University of Southampton

Faculty of Medicine

Human Development and Health

The metabolism of vitamin D and its effect on the epigenetic regulation of gene expression within the human placenta

by

Brogan Ashley

Thesis for the degree of Doctor of Philosophy

April 2019

University of Southampton

Abstract

Faculty of Medicine

Human Development and Health

Thesis for the degree of Doctor of Philosophy

The metabolism of vitamin D and its effect on the epigenetic regulation of gene expression within the human placenta

by

Brogan Ashley

Poor placental function impairs fetal growth and development. Suboptimal fetal growth is associated with an increased risk of disease in later life. Women of childbearing age have a high prevalence of 25-hydroxyvitamin D_3 ($25(OH)D_3$) deficiency, which is associated with reduced fetal growth and may impair placental delivery of vitamin D to the fetus. In this thesis I investigate which metabolites of vitamin D are passed from the mother to the fetus via the placenta, and how vitamin D directly affects placental tissue.

Placental $25(OH)D_3$ transfer and metabolism was investigated in *ex vivo* perfused placental cotyledons. Following perfusion of ^{13}C-$25(OH)D_3$ in the maternal circulation, vitamin D metabolites were measured in the maternal and fetal perfusate using liquid chromatography mass spectroscopy and enzyme-linked immunosorbent assay. Placental metabolism of ^{13}C-$25(OH)D_3$ was identified, and the metabolites ^{13}C-$25(OH)D_3$, ^{13}C-24,25-dihydroxyvitamin D_3 ($24,25(OH)_2D_3$) and 1,25-dihydroxyvitamin D_3 ($1,25(OH)_2D_3$) were transferred from the placenta to the fetal circulation. This study suggests that the placenta produces $1,25(OH)_2D_3$, and releases it to both the mother and the fetus.

The effects of short term $25(OH)D_3$ treatment on the placenta were determined in villous fragments and cultured syncytiotrophoblast cells. $25(OH)D_3$ altered DNA methylation in villous fragments when measured by Illumina 850K DNA methylation array, demonstrating alterations to placental epigenetics with $25(OH)D_3$. In addition $25(OH)D_3$ treatment of villous fragments resulted in altered RNA and protein expression, measured by RNA sequencing and liquid chromatography mass spectroscopy. Altered RNA expression was also observed in $25(OH)D_3$ treated cultured syncytiotrophoblast, measured by quantitative real time polymerase chain reaction. Altered DNA methylation, RNA and protein expression mapped to biological pathways of transcriptional

regulation, histone protein activity, immune function and inorganic ion transport. Components of the altered biological pathways may alter placental function in ways that could impact upon fetal growth.

Long term vitamin D (cholecalciferol) treatment was investigated in placentas from the Maternal Vitamin D and Osteoporosis Study (MAVIDOS) and the Southampton Pregnancy Intervention for the Next Generation (SPRING) studies. Pyrosequencing identified increased DNA methylation at one CpG site of the RXRα gene in MAVIDOS with 1000 IU cholecalciferol daily treatment, but no other changes in DNA methylation with treatment in either MAVIDOS or SPRING.

Data presented in this thesis suggest that the metabolites $25(OH)D_3$, $24,25(OH)_2D_3$ and $1,25(OH)_2D_3$ are transferred across the placenta to the fetal circulation, were they could act directly on the fetus. $25(OH)D_3$ is metabolised within the placenta, and this metabolism potentially alters levels of vitamin D metabolites in both the fetal and maternal circulation. $25(OH)D_3$ may also indirectly impact fetal growth and development via its actions on the placenta, which alter placental functions important for fetal growth. The data presented here helps explain the relationships underlying the observed association between maternal $25(OH)D_3$ concentration and fetal growth.

Table of Contents

Table of Tables

Table of Figures

Research Thesis: Declaration of Authorship

Print name:	Brogan Ashley

Title of thesis:	The metabolism of vitamin D and its effect on the epigenetic regulation of gene expression within the human placenta

I declare that this thesis and the work presented in it are my own and has been generated by me as the result of my own original research.

I confirm that:

1. This work was done wholly or mainly while in candidature for a research degree at this University;
2. Where any part of this thesis has previously been submitted for a degree or any other qualification at this University or any other institution, this has been clearly stated;
3. Where I have consulted the published work of others, this is always clearly attributed;
4. Where I have quoted from the work of others, the source is always given. With the exception of such quotations, this thesis is entirely my own work;
5. I have acknowledged all main sources of help;
6. Where the thesis is based on work done by myself jointly with others, I have made clear exactly what was done by others and what I have contributed myself;
7. Parts of this work have been published as:

EM Curtis, N Krstic, E Cook, S D'Angelo, SR Crozier, RJ Moon, R Murray, E Garratt, P Costello, J Cleal, **B Ashley**, NJ Bishop, S Kennedy, AT Papageorghiou, I Schoenmakers, R Fraser, SV Gandhi, A Prentice, MK Javaid, HM Inskip, KM Godfrey, CG Bell, KA Lillycrop, C Cooper, NC Harvey and the MAVIDOS Trial Group (2019). Gestational vitamin D supplementation leads to altered perinatal RXRα promoter DNA methylation: results from the MAVIDOS trial. Journal of Bone and Mineral Research 34(2) 231-240.

Signature:		Date:	12/04/2019

Acknowledgements

I wouldn't have been able to complete this thesis without the support, advice and guidance of so many people. I would like to say thank you to some of those people here.

Firstly, I would like to thank my supervisor Dr Jane Cleal. Thank you for imparting your knowledge of the placenta and vitamin D upon me, and for all of your help during the learning curve of a PhD. Thank you for your patience, encouragement and understanding throughout.

Professor Rohan Lewis, thank you for freely sharing your knowledge of the placenta with me, and encouraging me to proactively seek opportunities for learning and research.

Professor Nick Harvey, thank you for your support and guidance. In particular thank you for allowing me to work with the cohort studies, and for your help in understanding how to interpret and understand data from large trial studies.

Thank you to all of the research midwives, nurses and administrators whose help, advice and assistance have been invaluable to my studies. Having no prior experience working with patients, your knowledge and support gave me the confidence I needed to consent and collect samples for this research. The dedication to research and improving health during pregnancy shown by all of you is inspiring, and thank you for supporting me in making my little mark in this field.

Thank you to the patients of Princess Anne Hospital for allowing this research to take place, through the selfless act of donating their placental tissue. Thank you to the midwives and doctors at Princess Anne Hospital for allowing me to collect placental samples and for taking the time for research when your jobs are already so busy.

Dr Kerry Jones, and Felicity Hey, thank you for your expertise in measuring metabolites in my perfusate samples.

Dr Faisal Rezwan and Dr Christopher Bell, thank you for providing your expertise in the analysis of the DNA methylation array data. Dr Cory White, thank you for your expertise in analysing the RNA sequencing data. Dr Spiros Garbis and Dr Antigoni Manousopoulou, thank you for your expertise in analysing the proteomic data.

Thank you to Dr Susan Greenwood for your advice and expertise in establishing primary placental cell culture experiments.

Nevena Krstic, thank you for carrying out the pyrosequencing, even though you were at such a busy part of your own PhD.

Thank you to all of the IDS technical team, in particular Melissa Doherty and Georgie Hudson, for your technical expertise. Thank you for always providing an extra pair of hands when needed.

Dr Judith Holloway, the wisest person I know. I have been so fortunate to have your mentorship, through this PhD. Thank you for your understanding, advice and encouragement, it has been invaluable.

I have been fortunate to have lab mates who I also consider good friends. Thank you to Dr Emma Lofthouse, Jennifer Pearson-Farr, Dr Lisa Jones and Dr Claire Simner for all of the training, maths

checking and general support. But most importantly thank you for keeping me (mostly) sane with tea breaks!

Lance Morgan, I don't know what I did to deserve you. Thank you for moving across the country for me multiple times, for putting my education before your career. Thank you for your belief in me, and for looking after me every single day.

To Mum, Dad, Conor and Neve, my crazy, amazing family. Thank you for your love and support throughout my entire education. Thank you for your unwavering belief that I can achieve anything I put my mind to, I couldn't have done this without you.

Finally thank you to my funding bodies, RANK prize funds, Medical Research Council and the Faculty of Medicine Vice Chancellors Awards.

Definitions and Abbreviations

Abbreviation	Definition
$1,24,25(OH)_3D$	1,24,25-trihydroxyvitamin D
$1,25(OH)_2D$	1,25-dihydroxyvitamin D, calcitriol
$24,25(OH)_2D$	24,25-dihydroxyvitamin D
25(OH)D	25-hydroxyvitamin D, calcifediol
5hmC	5-hydroxymethylcytosine
5mC	5-methylcytosine
B&H	Benjamini & Hochberg
BCA	Bicinchoninic acid
BM	Basal membrane
BMC	Bone mineral content
BMD	Bone mineral density
bp	Base pairs
cDNA	Complementary DNA
ChIP	Chromatin immunoprecipitation
cp	Crossing point
CPM	Counts per million
CRH	Corticotropin-releasing hormone
CV	Coefficient of variation
CYP	Cytochrome P450
DBP	Vitamin D binding protein
DMEM	Dulbecco's modified Earle's medium
DNMT	DNA methyltransferase
DOHaD	Developmental Origins of Health and Disease
DXA	Dual energy x-ray absorptiometry
EBB	Earle's bicarbonate buffer
ELISA	Enzyme-linked immunosorbent assay
FDR	False discovery rate
FGR	Fetal growth restriction

GDM	Gestational diabetes mellitus
HAT	Histone acetyltransferase
HBSS	HEPES-buffered salt solution
hCG	Human chorionic gonadotrophin
HCS	Healthy Conversation Skills
HEPES	4-(2-hydroxyethyl)-1-piperazineethanesulfonic acid
HKG	Housekeeping gene
HMT	Histone methyltransferase
HP	Horseradish peroxidase
ICR	Imprinting control region
ID	Inner diameter
IGF2	Insulin-like growth factor II
IGF2R	Type-II Insulin-like Growth Factor Receptor
IU	International Unit
IVF	In vitro fertilisation
LCMS	Liquid chromatography mass spectroscopy
LGA	Large for gestational age
LH	luteinizing hormone
LINE1	Long interspersed elements
MAVIDOS	Maternal Vitamin D Osteoporosis Study
MBD	Methyl-CpG binding domain
MHRA	Medicines and Healthcare products Regulatory Agency
mRNA	Messenger RNA
mTOR	Mammalian target of rapamycin
MVM	Microvillous membrane
NCS	Newborn calf serum
NEC	No enzyme control
NTC	No template control
OD	Outer diameter
PBS	Phosphate buffered saline

PHLDA2	Pleckstrin homolog-like domain family A member 2
PMCA	Plasma membrane Ca-ATPase
Pro-vitamin D3	7-dehydrocholesterol
PTH	Parathyroid hormone
qRT-PCR	Quantitative reverse transcription polymerase chain reaction
RISC	RNA-induced silencing complex
RP	Reverse-phased
rRNA	Ribosomal RNA
RT	Room temperature
RXRα	Retinoid X receptor α
RXRβ	Retinoid X receptor β
RXRγ	Retinoid X receptor γ
SEM	Standard error of the mean
SGA	Small for gestational age
SPRING	Southampton Pregnancy Intervention for the Next Generation
SWS	Southampton Women's Survey
TBE	Tris Borate Ethylenediaminetetraacetic acid
UHRF	Ubiquitin-like, containing PHD and RING finger domain
UPL	Universal probe library
UVB	Ultraviolet B
VDIR	Vitamin D interacting repressor
VDR	Vitamin D receptor
VDRE	Vitamin D receptor element

Chapter 1 Introduction

1.1 Overview

Study of the human placenta has allowed researchers not only to gain an understanding of the anatomy and functioning of the organ, but also to understand the role it plays in fetal development. The delivery of the placenta following delivery of the baby has provided an opportunity for researchers to study the organ, generating information that has both advanced our scientific understanding and translated into improved clinical care. Research has allowed us to better develop and predict the effects of therapeutic drugs on the mother and fetus when used in pregnancy, both when administered for a pregnancy complication or for another health condition in the mother.

The placenta is a complex organ with multiple functions that we still do not fully understand. A healthy functioning placenta is necessary for healthy fetal growth, which in turn affects lifelong health and disease risk. Deficiency of vitamin D in pregnant mothers has been linked to poor fetal growth and increased disease risk in the offspring's later life. The precise mechanisms that link maternal vitamin D to fetal outcomes are unclear, however the placenta, as the conduit for nutrient transfer to the fetus must play a role in this relationship. The placenta mediates transfer of maternal vitamin D to the fetus and may also be affected by vitamin D levels at both the gene expression and epigenetic level. At present the interactions between vitamin D and the placenta are unclear and are the focus of this thesis.

1.2 Developmental Origins of Health and Disease

1.2.1 Fetal development and health

The risk of developing a number of non-communicable diseases in adult life has been associated with *in utero* development and birth weight by epidemiological studies in human populations. Population studies identified a link between a poor intrauterine environment and low birth weight with an increased risk of cardiovascular disease in later life (Barker, 1989, Barker, 1990). Further studies also identified an increased risk of cardiovascular disease, in addition to an increased risk of insulin resistance, high blood pressure and osteoporosis with a poor intrauterine environment and low birth weight (Barker, 1995, Cooper et al., 1997, Huxley et al., 2000). Offspring from mothers who experienced famine during early gestation in the Dutch Hunger Winter of 1944-45 show increased risk of obesity, despite not being born smaller (Painter et al., 2005), and of schizophrenia in later life (Hoek, 1998). Whereas offspring from mothers who experienced famine during late gestation in the Dutch Hunger Winter were born smaller, and had decreased glucose tolerance in later life (Hanson and Gluckman, 2014). The risk of developing non-communicable diseases is graded across the normal range of development, with greater deviation from 'normal' resulting in higher later life disease risk (Hanson and Gluckman, 2011). The associations seen in these studies have led to the development of the Developmental Origins of Health and Disease (DOHaD) hypothesis.

The DOHaD hypothesis suggests that the *in utero* physiological changes a fetus undergoes to increase its chances of survival in a particular environment persist into adult life, and subsequently can lead to the development of disease due to a mismatch in the adult and fetal environmental conditions (Eriksson, 2016, Hanson and Gluckman, 2015). Fetuses may also undergo predictive adaptive responses, which are physiological changes which do not provide an immediate survival advantage, but are made in anticipation of providing a future advantage. However if the prediction is inaccurate, the change can increase the risk of poor health or disease in later life (Gluckman and Hanson, 2004). Physiological changes are possible during fetal development due to developmental plasticity, which allows a number of possible phenotypes to develop from a specific genotype in response to differing environmental conditions (Gluckman and Hanson, 2004).

Non-communicable diseases present a huge challenge to healthcare. They reportedly account for 35 million deaths annually, of which 80% occur in low and middle income countries (Hanson

and Gluckman, 2011). In response to this the United Nations have included as part of the goal 'Good Health and Wellbeing' from their 17 Sustainable Development Goals, the following target:

> *By 2030, reduce by one third premature mortality from non-communicable diseases through prevention and treatment and promote mental health and wellbeing.*

Working towards ensuring women have healthier pregnancies could be the first step in reducing the lifelong risk of a number of non-communicable diseases.

1.2.2 Placental function and health

The placenta acts as a barrier between the maternal environment and the fetus. It acts to regulate what is able to pass from the mother to the fetus, and therefore regulates fetal exposure to both the nutrients and hormones necessary for fetal development, as well as possibly harmful compounds from the maternal environment. However, as shown in Figure 1-1 a sub-optimal maternal environment can lead to sub-optimal placental function, which can in turn lead to poor fetal growth. Placental function thus plays a vital role in mediating fetal growth and determining the offspring's future health.

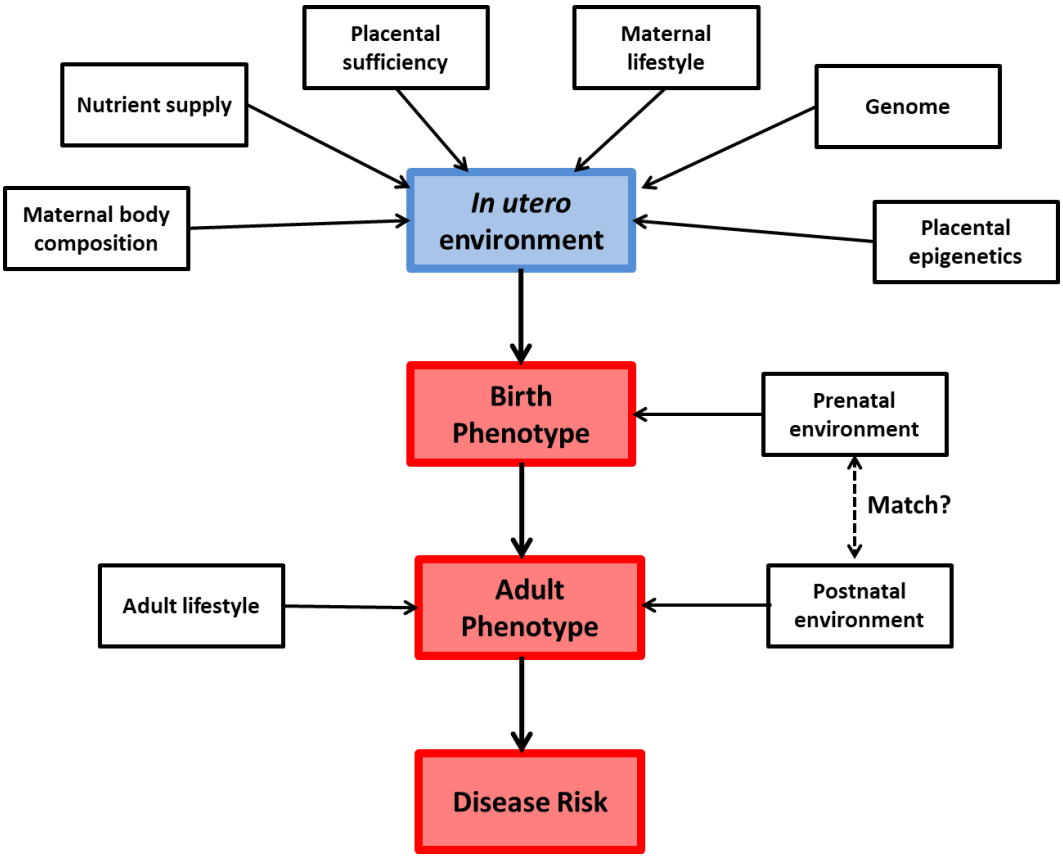

Figure 1-1 ***Factors affecting lifelong disease risk*** *An individual's risk of disease is affected by a number of factors, starting with those that effect the in utero environment and continuing throughout life.*

A high placental to birth weight ratio, indicating a fetus that has not reached its potential size due to placental inefficiency or other growth limiting factors, has been linked to poor cardiovascular outcomes for the offspring (Godfrey, 2002). A high placenta to birth weight ratio has also been linked to increased blood pressure at age seven years (Hemachandra et al., 2006), and an increased risk of cardiovascular disease associated death (Risnes et al., 2009). Placental shape, which can be altered by factors including maternal nutritional status, timing of periods of nutrient restriction and by fetal sex has also been linked with increased blood pressure in both childhood and adult life (Barker et al., 2010, Winder et al., 2011a, Winder et al., 2011b). A more oval shaped placenta was also linked to an increased risk of colorectal cancer in later life (Barker et al., 2013). These observations support a role for the placenta in mediating fetal development.

As shown in Figure 1-2, developmental plasticity may therefore make *in utero* intervention a valuable tool in fighting non-communicable diseases, with the placenta being an important target. Therapeutic or lifestyle interventions that improve placental function may allow for healthier fetal growth and a reduced lifetime risk of a number of diseases.

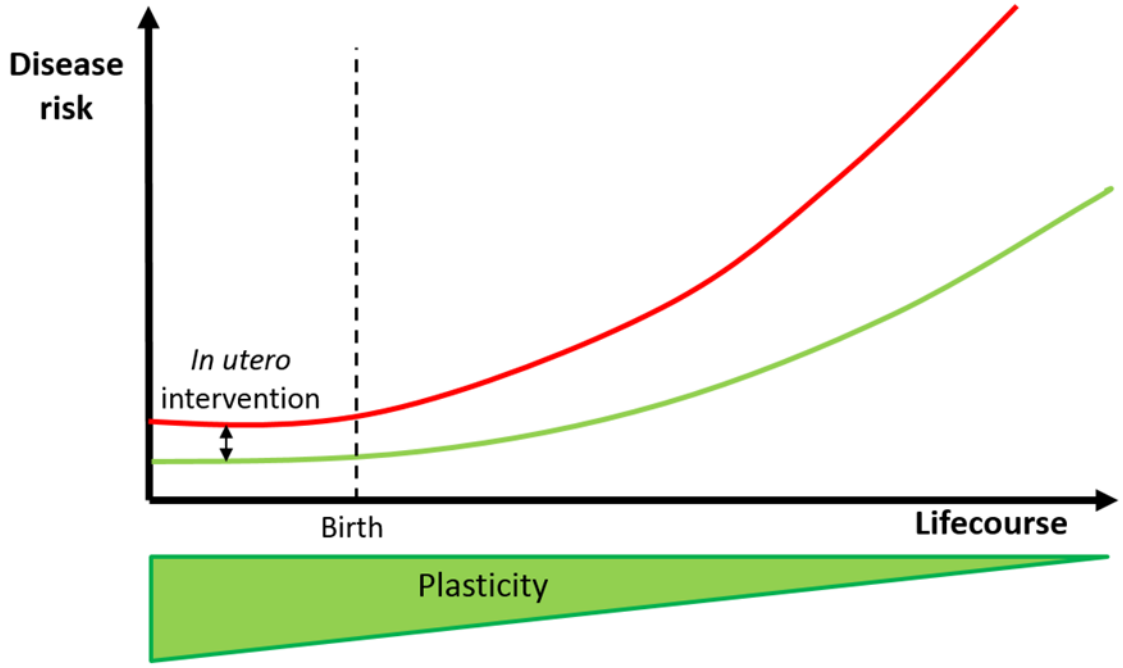

Figure 1-2 ***A life course approach to chronic disease risk.*** *Reducing disease risk in utero when the fetus demonstrates greatest plasticity may reduce lifelong risk of chronic diseases.*

1.3 Embryonic and fetal development

Fetal growth is determined by many factors, including but not limited to genetic growth potential, nutrient availability and exposure to environmental toxins. Over normal human gestation, development from fertilisation to birth can be divided into three periods, pre-embryonic (weeks 1-3), embryonic (weeks 4-8) and fetal (weeks 9-38).

1.3.1 Pre-embryonic human development

During fertilization sperm must travel to the fallopian tube and digest through the glycoprotein layer of the zona pellicuda surrounding the oocyte to reach and fertilise the cell. Cell division begins to occur as the fertilised oocyte is moved down the fallopian tube towards the endometrium. By three days after fertilisation cell division has produced a solid ball of cells, termed the morula. Cell division continues to occur, and by day five cells begin to move towards the outer edge of the ball, with one inner mass of cells, forming a hollow ball termed the blastocyst. The blastocyst escapes the zona pellicuda , consisting of the inner cell mass and outer wall of cells called the trophoblast layer. The inner cell mass continues to divide, and gastrulation occurs producing three germs layers, the endoderm, mesoderm, and ectoderm, from which all organs and tissues will develop. The notochord forms, inducing development of the neural plate from overlying ectoderm cells (Coad and Dunstall, 2011, Stables. D and Rankin. J, 2010, Aplin, 2000).

1.3.2 Normal human embryonic development

Implantation begins when close contacts are established between the fetal membranes and the uterine mucosa. The first stage of implantation occurs at around day 6-7 after conception, and is called apposition. At around this time point, the blastocyst has escaped the zona pellicuda, and consists of 107–256 cells (Aplin, 2000, Benirschke et al., 2006, Huppertz, 2008). As depicted in Figure 1-3 the blastocyst consists of an outer wall of trophoblast cells that surrounds the blastocyst cavity. Inside is the inner cell mass which contains larger cells that form the embryoblast (Benirschke et al., 2006). Trophoblast cells will develop into placental tissue while those of the inner cell mass become the embryo proper (Huppertz, 2008).

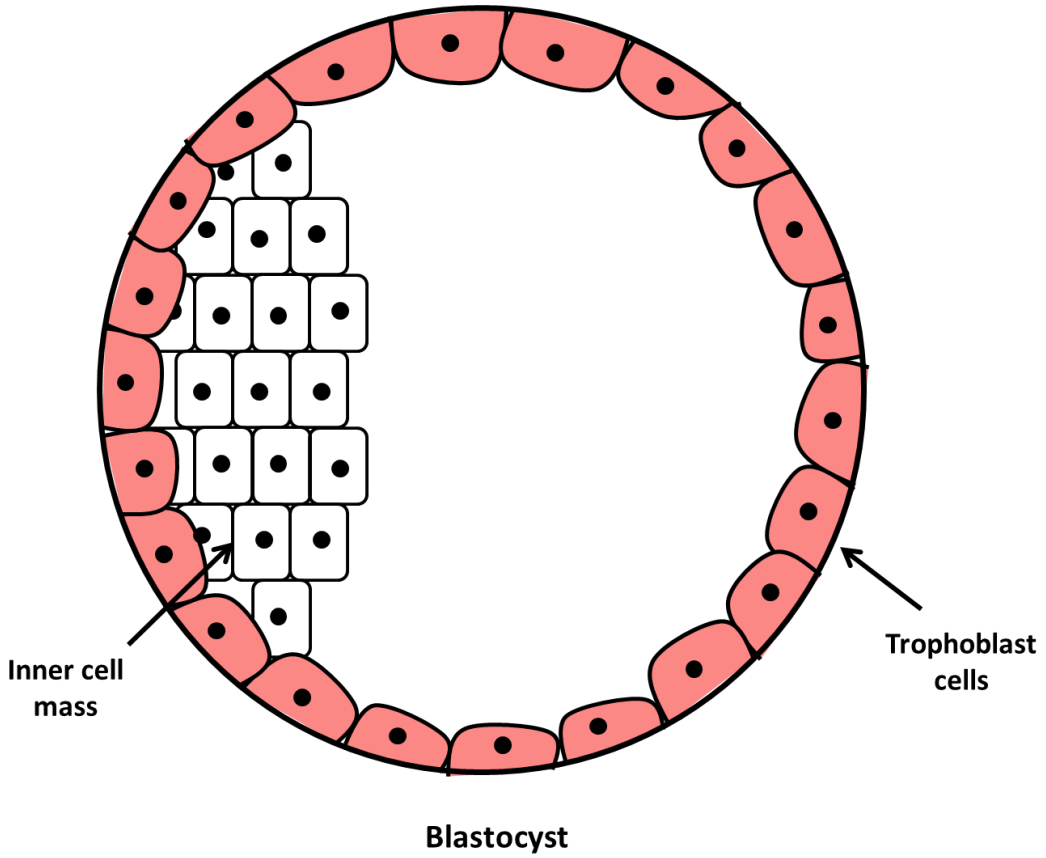

Figure 1-3 ***Diagram of the blastocyst 6-7 days after conception.*** *The inner cell mass, which will develop into fetal tissue, is surrounded by trophoblast cells, which develop into the placenta.*

Next the prelacunar stage of development occurs, and is depicted in Figure 1-4. Trophoblast cells overlying the inner cell mass form the implantation pole, the part of the trophoblast which will attach to and invade the uterine epithelium (Benirschke et al., 2006, Huppertz, 2008). Implantation occurs through the formation of attachments between membranes of the trophoblast and membranes of the uterine epithelium. This occurs during an implantation window during which the uterine epithelium displays this adhesive phenotype (Benirschke et al., 2006). Studies of *in vitro* fertilisation (IVF) have suggested that this implantation window occurs over four days, from 7-11 days after the peak in luteinizing hormone experienced around the time of ovulation (Bergh and Navot, 1992, Aplin, 2000). Once attached to the uterine epithelium, the mononuclear trophoblast cells begin to fuse, forming multinucleated syncytiotrophoblast, which has an invasive phenotype. The trophoblast cells which are still mononucleated and have not fused are now termed cytotrophoblast. At this stage only the syncytiotrophoblast is in contact with maternal tissue. Cytotrophoblast cells continue to divide, fusing with and maintaining the syncytiotrophoblast as it expands (Potgens et al., 2002, Benirschke et al., 2006, Huppertz, 2008).

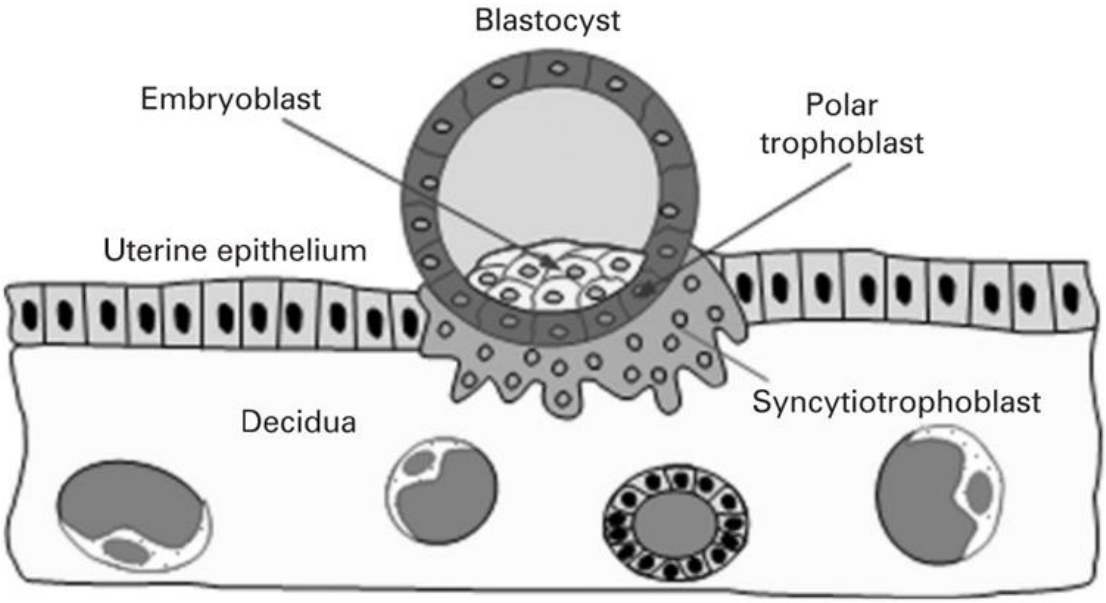

Figure 1-4 ***Implantation of the blastocyst.*** *Polar trophoblast cells of the implantation pole fuse to form syncytiotrophoblast during endometrial invasion. Adapted from The anatomy of the normal placenta (Huppertz, 2008).*

At eight days after conception, small fluid-filled intrasyncytial vacuoles begin to appear in the syncytiotrophoblast, which are called lacunae. This is the lacunar stage of development. The syncytiotrophoblast separating the lacunae are now termed trabeculae. With expansion of the syncytiotrophoblast, the lacunae continue to form and grow, creating a system of lacunae throughout the syncytiotrophoblast. This occurs from days 8 to 13 post conception. At this point the three basic structures which are still present at term can be identified, an early chorionic plate, the lacunar system which will become the intervillous space and a basal plate which is in contact with maternal tissue (Benirschke et al., 2006, Huppertz, 2008). At 12 days post conception implantation is finalised, as the embryo is completely embedded in the endometrium (Huppertz, 2008).

The embryonic period covers organogenesis, when all of the major organ systems and fetal structures are established, although most do not start functioning yet. This occurs through cellular differentiation of the inner cell mass, with totipotent cells specialising for a particular function. Folding occurs in which the embryo changes from being disk like in structure to cylindrical and curved into a ‘c’ shape. Growth is achieved through both cell division and increasing cell size (Coad and Dunstall, 2011, Stables. D and Rankin. J, 2010).

Table 1-1 *Normal in utero developmental features from gestational weeks 1 to 38. Information obtained from (Coad and Dunstall, 2011) and (Stables. D and Rankin. J, 2010).*

Developmental Period	Gestational age (weeks)	Developmental features
Pre-embryonic	1	Cell division to form morula Fluid accumulation to form blastocyst Blastocyst differentiation into trophoblast and inner cell mass Implantation
	2	Trophoblast differentiation and early placenta formation Formation of extraembryonic mesoderm Development of primitive streak
	3	Invagination of cells of the primitive streak to form mesoderm Formation of three germ layers Formation of notochord and beginning of neurulation
Embryonic	4	Neural tube fusing Folding into 'c' shape Appearance of upper and lower limb buds Beginnings of organ development
	5	Rapid brain development Facial development, upper and lower limb buds develop
	6	Joints and fingers in upper limbs begin to form External ear and retinal pigment form
	7	Liver becomes prominent Rapid growth of intestines
	8	Fingers separated and toes develop Limb movement can occur
Fetal	9-12	Body and limbs rapidly increase in length Ossification of skull and long bones Amniotic swallowing occurs Erythropoiesis begins in spleen and decreases in liver
	13-16	Period of rapid growth Active skeletal ossification
	17-20	Skin covered with protective vernix caseosa, held in place by lanugo (downy hair) Brown fat formed
	21-25	Surfactant secretion in lungs begins Rapid eye movement begins
	26-29	Lungs mature Central nervous system controls breathing Eyes open Subcutaneous fat laid down Erythropoiesis begins in bone marrow and ceases in spleen
	30-34	Body fat reaches 8% of fetal weight Fetus begins to store iron
	35-38	Head and abdomen circumference similar Body fat reaches 16% of fetal weight

1.3.3 Normal human fetal development

During the fetal period the rate of development is rapid, with organ systems maturing and becoming functional. Growth is primarily achieved through increasing cell size, although cell division is still taking place. The rate of growth of the head and brain slows compared to the rest of the body, so the head reduces from measuring half of the crown to rump length at 9 weeks to a quarter at term. Body fat is laid down in preparation for after birth (Coad and Dunstall, 2011, Stables. D and Rankin. J, 2010).

In utero development is a highly organised series of events and sensitive to a number of regulatory factors. Further details of these events are described in Table 1-1. Abnormal or altered development can have both short and long term consequences for the fetus, and therefore it is vitally important that we understand these.

1.3.4 Abnormal human fetal development

Abnormal fetal growth describes *in utero* development that results in the fetus growing at a different rate than is considered normal. Abnormal fetal growth is commonly classified as one of three conditions, small for gestational age (SGA), fetal growth restricted (FGR) or large for gestational age (LGA).

SGA describes a fetal estimated or actual birth weight of below the tenth percentile for their gestational age (Al-Amin et al., 2015). SGA fetuses have an increased risk of morbidity and mortality, and a number of poor postnatal health outcomes, including cardiovascular disease, osteoporosis, diabetes and high blood pressure (Barker, 1990, Barker, 1995, Cooper et al., 1997, Huxley et al., 2000). Poor maternal nutrition, hypertension and use of a number of therapeutic and recreational drugs are all risk factors for a SGA baby (Das and Sysyn, 2004).

FGR is a pathological condition that occurs when growth is prevented from reaching or maintaining its potential rate. Maternal over/under weight, smoking, history of preeclampsia, anaemia and chronic disease are all risk factors for FGR (Albu et al., 2014). FGR fetuses have an increased risk of perinatal mortality and lifelong poor health similar to SGA infants.

Infants are defined as being LGA if their birth weight is over the 90th percentile for their gestational age. Before birth a fetus is described as being macrosomic if its estimated weight is over the ninetieth percentile for their gestational age (Das and Sysyn, 2004, Mohammadbeigi et al., 2013). Diabetes mellitus, maternal obesity and family history are all risk factors for a fetus being LGA, and it is associated with a number of poor outcomes. There is an increased risk of

delivery complications, and infants have a higher incidence of obesity and diabetes in later life (Das and Sysyn, 2004).

Not all SGA babies are growth restricted, as some are simply at the lower end of the normal growth range. Similarly not all FGR babies are SGA. For example an appropriate for gestational age or LGA baby may subsequently become growth restricted, but its overall size is still appropriate or large for its gestational age. It is therefore not always simple to determine FGR clinically. Abnormal growth is caused by a large number of factors, with the placenta playing a significant role.

1.4 Human placental development

The placenta is a fetal organ that creates the barrier between the mother and the fetus. Even during its own development, the placenta must be able to function in accordance with that particular stage of embryonic development (Huppertz, 2008). With increasing gestation fetal demand for nutrients increases and the placenta must be able to meet this demand for nutrient transfer.

1.4.1 Trophoblast invasion

After implantation of the blastocyst around day 12 (see section 1.3.2) the invading syncytiotrophoblast, which is developing into the placenta, comes into contact with maternal capillaries. The capillaries are eroded allowing the first maternal blood cells into the lacunar system with a slow flow of venous blood. At 12 days post conception cytotrophoblast cells of the early chorionic plate also begin to penetrate into the trabeculae, and by 15 days post conception have reached the maternal side of the placenta. Here they begin to join together in an outermost layer to the placenta known as the trophoblastic shell (Benirschke et al., 2006, Huppertz, 2008). These are extravillous trophoblast cells, and display an invasive phenotype.

As shown in Figure 1-5 the extravillous trophoblast cells invade into the endometrium and into maternal spiral arteries. Here they replace the smooth muscle lining of the arteries with trophoblast cells. This reduces the elasticity of the vessels, reducing resistance and allowing for greater blood flow. However, during the first trimester of pregnancy the blood flow is not needed, and hence the trophoblast cells form a plug which occludes the spiral arteries. After 10-12 weeks gestation the plugs are dislodged and full placental blood flow is established (Zhou et al., 1997, James et al., 2006, Burton and Fowden, 2015).

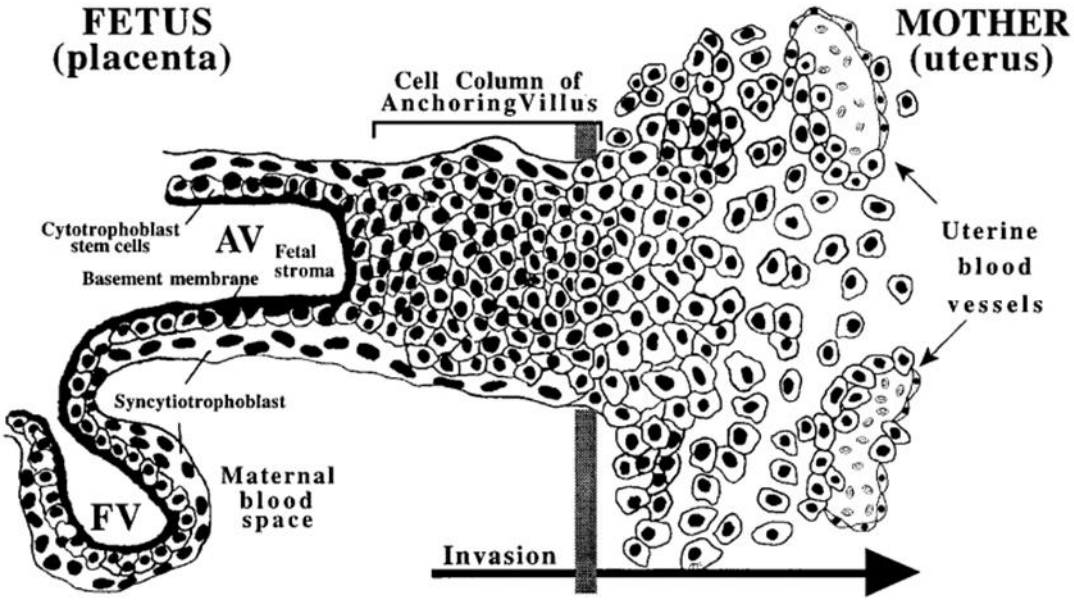

Figure 1-5 ***Trophoblast invasion of the endometrium.*** *Extravillous trophoblast cells invade the endometrium and remodel maternal spiral arteries in preparation for maternal blood flow into the placenta. Adapted from Human cytotrophoblasts adopt a vascular phenotype as they differentiate (Zhou et al, 1997).*

1.4.2 Villous development

At about 13 days after conception the villous stage of development begins. The trabeculae begin to develop small side branches, formed from syncytiotrophoblast protrusions. A core of cytotrophoblast cells develop in these protrusions and these structures become known as primary villi. The villi protrude into the intervillous space, the mature lacunae system. Extraembryonic mesenchyme cells (also known as allantois), a type of primitive connective tissue derived from the embryonic disk and found in the chorionic plate from 14 days post conception, also begin to penetrate into the trabeculae. They penetrate into the primary villi creating a mesenchymal core, and turning the structures into secondary villi. At 20 days post conception, hemangioblastic progenitor cells, derived from the mesenchyme, begin to form the first fetal capillaries. This formation of vasculature within the secondary villi turns them into tertiary villi. Villi continue to branch, creating structures known as villous trees. The number of tertiary villi increases throughout gestation (Benirschke et al., 2006, Huppertz, 2008). During the first trimester of pregnancy, from conception to week 12, the majority of villi are primary villi. This reflects the minimal blood flow in the placenta at this time as efficient transfer of nutrients from maternal to fetal circulations is not necessary. At eight weeks secondary villi begin to form, and these are the most predominant type of villi during the second trimester, from weeks 13 to 27. Tertiary villi are most abundant in the third trimester of pregnancy, from 28 weeks until term,

reflecting the high rate of nutrient transfer that occurs during this period (Huppertz, 2008, Burton and Fowden, 2015).

Human villous development results in the formation of a haemochorial placenta, in which maternal blood is able to come into direct contact with fetal trophoblast cells for nutrient transfer, as shown in Figure 1-6. At term the umbilical cord inserts into the chorionic plate, and fetal vessels from the umbilical cord branch into the network of villous trees. The villous trees bathe in maternal blood which has entered the intervillous space through maternal spiral arteries. The intervllious space is enclosed on the maternal side by cells of the basal plate, which are embedded in the uterine wall until delivery. Upon delivery detachment of the basal plate from the uterine wall reveals the maternal surface of the placenta, described as a false or artificial surface due to its attachment *in utero*. At the edge of the placenta where intervillous space has not formed the basal plate and chorionic plate are fused and form the chorion laeve. Placental membranes are composed of the amnion, a layer of epithelial cells and connective tissue that constitute the outermost layer of the fetal surface of the placenta, and the chorion, a connective tissue within which fetal vessels are found.

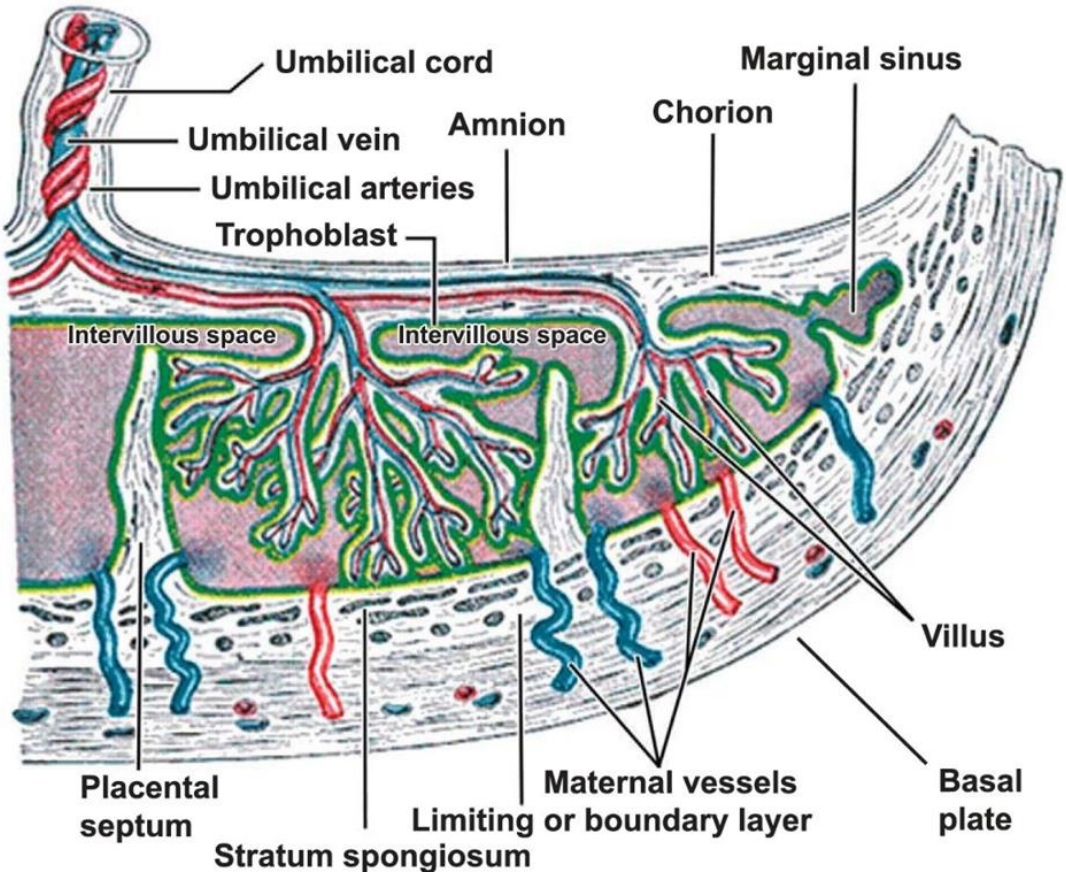

Figure 1-6 ***Diagram of the term human placenta.*** *Diagram demonstrating the main structures of a term placenta. Adapted from The role of morphology in mathematical models of placental gas exchange (Serov et al., 2016).*

Human placental structure is displayed in Figure 1-7. A full term human placenta is a discoidal organ that has been reported to be 22 cm in diameter, have a central thickness of 2.5 cm and a weight of 470 g on average. However these values vary extensively, and are subject to a number of influencing factors, including the timing and location of cord clamping (Bouw et al., 1976, Huppertz, 2008).

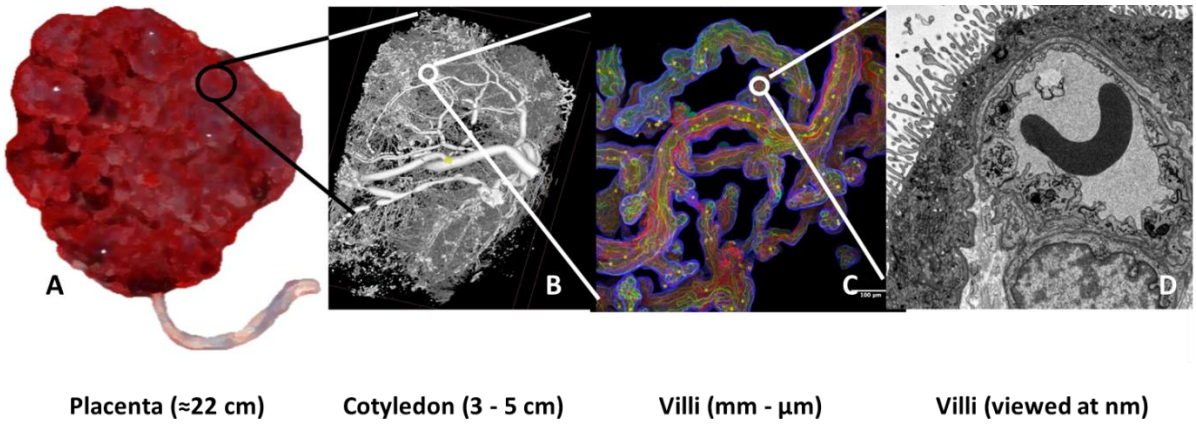

Figure 1-7 ***Scale of structures in the human placenta.*** *A) An image of the maternal side of a full term human placenta. B) A single cotyledon, imaged using computer micro-tomography. C) A small section of a villous tree imaged using fluorescence confocal microscopy demonstrating branching villi. D) Electron microscopy image of a cross section of a term placental villi.*

1.5 Placental function

Placental function is vital for pregnancy. While an important function of the placenta is the transport of nutrients to and removal of waste products from the fetus, it also carries out a number of other functions vital for successful pregnancy, including providing a barrier between the maternal and fetal circulations, and the endocrine regulation of metabolism.

1.5.1 Nutrient transfer

Transfer of nutrients through the placenta from the mother to the fetus is vital for fetal growth. Due to the large range of physical properties of substances to be transferred, as well as the need to regulate transfer, a number of different mechanisms are utilised. As shown in Figure 1-8, for a substance to transfer from the maternal to fetal circulation it must pass from the intervillous space, across the microvillous membrane (MVM) of the syncytiotrophoblast, through the syncytiotrophoblast, across the basal membrane (BM) of the syncytiotrophoblast and finally through the fetal capillary endothelium, (Gaccioli and Lager, 2016). A number of factors influence the rate of nutrient transfer between maternal and fetal circulations, including utero-placental and umbilical cord blood flow, concentration gradient, membrane thickness and exchange area (Gaccioli and Lager, 2016, Myren et al., 2007). The placenta regulates exchange of nutrients to the fetus by modulating transfer, placental consumption and placental metabolism of nutrients (Gallo et al., 2016).

Membrane permeable substances, such as the small hydrophilic compounds oxygen and carbon dioxide, are able to diffuse across the placenta between maternal and fetal circulations. The rate of transfer of oxygen and carbon dioxide is greatly influenced by rate of blood flow, membrane thickness and exchange area (Gaccioli and Lager, 2016, Myren et al., 2007). The concentration of oxygen is higher in maternal than fetal circulation, and hence oxygen diffuses from the maternal circulation to the fetal circulation (Murray, 2012).

Glucose moves down its concentration gradient from the maternal to the fetal circulation across the placenta via facilitated diffusion. This occurs via the GLUT (facilitated glucose transporter) family of facilitated transporter proteins (solute carrier family SLC2A gene family) (Gallo et al., 2016). GLUT1 (GLUT member 1; *SLC2A1*) is the primary glucose transporter found in the placenta, and it is located on both the MVM and BM. Expression of GLUT1 is around three times higher on the MVM than BM, meaning that more glucose is moved into the syncytiotrophoblast than undergoes efflux and thus transport across the BM is the rate limiting step (Jansson et al., 1993). Placental glucose metabolism, transporter density and maternal to

fetal concentration gradient all act to regulate glucose transfer to the fetus. It has been observed that between 16-22 weeks and 27-30 weeks gestation the expression and activity of the GLUT1 protein approximately doubles. This may allow for the necessary increase in glucose transfer to the fetus nearer term (Illsley, 2000).

The concentration of amino acids is higher in the fetal than maternal circulation, and so amino acids must be actively transported against their concentration gradient to the fetus (Cetin et al., 2005). Accumulative amino acid transporters take up a range of amino acids from the maternal circulation across the MVM into the syncytiotrophoblast, resulting in a net increase in the concentration of amino acids within the syncytiotrophoblast. These accumulative transporters include system A and system X^-_{AG} transporters (Cleal et al., 2018). System L exchange transporters that are also present on the MVM are then able to modify the composition of the pool of amino acids in the syncytiotrophoblast by exchanging one amino acid in the syncytiotrophoblast with a different amino acid from maternal circulation. This allows for less abundant amino acids to be selectively concentrated within the syncytiotrophoblast and thus available for transport to the fetus (Cleal et al., 2018). Facilitated transporters present on the BM are responsible for the net increase in amino acid concentration in the fetal circulation through efflux of amino acids. This occurs through the facilitated transporters TAT1 (T-type amino acid transporter 1/ *SLC16A10*), LAT3 (Large neutral amino acids transporter small subunit 3/ *SLC43A1*) and LAT4 (Large neutral amino acids transporter small subunit 4/ *SLC43A2*) (Cleal et al., 2011). Exchange transporters present on the BM are then able to modify the composition of the fetal amino acid pool. They exchange amino acids from the fetal circulation for one from the syncytiotrophoblast which is not transferred by the facilitated transporters (Cleal et al., 2007, Cleal et al., 2018). Amino acid transporters are also responsible for the transport of thyroid hormones across the placenta from the maternal to fetal circulations (Taylor and Ritchie, 2007).

Although fatty acids are able to diffuse across plasma membranes, the concentration of most fatty acids is higher in the fetal than maternal circulations and so they must be transported to the fetus (Haggarty, 2010). Fatty acids are taken up into the placenta crossing the MVM via fatty acid transport proteins, plasma membrane fatty acid binding protein and fatty acid translocase. They then undergo efflux across the BM into the fetal circulation via fatty acid translocases, fatty acid transport proteins or by passive diffusion (Gallo et al., 2016). Modelling of placental fatty acid transport has demonstrated that metabolism of fatty acids within the placenta regulates the transfer of fatty acids to the fetus (Perazzolo et al., 2015).

Calcium is transported across the placenta against its concentration gradient via plasma membrane Ca-ATPase (PMCA) proteins. PMCA proteins are located on both the MVM and BM,

and thus take up calcium from the maternal circulation into the syncytiotrophoblast, and then transport it to the fetal circulation. There is a higher concentration of PMCA proteins on the MVM than BM allowing for the BM to regulate calcium transfer to the fetus (Marin et al., 2008).

The placenta not only transports nutrients from the maternal to fetal circulations but also regulates the rate of transfer and composition of the nutrients that pass through it. Different transporters must work together to ensure suitable nutrient transfer. Changing fetal requirements throughout gestation alter what needs to be transported to the fetus, and placental regulation of nutrient transport accommodates for this.

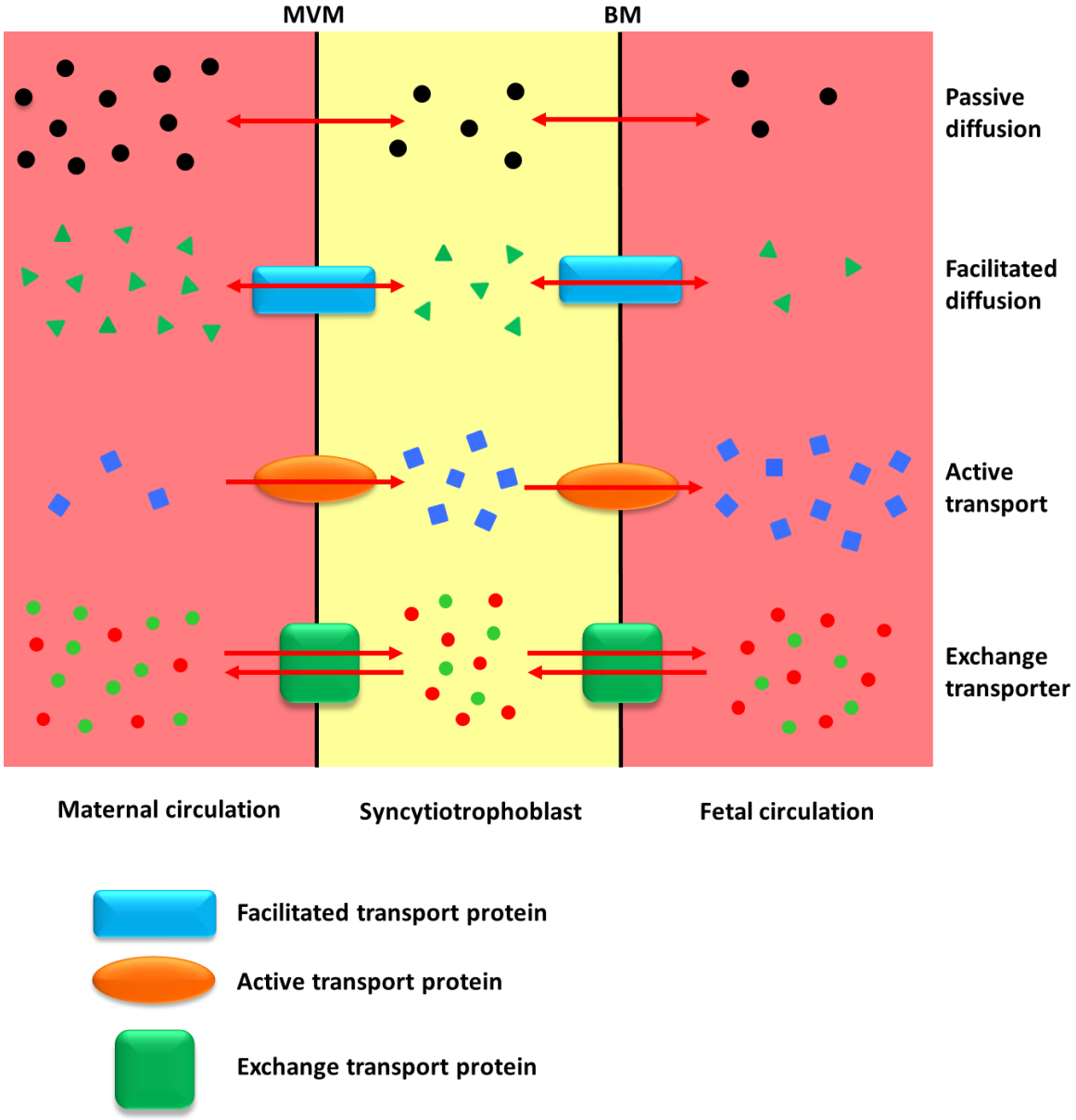

Figure 1-8 ***Placental nutrient transport.*** *Nutrients, gases and waste products must cross through the microvillous membrane (MVM) and basal membrane (BM) of the syncytiotrophoblast to pass from the maternal to fetal circulation. A number of mechanisms allow for this, including passive diffusion, facilitated diffusion, active transport and exchange transport.*

1.5.2 Immune regulation

One of the initial functions of the developing placenta is to prevent immune rejection of the fetus by the mother, and this immune tolerance must be maintained throughout pregnancy. Cells and proteins of the immune system within the decidua at the maternal-fetal interface play an important role in the growth and maintenance of a healthy functioning placenta. Immune cells include lymphocytes (T-cells, B-cells and natural killer cells), neutrophils, and monocytes/macrophages, which are all types of white blood cell (leukocyte). Many of these cells produce signalling proteins, such as cytokines, complement and antibodies, which act upon other cells and initiate a response.

The main immune cell class at the maternal-fetal interface are the lymphocytes. Uterine natural killer cells represent approximately 70% of lymphocytes cells within the decidua. These have been suggested to secrete pregnancy promoting cytokines that allow for trophoblast invasion into the endometrium, and for spiral artery formation. The lymphocyte regulatory T cells are also present in the decidua and have an immunosuppressive effect, downregulating the proliferation of effector T-cells (Racicot et al., 2014).

Macrophages are present in the decidua throughout gestation (Faas and De Vos, 2018). They make up 20–30% of decidual leukocytes in early pregnancy and decrease in number towards term, supporting an important role in implantation and placental development (Racicot et al., 2014, Abrahams et al., 2004, Heikkinen et al., 2003). Macrophages remove the cellular debris that results from apoptosis, and the uptake of apoptotic bodies can result in an immunosuppressive response. They also synthesise and secrete cytokines that act upon the local tissues (Abrahams et al., 2004).

Trophoblast cells secrete factors such as interleukin 10, an anti-inflammatory cytokine, which induce maternal regulatory T-cells and macrophages and hence support immune tolerance of the fetus (Svensson-Arvelund et al., 2015). Trophoblast cells also express pattern recognition receptors that can recognise the presence of viruses, bacteria, apoptotic cells and tissue damage. In response to this cytokines are released, which act upon macrophages in the decidua to elicit a response and protect the fetus (Racicot et al., 2014, Fest et al., 2007). The placenta therefore acts to prevent immune rejection of the fetus during pregnancy and also to modulate the local immune cells to protect the fetus from pathogens.

In addition to protecting the fetus from infection whilst *in utero*, the placenta also mediates the transfer of maternal antibodies to the fetus to provide immune protection during the neonate's early life. Immunoglobulin G (IgG) is the primary antibody transferred to the fetus, with

transfer thought to occur via binding to the neonatal Fc receptor (FcRn) in the syncytiotrophoblast. However differing concentrations of immunoglobulins in the maternal and fetal circulations suggest transfer is selective, and the exact mechanisms of this are unclear (Wilcox et al., 2017, Lozano et al., 2018).

1.5.3 Placental metabolism

The placenta is a highly metabolically active organ (Gallo et al., 2016). Metabolic activity within the placenta allows for the maintenance of placental tissues, as well as for regulation of the amount and type of different nutrients that are transferred to the fetus. Placental metabolism therefore regulates fetal exposure and influences fetal growth and development (Gallo et al., 2016).

Glucose is the main source of energy for placental and fetal tissues, with the mother supplying the glucose to both (Gallo et al., 2016, Hauguel et al., 1983). Around a quarter of glucose that enters the placenta is metabolised, and the rest is transferred directly to the fetus (Hauguel-de Mouzon and Shafrir, 2001). The majority of glucose that is metabolised within the placenta is converted to lactate via glycolysis, and transferred to the fetus where it acts as an alternative energy source (Hauguel-de Mouzon and Shafrir, 2001). Glucose is also metabolised to glycogen (Hahn et al., 2001), which is used within the placenta, and into lipids, as a stored energy source (Visiedo et al., 2013). Fatty acids are also metabolised within the placenta, where they are used as an energy source or can be stored in lipid droplets (Gallo et al., 2016).

Amino acids are another important metabolite within the placenta. They are taken up by the placenta and incorporated into a number of different proteins, including human placental lactogen , pregnancy-associated plasma protein A, human chorionic gonadotropin and pregnancy protein 1 (Schneider, 2015). This is important for the production of proteins and hormones that allow for the maintenance and success of pregnancy. The majority of net amino acid transfer across the placenta occurs in the mother to fetus direction (Gallo et al., 2016). Glutamate is taken up from both the maternal and fetal circulations and converted to glutamine within the placenta. The majority of this glutamine is then released to the maternal circulation, leaving a pool within the placenta to ensure there is sufficient glutamine to meet fetal demand. This is important as glutamine is a conditionally essential amino acid, whereby the fetus cannot synthesis sufficient amounts and thus requires a supply from the mother. The placenta is regulating glutamine metabolism to meet fetal demand (Day et al., 2013, Parimi and Calhan, 2007).

Although it is not synthesised within the placenta, the placenta plays an important role in the regulation of cortisol during pregnancy. Near term a rise in fetal cortisol levels causes a change

from fetal tissue growth to fetal tissue differentiation, allowing for maturation of organs and survival after birth. However cortisol is able to diffuse across the placenta, and thus could pass from maternal to fetal circulation throughout pregnancy, not just near term. The placenta expresses the enzyme 11β-hydroxysteroid dehydrogenase in order to protect the fetus from high levels of maternal cortisol. 11β-hydroxysteroid dehydrogenase type I interconverts cortisol and cortisone. The placenta expresses the enzyme 11β-hydroxysteroid dehydrogenase type II, which only converts active cortisol to inactive cortisone. Conversion of cortisol to cortisone within the placenta prevents cortisol from diffusing across to the fetus, thus preventing early differentiation of fetal tissues (Fowden et al., 2016, Cottrell et al., 2014).

1.5.4 Placental hormone synthesis

The synthesis and regulation of hormones by the placenta is vital for successful pregnancy. The placenta synthesises a number of hormones, which have roles in uterine invasion, pregnancy maintenance and labour. Most of these are synthesised in the syncytiotrophoblast, however other trophoblast cells such as extravillous trophoblasts also play an important role (Costa, 2016). Placental derived hormones also act upon the mother, mediating physiological changes necessary to support pregnancy, birth and lactation (Napso et al., 2018).

Human chorionic gonadotrophin (hCG) is a glycoprotein family hormone that is synthesised mainly in the syncytiotrophoblast, and released into the maternal circulation. Some hCG is also synthesised in extravillous cytotrophoblast cells (Handschuh et al., 2007), and hCG can be detected from embryos before implantation (Hay and Lopata, 1988, Costa, 2016). hCG is found in the maternal blood from two weeks of gestation, and peaks at 12 weeks (Handschuh et al., 2007, Jaffe et al., 1969). It acts to prevent regression of the corpus luteum, which subsequently allows for continued progesterone release from the corpus luteum and maintenance of early pregnancy.

Progesterone is a steroid hormone produced in the syncytiotrophoblast that is essential for the maintenance of pregnancy (Costa, 2016). During early pregnancy progesterone is released from the corpus luteum under hCG stimulation, however the placenta takes over this role by 6-8 weeks due to degeneration of the corpus luteum (Tuckey, 2005). Levels of progesterone increase in the maternal circulation until term (Tuckey, 2005). Progesterone acts to promote implantation of the embryo by inhibiting the action of oestrogen which causes epithelial cell proliferation and by inducing the expression of genes that allow for uterine receptivity (Halasz and Szekeres-Bartho, 2013). It then regulates the amount of trophoblast invasion by inhibiting matrix metalloproteinase activity, preventing over-invasion of the endometrium (Halasz and Szekeres-Bartho, 2013). Progesterone promotes immune tolerance throughout pregnancy by promoting Type 2 T-helper

cells to release cytokines which have anti-inflammatory effects and inhibiting the production of cytokines from Type 1 T-helper cells, which have pro-inflammatory effects (Raghupathy et al., 2005). It also acts to prevent pre-term labour by suppressing myometrium contractility (Ruddock et al., 2008). Progesterone also acts to regulate the production of other hormones, as well as to prepare the mammary glands for lactation (Costa, 2016).

Oestrogens are a group of four steroid hormones, oestrone, 17β-oestradiol, oestriol and oestetrol, that are produced in the syncytiotrophoblast in the placenta, or in the case of oestetrol in the fetal liver (Costa, 2016). Oestrogen levels increase throughout pregnancy to a peak at term (Costa, 2016). Oestrogens act to increase uteroplacental blood flow by causing vasodilation of placental and uterine arteries (Corcoran et al., 2014). They act to increase the number of gap junctions between myometrial cells, which promotes their contractile capability and may play a role in causing the onset of labour (Di et al., 2001). During pregnancy oestrogens play a role in regulating insulin and glucose homeostasis (Napso et al., 2018). Oestrogens also play a role in preparing the mother for after birth, promoting proliferation of the mammary gland epithelium and encouraging fat storage (Costa, 2016).

A number of placental derived hormones function to adapt maternal metabolism for pregnancy, including human placental lactogen and placental growth hormone. Both are mainly synthesised in the syncytiotrophoblast, but can also be produced by extravillous trophoblast cells (Costa, 2016). Human placental lactogen functions to regulate carbohydrate and lipid metabolism, increasing fatty acid concentration in the circulation by increasing lipolysis. Placental growth hormone functions to increase maternal secretion of IGF-1, and alter maternal metabolism to increase the availability of nutrients such as fatty acids and glucose in maternal blood (Costa, 2016, Napso et al., 2018).

Other hormones produced in the placenta include leptin, resistin, pregnancy-associated plasma protein A, placental protein 13, inhibins and activins (Costa, 2016). Collectively the endocrine functions of the human placenta allow for the establishment and maintenance of pregnancy, through alterations to maternal physiology that result in a pro-pregnancy state.

1.5.5 Regulation of placental function

Placental function in terms of nutrient transport, metabolic regulation, endocrine regulation and immune tolerance mean it has a large influence on fetal growth and development. Placental functions can be regulated by factors in both the maternal and fetal environments.

The Southampton Women's Survey (SWS; see section 1.8.1), is a longitudinal study looking at how pre-pregnancy and intrauterine factors affect the placenta, fetal and childhood growth. Data

from the SWS supports the hypothesis that maternal factors, such as nutritional status and reserves impact upon the development of the placenta, which in turn impacts upon fetal growth. Maternal body fat prior to pregnancy, maternal height and age at child's birth was positively associated with placental volume at 19 weeks. In turn placental volume at 19 weeks gestation was associated with a significant increase in offspring bone area, bone mineral content and bone mineral density, measured by DXA scan within two weeks of birth. Placental volume at 19 weeks was also associated with a significant increase in total percentage fat mass at birth and a decrease in total percentage lean mass (Holroyd et al., 2012).

Further supporting evidence linking maternal factors to placental function and fetal development is shown in mothers who carry out strenuous exercise in pregnancy. The activity of placental system A amino acid transporters (*SNAT1, SNAT2* and *SNAT4*) was shown to be significantly decreased in mothers who undertook strenuous exercise, and in mothers who had a smaller pre-pregnancy upper arm muscle area (Lewis et al., 2010). This suggests an adaptation of reduced amino acid transport to the fetus, conserving reserves in the mother when the mother has either low reserves or high demand for the reserves. Mothers who undertook strenuous exercise also had higher placental expression of *Pleckstrin homolog-like domain family A member 2* (*PHLDA2*). Greater placental expression of *PHLDA2* at term was associated with a decreased fetal femoral growth velocity between 19 and 34 weeks gestation, and reduced bone mineral content at four years of age (Lewis et al., 2012). *PHLDA2* is an imprinted gene expressed only from the maternal allele, and is expressed primarily in villous cytotrophoblast tissue. This again suggests an adaptation to conserve maternal reserves when demand is higher.

Other studies have also had similar findings. Higher maternal fat mass, an indicator of the mother's current nutritional state, was associated with a larger placental surface. Head circumference and birth weight are indicative of fetal and infant growth. Both higher maternal fat mass, larger maternal head circumference and higher maternal birth weight were associated with increased placental efficiency (Winder et al., 2011b). This suggests that nutritional statuses at different points throughout life are able to effect placental development and efficiency, and therefore influence fetal growth. These findings demonstrate how the placenta adapts to alterations in maternal environment or lifestyle and these changes subsequently impact upon fetal growth.

1.5.6 Placental sensing of the environment

The placenta acts to sense signals from the maternal and fetal environments, altering its activity in response. This allows the placenta to adapt to changing conditions, optimising its functions throughout pregnancy.

Studies suggest that the nutrient sensing capabilities of the placenta may in part be regulated by the mammalian target of rapamycin (mTOR) signalling pathway. mTOR is a serine/threonine protein kinase that is found as either mTOR complex 1 or mTOR complex 2. Within the cell mTOR acts as a nutrient sensor and is inhibited by the drug rapamycin (Roos et al., 2009b). mTOR is found within the syncytiotrophoblast in the placenta (Roos et al., 2007). Inhibition of mTOR activity by incubation with rapamycin significantly decreased system L amino acid transporter activity, but had no effect on system A activity in placental villous fragments (Roos et al., 2007). Further studies utilising cultured placental cytotrophoblast cells showed decreased activity of system L, system A and taurine amino acid transporters upon inhibition of mTOR with rapamycin (Roos et al., 2009a). The difference in system A response in the two studies may be a result of a much longer incubation with rapamycin in the cultured cells.

The imprinted *Igf2* gene may also act to regulate placental nutrient transfer. *Igf2* is paternally expressed, and loss of expression is associated with fetal and placental growth restriction in humans (Harris et al., 2011). Studies have shown that mice that do not express the placental-specific *Igf2* transcript have increased expression of glucose and system A amino acid transporters in their placentas, and that this is in response to fetal signals (Constancia et al., 2005). Whereas, in mice where the fetus does not express IGF2, placental amino acid transfer is reduced (Sferruzzi-Perri, 2018). In humans increased methylation of the *IGF2* gene in placental tissue is associated with a higher birth weight and greater height (St-Pierre et al., 2012). This suggests that within the placenta IGF2 may be acting in response to signals from the fetus to regulate the transfer of nutrients.

Studies have demonstrated that low maternal vitamin D levels are associated with reduced offspring birthweight (Harvey et al., 2014a), and this may be mediated by the actions of vitamin D on the placenta. Maternal vitamin D has been associated with placental function (Cleal et al., 2015), and thus reduced placental supply of vitamin D may have adverse effects on placental transfer of vitamin D and other important nutrients.

1.6 Vitamin D

Vitamin D, a nuclear receptor binding hormone, is one of the many nutrients that must pass from the mother to the fetus via the placenta during pregnancy. Vitamin D has a number of functions within the body, and acts primarily by altering gene expression. It is misleadingly named, not fitting the classical definition of a vitamin as only small amounts are obtained from dietary sources, and instead is better classified as a hormone (Grundmann and von Versen-Höynck, 2011).

Vitamin D is a secosteroid hormone, a hormone that is derived from a steroid compound that has undergone a cleavage to one of its ring structures (Shin et al., 2010). The term 'vitamin D' encompasses both vitamin D_2 (ergocholecalciferol), and vitamin D_3 (cholecalciferol), displayed in Figure 1-9. Vitamin D_2 is obtained solely from dietary sources, being produced in plants in an ultraviolet B (UVB) catalysed reaction of ergosterol, a fungal membrane sterol. Small amounts of vitamin D_3 are obtained in the diet, from sources such as dairy and oily fish, but most is synthesised in the skin from 7-dehydrocholesterol (pro-vitamin D_3) (Shin et al., 2010, Tuckey et al., 2018). Vitamin D_2 is only around one third as potent as vitamin D_3, and has a much shorter half-life (Armas et al., 2004). 'Vitamin D' will be used to refer to vitamin D_2 and vitamin D_3 collectively. As shown in Figure 1-10 vitamin D undergoes metabolism within the body to its active form, 1,25-dihydoxyvitamin D ($1,25(OH)_2D$), which then acts upon target tissues.

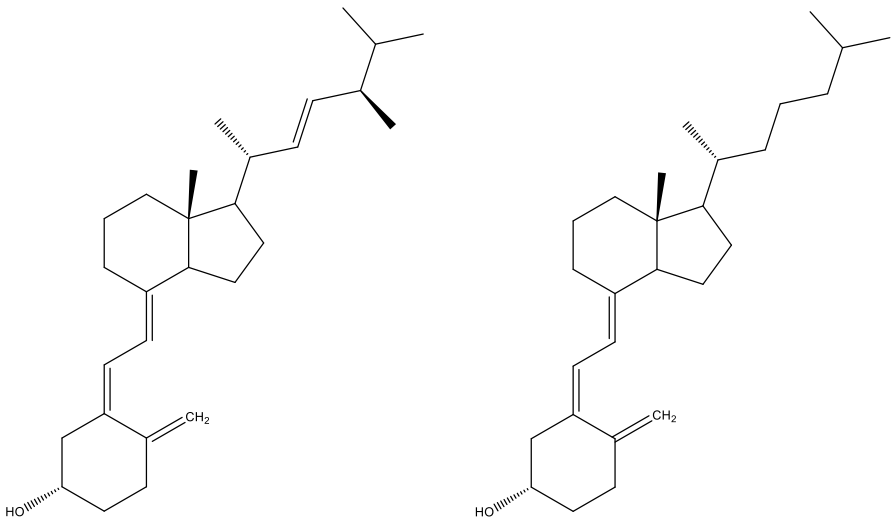

Vitamin D_2 (ergocholecalciferol)

Vitamin D_3 (cholecalciferol)

Figure 1-9 ***Chemical structures of Vitamin D_2 and Vitamin D_3.*** *Vitamin D_2 (ergocholecalciferol) and Vitamin D_3 (cholecalciferol).*

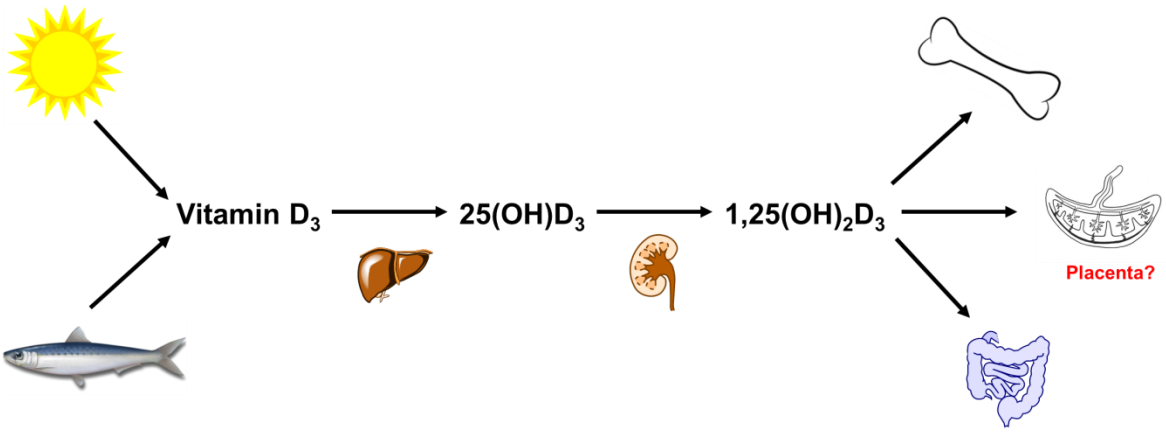

Figure 1-10 ***Pathway of vitamin D metabolites in the human body.*** *Vitamin D_3, obtained either through the diet or synthesised in the skin via a UVB catalysed reaction is converted to 25-hydroxyvitamin D_3 (25(OH)D_3) in the liver. It is further metabolised in the kidney to active 1,25-dihydroxyvitamin D_3 (1,25(OH)$_2D_3$), which acts on target organs, possibly including the placenta.*

1.6.1 Vitamin D metabolism

The metabolism of Vitamin D is displayed in Figure 1-11. 7-dehydrocholesterol, the precursor of vitamin D, is present in the epidermis of the skin. Upon exposure to sunlight, UVB radiation of wavelengths 290-315 nm penetrate the skin and are absorbed by 7-dehydrocholesterol. The UVB radiation acts on double bonds present in 7-dehydrocholesterol's B-ring, causing it to open and producing pre-vitamin D_3. Pre-vitamin D_3 then interacts with membrane phospholipids, stabilising it in its cZc conformer, which over a period of hours isomerises into vitamin D_3. With prolonged UVB exposure vitamin D_3 will isomerize into two further compounds, lumisterol and tachysterol, or back into 7-dehydrocholesterol. This prevents hypervitaminosis D from occurring through the over-production of vitamin D_3 (Tian and Holick, 1999, Wacker and Holick, 2013, Tuckey et al., 2018). Vitamin D_3 is then released from the plasma membrane into the extracellular space, where it diffuses into circulation. Vitamin D is hydrophobic, and in circulation approximately 90% is bound to vitamin D binding protein (DBP), approximately 10% to albumin or lipoprotein and only < 1% is free and unbound (Zerwekh, 2008, Wacker and Holick, 2013).

Vitamin D is next hydroxylated at carbon 25 by enzymes of the cytochrome P450 (CYP) family, primarily in the liver, into 25-hydroxyvitamin D (25(OH)D or calcifediol). This is the major circulating form of vitamin D in the blood. The enzyme CYP2R1 is the physiological 25-hydroxylase in humans, with the enzymes CYP27A1, CYP2J2, CYP3A4, and CYP2C11 also expressing some vitamin D 25-hydroxylase activity (Zhu and DeLuca, 2012, Jones et al., 2014, Tuckey et al., 2018).

25-hydroxyvitamin D then undergoes a further enzymatic reaction primarily in the renal proximal tubules of the kidney. Within the kidney the enzyme 25-hydroxyvitamin D 1α-

hydroxylase (CYP27B1), another cytochrome P450 enzyme, hydroxylates carbon 1 in the A ring, forming 1,25-dihydroxyvitamin D (1,25$(OH)_2$D or calcitriol). 1,25$(OH)_2$D is the main active form of vitamin D in the body. CYP27B1 has also been identified in a number of extra-renal sites, including in the placenta, bone and macrophages (Jones et al., 2014, Shin et al., 2010, Tuckey et al., 2018).

In both 25(OH)D and 1,25$(OH)_2$D inactivation occurs via the hydroxylation of C24 by the cytochrome P450 enzyme 25-hydroxylase (CYP24A1), producing 24,25$(OH)_2$D and 1,24,25$(OH)_3$D respectively. These products are then both further oxidised by CYP24A1 at C23 or C24, entering a C23 or C24 oxidation pathway of metabolism. In the C24 oxidation pathway a total of four oxidation steps lead to the production of calcitroic acid. While the synthesis of 25$(OH)D_3$ is not tightly regulated, the synthesis and degradation of 1,25$(OH)_2D_3$ is highly regulated, and subject to feedback control. The expression of both 25-hydroxyvitamin D 1α-hydroxylase and 25-hydroxylase within target tissues suggests local control of 1,25$(OH)_2$D activity (Jones et al., 1998, Tuckey et al., 2018, Jones et al., 2014).

25$(OH)D_{2/3}$ can also be acted on by the enzyme 25-hydroxyvitamin $D_{2/3}$-3-epimerase. This exchanges the 3α-hydroxyl group present in 25$(OH)D_{2/3}$ for a 3β-hydroxyl group. This epimerisation also occurs to 1,25$(OH)_2$D. The 3-epimers display reduced activity but greater stability (Tuckey et al., 2018).

Within the human placenta, increased expression of the CYP24A1 gene in response to vitamin D treatment suggests that vitamin D undergoes local metabolism within the tissue (Novakovic et al., 2009). However what vitamin D metabolites are produced, and whether the metabolites are utilised by the placenta, passed back to the mother or passed to the fetus is not known.

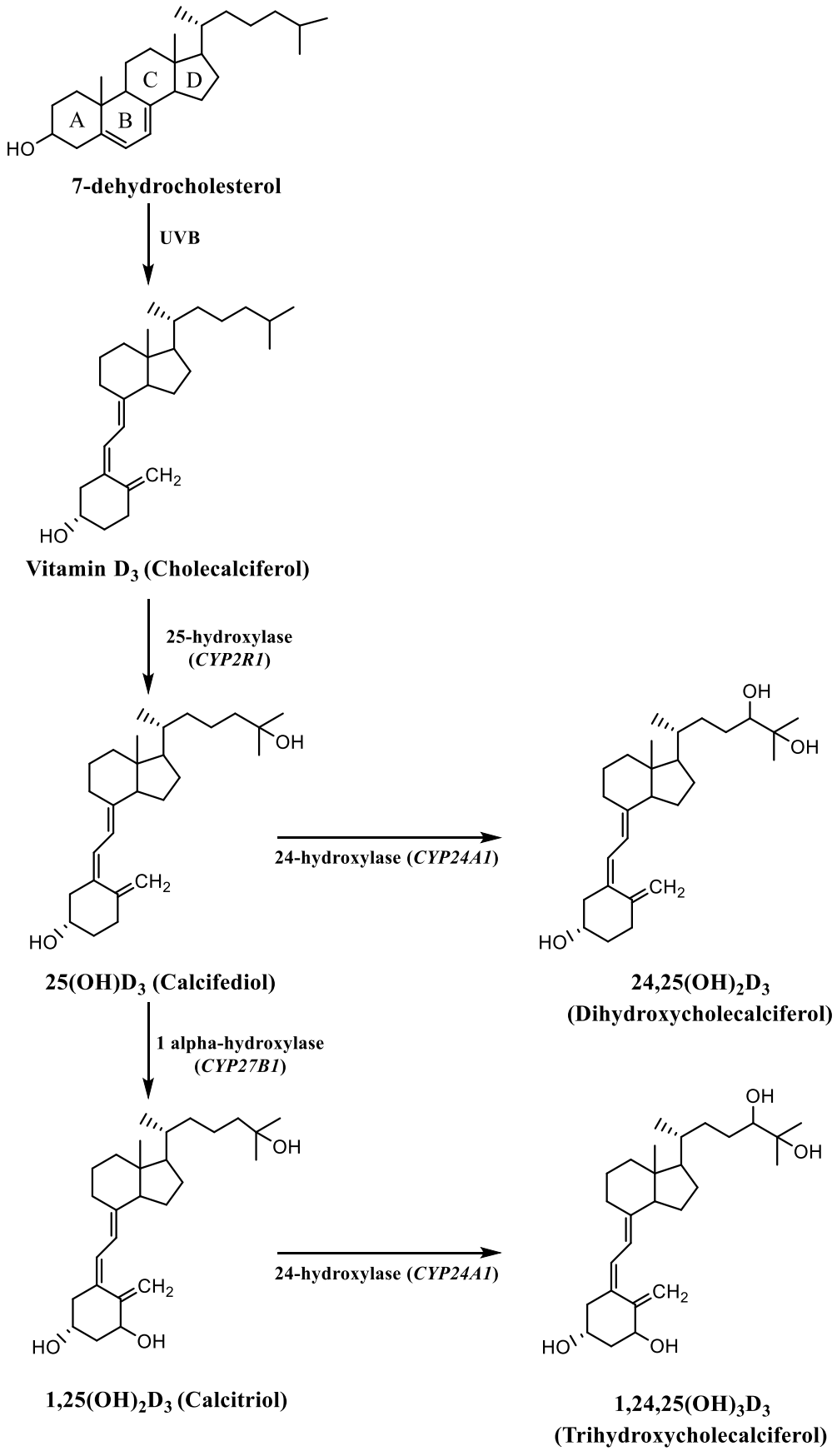

Figure 1-11 ***Vitamin D metabolic pathway.*** *The primary metabolic pathway of synthesis and degradation of 25-hydroxyvitamin D ($25(OH)D_3$) and 1,25-dihydroxyvitamin D ($1,25(OH)_2D_3$) within humans.*

1.6.2 Vitamin D functions

Vitamin D metabolites have multiple functions within the body, most notably in the maintenance of calcium homeostasis. Plasma calcium levels are tightly maintained within the human body, as physiological calcium levels are necessary for processes such as signalling in the nervous system and muscle contraction (Jones et al., 1998). Vitamin D carries out these functions by altering gene expression in target tissues (Molnar, 2014).

The parathyroid glands sense plasma calcium concentration, and in response to a decrease in calcium release parathyroid hormone (PTH) into the bloodstream (Carmeliet et al., 2015). PTH stimulates increased expression of *CYP27B1* in the renal proximal tubules of the kidney, which in turn results in increased metabolism of 25(OH)D to active $1,25(OH)_2D$ (Anderson et al., 2012). Calcium uptake in the intestine occurs through two mechanisms, paracellular and transcellular. Paracellular uptake occurs when dietary calcium levels are high, such as in breastfed infants, whereas transcellular uptake occurs when dietary levels are normal or low, through active uptake into the intestinal brush border enterocyte. $1,25(OH)_2D$ acts on the intestine to increase the expression of calcium uptake proteins, thus increasing intestinal calcium absorption and plasma calcium levels (Carmeliet et al., 2015). $1,25(OH)_2D$ also acts on bone osteoblast cells, increasing bone resorption leading to the transfer of calcium from the bone into the blood. Increased plasma calcium levels are sensed by the parathyroid glands, which then stop PTH production and prevent hypercalcaemia from occurring (Anderson et al., 2012).

Vitamin D metabolites have also been shown to play a role in modulating the immune system. A number of cells express *CYP27B1*, meaning they are able to locally synthesise $1,25(OH)_2D$. In the innate immune system monocytes exposed to a pathogen increase expression of *CYP27B1*, generating local $1,25(OH)_2D$. The $1,25(OH)_2D$ then acts back on the monocyte, increasing expression of antimicrobial peptides. Antigen presenting cells of the innate immune system play a role in stimulating the adaptive immune system, as they can present antigens to both T and B-cells, modulating them towards either an immunogenic or tolerogenic state. $1,25(OH)_2D$ acts on antigen presenting cells altering them towards promoting a tolerogenic state. In the adaptive immune system $1,25(OH)_2D$ acts on T-helper cells, suppressing their expression and modulating their cytokine production towards a tolerogenic state. The promotion of a tolerogenic environment in the presence of $1,25(OH)_2D$ is thought to play a role in preventing the inappropriate overresponse of the immune system seen in autoimmune diseases (Prietl et al., 2013).

A further function of vitamin D is in regulation of cell cycle progress and apoptosis. In a number of cell types $1,25(OH)_2D$ has been demonstrated to cause cell cycle arrest at the G1 to S

transition. It is thought to inhibit the activity of cyclins and cyclin dependent kinases necessary for cell cycle progression. 1,25$(OH)_2$D has also been observed to induce apoptosis in cells. Vitamin D can affect the expression levels of the pro-apoptotic proteins bak and bax, and the anti-apoptotic proteins bcl-2 and bcl-XL. Alteration to the expression levels of these proteins in the presence of vitamin D favours apoptosis (Samuel and Sitrin, 2008).

Vitamin D and pregnancy

During pregnancy, plasma levels of 1,25$(OH)_2$D become up to two and a half times higher than in that of a non-pregnant woman, strongly indicating an important role for vitamin D in pregnancy. CYP27B1 expression is upregulated in the kidneys during pregnancy, contributing to greater metabolism of 25(OH)D and resulting in the rise in 1,25$(OH)_2$D levels. DBP levels rise to up to double the pre-pregnancy level, altering free 25(OH)D availability (Besta et al., 2019).The effect of 1,25$(OH)_2$D on the immune system may help prevent rejection of the embryo during implantation by the mother, by promoting a tolerant environment. High 1,25$(OH)_2$D levels also result in increased intestinal calcium intake, with uptake two-fold higher than in the non-pregnant state. This provides the mother with the extra calcium needed to transfer sufficient amounts to the fetus throughout gestation (Karras et al., 2017, Christakos et al., 2013).

The placenta itself expresses the vitamin D receptor (VDR), CYP27B1 and CYP24A1 genes. CYP24A1, the gene responsible for the production of vitamin D 24-hydroxylase and hence for degradation of 1,25$(OH)_2$D is methylated within the placenta, inhibiting its expression and allowing for synthesis of 1,25$(OH)_2$D to exceed degradation (Novakovic et al., 2009). Within the human placenta, increased expression of the CYP24A1 gene in response to vitamin D treatment suggests that vitamin D undergoes local metabolism within the tissue.

1.6.3 Placental uptake and transfer

As a fetus is not exposed to ultraviolet light it is therefore unable to synthesise vitamin D. Vitamin D must instead be transferred from the mother to the fetus during pregnancy. However how vitamin D is transferred across the placenta is not well understood. Unpublished data from our laboratory suggests that this occurs through an active, likely endocytic mechanism. These mechanisms include clathrin-mediated endocytosis, clathrin-independent endocytosis and pinocytosis.

Clathrin-mediated endocytosis occurs when a vesicle containing cargo molecules is taken up into a cell coated in clathrin proteins. Clathrin-coated vesicles contain membrane receptors that are bound to specific ligands, allowing for the concentration and uptake of specific molecules. In the human placenta the endocytic receptor megalin is found in clathrin-coated pits,

the area where a clathrin-coated vesicle will form from (Burke et al., 2013). Clathrin-coated vesicles are formed when clathrin is nucleated at the membrane by accessory proteins. Clathrin molecules are then able to polymerise into a curved lattice that surrounds a section of membrane, forming the vesicle shape. This forms a “neck”, where the membranes are pulled closely together. Another membrane protein dynamin, which is a large GTPase, then wraps around the neck and upon GTP hydrolysis separates the vesicle from its membrane releasing it inside the cell. The clathrin coat is then released from the vesicle and recycled back to the membrane (Doherty and McMahon, 2009).

Like in clathrin-mediated endocytosis, in clathrin-independent endocytosis target compounds are also specifically bound and concentrated for uptake via membrane receptors. However there are a large number of different pathways of clathrin-independent endocytosis, with most cells displaying multiple pathways. These include RhoA-dependent, Cdc42-dependent, flotillin-dependent and Arf6-associated (Sandvig et al., 2011).

Unlike in clathrin-mediated endocytosis and clathrin-independent endocytosis, when macropinocytosis occurs compounds are taken up indiscriminately, without specifying or concentrating a specific substrate. In macropinocytosis membrane ruffles or protrusions extend from the membrane before fusing back to themselves, creating a vesicle. This is a largely dynamin independent pathway thought to be dependent on a number of proteins including Rac, Pak1, Cdc42, CtBP1/BARS and ARF6 (Sandvig et al., 2011).

The presence of megalin in the placenta is interesting as in the renal proximal tubule megalin, in association with another membrane protein cubilin, is responsible for the uptake of vitamin D binding protein. Megalin mediated uptake allows 25(OH)D to be taken up and converted to 1,25$(OH)_2$D in the kidney (Nykjaer et al., 2001). Within the placenta vitamin D needs to cross the MVM, pass through the syncytiotrophoblast, cross the BM and then pass through the fetal capillary endothelium to reach the fetus. Given the presence of megalin on the MVM it is possible that megalin plays a role in the uptake of vitamin D into the syncytiotrophoblast, but experimental evidence is needed to demonstrate this.

1.6.4 Mechanisms of vitamin D action

1,25$(OH)_2$D is the main active form of vitamin D within the body. 1,25$(OH)_2$D primarily acts by altering gene expression in a targeted manner, but is also reported to act via non-genomic pathways. Gene expression describes the process that takes place to produce RNA, and is regulated within cells to control the amount of product that is produced. Gene expression can be up or down regulated to suits the needs of the cell.

$1,25(OH)_2D$ exerts its effects in cells by altering gene expression at the transcriptional level. $1,25(OH)_2D$ binds to the VDR, a nuclear receptor protein located in the nucleus of target cells. The VDR, consisting of 427 amino acids, contains a DNA binding domain (domain C), a ligand binding domain (domain E), a connective hinge (domain D), and a short A/B domain on the N-terminus. The connective hinge links the DNA binding and ligand binding domains. The ligand binding domain contains a pocket in which $1,25(OH)_2D$ binds. This pocket contains about 40 non-polar amino acids as well as a number that are responsible for interacting with and binding to $1,25(OH)_2D$ (Rochel et al., 2000, Orlov et al., 2012, Molnar, 2014).

The DNA binding domain contains two zinc-finger motifs. Each zinc finger contains one zinc atom bonded with four cysteine residues, and this assists in the recognition and binding of vitamin D receptor elements (VDRE), found in the promoters of vitamin D responsive genes (Molnar, 2014). VDREs contain two half sites separated by a stretch of usually three neutral base pairs, called the DR3 element. The half sites have a consensus sequence of 5'-RGKTCA-3', where R is A or G, and K is G or T. The ligand binding domain of the VDR contains 12 α-helices (H1 – H12) and three β-sheets. Binding of $1,25(OH)_2D$ to the VDR causes a conformational change in H12 of the ligand binding domain allowing a region called activation function 2 (AF-2) to interact with other activating proteins. This allows it to form a heterodimer with a cofactor called the retinoid X receptor alpha (RXRα), and also to bind other co-activator proteins. Cofactors also bind to H3 and H5, stabilising the VDR-RXRα heterodimer (Haussler et al., 2013, Christakos et al., 2016).

As seen in Figure 1-12 the VDR-RXRα heterodimer then recognises and binds the VDRE, with the RXRα DNA binding domain binding the upstream half-site, and the VDR DNA binding domain binding the downstream half-site (Orlov et al., 2012). On positive VDREs, binding of the VDR-RXRα heterodimer induces transcription, whereas on negative VDREs (nVDRE), binding of VDR-RXRα represses transcription (Kim et al., 2007, Wan et al., 2015). Binding of the $1,25(OH)_2D$ activated VDR-RXRα heterodimer to positive VDREs results in conformational changes to the VDR-RXRα. This allows transcriptional activator proteins to bind forming a pre-initiation complex that recruits RNA polymerase to the promoter of the gene, initiating transcription (Haussler et al., 2013, Christakos et al., 2016).

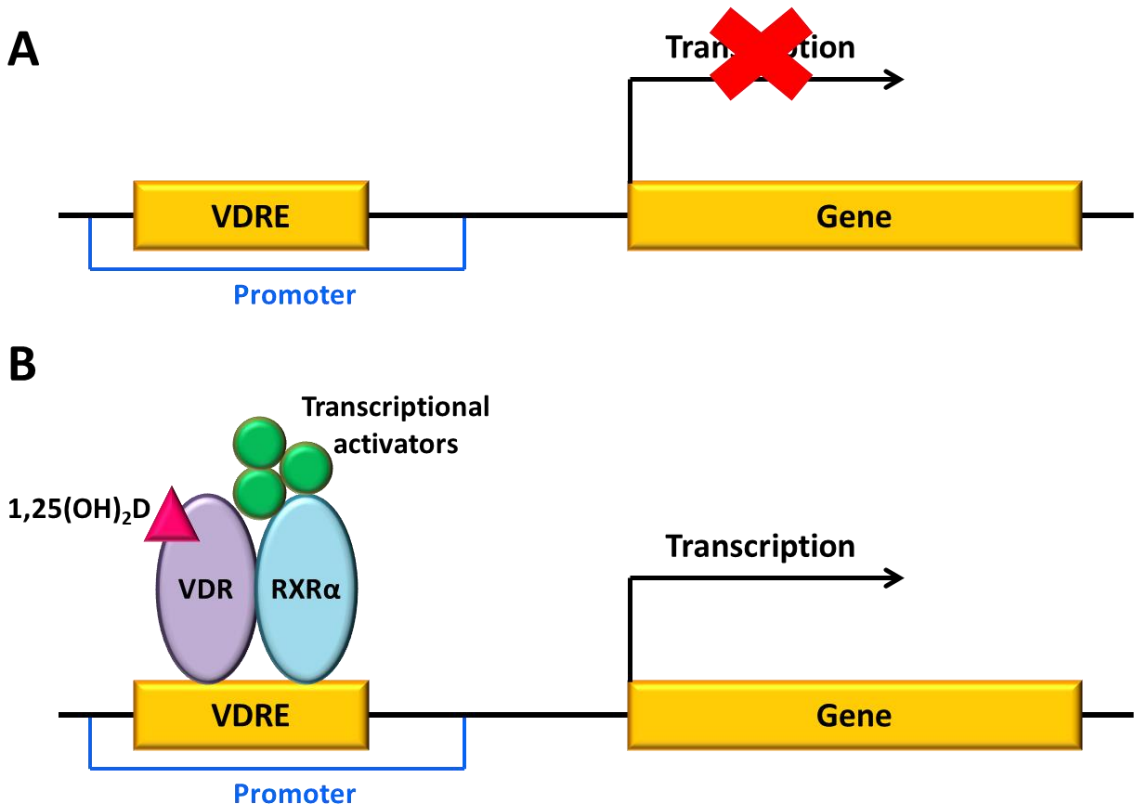

Figure 1-12 ***1,25(OH)$_2$D mediated mRNA transcription.*** *1,25(OH)$_2$D can activate gene transcription via its actions on the VDRE through the VDR-RXRα complex.* ***A)*** *In the absence of 1,25(OH)$_2$D genes controlled via VDRE are not transcribed.* ***B)*** *1,25(OH)$_2$D activated VDR-RXRα binds to the VDRE. This causes a conformational change that allows transcriptional activator proteins to bind and induces transcription of the downstream gene.*

Repression of transcription may occur in two ways, as shown in Figure 1-13. Binding of 1,25(OH)$_2$D activated VDR-RXRα heterodimer to nVDREs may induce a conformational change in the VDR-RXRα complex that allows transcriptional repressor proteins to bind, repressing transcription of the gene (Haussler et al., 2013). Alternatively nVDREs may be bound by a vitamin D interacting repressor (VDIR) protein. VDIR allows transcription of the gene to occur, but when bound by 1,25(OH)$_2$D activated VDR-RXRα any co-activating proteins are released and transcription is repressed (Lundqvist et al., 2012, Wan et al., 2015).

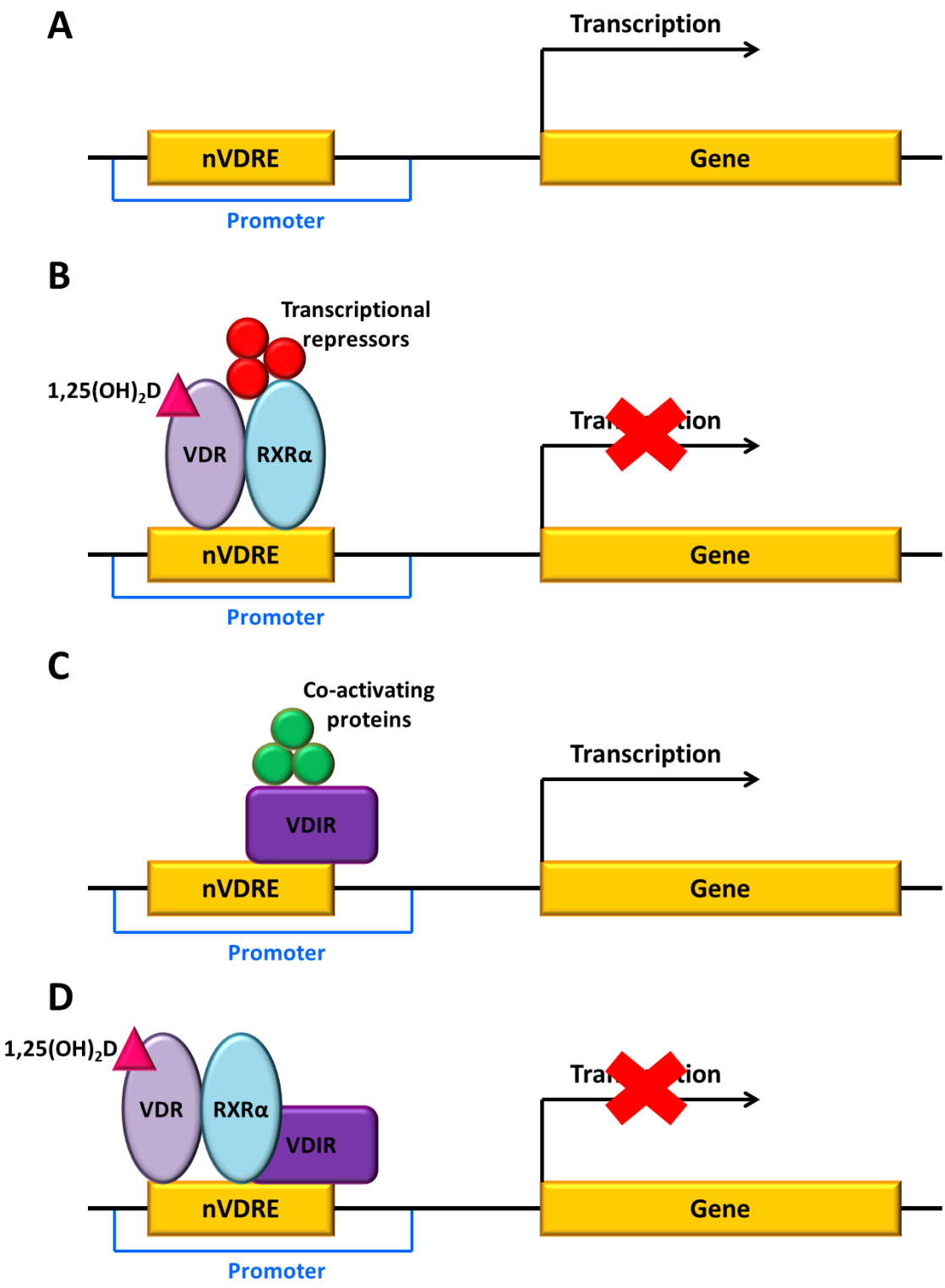

Figure 1-13 ***1,25(OH)$_2$D mediated repression of mRNA transcription.*** *1,25(OH)$_2$D can repress gene transcription via its actions on the VDRE through the VDR-RXRα complex.* ***A)*** *In the absence of 1,25(OH)$_2$D genes controlled via negative VDREs (nVDRE) are transcribed.* ***B)*** *1,25(OH)$_2$D activated VDR-RXRα binds to the nVDRE. This causes a conformational change that allows transcriptional repressor proteins to bind and repress transcription of the downstream gene.* ***C)*** *Alternatively the nVDRE may be bound by a vitamin D interacting repressor (VDIR) and co-activating proteins, inducing transcription of the downstream gene.* ***D)*** *1,25(OH)$_2$D activated VDR-RXRα binds VDIR occupied nVDREs, releasing the co-activating proteins and repressing transcription of the downstream gene.*

$1,25(OH)_2D$ also acts upon membrane localised VDR within cells such as neurons and skeletal muscle cells to exert non-genomic actions (Dursun and Gezen-Ak, 2017, Capiati et al., 2002). Binding of $1,25(OH)_2D$ to membrane bound VDR activates signalling molecules such as phospholipase C, which in turn results in the generation of second messengers or activated proteins to generate a response (Hii and Ferrante, 2016). In isolated cardiac myocytes, treatment with $1,25(OH)_2D_3$ results in altered sarcomere shortening and re-lengthening within minutes of $1,25(OH)_2D_3$ treatment, demonstrating that $1,25(OH)_2D_3$ can cause rapid non-genomic responses within a cell (Zhao and Simpson, 2010).

Whilst $1,25(OH)_2D$ is the most biologically active vitamin D metabolite, activity of other metabolites has also been reported. 25(OH)D has been observed to alter transcription via the action of VDR in a number of cell types, including mouse kidney, skin, prostate cells, and human MCF-7 breast cancer cells (Lou et al., 2010). 1,25-dihydroxy-3-epi-vitamin D_3 has been observed to alter transcription again via the VDR in a similar manner to $1,25(OH)_2D$ in human keratinocytes (Molnar et al., 2011).

Within the placenta the effects of vitamin D action are not well understood. The placenta expresses genes which have a VDRE in their promoter, although the number of genes which contain a VDRE is not known (Wang et al., 2018a). Vitamin D may also act to influence the expression of proteins such as transcription factors, which may have a downstream effect on the expression of other, non-VDRE controlled genes. Vitamin D may act to alter the transcription of genes such as DNA methyltransferases and histone modifiers, which may result in downstream epigenetic changes to placental gene expression, however further study is needed to understand this.

1.7 Epigenetic mechanisms

Epigenetics refers to the factors that alter gene expression without changing the DNA sequence itself. Epigenetic regulation of gene expression within the placenta is vital for normal fetal development, and vitamin D may play a role in regulating this.

1.7.1 DNA methylation

DNA methylation is one of the most studied epigenetic modifications. Methylation usually occurs on cytosine residues that precede a guanidine residue, termed CpG sites or CpG dinucleotides. CpG sites are found dispersed throughout the genome, and at a higher frequency in small approximately 1000 base pairs (bp) stretches of DNA called CpG islands. The majority of CpG sites throughout the genome are methylated, and are therefore termed hypermethylated, with the exception of CpG islands, which can have reduced methylation termed hypomethylated. Approximately 70% of gene promoters are located within CpG islands, which due to their high CpG site content are very susceptible to epigenetic regulation (Moore et al., 2013, Maccani and Marsit, 2009).

Methyl groups are added to DNA by members of the DNA methyltransferases (DNMT) family, Dnmt1, Dnmt3a and Dnmt3b. As shown in Figure 1-14, Dnmt1 is known as the maintenance methyltransferases as it methylates hemimethylated DNA produced during semi-conservative DNA replication. This conserves patterns of DNA methylation by copying the methylation found on the parent strand onto the daughter strand. Dnmt3a and Dnmt3b however are *de novo* methyltransferases as they introduce new patterns of methylation onto the DNA. Dnmt3L, another DNA methyltransferase, does not methylate DNA itself but binds to Dnmt3a and Dnmt3b, stimulating their methyltransferase activity. Transcription factors may bind Dnmt3a or Dnmt3b to target it to DNA, introducing new DNA methylation at a specific site. Dnmt1, Dnmt3a and Dnmt3b act to catalyse the transfer of a methyl group from the molecule S-adenyl methionine to the 5^{th} carbon of a cytosine reside, producing 5-methylcytosine (5mC) (Moore et al., 2013).

Patterns of DNA methylation sometimes need to be altered, for example genome wide demethylation occurs in the pre-implantation embryo before re-establishment of new patterns of DNA methylation. DNA undergoes demethylation via the action of TET enzymes. TET catalyses the oxidation of 5mC to 5-hydroxymethylcytosine (5hmC), which is then deaminated to thymine, before DNA repair enzymes replace the base with an unmethylated cytosine (Schuermann et al., 2016).

DNA methylation acts to reduce gene expression by inhibiting transcription factor binding by instead binding other proteins. Proteins with a high affinity for 5mC include those belonging to the families methyl-CpG binding domain (MBD) proteins, zinc finger proteins and ubiquitin-like, containing PHD and RING finger domain (UHRF) proteins. MBD family proteins contain a transcriptional repression domain. They are therefore able to bind methylated DNA and then recruit transcriptional repression complexes to inhibit gene expression. Zinc finger family proteins act in a similar fashion, to recruit transcriptional repression complexes to the methylated DNA and inhibit gene expression. UHRF family proteins however act to recruit Dnmt1 to hemimethylated DNA, maintaining DNA methylation and inhibition of gene expression (Moore et al., 2013).

Alterations to cytosine methylation in CpG islands therefore is able to switch on or off gene expression, by either inhibiting or allowing transcriptional machinery to bind to the promoter of the genes.

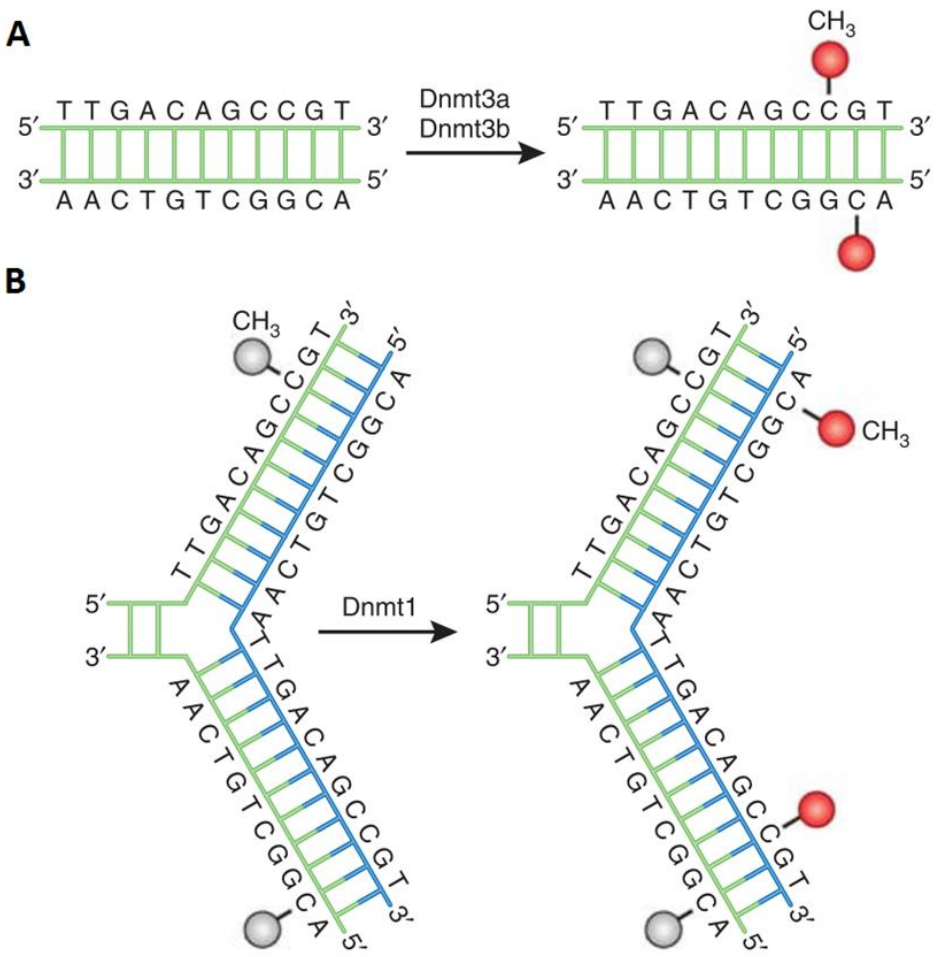

Figure 1-14 ***DNA methylation pathways.*** *DNA methyltransferases (DNMT) catalyse the addition of a methyl group (red) to DNA. A) Dnmt3a and Dnmt3b catalyse the addition of methyl groups onto naked DNA. B) Dnmt1 catalyses the addition of methyl groups onto daughter strands (blue) after DNA replication. Adapted from DNA methylation and its basic function (Moore et al., 2013).*

1.7.2 Histone modifications

Histone modifications are also an important mode of epigenetic regulation. Histone proteins form the core of nucleosomes. Two each of the four histone proteins, H2A, H2B, H3 and H4, interact to form an octomer around which 147 bp of DNA wrap, compacting the DNA. Around 25% of the mass of each histone protein is found in an unstructured N-terminal (and C-terminal in histones H2A and H2B) tail. The N-terminal tails of the histone proteins are not tightly packed into the nucleosome core and so are susceptible to post translational modifications (Cutter and Hayes, 2015).

The histone tails undergo methylation, acetylation, phosphorylation and ubiquitinylation at specific nucleotides, as shown in Figure 1-15. Enzymes responsible for the addition of these epigenetic modifications include histone methyltransferases (HMTs), histone acetyltransferases (HATs), kinases and ubiquitylases. Enzymes responsible for the removal of these epigenetic modifications include histone demethylases, histone deacetylases, phosphatases and deubiquitylases. Histone modifications can interact with chromatin, modifying whether the DNA is accessible to transcription factors or not. Active histone modifications act to create an open chromatin structure by inhibiting proteins that act to condense the DNA, thus allowing access of transcription factors to the DNA. Active histone marks include acetylation of H3 and H4, tri-methylation of H3 lysine 4 (H3K4me3) and tri-methylation of H3 lysine 36 (H3K36me3). Repressive histone modifications act to condense chromatin by allowing for interaction with the DNA and/or proteins that act to condense the chromatin, inhibiting the access of transcription factors. Repressive histone marks include methylation of H3 lysine 27 (H3K27me2/3) and methylation of H3 lysine 9 (H3K9me2/3). Histone modifications provide shorter term alterations to gene expression than DNA methylation (Nelissen et al., 2011, Zhang et al., 2015b).

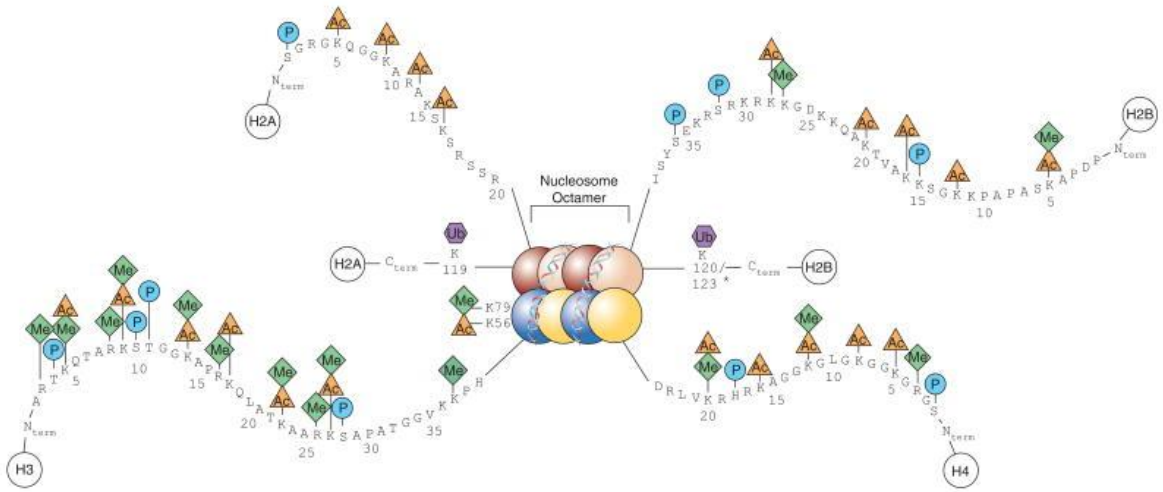

Figure 1-15 ***Histone modifications.*** *Nucleosomes consist of two each of the four core histones, H2A, H2B, H3 and H4. N and C-terminal tails protrude from the core of the nucleosome, and are subject to methylation (Me), acetylation (Ac), phosphorylation (P) and ubiquitination (Ub). Adapted from Chromatin-modifying enzymes as therapeutic targets (Keppler and Archer, 2008).*

1.7.3 microRNA

A third type of epigenetic regulation includes microRNAs (miRNA), which are small non-coding RNA molecules of approximately 22 nucleotides in length. miRNA processing is displayed in Figure 1-16. Primary miRNAs are transcribed by RNA polymerase II and have a 5' cap and a 3' poly-A tail. They form a hairpin structure, which then undergoes digestion by the enzyme Drosha. Drosha acts to remove to 5' cap and 3' poly-A tail, leaving a two nucleotide 3' overhang. This is now called a precursor miRNA (pre-miRNA). The pre-miRNA is exported from the nucleus via the protein Exportin-5, where it undergoes a further cleavage by the enzyme Dicer, leaving a double stranded RNA with short 3' overhangs on each strand. One strand of this complex is the mature miRNA and associates with the RNA-induced silencing complex (RISC) (Maccani and Marsit, 2009, McCreight et al., 2017).

miRNAs bind target RNAs with sequence complementarity, recruiting RISC to the target RNA. Target RNAs can be protein coding mRNA or other non-coding RNAs. RISC contains a protein called Argonaute, which can catalyse cleavage of mRNAs, resulting in their degradation. This often occurs when sequence complementarity between the target RNA and the miRNA is perfect. When sequence complementarity is not perfect, miRNAs still inhibit translation of the target RNA through blocking of translational machinery binding to the RNA. miRNAs can therefore act to either reduce or silence the protein expression resulting from a specific gene (Maccani and Marsit, 2009, Mohr and Mott, 2015).

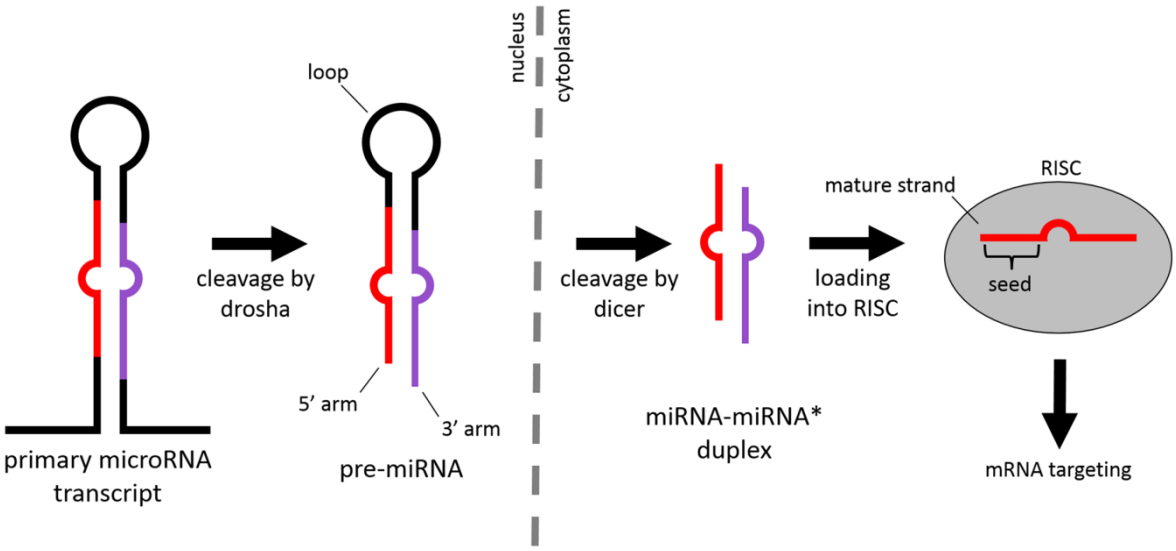

Figure 1-16 ***microRNA processing.*** *Primary microRNA transcripts are cleaved by Drosha, transported to the cytoplasm, cleaved again by Dicer and then interact with RISC to target mRNA. Adapted from Evolution of microRNA in primates (McCreight et al., 2017).*

1.7.4 Imprinting

Imprinting describes the process in which either the maternal or paternal allele of a gene is silenced through epigenetic modifications. Imprinted genes tend to occur in clusters throughout the genome, with each cluster controlled by an imprinting control region (ICR). Most ICRs have a number of sites of potential DNA methylation. DNA methylation in the ICR inhibits transcription of the downstream genes, silencing the imprinted genes. Imprinted genes also experience histone modifications to inhibit their transcription, and miRNAs target mRNA from these genes to further silence them. ICRs demonstrate that imprinting is usually controlled at the chromosomal rather than single gene level (Nelissen et al., 2011).

Genome wide demethylation and subsequent remethylation takes place shortly after fertilisation, but imprinted genes do not lose their methylation during this period as it is important for normal development of the embryo. The ‘parent-conflict’ or ‘battle of the sexes’ theory may partially describe why imprinting occurs. There is conflict between maternal and paternal genes to allocate the mother’s resources to the fetus. Paternal genes want to maximise nutrients and other resources transferred to the fetus to increase the chance of survival of the paternal genes, however maternal genes want to limit transfer of resources to any one fetus, to leave the mother better equipped to bear further children (Maccani and Marsit, 2009, Nelissen et al., 2011). Silencing of specific maternal or paternal alleles allows a balance between these.

Imprinted genes are expressed in the placenta, and are important for normal development. *Insulin-like Growth Factor-II* (*IGF2*) is a paternally expressed gene, and is involved in nutrient transport and fetoplacental growth. However the *Type-II Insulin-like Growth Factor Receptor*

(*IGF2R*) is a maternally expressed gene, and negatively regulates the effects of *IGF2*. Maternal expression of *IGF2R* may therefore be necessary to prevent fetal over nutrition resulting from unchecked *IGF2* action. Imprinted genes within the placenta play an important role in determining resource allocation, so the current baby receives the resources it needs whilst leaving the mother healthy enough to bear future children (Cleal and Lewis, 2016).

1.7.5 Placental epigenetics

The regulation of gene expression by epigenetic factors, such as DNA methylation and miRNA expression is important for placental development and function, however it may be altered by many maternal and environmental factors (Novakovic and Saffery, 2012). Placental epigenetic mechanisms are important determinants of the placental phenotype, which in turn affects placental function and fetal development.

After genome wide demethylation takes place in the pre-implantation embryo, methylation patterns are re-established, but cells of the trophoblast remain hypomethylated in comparison to those of the inner cell mass. Trophoblast cells are responsible for implantation and develop into placental tissue. The invasive behaviour of these trophoblast cells is required for successful implantation and is regulated by epigenetic mechanisms, such as DNA methylation. DNA methylation represses the expression of plakoglobin and E-cadherin, which allows the cells to display an invasive phenotype. Dnmt3a and Dnmt3b are responsible for this DNA methylation (Rahnama et al., 2006). This early period of re-methylation may be important for establishing appropriate placental epigenetic patterns, and thus during this time period environmental factors may have the potential to significantly alter the placental epigenome (Cleal and Lewis, 2016). The placenta is hypomethylated compared to healthy somatic tissues, with a 5mC content of 2.5-3% compared to 4-5% (Novakovic and Saffery, 2012). Most of this hypomethylation is found in repetitive DNA elements such as long interspersed elements (*LINE1*) (Perrin et al., 2007).

Epigenetic mechanisms influence the phenotype and behaviour of cells meaning different cell types may have differing patterns of epigenetic modifications. Investigations into DNA methylation differences between cytotrophoblast cells, fibroblast cells and whole placental tissue villous samples from 14-19 weeks gestation normal placentas suggest a similar global methylation pattern between the cells types, with specific genes displaying different methylation. Overall placental DNA methylation levels increase with increasing gestation, and therefore gestational age must be considered when evaluating placental methylation data. The most differentially methylated genes with increasing gestation included immune regulators, reflecting the changing placental adaptations to pregnancy (Chavan-Gautam et al., 2011, Novakovic et al., 2011).

Maternal factors, including lifestyle and health conditions can alter the placental epigenome (Reynolds et al., 2013). Studies have shown conflicting results on the effect of gestational diabetes mellitus (GDM) on global placental DNA methylation levels. A small study with 50 participants, eight of whom had GDM, showed reduced global placental methylation levels in those with GDM compared to non-diabetic controls (Nomura et al., 2014). However another study including 1030 participants, of whom 56 women developed GDM, showed significantly higher global placental methylation of those with GDM compared to controls (Reichetzeder et al., 2016). The differences seen here may be explained by the small sample size in the first study and differing participant demographics. The first study also showed significantly higher global placental methylation in obese mothers (n = 18) compared to non-obese controls (Nomura et al., 2014).

GDM has also been associated with gene specific differential methylation within the placental DNA. The imprinted gene *MEST* and the non-imprinted glucocorticoid receptor gene *NR3C1* both show significantly decreased DNA methylation levels in GDM compared to control placentas (El Hajj et al., 2013). Pathway analysis has observed altered DNA methylation in genes involved cardiovascular disease and metabolic disease pathways (Ruchat et al., 2013). GDM may therefore be acting to alter placental function by altering DNA methylation.

Preeclampsia has been associated with alterations to the methylation status of a number of genes within the placenta, including *SERPINB5, SERPINA3, MMP9* and *cullin-7*. Studies have also identified differential expression of miRNAs in preeclampic placentas, in particular miR-210, which is being investigated as a potential biomarker for the disease. Epigenetic mediated changes in gene expression may therefore be playing a role in the pathogenesis of preeclampsia (Deshpande and Balasinor, 2018).

Maternal alcohol consumption during pregnancy has been associated with increased placental DNA methylation of *LINE1* elements (Wilhelm-Benartzi et al., 2012). Maternal tobacco cigarette smoking was also associated with altered DNA methylation at *LINE1* elements, as well as alterations to specific genes. Smoking reduces the methylation of the gene *CYP1A1*, resulting in an increase in the genes expression (Wilhelm-Benartzi et al., 2012, Suter et al., 2010). *CYP1A1* plays a role in detoxification of harmful compounds in tobacco, and therefore reduced methylation in the promoter of *CYP1A1* may be an adaptation of the placenta to deal with increased exposure of maternal toxins.

miRNAs also have a role in the epigenetic regulation of placental gene expression. Maternal tobacco cigarette smoking has been associated with reduced expression of the developmentally important miRNAs *miR-16, miR-21* and *miR-146a* in placental tissue (Maccani et al., 2010). Altered expression of miRNAs has also been observed in placentas from GDM (Zhao et al., 2014), and

preeclamptic pregnancies (Zhu et al., 2009, Zhang et al., 2015a, Li et al., 2014). Trophoblast invasion is also regulated by miRNAs, with the chromosome 19 miRNA cluster targeting mRNAs of proteins involved in cellular movement (Xie et al., 2014).

Placental epigenetics have been associated with abnormal fetal outcomes. Distinct patterns of altered DNA methylation are observed in the placentas of FGR and SGA babies (Banister et al., 2011), and placentas from low birth weight babies show increased DNA methylation in the promoter of the gene *WNT2* (Ferreira et al., 2011). LGA babies show differential methylation of the glucocorticoid receptor gene promoter (Filiberto et al., 2011), and increased methylation of *LINE1* elements is also associated with increased birth weight (Wilhelm-Benartzi et al., 2012). Maternal 25(OH)D_3 levels have also been associated with offspring birth weight (Harvey et al., 2014a), and it is possible that vitamin D induced alterations to the placental epigenome underlie the altered offspring outcomes.

1.7.6 Vitamin D and epigenetics

In addition to acting at the transcriptional level to modulate gene expression, vitamin D can also act at an epigenetic level. Vitamin D repression or stimulation is associated with a number of epigenetic changes, and genes involved in the vitamin D pathway may also be regulated in an epigenetic manner.

Vitamin D and DNA methylation

Vitamin D has been observed to cause gene specific changes in DNA methylation. A small study measured cord blood 25(OH)D levels and found that in children with higher levels of 25(OH)D, there was a reduction in DNA methylation in the promoter of the gene *thymic stromal lymphopoietin (TSLP).* Consequently they also observed increased *TSLP* mRNA levels (Junge et al., 2016). *TSLP* has been linked to allergy development, and so vitamin D may be playing a role in allergic responses.

A further study in mice has observed changes in DNA methylation with low levels of vitamin D, but this time at imprinted regions. The male offspring of dams fed a low vitamin D diet had reduced methylation of the imprinted *H19/Igf2* ICR, *H19/PP* and *Grb10 DMR* in liver tissue, but not in sperm (Xue et al., 2016). It is possible that a similar effect may be seen in humans, but further research is needed to determine this.

The vitamin D pathway can also be regulated in an epigenetic manner by changes to DNA methylation, which has been associated with disease. Methylation has been observed in the promoter of the VDR gene in some adrenocortical carcinoma tissues, whereas no methylation was

observed in control adrenal tissue (Pilon et al., 2015). VDR mRNA and protein levels were also reduced, suggesting that this inappropriate methylation may play a role in adrenocortical carcinogenesis.

Vitamin D and histone modifications

The N-terminal tails of histone proteins can be methylated on either lysine or arginine residues. $1,25(OH)_2D$ induces the expression of the gene encoding for the enzyme JMJD3. JMJD3 is a member of the JmjC domain family of histone demethylase proteins, and acts to remove methyl groups from methylated lysine residues in histone proteins. It is one of only two proteins (the other being a member of the same family called UTX), known to be able to demethylate the H3K27me3 (trimethylated lysine 27 of histone 3) repressive mark. JMJD3 upregulation in turn has been shown to upregulate the expression of some $1,25(OH)_2D$ target genes including *CYP24A1*, *CDH1/E-cadherin* and *CST5/cycstatin D* (Pereira et al., 2012). Vitamin D is therefore able to act to alter histone methylation mediated epigenetic regulation of gene expression.

Vitamin D and miRNA expression

$1,25(OH)_2D$ treatment was demonstrated to significantly up or down regulate 111 miRNAs across seven different malignant and non-malignant prostate cell lines (Singh et al., 2015). They found VDR binding sites were enriched in the regions surrounding the miRNAs, suggesting a VDR mediated mechanism of action. Of the 111 altered miRNAs, only five were altered in more than one cell line, suggesting that $1,25(OH)_2D$ alters miRNA expression in a cell specific manner. Altered miRNAs are able to epigenetically regulate gene expression and therefore vitamin D is also able to effect the epigenetic regulation of gene expression in this manner.

Vitamin D and placental epigenetics

Within the human placenta there is specific methylation of the *CYP24A1* gene, but no methylation of *CYP27B1* or the *VDR*. This methylation is not observed in other somatic tissues, and directly reduces expression of the CYP24A1 enzyme uncoupling normal vitamin D regulation (Novakovic et al., 2009). This decreases the inactivation of $1,25(OH)_2D$, allowing for the increase in $1,25(OH)_2D$ concentration observed during pregnancy to occur.

DNA methylation has been observed to regulate vitamin D pathway genes within the placenta, and vitamin D has been observed to alter DNA methylation in other tissues (Novakovic et al., 2009, Junge et al., 2016). Vitamin D has also been observed to play a role in modifying epigenetic histone marks (Pereira et al., 2012), suggesting that vitamin D may act within the placenta to modify gene expression in an epigenetic manner, however experimental evidence is needed to demonstrate this.

1.8 Vitamin D, pregnancy and the placenta

Numerous links between vitamin D deficiency and adverse health outcomes during pregnancy suggest vitamin D plays an important role. Significant numbers of women of childbearing age are vitamin D deficient, but the effect of this on both the mother and the fetus during pregnancy is not fully understood. This has led to a number of studies which have aimed to observe and understand the role of vitamin D metabolites in both pregnancy disorders and offspring outcomes. A meta-analysis by *Harvey et al* identified associations between maternal 25(OH)D status and offspring birth weight, calcium status and bone mass. However it also highlighted the need for further research to explore these and other links to poor maternal and fetal outcomes (Harvey et al., 2014a).

1.8.1 Vitamin D and pregnancy disorders affecting the mother

Preeclampsia

Preeclampsia is a condition that develops during pregnancy that is characterised by new-onset hypertension and proteinuria after 20 weeks gestation. Preeclampsia results in an increased maternal risk of pulmonary edema, renal failure, cardiovascular disease, seizures and death. For the fetus preeclampsia increases the risk of premature delivery, fetal growth restriction and later life cardiovascular disease. Whilst the causes of preeclampsia are not well defined, they are thought to involve poor trophoblast invasion of the decidua, inflammation, oxidative stress and immune dysregulation (Burton et al., 2019).

It has been observed that pregnant mothers diagnosed with preeclampsia often have low plasma levels of vitamin D, but whether this deficiency is apparent before the onset of preeclampsia is not well understood (Seely et al., 1992). One study aimed to investigate this (Baker et al., 2010). 25(OH)D levels were measured in plasma samples taken between 15 and 20 weeks of gestation from 241 women, of which 43 developed severe preeclampsia after the time of taking the sample. Of the women who developed severe preeclampsia 25(OH)D deficiency, defined as < 50 nmol/l, was more common than compared to women with > 50 nmol/l. When adjusted for variables they found women with 25(OH)D levels of < 50 nmol/l had over a fivefold increased risk of developing severe preeclampsia than women with 25(OH)D levels ≥ 75 nmol/l. This suggests that vitamin D deficiency early in pregnancy could be contributing to the development of severe preeclampsia.

Another study also looked at the risk of low levels of vitamin D in pregnancy and the risk of preeclampsia, however both mild and severe preeclampsia were included (Bodnar et al., 2014). This study was much larger, with 25(OH)D levels from 717 women with and 2986 women without preeclampsia measured. After adjustment for variables this study found no significant increase in the risk of mild preeclampsia with low levels of 25(OH)D, characterised as < 30 nmol/l. The risk of severe preeclampsia was reduced by 40% in women with plasma 25(OH)D levels > 50 nmol/l in this study compared to those who had less than this. While both these studies agree that 25(OH)D deficiency increases the risk of developing severe preeclampsia, the 2010 Baker study showed a greater increase in risk. The sample size of this study was however small, which may have influenced the results.

A more recent study also aimed to look at the effect of low vitamin D levels in early pregnancy on the risk of developing preeclampsia (Achkar et al., 2015). 2144 women had their 25(OH)D concentration measured at 20 weeks or less gestation. 169 of these women subsequently developed preeclampsia. They found that vitamin D deficiency, defined in this study as < 30 nmol/l, doubled the chance of developing preeclampsia compared to those who had sufficient vitamin D, defined as > 50 nmol/l. The mean concentration of maternal 25(OH)D was significantly lower in the preeclamptic compared to control group. This agrees with previous studies that vitamin D deficiency increases the chance of developing preeclampsia, but comparisons of the results are difficult to make due to differing levels of vitamin D being classified as deficient in each study.

Gestational diabetes mellitus

Gestational diabetes mellitus (GDM) describes the onset of glucose intolerance during pregnancy, and is associated with poorer outcomes for both the mother and the fetus. In the mother GDM increases the risk of hypertension and caesarean section delivery, as well as later development of type 2 diabetes. GDM increases the risk of the fetus being LGA, as well as increasing the risk of obesity and type 2 diabetes in later life (Hashmi et al., 2019).

$1,25(OH)_2D$ action in pancreatic β-cells reportedly stimulates insulin receptors increasing insulin sensitivity. An observational study of 80 pregnant women, 40 with GDM and 40 without, found significantly lower serum 25(OH)D levels in women with GDM compared to those without at 24-28 weeks gestation (Ede et al., 2019). They reported at 1.69 fold increased risk of GDM in women with 25(OH)D deficiency (< 20 ng/ml, 50 nmol/l) compared to those with sufficient 25(OH)D levels (> 30 ng/ml, 75 nmol/l). This suggests that maternal vitamin D levels during pregnancy could be contributing to the development of GDM.

A meta-analysis investigating the link between maternal vitamin D levels and GDM risk analysed 87 observational studies and 25 randomised controlled trials (Zhang et al., 2018). They concluded that low 25(OH)D levels increases the risk of GDM, and that vitamin D supplementation may attenuate this risk. This data suggests that vitamin D may be a modifiable risk factor in the pathogenesis of GDM.

1.8.2 Vitamin D and pregnancy disorders affecting the fetus

Cohort Studies

Cohort studies are very useful to study pregnancy related conditions as they allow for the collection of a large amount of data about a high number of individuals. This means that not only is it possible to get a good number of both healthy and unhealthy subjects to study reducing bias in results, but that data on possible confounding factors is also often available. Factors such as maternal obesity, lifestyle, and health conditions may affect the concentration and actions of vitamin D metabolites during pregnancy. As such a number of cohort studies looking at women's reproductive health have taken place, of which some have provided us with important information on the how maternal vitamin D metabolite levels relate to offspring outcomes, as shown in Table 1-2.

Southampton Women's Survey

The aim of the Southampton Women's Survey (SWS) was to investigate how pre-pregnancy and intrauterine factors interact with the offspring's genes and environment to affect fetal growth and childhood development. 12,579 non-pregnant women aged between 20 – 34 years from the Southampton (UK) area were recruited, and were interviewed about their diet, body composition, physical activity, social circumstance and lifestyle (Inskip et al., 2006). Women who subsequently became pregnant underwent ultrasound scans at 11, 19 and 34 weeks gestation, and were interviewed again at 11 and 34 weeks gestation. Within 48 hours of birth neonatal anthropometry measurements were taken, along with umbilical cord blood and placental samples for analysis. A total of 2567 babies were born to SWS mothers. Infants have been followed up at 6 months, 1, 2, 3, 4, 6, 8 and now 10-12 years of age (Inskip et al., 2006). Analysis of this data has provided interesting results with regards to maternal vitamin D levels, some of which will be discussed below.

The Maternal Vitamin D Osteoporosis Study

The aim of the Maternal Vitamin D Osteoporosis Study (MAVIDOS) was to investigate if maternal supplementation with vitamin D in pregnancy resulted in offspring with a higher bone

mass at birth than those who were not supplemented. Bone mass increases through childhood to a peak in early adulthood, and then begins to decline. As shown in Figure 1-17 declining bone mass as an adult increases the risk of osteoporosis, and subsequently increases the risk of fracture. Studies have demonstrated that a higher weight at birth or 1 year of age results in a greater bone mass in adulthood (Dennison et al., 2005, Gale et al., 2001). It reasons that obtaining a higher peak bone mass would therefore decrease the risk of osteoporosis and fracture in later life, as the natural decline in bone mass would not reach as low a level of bone mass as would be reached if a lower peak bone mass had been obtained. One study which modelled the influence of different factors on the development of osteoporosis predicted that a 10% increase in peak bone mineral density delays the onset of osteoporosis by 13 years (Hernandez et al., 2003). As vitamin D is important to bone development, sufficient levels of vitamin D were predicted to be important for good levels of fetal bone growth.

1134 women were recruited and randomized to either receive 1000 International Units (IU)/day cholecalciferol or a placebo. Women were interviewed to determine their parity, lifestyle, diet, supplement intake, exercise, sunlight exposure and overall health and medications. At 19 and 34 weeks gestation they were followed up with ultrasound scans, and after birth infants underwent a DXA (dual energy x-ray absorptiometry) scan. Offspring have been followed up yearly and undergone a repeat DXA scan at 4 years of age (Harvey et al., 2012, Cooper et al., 2016).

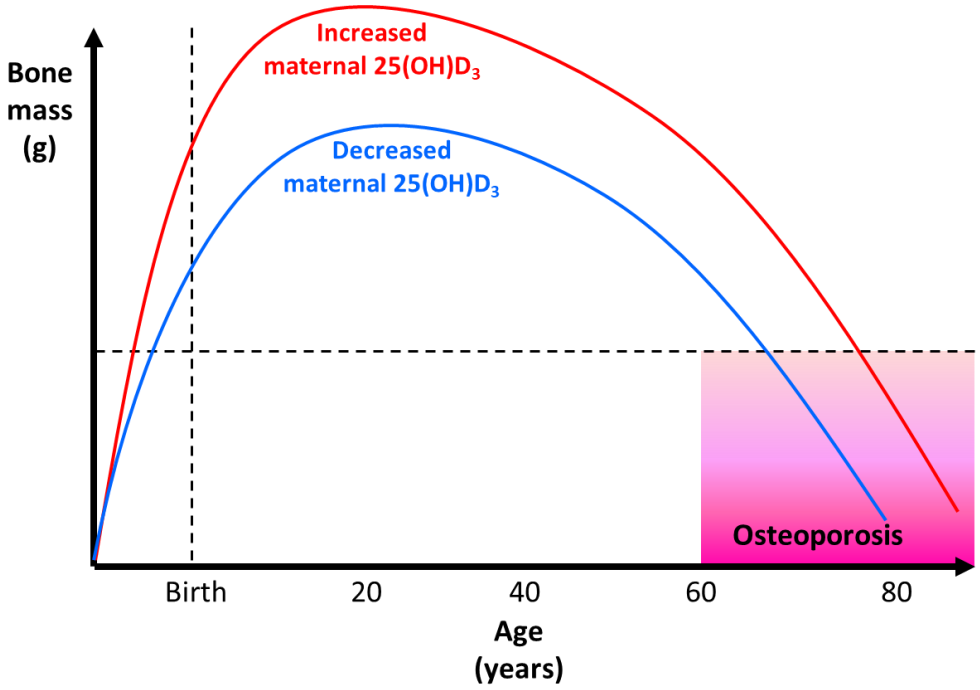

Figure 1-17 ***Relationship between vitamin D, bone mass and osteoporosis.*** *Peak bone mass is obtained in early adulthood, and declines with increasing age. Obtaining a higher peak bone mass may increase the age at which bone mass declines to osteoporosis levels.*

Southampton Pregnancy Intervention for the Next Generation

The Southampton Pregnancy Intervention for the Next Generation (SPRING) trial is an ongoing study in Southampton (UK). It aims to investigate whether a behaviour change intervention can lead to improved diet quality in pregnancy, the effect of oral vitamin D supplementation on vitamin D status of pregnant woman, and if the combination of both leads to improved overall nutritional status in the woman. The behaviour change intervention is administered through healthy conversation skills, and the vitamin D supplementation consists of 1000 IU/day cholecalciferol supplementation. Women are currently being recruited at the Princess Anne Maternity hospital in Southampton, and are followed up throughout pregnancy and after birth (Baird et al., 2016).

Table 1-2 *Overview of Southampton cohort studies used to investigate the role of vitamin D in pregnancy outcomes.*

Study	Study type	Intervention	Starting point	Inclusion criteria
Southampton Women's Survey	Observational	No intervention	Pre-pregnancy	Aged 20–34 years. Resident of Southampton (UK)
Maternal Vitamin D Osteoporosis Study	Supplementation	1000 IU cholecalciferol daily	14 weeks gestation	Singleton pregnancy. Maternal 25(OH)D level of 25-100 nmol/l.
Southampton Pregnancy Intervention for the Next Generation	Supplementation and behaviour change	1000 IU cholecalciferol daily. Healthy conversation skills sessions.	14 weeks gestation	Singleton pregnancy

1.8.3 Findings from vitamin D pregnancy studies

Numerous studies have investigated a link between maternal vitamin D status and development during pre-natal and postnatal life for the offspring. These studies have suggested that vitamin D influences a number of factors, including *in utero* growth of the fetus and therefore birth weight, and both fetal and postnatal body composition in terms of bone health and adiposity. Findings indicate that the effects of vitamin D may be via changes to gene expression, with epigenetic modifications potentially mediating the long term effects on gene expression.

Associations between maternal vitamin D levels and birth weight

Poor maternal vitamin D levels have been associated with reduced offspring birth weight (Harvey et al., 2014a). Investigating this in a cohort of 747 Chinese women with maternal $25(OH)D_3$ levels measured at the first prenatal visit, a nonlinear relationship between birthweight and $25(OH)D_3$ was found (Wang et al., 2018b). For every 1 ng/ml (2.5nmol/l) increase in maternal $25(OH)D_3$ a 69 g increase in birth weight was observed, up to 20 ng/ml (50 nmol/l) $25(OH)D_3$ at which point the relationship levelled out.

However another study investigating the relationship between maternal vitamin D deficiency and birth weight found a less clear relationship (Eggemoen et al., 2017). Maternal $25(OH)D_3$ deficiency of < 50 nmol/l at 15 and 28 weeks gestation was significantly associated with reduced birth weight when adjusted for maternal age, parity, education, pre-pregnancy BMI, season, gestational age and neonate sex. When adjusted for ethnicity however, this relationship between deficient maternal $25(OH)D_3$ and birth weight was no longer significant. These studies suggest that maternal vitamin D status may play a role in altering birth weight outcomes, but that other factors such as ethnicity may have a bigger effect.

Associations between maternal vitamin D levels and offspring bone health

Our understanding of the role that vitamin D plays in bone health has made the effect of vitamin D during pregnancy on fetal and childhood bone development an exciting area of research. One longitudinal study aimed to look at the effect of vitamin D deficiency during pregnancy on bone mass throughout childhood (Javaid et al., 2006). 198 children whose mother's plasma 25(OH)D levels had been measured in late pregnancy (34 weeks) had their whole body and lumbar spine bone mineral content measured using DXA at 9 years of age. Children of mothers who were deficient in vitamin D in late pregnancy had a significantly lower whole body bone mineral content and lumbar spine bone mineral content than those whose mothers had sufficient vitamin D. Deficiency in this study was classified as a 25(OH)D concentration of < 11 µg/L (27.5 nmol/l), and sufficiency as > 20 µg/L (50 nmol/l). This study suggests that inadequate vitamin D levels during pregnancy have a lasting effect on subsequent bone development in childhood. This could have much longer lasting consequences throughout life. However conclusions from this study are limited by sample size and the fact that only 25(OH)D concentration was measured, so the effect of $1,25(OH)_2D$ is not known.

Another study investigated the effects of maternal vitamin D status on fetal bone development (Mahon et al., 2010). 424 pregnant mothers who were participating in the SWS (Inskip et al., 2006) had their 25(OH)D levels measured at 34 weeks of gestation. 3D ultrasound was performed at 19 and 34 weeks gestation and used to measure fetal femur length and femoral

metaphyseal cross sectional area. These measurements were used to calculate femoral splaying index, with higher splaying index indicating a phenotype similar to rickets. Vitamin D deficiency, defined in this study as a 25(OH)D concentration of ≤ 25 nmol/l, was associated with higher femoral splaying index at both 19 and 34 weeks gestation than in mothers with sufficient vitamin D, > 70 nmol/l. This suggests that vitamin D plays an important role in bone development during pregnancy and that vitamin D deficiency has consequences for bone development at as early as 19 weeks. However again in this study only 25(OH)D was measured so the effect of $1,25(OH)_2D$ was not known. 25(OH)D was also only measured at 34 weeks, so it may have been very different in early pregnancy, meaning conclusions about the link between 25(OH)D and femoral splaying index at 19 weeks cannot be reliably made.

The effect of supplementation with vitamin D during pregnancy on fetal bone growth was investigated in a recent study (Vaziri et al., 2016). 62 women were supplemented with 2000 IU $25(OH)D_3$ daily from 26-28 weeks gestation till term, with a further 65 women receiving a placebo. At birth, 4 weeks and 8 weeks of age the babies had their weight, height and head circumference measured. No significant differences were identified between the two study groups. 25 infants underwent bone densitometry measurements, and again no significant differences were identified between the two groups for total body bone mineral content, bone mineral density and bone area. Mothers receiving vitamin D supplementation had a significant increase in their plasma 25(OH)D levels at childbirth compared to baseline measurements. There was no increase in vitamin D concentration of placebo participants. This study might suggest that vitamin D supplementation during pregnancy does not result in improved bone measurements in the infant. However, this study is limited by a small sample size, late starting point of supplementation and by > 85% of the mothers suffering from vitamin D deficiency or insufficiency at the start of the study.

The MAVIDOS study aimed to investigate if supplementation with vitamin D during pregnancy would result in greater whole body bone mineral content in infant offspring (Cooper et al., 2016). 479 women were randomised to receive 1000 IU $25(OH)D_3$ per day, with a further 486 receiving a placebo, from 14 weeks of gestation until term. Within two weeks of birth neonates underwent a DXA scan. There was no significant difference in whole body bone mineral content between the placebo and vitamin D supplemented groups. There was also no difference in bone area, bone mineral density, birth weight, length, fat mass, head circumference or abdominal circumference. When results were strengthened by season of birth, there was a significant increase in the bone mineral content of infants whose mothers received vitamin D supplementation when born during the winter months. However this study was limited by not

including mothers whose 25(OH)D levels at recruitment were less than 25 nmol/l, and conclusions from season of birth are limited by reduced sample size.

Associations between maternal vitamin D levels and offspring obesity

Reduced levels of vitamin D have been linked to an increase in obesity, however whether maternal vitamin D levels in pregnancy influence fat mass in the child was not known. The relationship between maternal vitamin D levels and offspring fat mass in childhood was therefore investigated in the SWS study (Crozier et al., 2012). 977 children whose mothers serum 25(OH)D levels had been measured at 34 weeks gestation and who had undergone a DXA scan at birth and/or age 4 or 6 years were included in the study. They found that at birth the fat mass of babies born to mothers with lower 25(OH)D levels (≤ 50 nmol/l), was lower than that of babies whose mothers had higher 25(OH)D levels (> 75 nmol/l). However at both 4 and 6 years of age this relationship was reversed with fat mass significantly lower in children of mother who had sufficient or good levels of 25(OH)D (> 50nmol/l) compared to those from mothers with low levels. This suggests that maternal vitamin D deficiency may result in increased fat mass and hence obesity in the offspring during childhood.

Another study investigating the relationship between maternal vitamin D status and offspring adiposity involved a prospective pregnancy cohort called Rhea (Daraki et al., 2018). 532 children whose mothers 25(OH)D levels had been measured at 14 weeks gestation had their BMI and waist circumference measured at 4 and 6 years of age. Deficient 25(OH)D levels (< 37.7 nmol/l) at 14 weeks gestation was associated with an increased waist circumference and BMI at both 4 and 6 years of age, compared to those with sufficient 25(OH)D levels (> 51.2 nmol/l). This suggests that vitamin D deficiency during pregnancy could have a lasting impact on adiposity in childhood.

Potential mechanisms linking vitamin D to offspring outcomes

The actions of $1,25(OH)_2D_3$ to alter gene expression may underlie the altered offspring outcomes observed when the mother is deficient in $25(OH)D_3$. The actions of $1,25(OH)_2D_3$ on the placenta may play a role in this by altering placental efficiency or function, changing what nutrients are passed to the fetus during development.

The transfer of amino acids from the mother to the fetus via the placenta is vital for fetal growth. As the regulation of many placental nutrient transporter genes is unknown and several contain VDREs within their promoter regions, the link between vitamin D and placental amino acid transporters was investigated in the SWS (Cleal et al., 2015). The mRNA levels of a range of known amino acid transporter genes were measured in 102 SWS placental samples from mothers

whose 25(OH)D and DBP levels had been measured at 34 weeks gestation. They showed a positive correlation between maternal 25(OH)D and expression of the amino acid transporter *LAT3*. They also showed a positive correlation between DBP and the expression of the amino acid transporters *LAT3, LAT4, SNAT1, SNAT2, y^+LAT2* and *EAAT3*. This suggests that vitamin D may be important for the regulation of amino acid transfer to the fetus during pregnancy. The link between DBP and amino acid transporter gene expression shown in this study suggest that vitamin D may be playing a regulatory role. These results may partially explain why fetal growth restriction is observed in mothers deficient in vitamin D. However again this study is limited by not having measured $1,25(OH)_2D$, which acts directly with DBP and could therefore have given further insight into the link between vitamin D and amino acid transporter gene expression in the placenta.

In support of these findings a subsequent study also identified increased gene expression of system A (including *SNAT2* identified above) and system L amino acid transporters in a cultured placental trophoblast cells treated with $1,25(OH)_2D_3$ (Chen et al., 2016).

Conclusions

Collectively these studies have demonstrated that maternal vitamin D deficiency during pregnancy is a risk factor for poor health outcomes. Despite the numerous studies linking vitamin D deficiency during pregnancy to adverse health outcomes a lack of consensus between what levels of 25(OH)D count as sufficient and deficient make studies difficult to compare. A large number of studies also only measure 25(OH)D and not $1,25(OH)_2D$, the active form within the body. 25(OH)D levels may be low whilst still maintaining sufficient levels $1,25(OH)_2D$, but due to their different biological activity it is critical to distinguish between them when considering their effects. However plasma 25(OH)D levels are a good indicator of maternal vitamin D reserves, as with very low maternal 25(OH)D it is difficult to maintain adequate $1,25(OH)_2D$ levels in the longer term. The large number of studies which link low vitamin D levels to adverse health outcomes suggests that vitamin D is playing a vital role in pregnancy; however the mechanisms underlying these effects are not understood. Further studies to determine how vitamin D interacts with and alters functioning of the placenta will allow us to better understand vitamin D deficiency adversely affects pregnancy.

1.9 Summary

A significant volume of research has been published in recent years in support of the hypothesis that the *in utero* environment has long term effects on the health of the individual. The placenta, at the interface between the maternal and fetal environments, provides a protective barrier and acts to optimise conditions *in utero*. However healthy functioning of the placenta is limited by maternal resources. Sufficient levels of vitamin D have long been regarded as important for bone health, but more recently also considered important for positive pregnancy outcomes. Poor maternal vitamin D levels have been associated with numerous pregnancy complications and longer term health implications for the offspring. However the mechanisms underlying these associations are not understood. Vitamin D must cross the placenta from the mother to the fetus, but what happens to vitamin D within the placenta, and how vitamin D acts on the placenta is not clear from current research. Gene expression data suggest that vitamin D is metabolised within the placenta, but what metabolites are present, and what metabolites pass to the fetus are not known. Vitamin D has been observed to alter epigenetics in a number of tissues, and it is therefore likely that it is also acting in this manner in the placenta, but studies are needed to confirm this. Vitamin D mediated effects on the placental transcriptome and epigenome may result in changes to placental functions that are responsible for altered fetal outcomes.

1.10 Hypothesis and aims

Hypothesis: 25(OH)D_3 will be metabolised within the human placenta and both 25(OH)D_3 and its metabolites will be transferred to the fetus. Within the placenta, vitamin D will mediate epigenetic regulation of gene expression, which may relate to fetal phenotype.

Aims:

1. To investigate how 25(OH)D_3 is metabolised within the human placenta and which forms are transferred to the fetal circulation using the isolated perfused placental cotyledon method.
2. To investigate how short term 25(OH)D_3 treatment alters DNA methylation, mRNA and protein expression in term human villous tissue.
3. To relate placental vitamin D mediated epigenetic changes to gene expression in an isolated human cytotrophoblast cell model.
4. To relate placental vitamin D mediated epigenetic changes to gene expression and fetal phenotype using two human cohorts.

Chapter 2 General Methods

2.1 Cohort Studies

Two human cohort studies were used to investigate the relationships between DNA methylation and gene expression with vitamin D supplementation. These were the Maternal Vitamin D Osteoporosis Study (MAVIDOS) and Southampton Pregnancy Intervention for the Next Generation study (SPRING). The MAVIDOS study was carried out with approval from the Medicines and Healthcare products Regulatory Agency, Southampton and Southwest Hampshire Research Ethics Committee, University Hospital Southampton (UHS) Trust R and D and Data Protection Office. The SPRING study is being carried out with approval from the Medicines and Healthcare products Regulatory Agency and the Southampton and South West Hampshire Research Ethics Committee.

2.1.1 Maternal Vitamin D Osteoporosis Study

MAVIDOS was a randomised double-blind trial investigating whether supplementing mothers with vitamin D during pregnancy results in offspring having a higher bone mass at birth than those whose mothers were not supplemented, as shown in Figure 2-1. Women were recruited at around 12 weeks of gestation when attending an antenatal appointment at one of three study centres, Southampton, Oxford and Sheffield. In our studies only samples from women attending the Southampton centre have been utilised. Women are screened, and those with circulating 25(OH)D levels of between 25 and 100 nmol/l are recruited. At 14 weeks of gestation women were assessed and randomly assigned to either once daily oral supplementation of 1000 IU cholecalciferol or matched placebo (Bilcare GCS (Europe) Ltd). Women were interviewed to collect information on parity, demographic features, exercise, smoking, alcohol intake, diet, sunlight exposure, health and medication. Anthropometry measurements were taken including height, weight, skinfold thickness and grip strength. A blood sample was also taken at this visit. At 18-21 weeks gestation participants underwent a high-resolution 3D ultrasound scan, alongside their NHS anomaly scan. At 34 weeks gestation further blood samples were taken. Anthropometry measurements and interview questions were repeated, and participants underwent another 3D ultrasound scan. Upon delivery of the baby umbilical cord blood, umbilical cord and placental samples were taken. Neonatal anthropometry measurements were taken, including length, weight, skinfold thickness, head and abdominal circumference. A neonatal DXA scan (Holographic Discovery Instrument) was carried out as soon as possible after birth, within 14 days, to measure whole body and lumbar spine bone area, bone mineral content and bone mineral density.

Offspring were followed up at 1, 2, 3, and 4 years of age to obtain health, diet and exercise information. At 4 years of age a repeat DXA scan was carried out (Harvey et al., 2012). Follow up is currently taking place at 6 years of age.

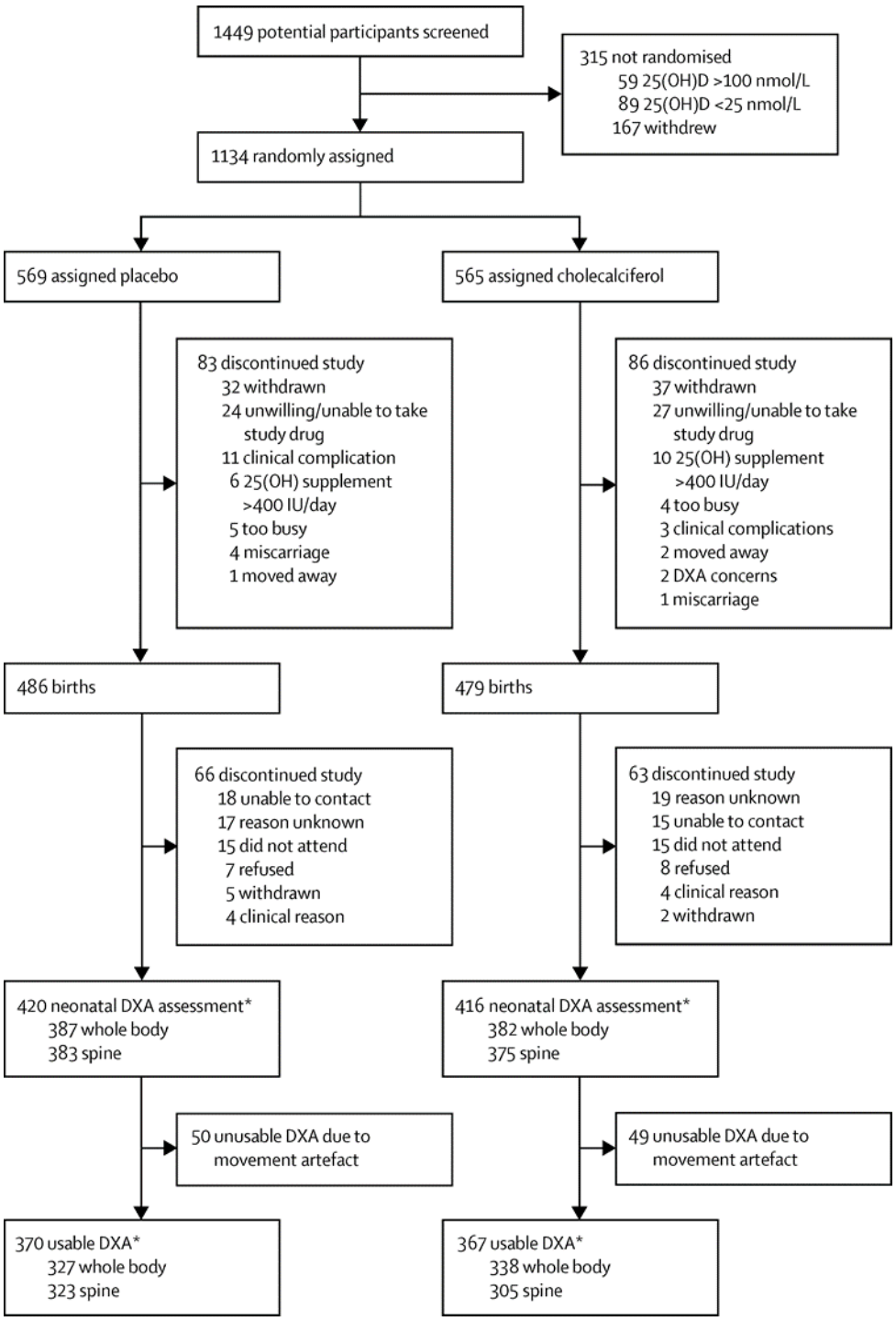

Figure 2-1 ***The Maternal Vitamin D and Osteoporosis Study (MAVIDOS) trial outline*** *(Cooper et al., 2016)*

2.1.2 Southampton Pregnancy Intervention for the Next Generation

SPRING is a randomised controlled trial investigating two different interventions (Baird et al., 2016), as shown in Figure 2-2. Women are being recruited at 8-12 weeks of gestation when attending an antenatal appointment at the Princess Anne Maternity Hospital Southampton. Women are randomised to receive either Healthy Conversation Skills (HCS) support and vitamin D supplementation, Healthy Conversation Skills and a placebo, normal care and vitamin D supplementation or normal care and a placebo. The HCS support is a behavioural intervention carried out by trained nurses to encourage and give women the personal tools to make healthy changes to their diet and lifestyle. The vitamin D supplementation consists of a once daily oral supplement of 1000 IU cholecalciferol or a matched placebo (Sharp Clinical Services (UK) Ltd).

At 14 weeks gestation women are interviewed to collect information on parity, demographic features, diet, lifestyle, exercise, exposure to sunlight and general health and medication. A food frequency questionnaire is used to determine a prudent diet score. Anthropometry measurements are taken including height, weight, skinfold thickness and grip strength, as well as a blood sample. Women receiving HCS support have their first session with a research nurse, and the vitamin D supplement or placebo is prescribed. Participants are blind to whether they are receiving vitamin D or a placebo, and if they are having behavioural intervention or normal care. Researchers are blind to whether the participants are receiving vitamin D supplementation or placebo, but are aware of whether the participant is having a behavioural intervention or normal care. At 18-21 weeks gestation participants undergo a high-resolution 3D ultrasound scan, and a further HCS support session if receiving that intervention. At 26 weeks gestation participants receive a phone call to arrange their next appointment, and for those receiving HCS support they also have their third session over the phone. At 34 weeks gestation all participants undergo the 3D ultrasound, interview, anthropometry measurements again and give another blood sample. Upon delivery of the baby, umbilical cord blood, umbilical cord and placental samples are collected. Neonatal anthropometry measurements are taken, including length, weight, abdominal circumference and skinfold thickness. A neonatal dual-energy X-ray absorptiometry scan (Holographic Discovery Instrument) is carried out as soon as possible after birth, within 14 days, to measure whole body and lumbar spine bone area, bone mineral density and bone mineral content.

One month after birth the mothers are visited and interviewed again, this time with the inclusion of questions about infant feeding. Participants receiving HCS support have their final session with the research nurse. There are plans to follow up the children throughout childhood (Baird et al., 2016)

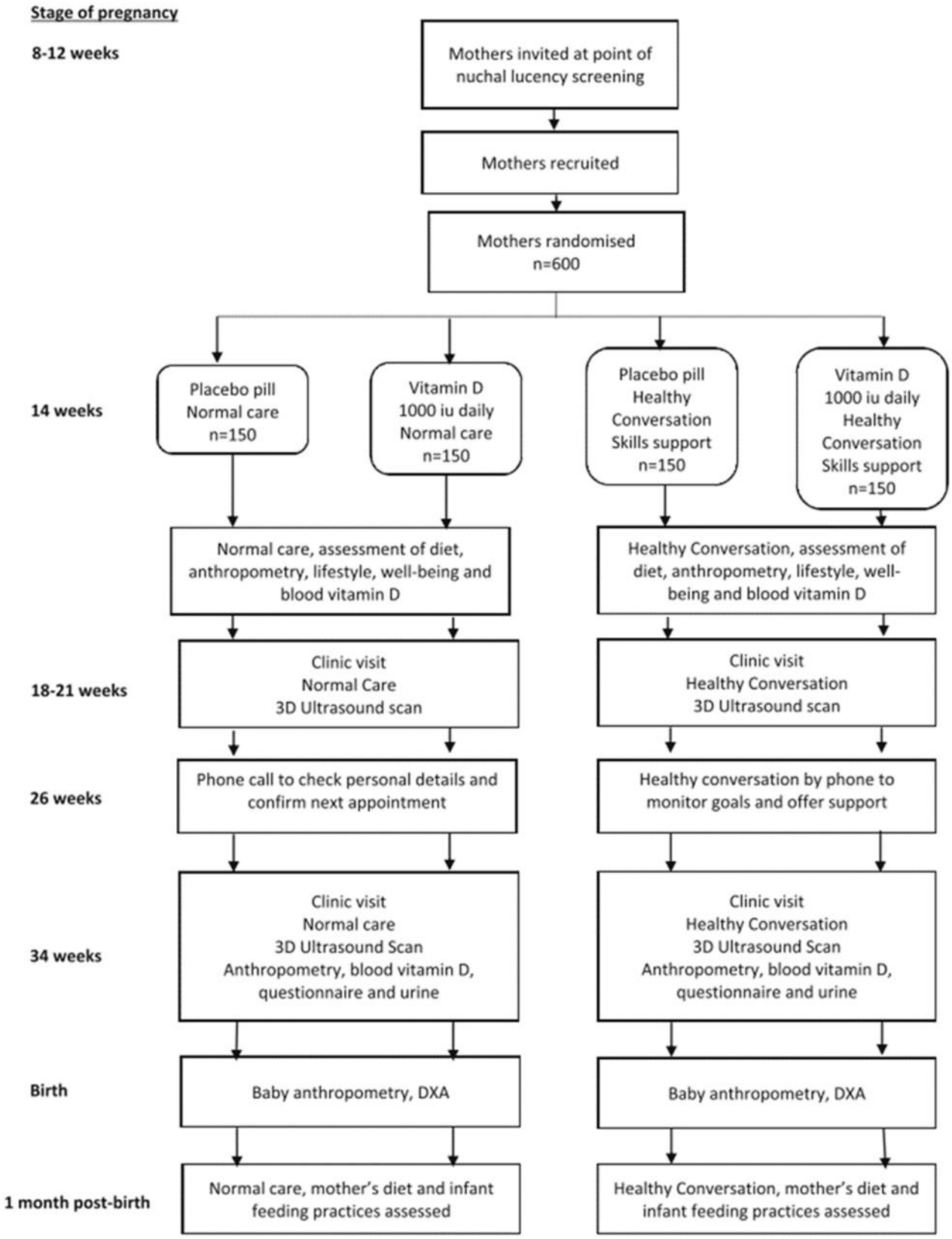

Figure 2-2 ***Southampton PRegnancy Intervention for the Next Generation (SPRING) study design*** *(Baird et al., 2016)*

2.2 Placental collection

2.2.1 General collection

Term placentas were collected from healthy, uncomplicated pregnancies within 30 min of delivery at the Princess Anne Hospital, Southampton. This study gained informed, written consent from the participants and ethical approval from the Southampton and South West Hampshire Research Ethics Committee. Once obtained, the tissue was sealed into a plastic bag, placed into a box and transported to the laboratory as quick as possible ready for *ex vivo* experiments such as placental perfusion, fragment culture and primary cell culture (sections 2.3, 2.4 and 2.5 respectively).

2.2.2 Cohort study collection

94 placenta samples were collected from the SPRING study participants as described in section 2.1.2 as soon as possible after birth. Upon collection the umbilical cord, membranes and any blood clots were removed. The placenta was weighed and ten 0.5 cm^3 villous tissue samples were cut from the maternal side of the placenta with decidua removed via random sampling with a stratified random sampling grid, as shown in Figure 2-3. The samples were then snap frozen in liquid nitrogen and stored at -80°C.

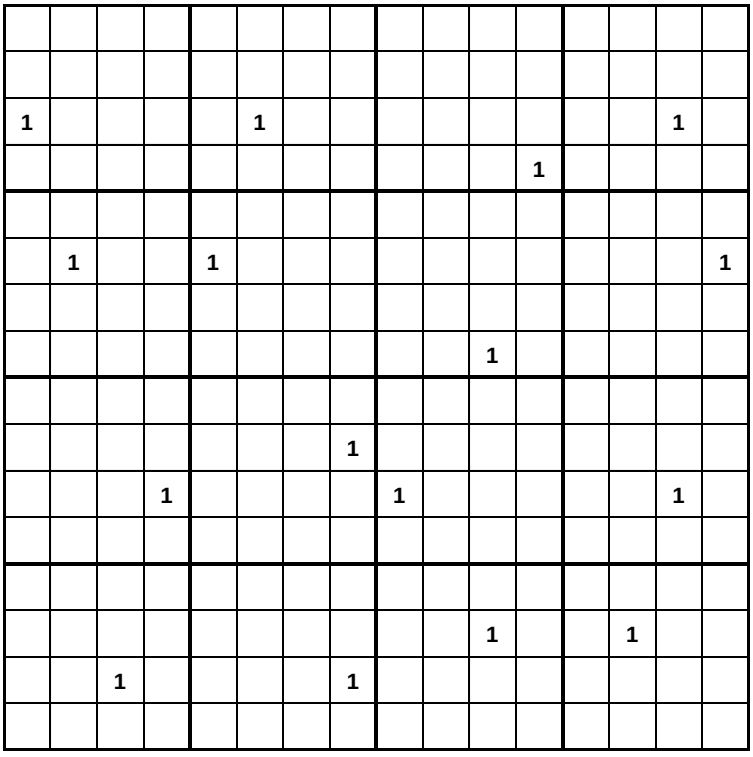

Figure 2-3 ***Random sampling grid*** *Example of the stratified random sampling grid used to obtain placental tissue samples from the MAVIDOS and SPRING studies.*

2.3 Placental perfusion

Ex vivo placental perfusion techniques as adapted in our laboratory (Cleal et al., 2007) were used to investigate 25(OH)D metabolism and transfer across the placenta, as shown in Figure 2-4. Term human placentas were collected within 30 min of delivery and a selected cotyledon perfused with a physiological buffer. Perfusate was collected at specific time intervals.

Upon collection the placenta was examined, and blood clots removed to allow for inspection of the cotyledons. An undamaged cotyledon with a clear artery and vein pair was selected. Larger arteries and vessels that did not sharply bend or cross other vessels were preferentially selected for ease of cannulation. Using a pair of fine nosed scissors and tweezers, the artery was cut as close to the umbilical cord insertion as practical, without damaging the surrounding tissue. A 20 ml Leur-Lok syringe was filled with Earle's bicarbonate buffer (EBB; see Table 2-1), heated to 37°C and gassed with 95% O_2, 5% CO_2. The syringe was attached to the fetal arterial catheter; a 15cm length of tubing (Portex PVC tubing, inner diameter (ID) = 0.86 mm, outer diameter (OD) = 1.52 mm), and EBB was pushed through to ensure there were no bubbles in the tubing. The feto-placental arterial catheter was inserted approximately 2-4 cm into the cut artery, and sutured tightly in place using vicryl absorbable coated braided suture with a 26 mm ½ circle tapercut needle (Johnson & Johnson Medical Ltd). EBB was then flushed into the cotyledon to allow the heparin within it to inhibit further blood clotting from taking place. Again using a pair of fine nosed scissors and tweezers, the corresponding vein was cut as close to the umbilical cord insertion as practical, without damaging the surrounding tissues. The feto-placental venous catheter (Portex PVC tubing, ID = 2 mm, OD = 3 mm, 15 cm length), was then inserted 2-4cm into this vein and sutured tightly in place. Further EBB was flushed through the cotyledon, ensuring there were no leaks and that circulation was not flowing into any other cotyledons. The placenta was then assembled onto the perfusion equipment, ensuring the cotyledon to be perfused was not damaged or trapped between the two sides of the perfusion clamp. Excess placental tissue was cut away from the perfused cotyledon and discarded. EBB was flushed through the cotyledon again to ensure that both tubes were still in place, not leaking, and that there was free flow of buffer.

The placenta was moved to the perfusion cabinet, which is maintained at 37°C and fetal circulation established at a rate of 6 ml/min using a roller pump. If after 15 min, the recovery from the fetal circulation was over 95% (5.7 ml/min), the maternal circulation was established at a rate of 14 ml/min by inserting the five maternal cannulae (ID = 0.58 mm, OD = 0.96 mm, 15 cm length), spread across the perfused cotyledon. Once the maternal circulation was established both the

maternal and fetal circulations were perfused for 45 min with EBB buffer warmed to 37°C and gassed with 95% O_2, 5% CO_2. At 45 min the maternal and fetal circulation was transferred to the corresponding experimental EBB buffer warmed to 37°C and gassed with 95% O_2, 5% CO_2 and the experiment was started. Perfusate samples were collected from the maternal and fetal vein at set time intervals throughout the experiment. One unperfused cotyledon was cut from the placenta, weighed, and then cut into ~1 cm^3 chunks and stored at -80°C. After the last experimental time point the fetal and maternal circulations were both returned to general EBB buffer and perfused for a further 5 min. Circulation was stopped, and the placenta removed from the perfusion cabinet. The placenta was disassembled from the perfusion set up, and non-perfused tissue was carefully trimmed from around the edge of the perfused cotyledon. The perfused cotyledon was weighed, cut into ~1 cm^3 chunks and frozen at -80°C. Perfusate samples were stored at -80°C.

Table 2-1 *Composition of Earle's bicarbonate buffer (EBB).*

Reagent	Concentration	Supplier
$CaCl_2H_2O$	1.8 mmol/l	Thermo Fisher Scientific
$MgSO_4.7H_2O$	0.4 mmol/l	BDH Laboratory Supplies
D-Glucose	5.5 mmol/l	Sigma Aldrich
NaCl	116.4 mmol/l	Thermo Fisher Scientific
KCl	5.36 mmol/l	Thermo Fisher Scientific
$NaH_2PO_42H_2O$	0.9 mmol/l	BDH Laboratory Supplies
$NaHCO_3$	26.2 mmol/l	Sigma Aldrich
Bovine serum albumin (Heat shock fraction, pH7, ≥ 98%)	1 g/L	Sigma Aldrich
Heparin	5000 IU	Sigma Aldrich

IU = International Unit

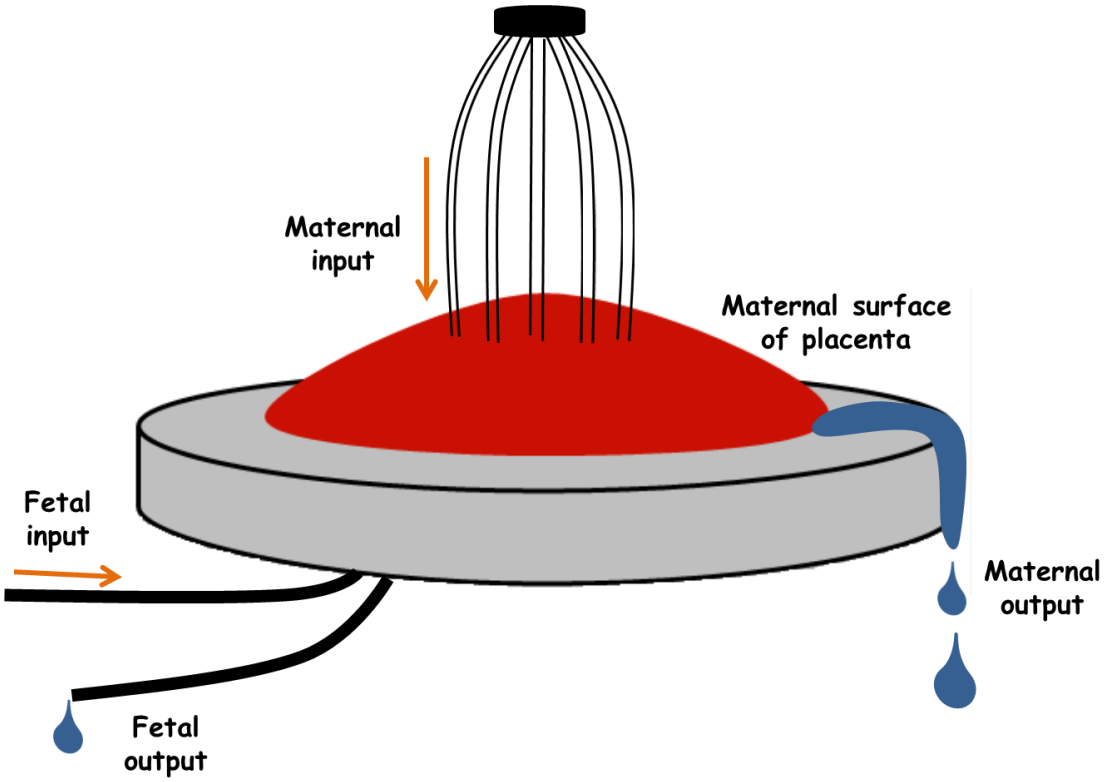

Figure 2-4 ***Placental perfusion arrangement.*** *A placental cotyledon has the fetal circulation re-established via fetal arterial and venous catheters and maternal circulation re-established with five maternal spiral artery catheters. Perfusate is collected from the fetal and maternal outputs.*

2.4 Placental fragment culture

To investigate the effects of vitamin D treatment placental tissue fragments have been incubated with vitamin D.

Term human placentas were collected as described in section 2.2.1 from healthy, uncomplicated pregnancies within 30 min of delivery. Villous tissue fragments of approximately 10 mg were cut from the maternal surface of the placenta, with decidual tissue removed. Fragments were stored at room temperature (RT) in Tyrode's buffer (see Table 2-2), whilst remaining fragments were dissected. 3 x 10 mg fragments were incubated in a 2 ml Eppendorf tube with 0.5 ml Tyrode's buffer containing 20 µmol 25(OH)D_3 (dissolved in ethanol) and 0.7 mmol/l bovine serum albumin (BSA; Sigma Aldrich) or ethanol control with 0.7 mmol/l BSA, or 20 µmol 25(OH)D_3 + 9 µmol DBP or ethanol control + 9 µmol DBP, at 37°C for 8 h. After 8 h the buffer was removed, fragments washed in Tyrode's buffer and then snap frozen on dry ice. Fragments were stored at -80°C.

Fragments were incubated for a period of 8 h as in a previous time course experiment carried out by Dr Simner (Simner, 2015), this was shown to be the optimum time to observe gene expression changes for a known vitamin D responsive gene in vitamin D treated fragments. At 8 h housekeeper gene (HKG) expression was consistent with that seen in earlier time points. Beyond 12 h of incubation HKG expression began to decrease, suggesting cell death was occurring. The dosage of 25(OH)D_3 was in the micro-molar range rather than the physiological nano-molar range. This is within the concentration range used in previous vitamin D studies meaning we can compare our findings to the previous results (Deising et al., 2006).

Frequently in vitamin D treatment experiments, BSA is used as the vitamin D binding protein as it is affordable and readily available, however in normal physiological conditions most vitamin D is bound to DBP (Zerwekh, 2008). Therefore in this study we have included the use of both BSA and DBP as binding proteins to identify if the changes we observe are altered by the binding protein used.

Table 2-2 *Composition of Tyrode's buffer used in placental fragment culture experiments.*

Buffer	Components	Supplier
Tyrode's buffer	135 mmol/l NaCl	Thermo Fisher Scientific
	10 mmol/l HEPES	Thermo Fisher Scientific
	5.6 mmol/l D-Glucose	Sigma Aldrich
	5 mmol/l KCl,	Thermo Fisher Scientific
	1.8 mmol/l $CaCl_2 2(H_2O)$	Thermo Fisher Scientific
	pH to 7.4 with NaOH	Thermo Fisher Scientific

2.5 Primary cytotrophoblast cell culture

Primary cytotrophoblast cells were isolated from human placental tissue and cultured to investigate the effects of 25(OH)D on placental gene expression. Cells were investigated at both the cytotrophoblast cell stage and after syncytialisation into syncytiotrophoblast cells as they undergo morphological and functional changes during this process, which may alter their gene expression.

2.5.1 Cell isolation

Term placentas were collected as described in section 2.2.1 from healthy, uncomplicated pregnancies within 30 min of delivery.

The umbilical cord (if present) and membranes were removed, and the whole placenta cut into ≈2 cm^3 pieces, except ≈0.5 cm from around the edge, which was discarded. Placental cubes were washed three times in sterile 0.9% saline to remove maternal blood. The chorionic plate and underlying 3 mm of tissue, and decidua and underlying 3 mm of tissue were removed, and the remaining tissue cut into small pieces. Pieces were placed into sterile 0.9% saline and washed once. Tissue was then strained through sterile gauze and refined into smaller pieces by mincing with scissors. Vessels, blood clots and gritty tissue were removed with forceps and discarded. Minced tissue was then transferred into 0.9% saline and washed. Tissue was strained through a sterile gauze, removing any further visible vessels or blood clots. Tissue was rolled together to dry, weighed, and then placed into a 1 litre conical flask with 150 ml warmed HEPES-buffered salt solution (HBSS; see Table 2-3), pre-mixed with 30 mg DNAse (Sigma Aldrich) and 15 ml trypsin (Thermo Fisher Scientific). The contents of the flask was mixed by swirling and placed in a shaking water bath at 37°C and 80 rpm for 30 min to digest tissue. After digestion the flask was removed from the water bath and supported on its side on the benchtop, allowing the contents to settle to the bottom, as shown in Figure 2-5. 100 ml of supernatant was removed from the flask using a sterile stripette, being careful not to disturb the tissue, and placed into a sterile 250 ml beaker.

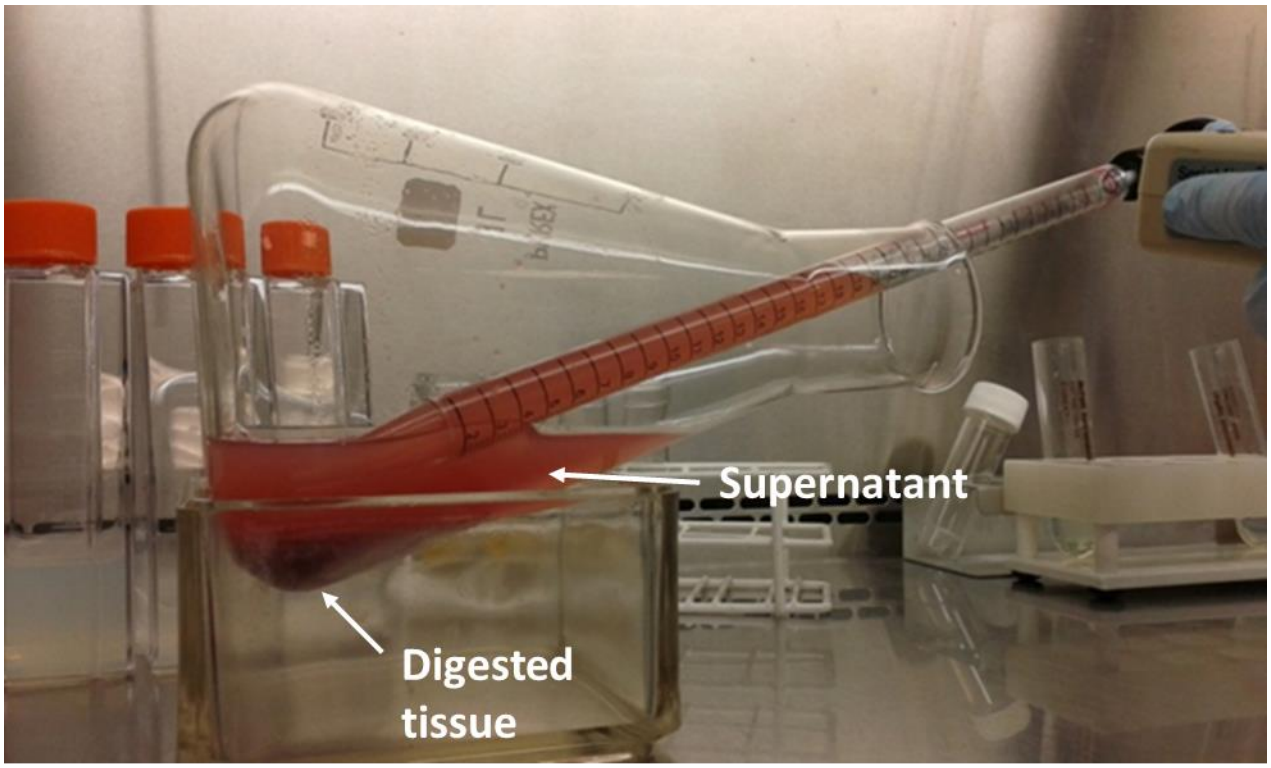

Figure 2-5 ***Placental tissue digestion*** *Representative image of supernatant being removed from digested tissue after the first digestion step, using a sterile 25 ml stripette. Image courtesy of Dr Susan Greenwood (University of Manchester).*

To the remaining tissue 100 ml of warmed HBSS, pre-mixed with 20 mg DNAse, and 10 ml trypsin was added. The contents of the flask was mixed by swirling and placed a shaking water bath at 37°C and 80 rpm for 30 min to digest. After the second digestion, 100 ml of supernatant was again removed from the flask using a sterile stripette and placed into a sterile 250 ml beaker. 75 ml of warmed HBSS, pre-mixed with 10 mg DNAse, and 7.5 ml of trypsin was added to the remaining tissue. The contents of the flask was mixed by swirling and placed in a shaking water bath at 37°C and 80 rpm for 30 min to digest. After the third digestion was complete the contents of the flask was strained through gauze, and then through a wire mesh (50 μm^2 hole, 0.036 mm wire), into a sterile 250 ml beaker. Starting after the first digestion the supernatant was layered over newborn calf serum (NCS; Sigma Aldrich). 25 ml of supernatant was layered over 5 ml of NCS in a sterile universal tube, as shown in Figure 2-6, and then centrifuged at 2200 rpm for 10 min to pellet cells. This was continued throughout digestion steps until all obtained supernatant had been centrifuged and cells pelleted.

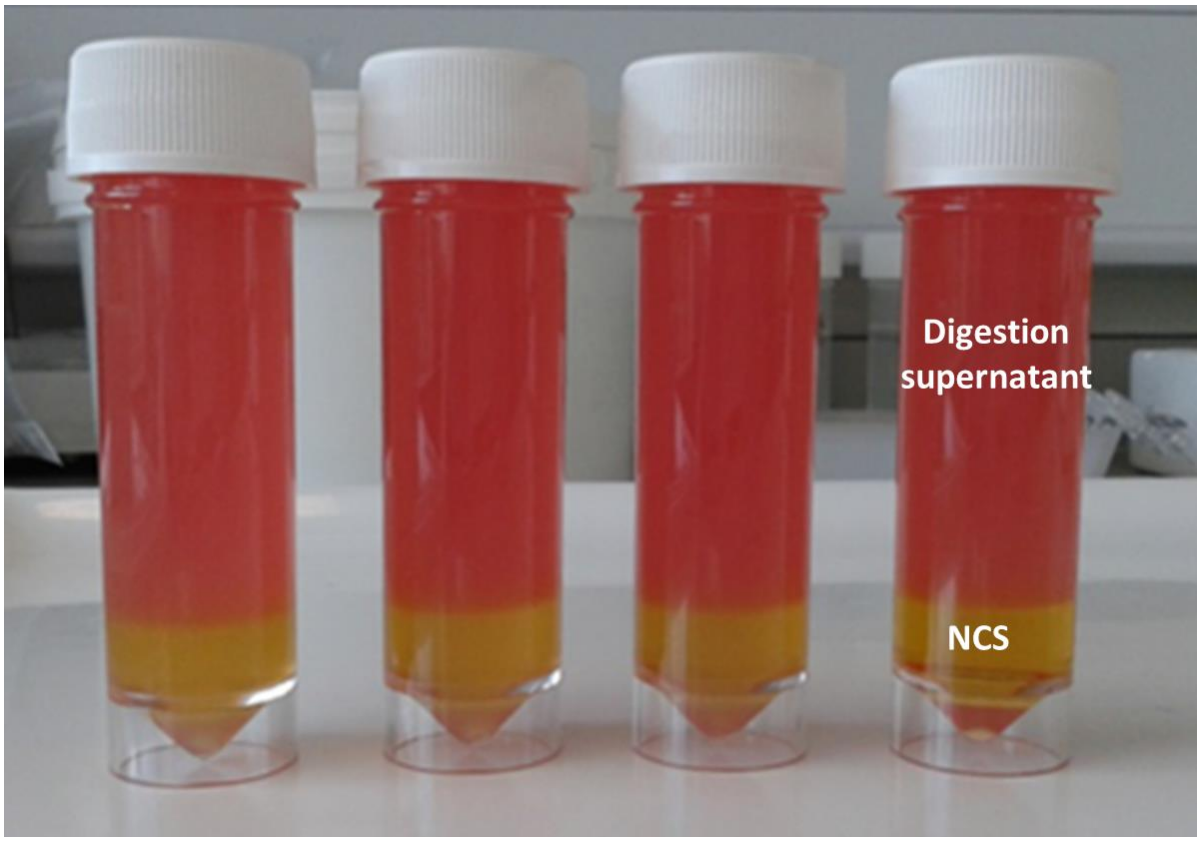

Figure 2-6 ***Placental digestion supernatant****. A representative image of digestion supernatant layered over newborn calf serum prior to centrifugation.*

A red pellet of erythrocytes with a thin pale layer above containing cytotrophoblast cells was obtained. Supernatant was removed and discarded and the pellets resuspended in 1 ml pre-warmed Dulbecco's modified Earle's medium (DMEM; Fisher Scientific). Resuspended pellets were combined into one sterile 30 ml universal tube. The tube was filled to the top with DMEM and centrifuged at 2200 rpm for 10 min. Supernatant was discarded and the pellet resuspended in 6 ml of DMEM. The cell suspension was pipetted equally on to the top of two Percoll gradients, prepared in cortex tubes as described in Table 2-4. The Percoll gradients were centrifuged for 30 min at 2800 rpm. After centrifugation bands were visible at the menisci separating the different concentration layers, as shown in Figure 2-7. Erythrocytes formed a dark red pellet at the bottom of the tube. DMEM and cell debris sitting at the top of the gradient was aspirated off and discarded. Cells were collected from the 35-55% region using a sterile pipette, and transferred a sterile 30 ml universal tube. The tube was filled with 37°C cell culture media (see Table 2-3), and centrifuged at 2200 rpm for 10 min. Supernatant was discarded and the pellet was resuspended in 2 ml 37°C culture media. Cells were counted as described in section 2.5.3 and plated at a density of $3x10^6$ cells per 32 mm diameter well in 6 well plates, with 2 ml of culture media.

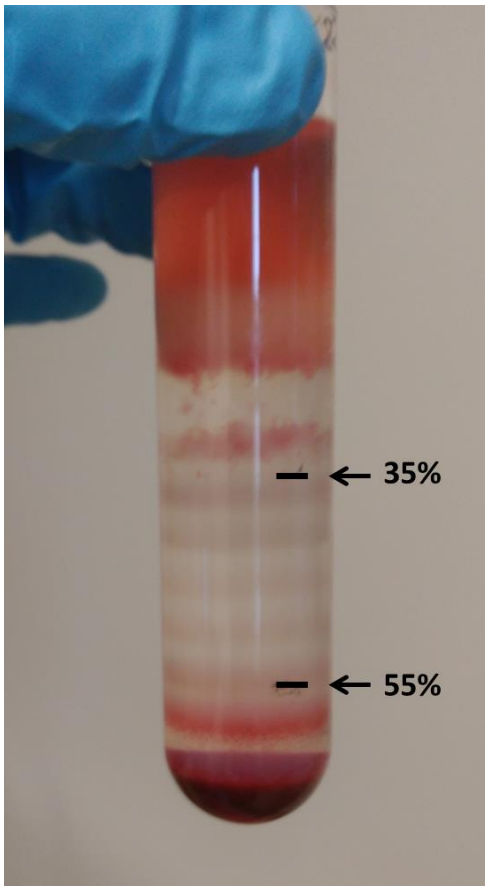

Figure 2-7 ***Percoll density gradient*** *Representative image of placental cells separated by centrifugation on a Percoll density gradient.*

Table 2-3 *Cell culture working solutions composition*

Solution	Components	Supplier
Phosphate buffered saline (PBS)	1PBS tablet dissolved in 200 ml dH20 = 10 mmol/l phosphate buffer, 2.7 mmol/l KCL and 137 mmol/l NaCl at pH 7.4.	Sigma Aldrich
DMEM/Ham's cell culture media	DMEM (225 ml) Ham's F12 (225 ml) 10% FBS (50 ml) 320 IU gentamicin Supplement mix (5 ml) containing 10,000 IU penicillin, 10 mg/ml streptomycin and 200 mmol/l glutamine	Thermo Fisher Scientific Thermo Fisher Scientific Thermo Fisher Scientific Sigma Aldrich Sigma Aldrich
10 x HEPES-buffered salt solution (HBSS)	54 mmol/l KCl 409 nmol/l KH2PO4 1.4 mol/l NaCl 3.3 mmol/l Na2HPO4.12H2O 55.5 mmol/l Glucose	Thermo Fisher Scientific Thermo Fisher Scientific BDH Laboratory Supplies Sigma Aldrich
1 M HEPES	1 mol/l HEPES at pH 7.4.	Thermo Fisher Scientific
1 X HBSS working solution	50 ml 10X HBSS 12.5 ml 1M HEPES at pH 7.4 made to a total volume of 500 ml with dH2O.	Thermo Fisher Scientific

Table 2-4 *Percoll gradient preparation*

Cortex tube markings	Percoll
	2 ml 10%
	2 ml 20 %
	4 ml 30%
Tube marked at boundary here	----------
	2 ml 35%
	2 ml 40%
	2 ml 45%
	2 ml 50 %
	2 ml 55%
Tube marked at boundary here	----------
	2 ml 60%
	3 ml 70%

2.5.2 Cytotrophoblast culture

18 h after cell plating the culture media was removed from each well of the plate and replaced with fresh, 37°C culture media. This was repeated every 24 h thereafter. Table 2-5 shows representative images of the cultured cytotrophoblast cells at each time point. A sample of the culture media removed at each time point was stored at -20°C for later analysis of human chorionic gonadotrophin (hCG) content, as described in section 2.8. At 90 h after plating, cells were collected for later analysis or fixed for imaging. Culture media was removed and cells washed once with phosphate buffered saline (PBS, Sigma Aldrich; see Table 2-3). To fix cells 1.5 ml of methanol, pre-chilled to -20°C, was added to the wells and stored at -20°C for 30 min. Methanol was removed and cells were washed once with PBS pre-chilled to 4°C. A further 2 ml of PBS was added and the plate was stored at 4°C prior to imaging. To collect for alternative analysis (RNA, DNA etc.) cells were scraped from the plate using a cell scraper (Fisher Scientific) and collected into an appropriate medium, before storage at -80°C.

2.5.3 Cell counting

Cells in solution were counted using a Beckman Coulter Z1 Particle Counter to determine concentration. 20 µl of the cell suspension was diluted in 10 ml of Isoton II Diluent (Beckman Coulter) and mixed well. The particle counter was set to record cells between 6–19 µm in diameter. Two readings were taken of the number of cells in 500 µl of the cell suspension and the

results added together. The number of cells in 1 ml of the diluted cell suspension was then multiplied by 500 to account for the dilution, giving the number of cells per ml of cell suspension.

Table 2-5 *Representative images of cultured cytotrophoblast cells at different time points. Red arrows indicate a single cytotrophoblast cell. White arrows indicate syncytiotrophoblast formation.*

18 h	**42 h**
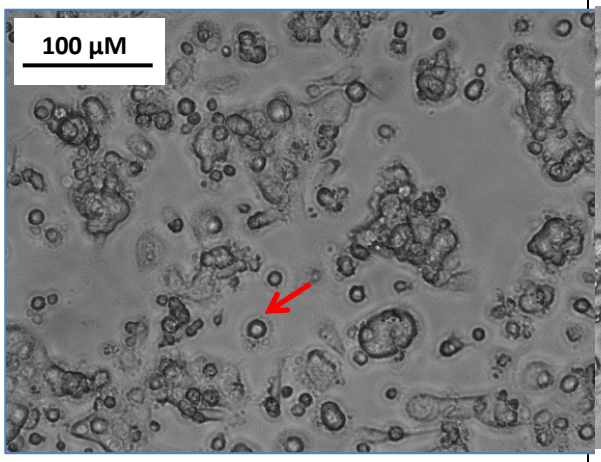	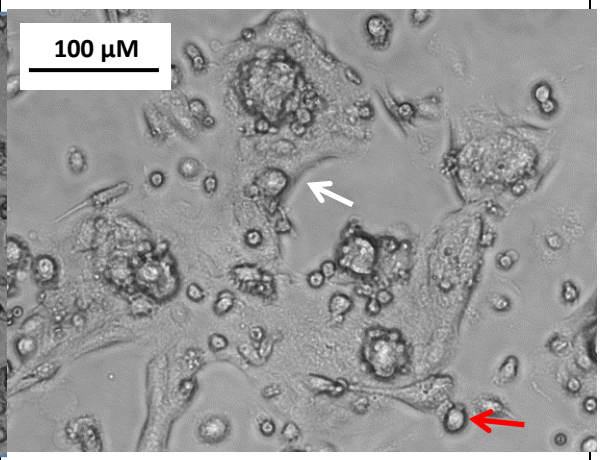
66 h	**90 h**
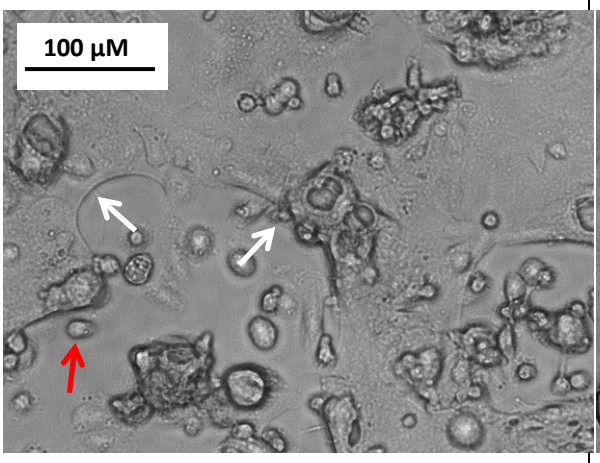	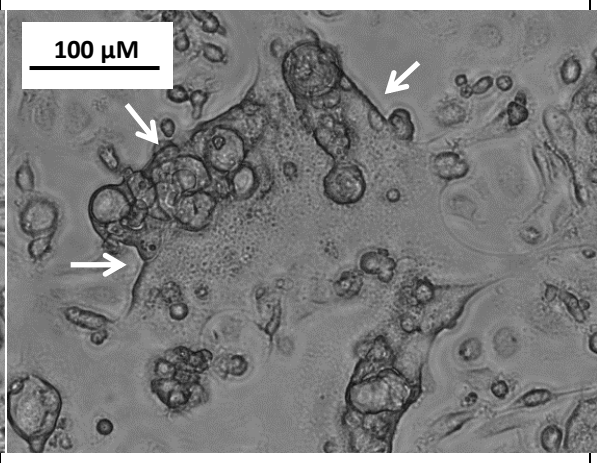

2.6 Stable isotope measurement

^{13}C-25(OH)D_3 and metabolites were measured in perfusate samples by Felicity Hey (University of Cambridge) using liquid chromatography mass spectroscopy (LCMS). LCMS is a technique that allows for the components of a sample to be separated and identified. A sample is introduced to a liquid that is passed under high pressure through a column that is lined with a stationary phase. This separates the sample by its weight and affinity for the stationary phase and causes it to fragment. The sample is then ionized, and separated according to its mass to charge ratio (*m/z*). A second ionisation causes the molecules to fragment again, and these daughter ions are detected.

Perfusate samples were diluted at a ratio of 1:2 in distilled water. 100 µl 0.1 M HCl was added and protein precipitated out of solution with 150µl of 0.2 M $ZnSO_4$ and 450 µl methanol. Samples were vortexed and centrifuged at 12500 rpm for 10 min at RT. 600 µl of supernatant was transferred to a 5 ml eppendorf. 700 µl hexane and 700 µl methyl-tert-butyl ether (MTBE) were added and vortexed to wash the sample of contaminants. Samples were centrifuged at 4500 rpm for 10 min at RT and 800 µl of the upper organic phase transferred to a 2 ml eppendorf. To the remaining residue 400 µl of hexane and 400 µl of MTBE were added, samples vortexed and again centrifuged at 4500 rpm for 10 min at RT. 800 µl of the upper organic phase was collected and combined with the first supernatant collected.

Samples were dried under nitrogen at 40°C and derivatised by dissolving in 50 µl of 0.5mg/ml 4-phenyl-1,2,4-triazoline-3,5-dione (PTAD) in acetonitrile (ACN) before vortexing for 1 h at RT. 50 µl of methanol was added before drying samples under nitrogen at 40°C. When dry the samples were reconstituted in 50 µl of 50:50 ACN/water.

Samples were analysed using a Waters (Manchester, UK) Acquity UPLC module interfaced to 5500 QTRAP quadruple –linear ion trap mass spectrometer (AB Sciex, Concord, ON, Canada). Separations were performed in a Waters CORTECS $C18^+$ column (2.1×150 mm, 1.6 µm) housed in a column oven at 45°C. Separated analytes were detected by the mass spectrometer using the electrospray ionisation mode with multiple reaction monitoring. Analytes were quantified by comparison to an external standard calibration curve, and the limit of quantification was 0.6 pmol/L.

2.7 $1,25(OH)_2D_3$ measurement

$1,25(OH)_2D_3$ in placental perfusate samples was measured using the 1,25-dihydroxy vitamin D EIA kit (Immunodiagnostic systems; UK). In this kit $1,25(OH)_2D_3$ undergoes immunoextraction from the perfusate followed by quantification by enzyme immunoassay.

Lipids were removed from the perfusate by the process of delipidation. 30 µl of delipidation reagent 1 was added to 300 µl of perfusate sample or controls and vortexed. Samples were centrifuged at 2000 g, RT for 15 min. Immunocapsules containing a monoclonal antibody to $1,25(OH)_2D_3$ linked to solid phase particles in a gel suspension with vitamin D binding protein inhibitor were provided. The immunocapsules were vortexed and the solid phase allowed to settle to the bottom of the capsule. 100 µl of the delipidated samples were added to the immunocapsules and rotated at 15 rpm for 90 min at RT on a roller. The bottom stopper was removed from the immunocapsules, and immunocapsules placed in a 12 x 75 mm borosilicate glass tubes. Immunocapsules were centrifuged at 750 g for 1 min at RT to remove sample. 500 µl deionized water was added to the immunocapsules and again centrifuged at 750 g for 1 min at RT to wash contaminants from the gel. This wash step was repeated a further two times. Immunocapsules were next placed in clean borosilicate glass tubes. 150 µl of elution reagent 2 (ethanol) was added to the immunocapsules and allowed to incubate for 2 min, before centrifuging at 750 g for 1 min at RT to elute $1,25(OH)_2D_3$ from the column. This elution step was repeated a further two times collecting a total of 450 µl of sample. Immunocapsules were discarded and tubes containing samples placed in a heat block at 40°C. Samples were evaporated under a flow of nitrogen until the tube was completely dry. 100 µl assay buffer was added to tubes to dissolve dried samples. Samples had now been immunoextracted, and were ready for quantification by immunoassay.

100 µl of calibrators (standards) were added to borosilicate glass tubes. 100 µl of primary antibody solution (sheep anti-$1,25(OH)_2D_3$) was added to each calibrator and sample. Samples vortexed and incubated overnight at 4°C. 150 µl of each sample was added to a well of an anti-sheep IgG coated microplate. The plate was covered and incubated on an orbital shaker at 500 rpm for 90 min at RT, allowing $1,25(OH)_2D_3$ to bind to the plate. 100 µl of $1,25(OH)_2D_3$ biotin solution was added to each well and incubated on an orbital shaker at 500 rpm for 60 min at RT, binding any unbound antibody on the plate to biotin labelled $1,25(OH)_2D_3$. Wells were washed three times with 250 µl wash solution. 200 µl of enzyme conjugate containing avidin linked to horseradish peroxidase was added to each well and incubated at RT for 30 min. Wells were washed three times with 250 µl wash solution. 200 µl of TMB substrate was added to each well

and incubated at RT for 30 min. 100 µl of stop solution was added to all wells, and absorbance at 450 nm measured on a plate reader (Promega GloMax Discover).

A higher concentration of $1,25(OH)_2D_3$ in the sample reduced binding of biotin labelled $1,25(OH)_2D_3$ to the plate, reducing the subsequent colour change. Therefore greater absorbance at 450 nm indicates a lower $1,25(OH)_2D_3$ concentration. Concentration was calculated by determining the percentage binding (B/Bo%) of each sample according to the following equation:

$$B/Bo\% = \frac{(mean\ abs - mean\ abs\ substrate\ blank)}{(mean\ abs\ for\ '0'\ calibrator - mean\ abs\ substrate\ blank)} * 100$$

Concentration of $1,25(OH)_2D_3$ in samples was then determined by comparing the percentage binding to percentage binding of the calibrators standard curve. All samples were measured in singleton on the same plate and the intra-assay coefficient of variation was 20.13%.

2.8 B-human Chorionic Gonadotrophin quantification

The level of β-human chorionic gonadotrophin (β-hCG) produced by cultured cytotrophoblast cells (see section 2.5), was measured using a β-hCG ELISA Kit (DRG Diagnostics; Germany), as shown in Figure 2-9. This ELISA (enzyme-linked immunosorbent assay) works via the 'sandwich principle', in which β-hCG binds to a bound antibody on the plate, and is detected with an anti-β-hCG antibody conjugated to horseradish peroxidase.

Microtiter wells are coated with a mouse monoclonal antibody directed towards a unique β-hCG molecule antigenic site. 25 µl of standard, control and media samples from cultured cytotrophoblast cells were added to wells. β-hCG present in the media samples binds to the antibody and becomes attached to the plate. 100 µl of enzyme conjugate, containing a human anti-β-hCG antibody conjugated to horseradish peroxidase, was then added to the wells. The plate was shaken thoroughly on a plate shaker for 10 s, and then incubated for 60 min at RT. After incubation the contents of the wells was discarded, and the wells washed five times with 400 µl distilled water. This removes any unbound enzyme conjugate from the wells. 100 µl of substrate solution, containing a substrate of the horseradish peroxidase enzyme, was added to each well, and incubated for 15 min at RT. During this time the enzymatic reaction produces a blue colour in the wells. After incubation the reaction was stopped with the addiction of 50 µl of stop solution. This changes the colour of the solution in the wells to yellow. The absorbance of each well at 450 nm was then determined by reading on a plate reader (Promega GloMax Discover) within 10 min. A greater concentration of β-hCG results in a higher absorbance reading, and concentration calculated by measurement from a standard curve, as shown in Figure 2-8. Samples were run in duplicate with all samples on the same plate and the intra-assay coefficient of variation was 0.63%.

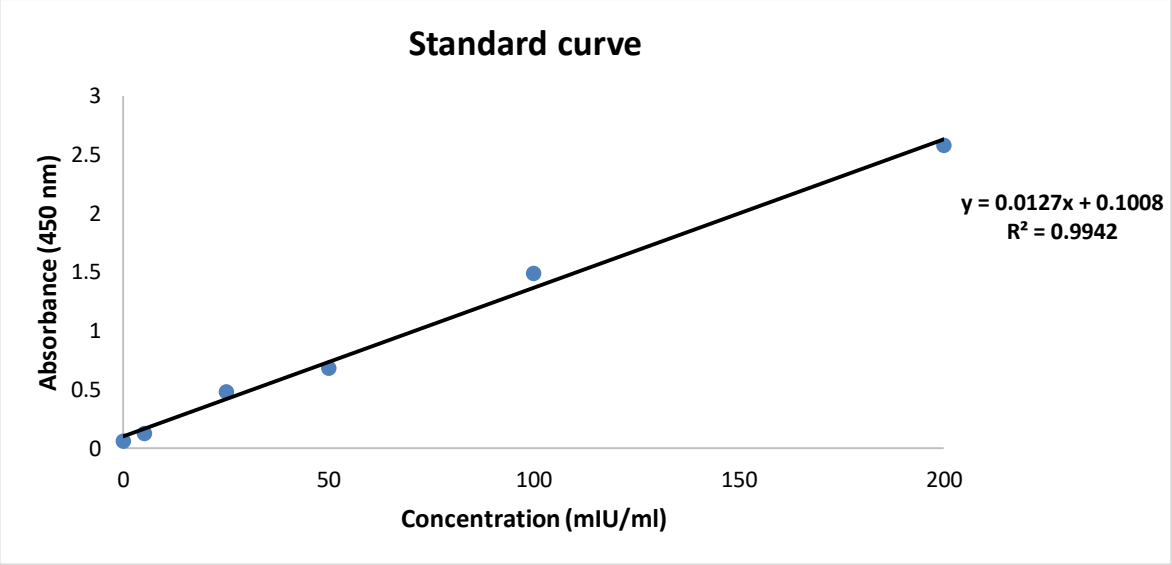

Figure 2-8 ***An example of a standard curve generated from the DRG β-hCG ELISA Kit.***

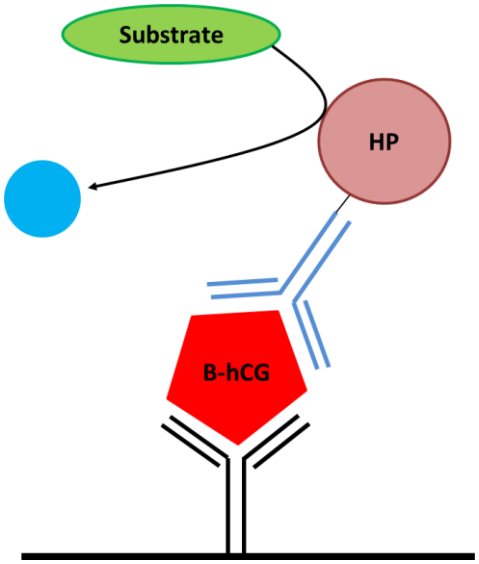

Figure 2-9 ***β-hCG ELISA diagram*** *β-hCG is measured via a sandwhich ELISA, in which the β-hCG molecule binds to an antibody bound to a microtitre well. An anti-hCG antibody conjugated to horseradish peroxidase (HP) is then bound to the β-hCG, and the addition of a substrate of HP produces a measurable change in colour.*

2.9 DNA and RNA

Analysis of DNA and RNA was used to identify and measure effects of 25(OH)D and $1,25(OH)_2D$ on placental tissue.

2.9.1 Tissue Crushing

Placental tissue that had been frozen and stored at -80°C from cohort studies and perfused cotyledons (see sections 2.2.2 and 2.3 respectively) was crushed to a fine powder. The crushing chamber is placed on dry ice and allowed to cool for a minimum of 15 min, as shown in Figure 2-10. The tissue sample is then removed from the freezer immediately on to dry ice. The top of the crushing chamber is dipped in liquid nitrogen, and then placed back on dry ice. A sample of tissue ~0.5 cm^3 is moved into the crushing chamber, and the top of the crushing chamber placed over the sample. A mallet is used to hit the top of the crushing chamber, forcing it into the chamber with the sample inside, and thus crushing the sample. The top of the crushing chamber is removed and the sample inspected. If the sample is a fine powder it is transferred from the chamber to pre-chilled cryovials for storage. If chunks of tissue are still present the top of the crushing chamber is replaced and the sample crushed until it reaches a fine powder. Tissue sample is kept frozen throughout.

Figure 2-10 ***Tissue crushing equipment*** *A) Crushing chamber. B) Crushing chamber assembled for use. C) Crushing chamber is cooled on dry ice prior to use.*

2.9.2 DNA extraction

DNA was extracted from crushed cohort study tissue (see sections 2.2.2 and 2.9.1), tissue fragments (see section 2.4), or cultured cytotrophoblast cells (see section 2.5). The Qiagen DNeasy Blood & Tissue Kit (Qiagen, UK) was used to carry out extractions, and all reagents and columns used were supplied in the kit.

Between 18 – 35 mg of frozen tissue, 3 fragments or 9 x 10^6 cells were placed into a pre-chilled, labelled 1.5 ml eppendorf tube and kept frozen on dry ice until all samples are weighed and ready for extraction. Samples were then processed as shown in Figure 2-11. Samples were removed from dry ice and placed into a rack at RT. 180 µl of buffer ATL was added immediately to each sample. Samples were mixed thoroughly by vortexing. 20 µl of proteinase K was added and samples were again mixed thoroughly by vortexing. Samples were next incubated at 56°C for between 1 and 3 h until completely lysed. Complete lysis was determined when no tissue fragments were left visible to the naked eye. After lysis samples were vortexed for 15 s, before adding 200 µl of buffer AL and again vortexing to mix. 200 µl of 100% ethanol was added and again mixed thoroughly by vortexing. At this stage a white precipitate formed in the samples. The whole sample, including precipitate, was moved on to a DNeasy Mini spin column placed in a 2 ml collection tube. The DNeasy Mini spin column contains a silica based membrane that binds DNA in the presence of a high concentration of chaotropic salt, which is provided by buffer AL. The sample was then centrifuged at 8000 rpm for 1 min and the flow-through and collection tube discarded. The spin column was placed in a new 2 ml collection tube, 500 µl of buffer AW1 was added to the spin column and centrifuged at 8000 rpm for 1 min. The flow-through and collection tube were discarded and the spin column placed in a new 2 ml collection tube. 500 µl of buffer AW2 was added to the spin column and centrifuged at 14000 rpm for 3 min. This step dried the DNeasy Mini spin column membrane to ensure residual ethanol is not present in the final product. The flow-through and collection tube were discarded and the spin column was placed in a new 2 ml collection tube. Buffers AW1 and AW2 remove contaminants such as proteins from the column, without disrupting DNA binding to the silica based membrane. The DNA was then eluted from the column in buffer AE (10 mmol Tris-Cl, 0.5 mmol EDTA, pH 9.0). 200 µl of buffer AE was pipetted onto the spin column and incubated at RT for 1 min. It was then centrifuged for 1 min at 8000 rpm to elute the DNA from the column. A further 200 µl of buffer AE was added to the spin column in a new collection tube, incubated for 1 min at RT, and centrifuged for 1 min at 8000 rpm to elute any remaining DNA on the column. The two eluted samples were not combined to prevent dilution of the more concentrated sample. Eluted DNA was stored at -20°C. For

samples with a low DNA yield, the volume of buffer AE was reduced to concentrate the eluted DNA.

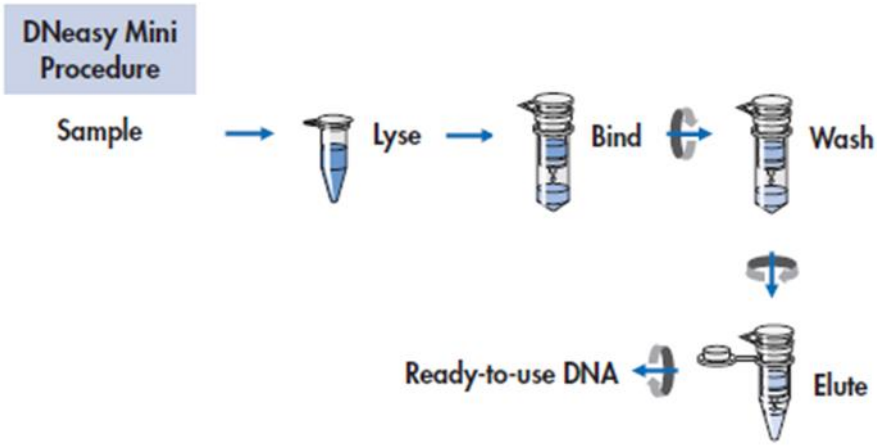

Figure 2-11 ***Qiagen DNeasy Blood and Tissue Kit*** *Procedure for extracting DNA from tissue and cells utilising the Qiagen DNeasy Blood and Tissue Kit. Adapted from the DNeasy Blood and Tissue Handbook.*

2.9.3 RNA extraction

RNA was extracted from crushed perfused placental cotyledons (see sections 2.3 and 2.9.1), tissue fragments (see section 2.4), or cultured cytotrophoblast cells (see section 2.5). Extraction was carried out using the Qiagen miRNeasy mini kit (Qiagen, UK), and all reagents and columns used were supplied in the kit.

Between 25-35 mg of frozen tissue, 3 fragments or 9 x 10^6 cultured cytotrophoblast cells were placed into a pre-chilled 2 ml eppendorf tube, keeping tissue frozen throughout. Samples were then processed as shown in Figure 2-12. 700 µl of QIAzol Lysis reagent was added to the tissue sample, and homogenised in 10 s bursts until tissue was completely homogenised (IKA T10 basic Ultra-Turrax ® homogeniser). When homogenisation was complete the sample was left to stand at RT for 5 min.

140 µl of chloroform (Acros Organics) was added to the sample, and the tube shaken vigorously for 15 s before being left to stand at RT for a further 3 min. The sample was then centrifuged for 15 min at 12000 rpm and 4°C. All centrifugation steps after this were carried out at RT. 350 µl of the upper aqueous phase was transferred to a clean tube, and 525 µl of 100% ethanol added. The sample was mixed thoroughly by pipetting up and down, at which stage a slight precipitate formed. 700 µl of the sample, including any precipitate, was transferred to an RNeasy mini spin column placed in a 2 ml collection tube. The sample was then centrifuged for 15 s at 8000 rpm and the flow through discarded. The remaining ethanol/aqueous phase sample was

added to the same RNeasy spin column and centrifuged for 15 s at 8000 rpm. Flow through was discarded. 350 µl of buffer RWT was added to the spin column and centrifuged for 15 s at 8000 rpm to wash contaminants from the membrane. Flow through was discarded. 80 µl of DNase I incubation mix (10 µl DNase I + 70 µl of Buffer RDD) was next added to the spin column, and left to sit at RT for 15 min to digest any remaining DNA. 350 µl of buffer RWT was added to the spin column, and centrifuged for 15 s at 8000 rpm. Flow through was discarded. 500 µl of buffer RPE was then added to the spin column and centrifuged for 15 s at 8000 rpm to wash contaminants from the column. Flow through was discarded. A further 500 µl of buffer RPE was added to the spin column and centrifuged for 2 min at 8000 rpm. The spin column was transferred to a clean 1.5 ml collection tube. 50 µl of RNase free water was added to the spin column and centrifuged for 1 min at 8000 rpm. Samples were stored at -80°C.

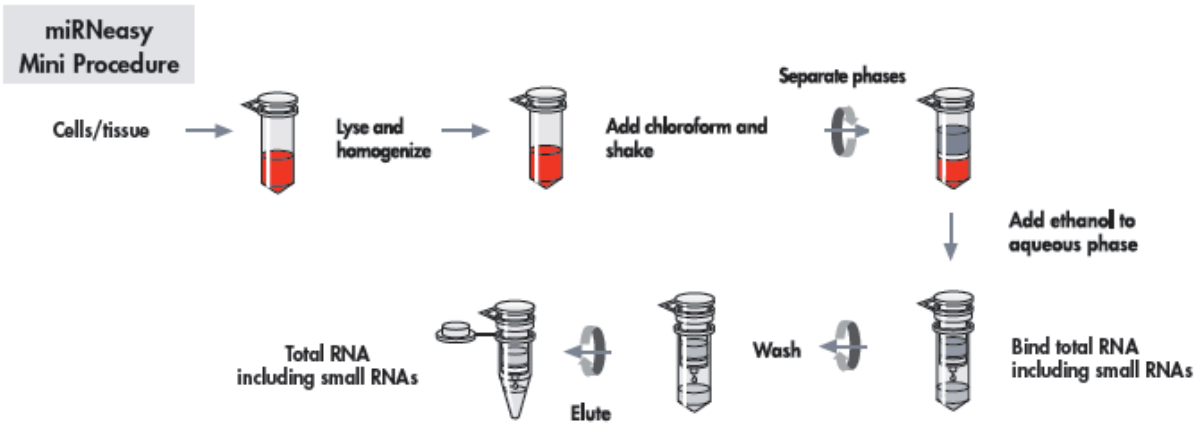

Figure 2-12 ***Qiagen miRNeasy mini kit*** *Procedure for extracting RNA from tissue and cells utilising the Qiagen miRNeasy mini kit. Adapted from Qiagen miRNease mini kit handbook*

2.9.4 Determination of DNA and RNA yield and quality

A Thermo Scientific Nanodrop 1000 Spectrophotometer (Thermo Scientific, UK) was used to determine the concentration and quality of DNA and RNA samples in solution.

The spectrophotometer was blanked by loading 1 µl of ddH_2O or elution buffer onto the pedestal and measuring the absorbance across the full range of wavelengths. For subsequent measurements this is subtracted from the value measured by the software to ensure background absorbance is not included in concentration calculations. 1 µl of sample is then loaded onto the pedestal and an absorbance spectrum measured. Concentration is calculated by the software using the Beer-Lambert equation:

$$A = E \times b \times c$$

Where A is absorbance represented in absorbance units, E is the wavelength dependent molar absorptivity coefficient, b is the path length in cm and c is concentration in moles/litre. The molar

absorptivity coefficient for DNA is A_{260} of 1.0 = 50 µg/ml of pure dsDNA, and for RNA A_{260} of 1.0 = 40 µg/ml. Values for the ratio of absorbance at 260/280 nm and 260/230 nm are also given. The 260/280 nm ratio indicates DNA/RNA purity. A value of around 1.8 indicates pure DNA/RNA, with values significantly lower than this indicating contamination with proteins, phenols or other substances absorbing around 280 nm. The 260/230 nm ratio also indicates DNA/RNA purity. Values in the range of 1.8 – 2.2 indicate pure DNA/RNA, with lower values suggesting co-purified contaminants.

2.9.5 Gel electrophoresis

Gel electrophoresis was also carried out to assess DNA and RNA quality. In gel electrophoresis molecules are separated based upon their size and charge. Nucleic acids such as DNA and RNA have a negative charge due to the presence of phosphate groups in their backbone. Therefore when DNA or RNA is placed in an agarose gel and an electric current is passed through the nucleic acid moves towards the positive electrode. The agarose in the gel forms a matrix, with higher concentration gels having smaller 'holes' within the matrix through which the DNA and RNA must pass. Smaller molecules are therefore less inhibited passing through the gel and will move further towards the positive electrode, separating the nucleic acid based upon its size. For DNA 0.8% agarose gels and for RNA 1% agarose gels were used.

Agarose (Sigma) and 1 x Tris Borate EDTA (TBE; Fisher Scientific) were mixed together and heated until the agarose dissolved. 14 µl of GelRed™ (Biotium) was added per 100 ml of gel so nucleic acids could be visualised under UV light once the gel had run. The gel was poured into a mould whilst still warm and left to set. When set the gel was moved to the electrophoresis tank, and the tank filled with 1 x TBE buffer. For each DNA sample 250 ng of DNA was diluted with 3 µl of loading dye (Ambion) and ddH_2O to a total volume of 15 µl and loaded onto the gel. For each RNA sample 250 ng of RNA was diluted with 2 µl of loading dye, 2 µl of deionised formamide to a volume of 12 µl and loaded on to the gel. DNA and RNA gels were ran at 100 V for approximately 1 h or 40 min respectively. Gels were then removed from the tank and visualised under UV light. For good quality DNA, one clear band is expected, and for RNA two bands, corresponding to 28S and 18S ribosomal RNA (rRNA), as shown in Figure 2-13.

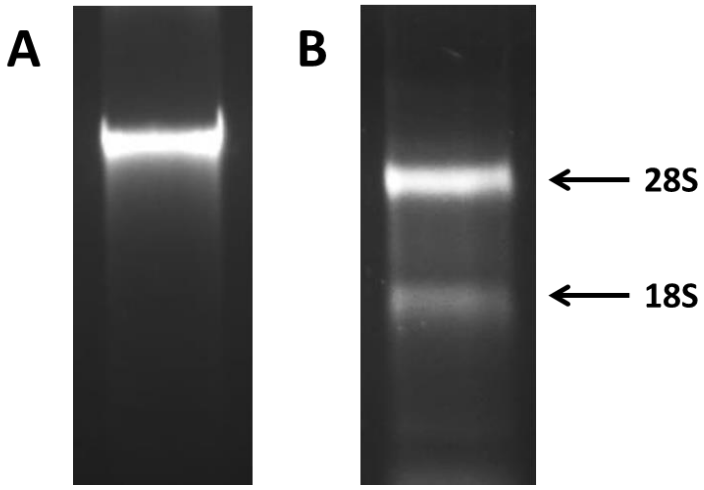

Figure 2-13 ***Example gel electrophoresis images*** *A) DNA gel. B) RNA gel, with bands representing 28S and 18S rRNA.*

2.9.6 Reverse transcription

To generate DNA from RNA, obtained as described in section 2.9.2, reverse transcription was carried out, generating complementary DNA (cDNA). Random primers bind to complementary sequences throughout the RNA, and reverse transcriptase's elongate the primers, producing cDNA.

All reagents used in this protocol were obtained from Promega (UK). 12 µg of RNA was added to 250 ng of random primers and made up to a volume of 7 µl with ddH_2O. Samples were briefly vortexed and centrifuged to equilibrate. Samples were heated for 5 min at 70°C (Veriti 96 well thermal cycler; Applied Biosystems), to melt secondary structures which may be present in the RNA. Samples were briefly vortexed and centrifuged. To each sample 2.5 µl of Moloney Murine Leukaemia Virus (M-MLV) 5X Reverse Transcriptase Buffer, 0.5 mmol/L PCR nucleotide mix, 12.5 units Recombinant RNasin® Ribonuclease Inhibitor, 100 units M-MLV Reverse Transcriptase were added and up made to a volume of 12.5 µl with ddH_2O. To prevent small volumes resulting in pipetting error a master mix was created to add these components to the samples. Samples were briefly vortexed and centrifuged to equilibrate, then heated at 37°C for 60 min to allow the reverse transcriptase to elongate the annealed primers. The temperature was then increased to 95°C for 10 min to inactivate the reverse transcriptase enzyme.

In addition to the reverse transcription of the samples, no enzyme controls (NECs) and coefficients of variation (CV) controls were also transcribed. NECs control for the presence of genomic DNA, and were made as described above except for the addition of extra ddH_2O in the place of M-MLV Reverse transcriptase. CV controls test for experimental variation. A small volume of RNA from multiple samples was pooled, and separated into six samples. These were all reverse transcribed alongside the sample set. Samples were briefly centrifuged and stored at -20°C.

2.9.7 Quantitative reverse transcription polymerase chain reaction

Quantitative reverse transcription polymerase chain reaction (qRT-PCR) was carried out to compare the messenger RNA (mRNA) levels of specific genes between samples, relative to HKG. qRT-PCR was carried on a Roche Lightcycler 480 using Roche Universal Probe Library (UPL; West Sussex, UK) or Perfect Probe (Primer Design, Southampton, UK) designed assays, with 2X MasterMix (Roche LightCycler 480 Probes 2X concentration MasterMix). For each qRT-PCR assay samples were run in triplicate with NECs, no template controls (NTCs) and CV controls to control for genomic DNA contamination, reagent contamination and experimental variation respectively. To calculate the concentration of cDNA for each gene 7 standards containing a known concentration were also run. Standards were generated from a pooled RNA stock and diluted as described in Table 2-6. Primers were designed using the Roche Universal Probe Library Assay Design Centre (https://lifescience.roche.com/en_gb/brands/universal-probe-library.html#assay-design-center).

Table 2-6 *Standard curve dilutions and concentration for qRT-PCR.*

Standard	Dilution		Concentration (ng/5µl)
S7	30 µl stock		100
S6	15 µl S7	15 µl ddH_2O	50
S5	15 µl S6	15 µl ddH_2O	25
S4	15 µl S5	15 µl ddH_2O	12.5
S3	15 µl S4	15 µl ddH_2O	6.25
S2	15 µl S3	15 µl ddH_2O	3.125
S1	15 µl S2	15 µl ddH_2O	1.5625

In this study three HKGs were used to normalise qRT-PCR data, as previously recommended for use in placental tissue (Cleal et al., 2009). HKGs were selected using the GeNorm HKG selection kit to identify the most stable HKGs in placental tissue and with 25(OH)D treatment by Dr Claire Simner, and displayed in Table 2-7. For each HKG tested the expression stability (M-value) was calculated and the genes were ranked in order of stability, with a higher M-value indicating a less stably expressed gene. Dr Simner then generated a value called the V score, which indicated how the normalisation factor changes upon addition of another gene. A V score of 0.15 or less indicates that the addition of an extra HKG would have no significant effect on normalisation factor and therefore is not necessary. This study therefore established that three

HKGs were preferred and these were UBC, YWHAZ and ATP5B (M-values < 0.2). The geometric mean of the HKGs was then used as the normalisation factor for the qRT-PCR in the current study.

Table 2-7 *Housekeeping genes used for qRT-PCR normalisation.*

Gene	Gene name	Accession number (GenBank)
UBC	Ubiquitin C	NM_021009
YWHAZ	Tyrosine 3-Monooxygenase/Tryptophan 5-Monooxygenase Activation Protein Zeta	NM_003406.3 NM_145690.2 NM_001135699.1 NM_001135700.1 NM_001135701.1 NM_001135702.1
ATP5B	ATP synthase	NM_001686

The qRT-PCR assay cycles through a number of temperatures to amplify the cDNA. An initial high temperature is applied to activate the polymerase, followed by a number of cycles of three temperatures to denature double stranded cDNA, allow the primers to anneal and for strand elongation. qRT-PCR reaction components and cycling conditions are described in Table 2-8 and 2-9 respectively.

Table 2-8 *PCR components used in Perfect Probe and Roche UPL assays.*

PCR component	Perfect Probe	Roche UPL
Master Mix stock (Roche, SUI)	5 µl	5 µl
Forward Primer (200 nM)	N/A	0.3 µl
Reverse Primer (200 nM)	N/A	0.3 µl
Probe (100 nM)	N/A	1.3 µl
Primer/Probe mix	0.5 µl	N/A
cDNA (4 ng/µl)	3 µl	3 µl
ddH_2O	1.5 µl	N/A
Total volume	10 µl	10 µl

N/A = not applicable. UPL = Universal Probe Library

Table 2-9 *qRT-PCR cycling conditions for Perfect Probe and Roche UPL assays.*

Cycling condition	Perfect Probe	Roche UPL
Polymerase activation	95°C for 10 min	95°C 10 min
Amplification	50 cycles of: 95°C for 10 s 50°C for 30 s* 72°C for 15 s	45 cycles of: 95°C for 10 s 60°C for 30 s 72°C for 1 s*
Cooling	50°C for 30 s	40°C for 1 s

** indicates data collection step. UPL = Universal Probe Library*

Crossing point (Cp) values were determined for each sample by the Roche Lightcycler 480 software using the Second Derivative maximum method. In this method the point at which the acceleration of the fluorescence signal is at its maximum on the amplification curve is taken as the Cp value. The second derivative of a function at a point on a curve tells you whether the curve is concave in an up or downwards direction at that point. Therefore the maximum second derivative value of the amplification curve is where the fluorescence signal is increasing at its maximum acceleration for the reaction. This method gives a Cp value in the middle of the log linear phase of the amplification curve.

The Cp values were then plotted against known log cDNA concentrations from the standard curve as shown in Figure 2-14. A concentration of cDNA for each sample was calculated using the

equation x = 10^((y-c)/m), where y refers to the sample Cp value, m to the gradient of the line and c to the y intercept.

cDNA concentration for samples and CV controls were then divided by the geometric mean of the HKGs. The coefficient of variation of the 6 CV controls was then calculated using the equation:

CV = (Standard deviation / mean) x 100

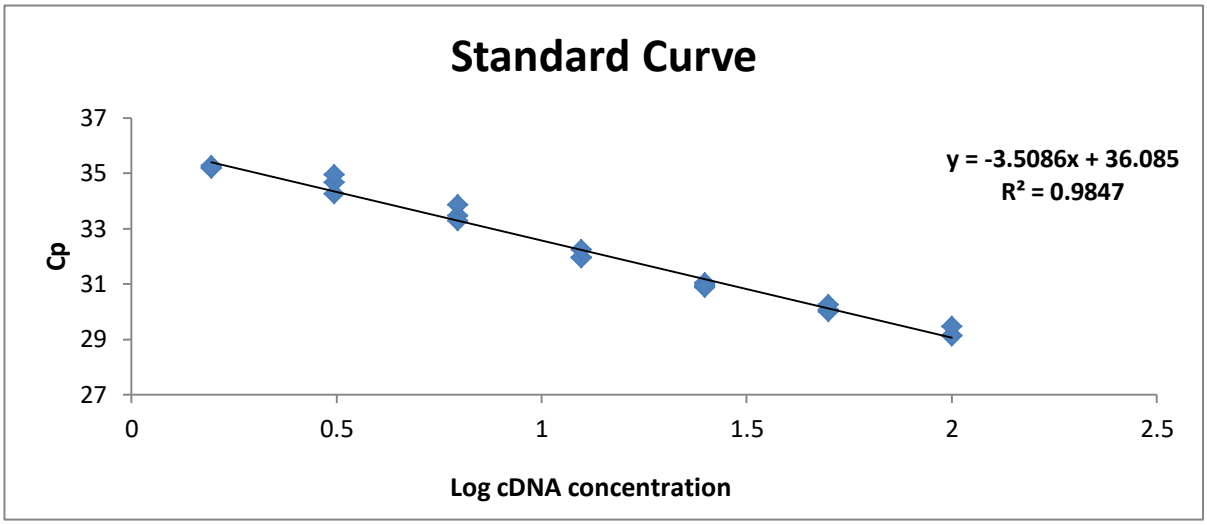

Figure 2-14 ***A representative example of a qRT-PCR standard curve***

2.10 Array data

2.10.1 Illumina 850K DNA methylation

DNA methylation analysis was carried using the Infinium® MethylationEPIC array at Barts and the London School of Medicine and Dentistry Genome Centre, on placental villous fragment samples (see section 2.4). The Infinium® MethylationEPIC quantifies the methylation status of over 850,000 cytosines within CpGs in the human genome, sampling 95% of CpG islands, 99% RefSeq promoters, and with coverage across the gene body. DNA underwent bisulphite conversion, in which unmethylated cytosine residues are converted to uracil, and methylated cytosines are not affected. Whole genome amplification was then carried out, in which uracil residues are converted to thymine. This allows for the distinction of methylation status at known methylation sites. Methylated sites will present with a cytosine base, and unmethylated a thymine base.

Over 850,000 individual CpG sites were then analysed for their methylation status using two Illumina Infinium Bead Chip assays, as shown in Figure 2-15. Beads display many target specific probes which allow investigation of individual CpG sites in bisulphite converted DNA. The Infinium I assay presents two 50 bp probes for each CpG site, one for methylated and one for unmethylated. The 3' terminus of the probe targets either the cytosine of a methylated site or the thymine of an unmethylated site. The Infinium II assay presents only one probe for each CpG locus. The 3' terminus of the probe binds the nucleotide directly upstream of the CpG site, and extension with either a labelled guanine or adenine base determines methylation status. Collectively these allowed for the investigation of methylation status at CpG sites present in CpG islands, CpG shores, CpG shelves as well as miRNA promoter regions.

Methylation data as β-values were normalised and differentially methylated CpGs were identified by a Wilcoxon signed-rank test with control versus vitamin D treated by Dr Faisel Rezwan. Initially data was filtered based on a probability of 5% and pathway analysis was carried out using Toppgene (Division of Bioinformatics, Cincinnati Children's Hospital Medical Centre). Data was then further filtered to a probability of 1% and pathway analysis carried out using GREAT V3.0.0 (http://great.stanford.edu/public/html/index.php, Bejerano Lab, Stanford University) by Dr Christopher Bell.

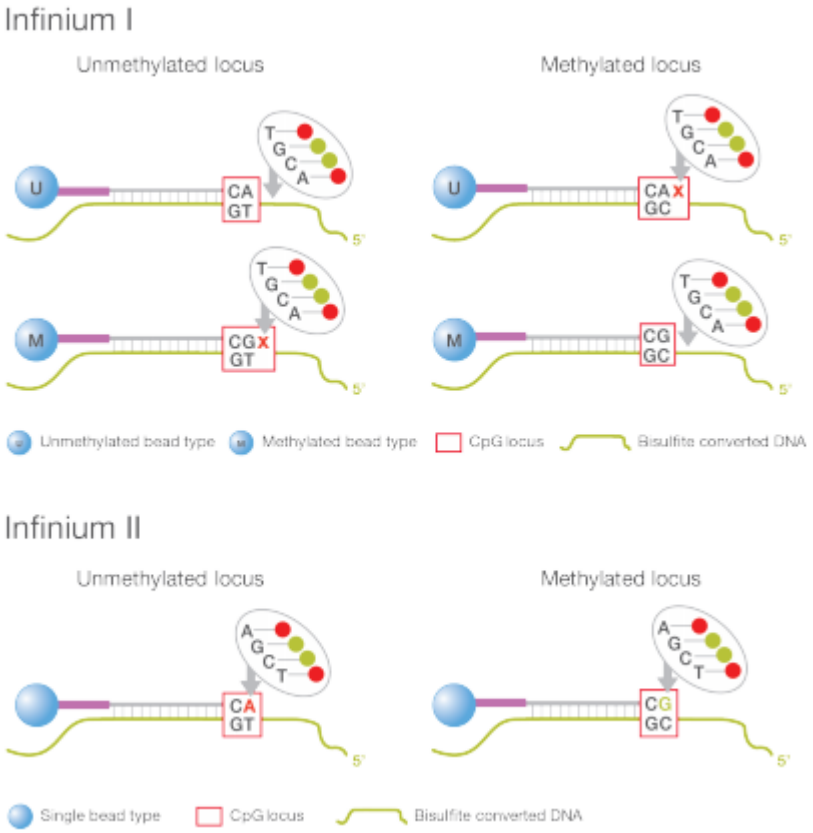

Figure 2-15 Illumina Infinium bead chip assays, Infinium I and II *The Infinium I assay presents two probes for each CpG site, one targeting the methylated CpG and one the unmethylated. The Infinium II presents only one probe per CpG site, targeting the nucleotide directly upstream of the site and performing a base extension with a labelled nucleotide to determine methylation status.*

2.10.2 RNA sequencing

RNA expression was investigated using stranded RNA sequencing (RNAseq; Expression Analysis, Durham, North Carolina, USA), using HiSeq 2x 50 bp paired-end sequencing on an Illumina platform in placental villous fragment samples (see section 2.4).

cDNA synthesis was carried out using the Illumina TruSeq Stranded mRNA sample preparation kit. Total RNA is purified to select for polyadenylated RNA (mRNA and some non-coding RNAs), before being heat fragmented in the presence of divalent cations. Double stranded cDNA is synthesised, with deoxyuridine triphosphate (dUTP) instead of deoxythymidine triphosphate (dTTP) present in the second strand master mix. An adenine residue is added to the cDNA and a barcode sequence attached via ligation. cDNA is amplified via PCR, during which the polymerase stalls at a dUTP base preventing second strand amplification, and preserving strand information.

The resultant library is quantified, normalised and pooled, before being bound to the surface of a flow cell. Each bound template molecule undergoes clonal amplification up to 1000 fold, creating individual clusters. The sequence is then determined by allowing the four fluorescently labelled nucleotides to flow over the flow cell, and be incorporated into the attached nucleic acid chains. Only a single nucleotide may be incorporated per cycle, as each nucleic acid acts as a polymerisation terminator. Fluorescence is measured for each cluster, before the dye is enzymatically cleaved and the next cycle begins.

After obtaining the sequencing data, Dr Cory White carried out demultiplexing, in which reads containing multiple barcodes were corrected or removed. Sequences were then clipped and trimmed to remove barcode sequences and poor quality bases at the ends of reads. Reads were mapped to hg38 (Ensemble; March 2017) using HISAT2 v2.0.5, and counted with HTSeq v0.6.1p1 using “union mode” and “stranded=reversed settings”.

Genes were filtered based upon counts per million (CPM) and genes with < 1 CPM in at least half of the samples were removed. Samples were normalized using the trimmed mean of M-values (TMM) method, and median plots demonstrated no samples outside two standard deviations. Differential expression analysis was carried out using EdgeR (Robinson et al., 2010).

2.10.3 Proteomics

Protein expression was investigated using LCMS to determine what proteins were present and at what level in villous tissue samples by Dr Antigoni Manousopoulou. The use of LCMS allows for the un-biased investigation of all detectable proteins in the sample, including those of which we have no prior knowledge of their relationship with vitamin D.

Frozen placental fragment samples (see section 2.4) were dissolved in triplicate in a buffer of 0.5 M triethylammonium bicarbonate and 0.05% sodium dodecyl sulphate before homogenisation using the FastPrep system (Savant Bio, Cedex, Fr). Samples were subjected to pulsed probe sonication (Misonix, Farmingdale, NY, USA), and lysates centrifuged at 16000 g for 10 min at 4˚C. The protein content from the supernatant was measured using the Direct Detect™ Spectroscopy system (Merck Millipore, Darmstadt, Germany). Lysates were then reduced, alkylated and subjected to trypsin proteolysis. Peptides were labelled using the eight-plex iTRAQ reagent kit (iTRAQ AbSciex, San Hose, CA, USA), then pooled and fractionated with high-pH reversed-phase (RP) chromatography. Resulting fractions were LCMS analysed with low-pH RP capillary chromatography (PepMap C18, 50 µm ID × 50 cm L, 100 Å pore, 3.5 µm particle) and nanospray ionization FT-MS (Ultimate 3000 UHPLC – LTQ-Velos Pro Orbitrap Elite, Thermo Scientific, Bremen, DE).

To analyse, unprocessed raw files were submitted to Proteome Discoverer 1.4 for target decoy searching against the UniProtKB homo sapiens database comprised, of 20,159 entries (release date January 2015). Parameters allowed for up to two missed cleavages, a precursor mass tolerance of 10 ppm, a minimum peptide length of six and a maximum of two variable (one equal) modifications of; iTRAQ 8-plex (Y), oxidation (M), deamidation (N, Q), or phosphorylation (S, T, Y). Methylthio (C) and iTRAQ (K, Y and N-terminus) were set as fixed modifications. False discovery rate (FDR) at the peptide level was set at < 0.05. The percent co-isolation excluding peptides from quantitation was set at 50. Reporter ion ratios from unique peptides only were taken into consideration for the quantitation of the respective protein. A permutation test using the normalised iTRAQ ratios of each vitamin D treated placenta compared to its respective control. Significance was set at $p < 0.05$. In adherence to the Paris Publication Guidelines for the analysis and documentation of peptide and protein identifications (http://www.mcponline.org/site/misc/ParisReport_Final.xhtml), only proteins identified with at least two unique peptides were further subjected to bioinformatics.

2.11 Cytotrophoblast imaging

Cytotrophoblast cells cultured for 18 h or 90 h and fixed as described in section 2.5.2 were imaged to determine if syncytialisation had occurred.

Cells, stored at 4°C under PBS, were washed three times with PBS. 2 ml of 2% BSA in PBS was added to each well and incubated for 60 min at RT to block nonspecific binding. Cells were washed three times with 2 ml PBS. 1 ml PBS was added to control wells. 1 ml Desmoplakin at 1/100 dilution (mouse anti-human Desmoplakin I+II, Abcam ab16434) was added to each experimental well. Cells were incubated overnight at 4°C. Cells were washed three times for 5 min each with 2% BSA in PBS. 1 ml of DAPI at 1/250 dilution (Sigma Aldrich D9542) + Alexa Fluor 568 at a 1/500 dilution (goat anti-mouse IgG H&L, Abcam ab175473) was added to each well. Cells were incubated for 2 h at RT. Cells were washed three times in PBS. Cells stored under 2 ml PBS in the dark at 4°C until imaging.

Once stained, cells were imaged using a Leica SP8 confocal microscope, as shown in Figure 2-16. A laser providing excitation light is reflected off a dichromatic mirror, towards two further mirrors which direct the laser beam onto the sample. Movement of these mirrors scans the laser beam across the sample. Fluorescent dyes in the sample which are excited at the wavelength of the laser beam emit photons, which are then reflected back along the path of the mirrors, through the dichromatic mirror, and through a pinhole which focuses the light onto a detector. The detector is attached to a computer, and an image is built up as the laser beam is scanned across the sample.

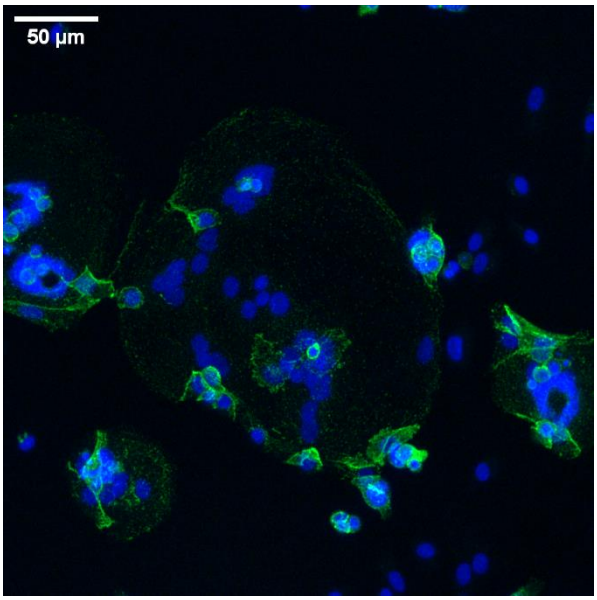

Figure 2-16 ***A representative image of cytotrophoblast cells cultured for 90 h*** *Cells stained with DAPI (nuclei; blue) and desmoplakin (green) before confocal imaging.*

2.12 Histone mark measurement

2.12.1 Histone extraction

Histones were extracted from crushed SPRING placental tissue (see sections 2.2.2 and 2.9.1) and villous fragments (see section 2.4) using the EpiQuik™ total histone extraction kit (Epigentek, USA). 30 mg of crushed or fragmented tissue was placed in a Dounce homogeniser with 0.5 ml of pre-lysis buffer, and tissue disaggregated with 60 strokes. The homogenised mixture was transferred to a 2 ml eppendorf tube and centrifuged at 10000 rpm for 1 min at 4°C. Supernatant was removed and discarded. The pellet was resuspended in 200 µl lysis buffer and incubated on ice for 30 min to lyse cells. After incubation the solution was centrifuged at 12000 rpm for 5 min at 4°C, and the supernatant (containing acid-soluble proteins), moved into a fresh tube. 60 µl of balance-dithiothreitol (DTT) buffer was added immediately to the supernatant, and protein concentration quantified with a BCA assay. Balance buffer is pH optimised for protein stability and DTT reduces disulphide bonds.

Histone protein concentration was measured using the Pierce™ Bicinchoninic Acid (BCA) Kit for Protein Determination (Thermo Scientific). In this assay peptides of three or more amino acid residues chelate with Cu^{2+} ions in an alkaline environment, producing Cu^{1+}, and a characteristic blue colour. BCA reacts with Cu^{1+} and produces a purple colour. This gives a linear increase in 562 nm absorption with increasing protein concentration.

25 µl of standard or sample was pipetted into a 96 well plate in duplicate. 200 µl of working reagent (50:1 Reagent A:B) was added to each well, the plate was mixed on a plate shaker for 30 sec and then covered and incubated for 30 min at 37°C. The plate was cooled and the absorbance measured at 562 nm on a plate reader (Promega GloMax Discover), and a standard curve used to determine concentration.

2.12.2 Histone methylation/acetylation measures

Measurement of histone methylation/acetylation at specific marks was carried out using purified histone proteins obtained as described in section 2.12.1 and using the EpiQuik™ Global Methyl/Acetyl Histone Quantification Colourimetric Kits (Epigentik). In this assay the targeted methylation or acetylation mark is captured to the well with an antibody. The captured histone is then bound by a labelled antibody and a measurable colour change produced.

50 µl of antibody buffer was added to each well of a 96 well plate. 300 ng of histone extract was added for each sample into a well, and 50 µl of standard control at concentrations 1-100 ng/µl added to generate a standard curve. Samples were covered, mixed thoroughly on a plate shaker and then incubated for 2 h at RT. The solution discarded from the wells, and these were washed three times with 150 µl wash buffer. 50 µl of detection antibody was added per well and incubated for 1 h at RT on an orbital shaker (100 rpm). Wells were again emptied and washed three times with 150 µl wash buffer. 100 µl of colour developer was added and incubated for 2-10 min at RT away from light. When colour turned a medium blue 50 µl of stop solution was added to each well, turning the samples a yellow colour. Absorbance at 450 nm was measured on a plate reader within 2-15 min, and the standard curve used to determine the amount of the methylation/acetylation mark being measured.

2.13 DNA methylation pyrosequencing measures

DNA samples (see section 2.9.2) from MAVIDOS and SPRING placental samples, 25(OH)D treated fragments and cultured cytotrophoblasts (see sections 2.2.2, 2.4 and 2.5.2 respectively) DNA underwent bisulfite conversion, PCR amplification and pyrosequencing to identify sites of DNA methylation. Bisulfite conversion, PCR and pyrosequencing was carried out by Nevena Krstic.

2.13.1 Bisulfite conversion

Bisulfite conversion can be used to analyse DNA methylation by deaminating cytosine residues to uracil, while leaving 5-methylcytosine residues intact. Downstream PCR then recognises uracil residues as thymine residues, changing the DNA sequence at unmethylated cytosine residues, whilst methylated sites remain the same.

DNA was bisulfite converted using the EZ-96 DNA Methylation-Gold Kit (Zymo Research; California, USA), as shown in Figure 2-17. 1 µg of DNA in a volume of 20 µl was added to 130 µl of CT conversion reagent, mixed and placed in a thermal cycler for 10 min at 98 °C, 2.5 h at 64 °C, and up to 20 h at 4 °C. Samples were placed in a spin column plate inside a collection plate, and 600 µl binding buffer added per well. The plate was centrifuged for 30 sec at 10000 rpm and flow through discarded. 100 µl wash buffer was added and the plate centrifuged for 30 sec at 10000 rpm with flow through discarded. 200 µl desulphonation buffer was added, incubated for 15 min at RT, and centrifuged for 30 sec at 10000 rpm, with flow through discarded. Wells were washed twice with 200 µl wash buffer and centrifuged for 30 sec at 10000 rpm with flow through discarded. The spin column plate was placed over an elution plate, with 30 µl elution buffer added per well and incubated for 1-2 min at RT. Following centrifugation for 30 sec at 10000 rpm the eluted DNA was stored in 2 µl aliquots at -20 °C.

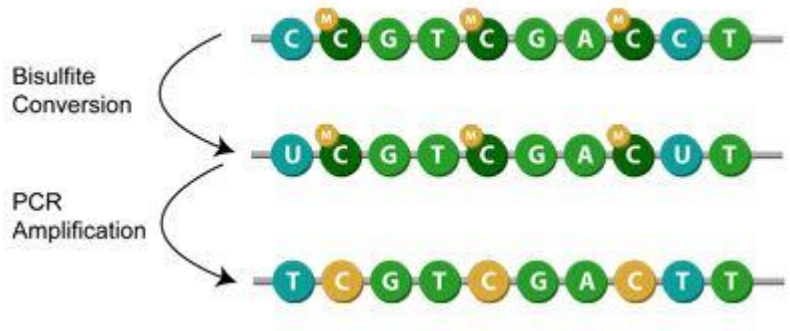

Figure 2-17 ***Bisulfite conversion of DNA*** *During bisulfite conversion unmethylated cytosine residues are converted to uracil, whilst methylated cytosine residues are unaffected. PCR amplification recognises the uracil residues as thymine thus changing the DNA sequence at unmethylated cytosine residues. Figure adapted from www.epigentek.com*

2.13.2 PCR amplification

PCR was prepared in a DNase free fume hood. 48 µl of mastermix (see Table 2-10) was added to 2 µl of bisulfite converted DNA. Plates were capped and covered in a thermos-safe seal, then placed in a thermal cycler for 45 cycles of amplification (see Table 2-11). Each plate contained three Promega controls, three Roche controls, a 0% methylated control, a 100% methylated control and three NTCs. After amplification 5 µl of each DNA sample was added per well of a 0.8% agarose gel and electrophoresis carried out at 100 V for 20 mins. Visualisation under UV light determined if amplification was successful and if contaminants were present.

Table 2-10 *Composition of mastermix used in the PCR amplification of bisulfite converted DNA samples.*

Reagent	Volume (µl)
Buffer	5
Forward Primer (10 µmol)	1
Reverse Primer (10 µmol)	1
dNTPs (10 µmol)	1
Hotstar Taq	0.25
dH_2O	39.75
Bisulfite DNA	2

Table 2-11 *Cycling conditions for the PCR amplification of bisulfite converted DNA samples.*

Temperature (°C)	Time	Cycles
95	5 mins	1
95	30 sec	45
60	30 sec	
72	1 min	
72	10 min	1
4	∞	

2.13.3 Pyrosequencing

10 µl of bisulfite converted and PCR amplified DNA was aliquoted into a plate with 30 µl water, 30 µl of binding buffer and 2 µl sepharose beads. Plate was continuously shaken until it was passed through the PyroMark workstation as per manufacturer's instructions. Beads were released into 0.5 µl of 10 µmol sequencing primer and 11.5 µl annealing buffer. The plate was heated to 80 °C then left to cool for 2 min before pyrosequencing occurred. Amplicons and sequencing primers are described in Table 2-12.

Table 2-12 *Amplicons and sequencing primers used in pyrosequencing.*

Gene		Amplicon		Sequencing Primer
RXRα	RXRα 0-5	F: TGGGAAGGTTGAAGGTTTTAGAA	RXRα 0-3	GTTATTTTTTGTTTTAGAGAT
		R: AACACAAAAACTAAATATAAACCCAAATCT	RXRα 4-5	AGAAGGGTTTTTTGTTTTTAA
	RXRα 6-7	F: GGAAGGTTGGGTTGAAGTGT	RXRα 6	GTTGTTGGTGTTTGGA
		R: ACCCACATAAAAATCTATCTACATATACC	RXRα 7	GTGTTTGAGGTTATTTTTTAATAG
	RXRα 8-12	F:TGGGATTATTGGTTTTTGAGTTAGGT	RXRα 8-11	CCCAACCTTCCCACC
		R: CCCACTATTAAAAAATAACCTCAAACACTT	RXRα 12	CCTACTACTCCTTCTCT

2.14 Data analysis

Data were analysed using IBM® SPSS® Statistics Version 20 (IBM®, Armonk, New York, USA). Graphs were created in GraphPad Prism 6 (GraphPad Software Inc., California, USA) or Microsoft Excel 2010. All data were tested for normal distribution before further statistical analysis. Normal distribution was assessed by analysis of frequency histograms as well as the skewness statistic. A skewness value between -1.0 to +1.0 was considered normally distributed. Non-normally distributed data were log transformed or square rooted and then re-tested for normal distribution. Data that were still not normally distributed were analysed using non-parametric methods. All normally distributed data were analysed using parametric statistical tests. For all statistical tests a p value of ≤ 0.05 was considered statistically significant. Data are presented as mean ± standard error of the mean (SEM) unless otherwise stated.

2.14.1 Array based data

DNA methylation

The Illumina 850K methylation array data was not normally distributed, and so a non-parametric Wilcoxon signed-rank test with control verses vitamin D treated was used. Data were filtered to a probability of 1% and pathway analysis carried out using GREAT V3.0.0 (http://great.stanford.edu/public/html/index.php, Bejerano Lab, Stanford University) by Dr Christopher Bell.

RNA sequencing

Raw data were analysed by Dr Cory White. Data were mapped to hg38 (Ensemble, March 2017), normalised, and differential expression determined using EdgeR (Robinson et al., 2010). Data were filtered to a Benjamini & Hochberg (B&H) FDR corrected probability of 5%. Genes with altered expression were mapped to pathways using Toppgene (Division of Bioinformatics, Cincinnati Children's Hospital Medical Centre). Pathways accepted with a minimum hit count of 4 and B&H FDR corrected q value of ≤ 0.05.

Proteomics

Differential expression of peptides with vitamin D treatment was determined by Dr Spiros Garbis and Dr Antigoni Manousopoulou. Permutation testing was carried out in which 3 out of 4 permutations with a probability of 5% was accepted as differentially expressed. Genes with

altered protein expression were mapped to pathways using MetaCore (Clarivate; USA). Pathways accepted with a B&H FDR corrected q value of ≤ 0.05.

2.14.2 Gene expression data

Gene expression was measured using qRT-PCR, as described in section 2.9.7. qRT-PCR data was normalised to HKG expression, and is presented as relative expression to HKG. Expression was tested for normal distribution, and if not normally distributed the log transformed or square rooted and re-tested. Data from these experiments required the comparison of two groups; control treated and vitamin D treated, so were analysed using a Student's t-test.

2.14.3 Epigenetic histone mark measures

Data were tested for normal distribution, and if not normally distributed log transformed and re-tested. Fragment samples were matched between treatment groups and therefore analysed by paired Student's t-test. SPRING samples were unmatched and therefore analysed by independent Student's t-test.

2.14.4 Pyrosequencing data

DNA methylation at CpG sites within the RXRα promoter were measured by pyrosequencing in placental fragment, cytotrophoblast cells, MAVIDOS and SPRING placenta samples. Data were tested for normal distribution, and if not normally distributed log transformed and re-tested. Cytotrophoblast and placental fragment samples were matched between treatment groups and therefore analysed by paired Student's t-test. MAVIDOS and SPRING placental samples were unmatched and therefore analysed by independent Student's t-test.

2.14.5 MAVIDOS data

MAVIDOS data was analysed by linear regression by Dr Stefania D'Angelo. Associations between maternal metabolites concentrations and placental DNA methylation were analysed with metabolite concentration as the predictor. Associations between placental DNA methylation and gene expression were analysed with DNA methylation as the predictor. Associations between placental gene expression and offspring body composition were analysed with gene expression as the predictor. The β-value gives the amount of change in the outcome with one unit change in the predictor. Data are presented as β-values, and were adjusted for appropriate variables.

2.14.6 Power (retrospective calculations)

Gene expression changes were measured in cultured cytotrophoblast and fragment samples. To determine the power reached in these studies a retrospective power calculation was carried out using the Inference for means software (University of British Columbia; www.stat.ubc.ca/~rollin/stats/ssize/n2.html). With a minimum 3-fold change in gene expression, and an average standard deviation of 5, 40% power was reached in this study. 11 samples per group would be required to obtain 80% power.

Chapter 3 The metabolism of vitamin D within the human placenta

3.1 Introduction

The placental transfer of maternal nutrients to the fetus is vital for optimal fetal growth and development. Nutrients can pass from the maternal to the fetal circulations by passive diffusion, facilitated diffusion or active transport, depending on the physical properties of the nutrient and the presence of appropriate transport proteins on the microvillous membrane (MVM) and basal membrane (BM). The placenta regulates transfer of nutrients to the fetus through a number of mechanisms, including selective uptake of substances into the placenta, transporter density and metabolism. Metabolism allows the placenta to utilise nutrients to meet its own demands, or to modify the pool of nutrients available for transfer to the fetus by degrading abundant compounds and synthesising nutrients in demand from precursors. Several nutrients required for fetal growth are known to be metabolised by the placenta, regulating their availability to the fetus and for usage by the placenta itself. Nutrients metabolised by the placenta include glucose, amino acids and fatty acids (Gallo et al., 2016, Hauguel-de Mouzon and Shafrir, 2001, Schneider, 2015). Maternal vitamin D is required by the fetus, and has been associated with fetal growth (Harvey et al., 2014a). Maternal vitamin D must therefore be transferred across the placenta to the fetus. However, how the placenta metabolises and regulates vitamin D transfer to the fetus is not understood.

In the mother, small amounts of vitamin D_3 are obtained in the diet, from sources such as fish and eggs, but most vitamin D_3 is produced in the epidermis of the skin from 7-dehydrocholesterol in a UVB catalysed reaction (Tuckey et al., 2018). UVB irradiation of 7-dehydrocholesterol produces pre-vitamin D_3, which isomerises into vitamin D_3, before diffusing into circulation (Wacker and Holick, 2013, Tuckey et al., 2018). Within circulation around 90% of vitamin D_3 is bound to DBP, 10% to albumin or lipoprotein and < 1% is free and unbound (Zerwekh, 2008, Wacker and Holick, 2013). In the liver vitamin D_3 is hydroxylated by the enzyme CYP2R1 creating $25(OH)D_3$, the main circulating form of vitamin D_3. $25(OH)D_3$ undergoes a further hydroxylation by the enzyme CYP27B1 within the kidney producing $1,25(OH)_2D_3$, the main active form of vitamin D. Both $25(OH)D_3$ and $1,25(OH)_2D_3$ are inactivated via hydroxylation by the enzyme CYP24A1, producing $24,25(OH)_2D_3$ and $1,24,25(OH)_3D_3$ respectively (Jones et al., 2014, Tuckey et al., 2018). Whilst the majority of vitamin D is produced in the kidneys and liver, there are also numerous other sites of local production, including bone and macrophages (Jones et al., 2014).

$25(OH)D_3$ is the main circulating metabolite of vitamin D present in the maternal circulation, but it is $1,25(OH)_2D_3$ that is widely reported to be the primary biologically active metabolite. However activity of other metabolites has also been reported. $25(OH)D_3$ and 1,25-

dihydroxy-3-epi-vitamin D_3 have both been observed to alter transcription by acting upon the VDR in a number of cell types, demonstrating their ability to alter tissue function (Lou et al., 2010, Molnar et al., 2011). Therefore the type and ratio of metabolites that are present may alter the effect that vitamin D is able to exert on a tissue.

Before the maturation of fetal organ function that occurs during the third trimester, a fetus lacks the capability to metabolise $1,25(OH)_2D_3$ from its precursor molecules. When organ function matures in later pregnancy and the fetus develops the capability to metabolise vitamin D, it is still reliant upon maternal vitamin D due to lack of dietary intake or exposure to UV light. Therefore vitamin D metabolites must be able to pass from the maternal blood in the intervillous space, across the MVM, through the syncytiotrophoblast, across the BM and through the fetal capillary endothelium to the fetal circulation. Establishing an understanding of what metabolites cross the placenta to the fetus may allow us to better understand the role of vitamin D in fetal development. Studies utilising rats which also have a hemochorial placenta like humans have shown that $25(OH)D_3$ crosses the placenta (Liu and Hewison, 2011). Conversely in a study looking at human placental samples, it was suggested that it is $1,25(OH)_2D_3$ that primarily crosses the placenta (Ron et al., 1984). However this study of human placentas had a number of limitations, including a varying protocol and samples being measured at the limits of detection. Hypothesised pathways of metabolism and transfer are displayed in Figure 3-1.

The placenta expresses the *VDR, CYP27B1* and *CYP24A1* genes, suggesting that it is capable of vitamin D metabolism (Novakovic et al., 2009). Indeed treatment of placental samples with $25(OH)D_3$ induces increased gene expression of *CYP24A1*, suggesting that $25(OH)D_3$ is being metabolised into a transcriptionally active form. If $25(OH)D_3$ is crossing the placenta to the fetus, it is possible that metabolism of $25(OH)D_3$ to $1,25(OH)_2D_3$ is one mechanism of regulating transfer. Conversion of $25(OH)D_3$ to $1,25(OH)_2D_3$ could limit the local pool of $25(OH)D_3$ available for transfer, and therefore regulate the transfer of vitamin D to the fetus, without limiting the pregnancy induced rising $1,25(OH)_2D_3$ levels. However $1,25(OH)_2D_3$ could be an alternative substrate that is also transferred to the fetus, and therefore placental conversion of $25(OH)D_3$ to $1,25(OH)_2D_3$ may ensure sufficient local supply of $1,25(OH)_2D_3$ to meet fetal demand. Although *CYP24A1* gene expression is reduced in placental tissues compared to other somatic tissues (Novakovic et al., 2009) its expression is not completely abolished, and therefore some conversion of $25(OH)D_3$ and $1,25(OH)_2D_3$ to $24,25(OH)_2D_3$ and $1,24,25(OH)_3D_3$ respectively may occur. Whether these degradation products would then undergo further inactivation in the placenta, or are transported back to the maternal circulation for further inactivation is not known.

Vitamin D and its metabolites have a number of impacts on fetal and maternal health outcomes. We therefore need to understand how the placenta metabolises and regulates vitamin D transfer to the fetus. This information may inform and direct future healthy pregnancy advice and interventions.

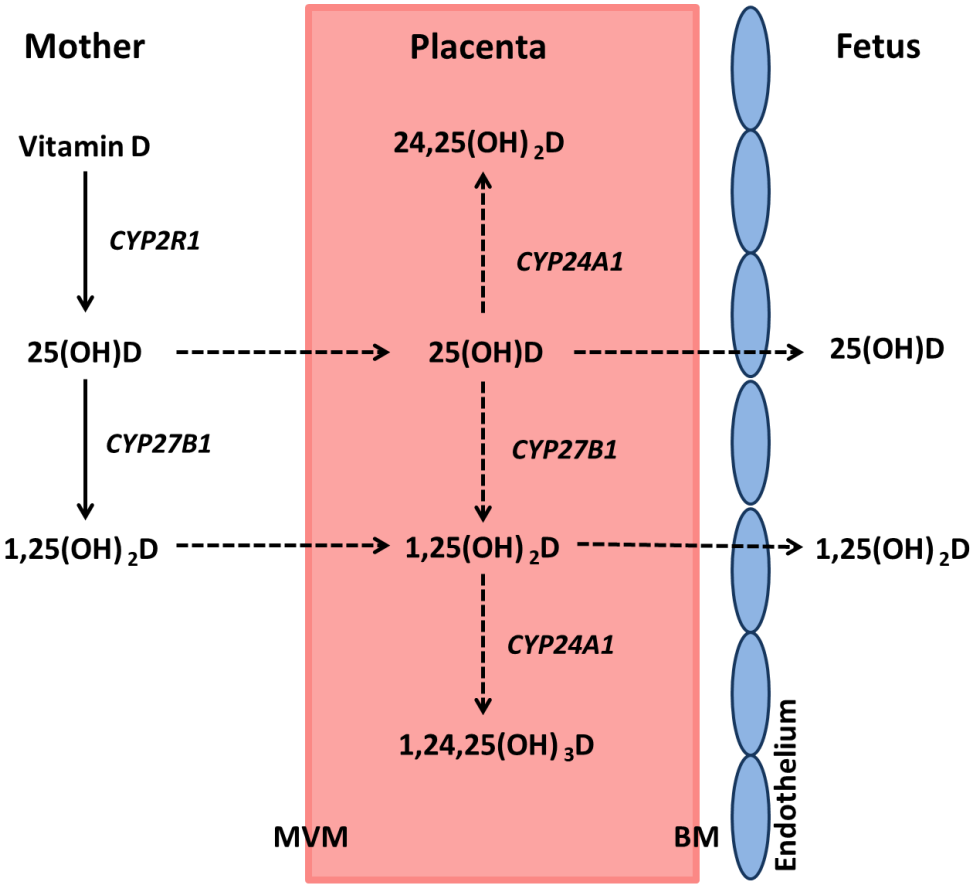

Figure 3-1 ***Placental vitamin D metabolism.*** *Metabolism of vitamin D within the human placenta, showing the pathway vitamin D must take from the maternal circulation, across the microvillus membrane (MVM), through the syncytiotrophoblast, across the basal membrane (BM) and through the fetal capillary endothelium to the fetal circulation. Solid arrows show known pathways, dashed arrows show hypothesised pathways.*

3.1.1 Aims

1. To investigate how 25(OH)D_3 is metabolised within the human placenta and which forms are transferred to the fetal circulation using the isolated perfused placental cotyledon method.

3.2 Methods

3.2.1 Placental collection

Term human placentas were collected within 30 min of delivery as described in Chapter 2.2.1, from women who had healthy, uncomplicated pregnancies. Tissue was transported to the laboratory as quickly as possible for experimentation.

3.2.2 Placental perfusion

Placental perfusion was carried out as described in Chapter 2.3. After 45 min of perfusion of both the fetal and maternal circulations with EBB (see Table 2-1), the maternal buffer was switched to EBB containing 30 nmol/l ^{13}C-25(OH)D_3. One 10 ml sample and two 1 ml samples were taken at time points 30, 60, 90, 120, 150, 180, 200, 220, 240, 260, 280 and 300 min from the experimental start time from both the maternal outflow and fetoplacental vein. Stock samples were taken of the maternal and fetal experimental buffers directly from their bottles. All samples were snap frozen on dry ice and stored at -80°C. At the end of the experiment the maternal buffer was returned to general EBB for 5 min before the perfusion was stopped, and the perfused cotyledon weighed and snap frozen. Perfused tissue was stored at -80°C. Unperfused placental samples were collected as controls, washed in EBB and snap frozen, before storage at -80°C.

3.2.3 Tissue crushing

Snap frozen villous tissue samples from perfused cotyledons and unperfused control placental samples were crushed to a powder as described in Chapter 2.9.1. Briefly samples were placed into a pre-chilled crushing chamber and crushed to a fine powder, keeping the samples frozen throughout. Powdered samples were stored at -80°C.

3.2.4 RNA extraction

RNA was extracted from placental villous tissue that had been stored at -80°C and then crushed to a fine powder as described in Chapter 2.9.1, using the Qiagen miRNeasy mini kit, as described in Chapter 2.9.3. The addition of chloroform separates RNA from DNA and protein, and RNA is selectively bound to a spin column. Contaminates are washed away and then the RNA is eluted from the column in RNAse free water. The quantity and integrity of total RNA was confirmed by Nanodrop 1000 Spectrophotometer and agarose gel electrophoresis, as described in Chapter 2.9.4 and 2.9.5.

3.2.5 Reverse transcription

To convert RNA to cDNA samples underwent reverse transcription as described in Chapter 2.9.6. Total RNA (12 µg) was reverse transcribed with 250 ng random hexamer primers, 100 units M-MLV reverse transcriptase, 25 units recombinant RNasin ribonuclease inhibitor and 0.5 mmol/L PCR nucleotuide mix in a final reaction volume of 12.5 µl in 1x MMLV reaction buffer (Promega, Wisconsin, USA). PCR conditions were 37°C for 60 min then 95°C for 10 min. Each of the samples was reverse transcribed individually at the same time to reduce variation. A standard curve, NECs and CVs were also reverse transcribed in the same batch.

3.2.6 Quantitative real-time polymerase chain reaction

CYP24A1 gene expression was measured using qRT-PCR as described in Chapter 2.9.7. Primer sequences are displayed in Table 3-1. mRNA expression was measured using Roche UPL assay. The HKG *YWHAZ* (as previously selected using geNorm analysis) was also measured using a Primer Design Perfect Probe assay. UPL qRT-PCR cycling conditions were 95°C for 10 min; 45 cycles of 95°C for 10 s, 60°C for 30 s and 72°C for 1 s; 50°C for 30 s, with data collection at the 72°C step. Perfect Probe HKG qRT-PCR cycling conditions were 95°C for 10 min; 50 cycles of 95°C for 10 s, 50°C for 30 s and 72°C for 15 s; 50°C for 30 s, with data collection at the 50°C step. For each qRT-PCR assay, samples (4 ng) were run alongside a standard curve, CV controls, NECs and NTCs in triplicate. Cp values were determined by the second derivative method and were converted to DNA concentration using a standard curve as described in Chapter 2.9.7. Expression levels of *CYP24A1* were normalised to the expression levels of the housekeeping gene *YWHAZ* for each sample. Due to having a limited amount of cDNA only one HKG was used normalise the qRT-PCR data here. Future work would look to repeat this with three HKGs.

Table 3-1 *Primers and probes used for qRT-PCR.*

Gene	Accession number	Primer sequence (5'-3')	UPL number	Amplicon (bp)
CYP24A1	NM_000782.4	F: GAAAGAATTGTATGCTGCTGTCA R: CACATTAGACTGTTTGCTGTCGT	78	1337-1359 1386-1408

UPL = Universal probe library, bp = base pairs, F = Forward, R = reverse

3.2.7 Vitamin D metabolite measurement

^{13}C labelled and unlabelled vitamin D metabolites were measured in perfusate samples by Felicity Hey (University of Cambridge), as described in Chapter 2.6. Briefly proteins were precipitated from the perfusate samples and centrifuged to remove contaminants. Supernatant

containing the vitamin D metabolites was further washed of contaminants, and then separated using ultra performance liquid chromatography. Separated analytes were detected by the mass spectrometer using the electrospray ionisation mode with multiple reaction monitoring (n = 5 per time point for maternal and fetal perfusate samples). Metabolites measured include $25(OH)D_2$, $25(OH)D_3$, ^{13}C-$25(OH)D_3$, $24,25(OH)_2D_3$, ^{13}C-$24,25(OH)_2D_3$ and 3-epi-$25(OH)D_3$.

3.2.8 $1,25(OH)_2D_3$ measurement

$1,25(OH)_2D_3$ in placental perfusate samples was measured using the 1,25-dihydroxy vitamin D EIA kit (Immunodiagnostic systems; UK), as described in Chapter 2.7. Briefly samples were delipidated through centrifugation, then contaminants removed by selective binding of $1,25(OH)_2D_3$ to the solid phase in an immunocapsule. Contaminants were washed from the immunocapsules, then $1,25(OH)_2D_3$ eluted, dried and re-dissolved in assay buffer. Samples were incubated overnight with a sheep anti-$1,25(OH)_2D_3$ antibody, then bound to a microplate coated with anti-sheep IgG. Biotin labelled $1,25(OH)_2D_3$ was then added to the plate, followed by horseradish peroxidase labelled avidin, and finally enzyme substrate to produce a colour change proportional to the amount of biotin labelled $1,25(OH)_2D_3$ that was able to bind the plate.

3.2.9 Data analysis

<u>Gene expression</u>

qRT-PCR data was normalised to HKG expression, and is presented as relative expression to HKG. Expression was tested for normal distribution, and as not normally distributed data was log transformed and re-tested. Data required the comparison of two groups; control treated and vitamin D treated, so were analysed using an independent Student's t-test. Data presented as mean ± SEM.

<u>Perfusate measures</u>

Perfusate samples were analysed to determine whether there was a change in concentration of a metabolite throughout the duration of the experiment. Maternal and fetal samples were analysed separately by paired Student's t-test to identify changes in concentration between the beginning and end of the experiment. Data presented as mean ± SEM.

3.3 Results

In order to determine what metabolites of vitamin D are produced in the placenta and transferred to the fetus placental cotyledons were perfused with ^{13}C-25(OH)D_3.

3.3.1 *CYP24A1* gene expression

Ex vivo placental cotyledons were perfused with 30 nmol/l ^{13}C-25(OH)D_3 for a period of 5 h (n = 5). A concentration of 30 nmol/l ^{13}C-25(OH)D_3 is within the normal physiological range for 25(OH)D_3. qRT-PCR measurements of the vitamin D response gene *CYP24A1* were used as a proxy for vitamin D uptake into the placenta.

CYP24A1 mRNA expression is displayed in Figure 3-2. *CYP24A1* mRNA expression was significantly upregulated (p = 0.017) in samples from cotyledons perfused with ^{13}C-25(OH)D_3 (n = 5), compared to control unperfused placental samples (n = 10).

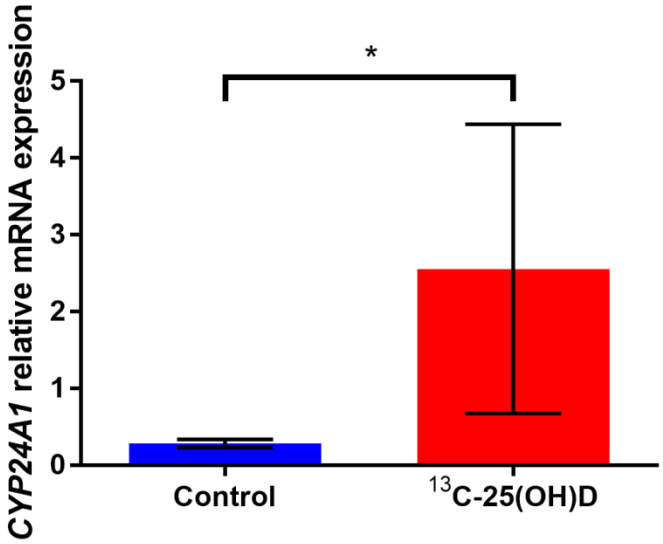

Figure 3-2 ***CYP24A1 mRNA expression in perfused placental cotyledons.*** *Relative mRNA expression of CYP24A1 in samples from placental cotyledons perfused with ^{13}C-25(OH)D_3 vs control unperfused placental samples. Data presented as mean ± SEM and analysed by independent Student's t-test. *p < 0.05.*

3.3.2 Metabolites in maternal and fetal perfusate

To determine what vitamin D metabolites were present in the maternal and fetal perfusate, samples were analysed by LCMS. Data displayed in Figure 3-3. Negative values are

obtained when the metabolite is present in a quantity below the limit of quantification, indicating minimal or no presence of that metabolite in the sample.

^{13}C-25(OH)D_3 perfusate measures are displayed in Figure 3-3a. The maternal circulation was perfused with ^{13}C-25(OH)D_3 at 125.0 ± 8.05 pmol/min (time point 0). The maternal perfusate output decreased to 100.9 ± 5.31 pmol/min by 300 min ($p = 0.029$) indicating uptake by the placenta. The fetal circulation was perfused with buffer containing no ^{13}C-25(OH)D_3 (measured at 0 pmol/min). The fetal perfusate, output of ^{13}C-25(OH)D_3 increased to 9.0 ± 2.48 pmol/min by 300 min ($p = 0.01$).

^{13}C-24,25$(OH)_2D_3$ perfusate measures are displayed in Figure 3-3b. ^{13}C-24,25$(OH)_2D_3$ was not present in either input buffer and could be measured in both the maternal and fetal output perfusate. Maternal output of ^{13}C-24,25$(OH)_2D_3$ increased from 0.03 ± 0.02 pmol/min at 30 min to 2.37 ± 0.43 pmol/min at 300 min ($p = 0.005$). In the fetal perfusate there was a small amount of ^{13}C-24,25$(OH)_2D_3$ at 60 min, , which increased to 0.72 ± 0.22 pmol/min by 300 min. There was a significant increase in ^{13}C-24,25$(OH)_2D_3$ output in the fetal circulations between 30 and 300 min ($p = 0.035$).

25(OH)D_3 perfusate measures are displayed in Figure 3-3c. 25(OH)D_3 was present in the maternal perfusate, and there was a very small amount of 25(OH)D_3 detected in the fetal perfusate, with values in the range of 0 – 0.2 pmol/min. There was no significant change in the concentration of 25(OH)D_3 in either the maternal or fetal perfusate between 30 and 300 min.

25(OH)D_2 perfusate measures are displayed in Figure 3-3d. A small amount of 25(OH)D_2 was identified in the maternal output perfusate, at 30 min and 60 min In the fetal perfusate output of 25(OH)D_2 was only identified at low levels at 60 min, There was no significant change in the concentration of 25(OH)D_2 in either the maternal or fetal perfusate between 30 and 300 min.

3-epi-25(OH)D_3 perfusate measures are displayed in Figure 3-3e. 3-epi-25(OH)D_3 was present in both the maternal and fetal perfusate. In the maternal perfusate, output of 3-epi-25(OH)D_3 fluctuated up to a maximum output of 2.3 pmol/min between 30 and 300 min. In the fetal output 3-epi-25(OH)D_3 was present at a value of 0.5 pmol/min at 30 min, with no further output after this timepoint. No statistics were carried out to determine if there was any significant change in output of 3-epi-25(OH)D_3 as all measures were below the limit of quantification.

24,25$(OH)_2D_3$ perfusate measures are displayed in Figure 3-3f. A very small amount of 24,25$(OH)_2D_3$ was present in the maternal perfusate. In the maternal perfusate output of 24,25$(OH)_2D_3$ was 0.02 pmol/min at 30 min, with no further output for the remainder of the experiment. In the fetal perfusate, no output of 24,25$(OH)_2D_3$ was measured. No statistics were

carried out to determine if there was any significant change in output of $24,25(OH)_2D_3$ as all measures were below the limit of quantification.

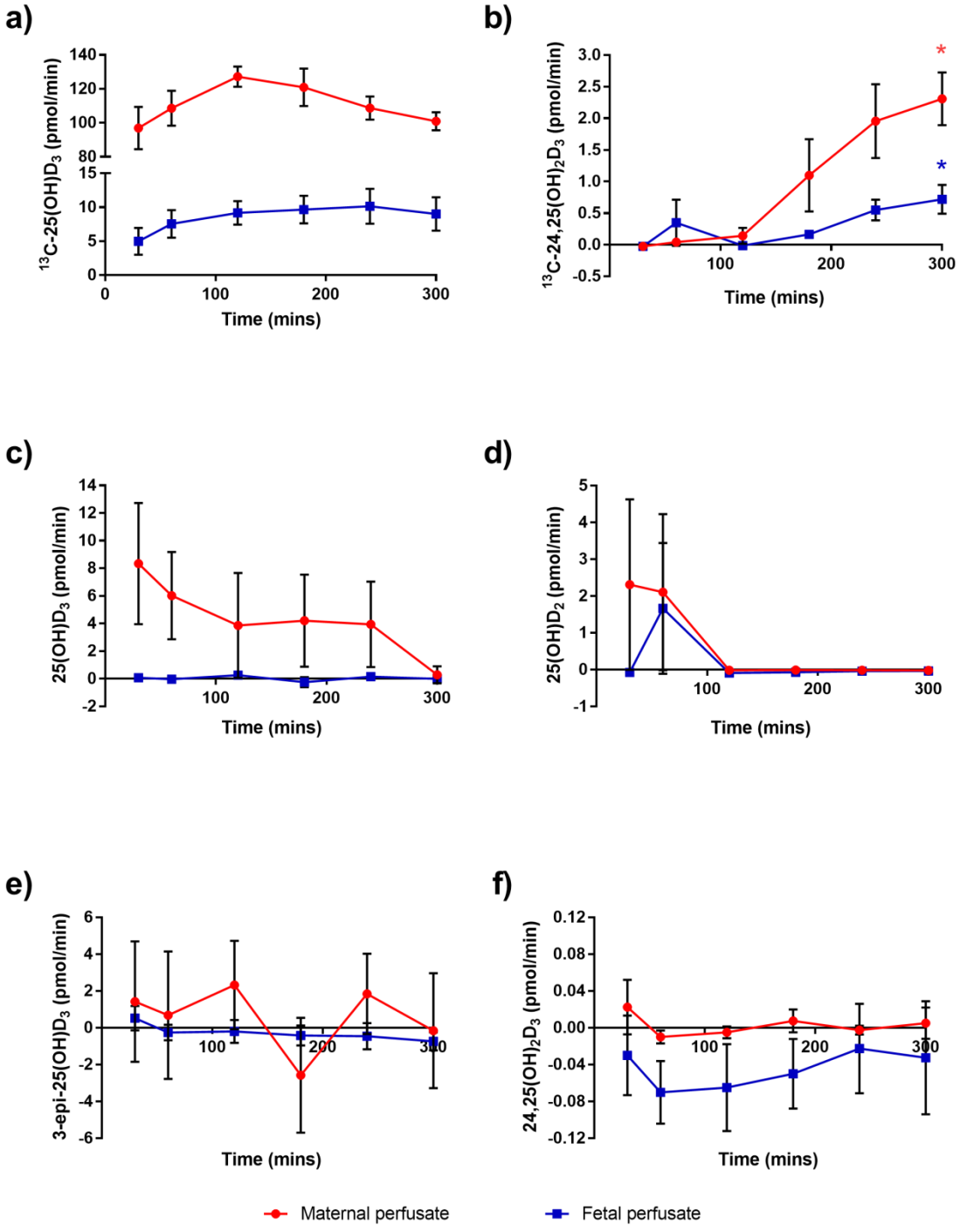

Figure 3-3 ***Vitamin D metabolites present in placental perfusate.*** *Vitamin D metabolites present in the perfusate of ^{13}C-25(OH)D$_3$ perfused ex vivo placental cotyledons.* ***a)*** *^{13}C-25(OH)D$_3$* ***b)*** *^{13}C-24,25(OH)$_2$D$_3$* ***c)*** *25(OH)D$_3$* ***d)*** *25(OH)D$_2$* ***e)*** *3-epi-25(OH)D$_3$* ***f)*** *24,25(OH)$_2$D$_3$. n= 5. Data presented as mean ± SEM.* indicates there is a significant difference ($p < 0.05$) between 30 min and 300 min samples, analysed by paired t test.*

$1,25(OH)_2D_3$ in maternal and fetal perfusate was measured using the 1,25-dihydroxyvitamin D EIA kit (Immunodiagnostic Systems; United Kingdom).

$1,25(OH)_2D_3$ perfusate output data are displayed in Figure 3-4. $1,25(OH)_2D_3$ was present in both the maternal and fetal perfusate. In the maternal perfusate, output of $1,25(OH)_2D_3$ fluctuated between 0.0007 pmol/min and 0.009 pmol/min. In the fetal perfusate, output of $1,25(OH)_2D_3$ had a value of 0.0005 ± 0.001 pmol/min at 30 min, before declining to 0.0001 ± 0.0002 pmol/min at 120 min and then increasing to 0.0029 ± 0.0007 pmol/min by 240 min for the remainder of the experiment. There was no significant change in the concentration of $1,25(OH)_2D_3$ in either the maternal ($p = 0.189$) or fetal ($p = 0.110$) perfusate between 0 and 300 min.

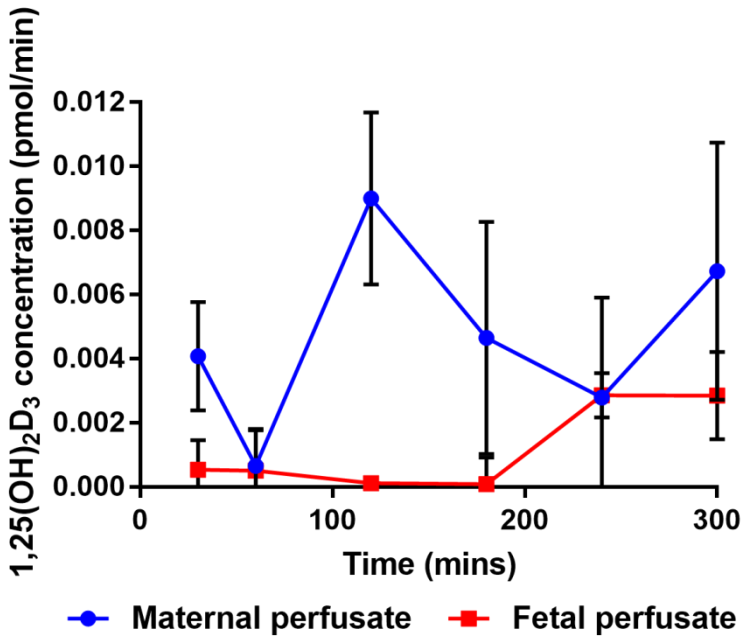

Figure 3-4 ***1,25(OH)$_2$D$_3$ present in placental perfusate.*** *1,25(OH)$_2$D$_3$ in the perfusate of ^{13}C-25(OH)D$_3$ perfused ex vivo placental cotyledons. Data displayed as mean ± SEM.*

Transfer of ^{13}C-25(OH)D$_3$ from the maternal circulation to the fetal circulation was calculated as a percentage of that entering the placenta in the maternal stock, and is displayed in Figure 3-5. 78% of the ^{13}C-25(OH)D$_3$ entering the placenta in the maternal stock was present in the maternal perfusate at 30 min, increasing to 102% at 120 min before declining again to 80% by 300 min. In the fetal perfusate 4% of the maternal stock ^{13}C-25(OH)D$_3$ was present at 30 min, increasing to 7-8% consistently between 120-300 min.

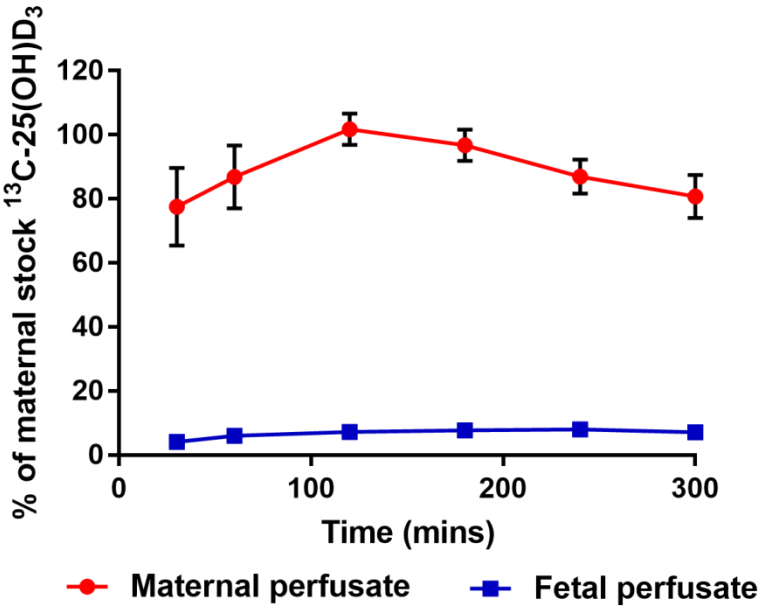

Figure 3-5 ***^{13}C-25(OH)D$_3$ in fetal and maternal placental perfusate.*** *Percentage of maternal stock ^{13}C-25(OH)D$_3$ in the perfusate of ex vivo placental cotyledons perfused with 30 nmol/l ^{13}C-25(OH)D$_3$. Data displayed as mean ± SEM.*

3.4 Discussion

This study has demonstrated that the human placenta metabolises 25(OH)D_3, and that its metabolites are released in both the maternal and fetal circulations. This data suggests that the placenta may regulate the transfer of vitamin D from the maternal to the fetal circulation.

3.4.1 Gene expression as an indicator of placental vitamin D uptake

CYP24A1 contains a VDRE in its promoter, and its transcription is increased in the presence of vitamin D. In this chapter increased *CYP24A1* gene expression was observed in placentas perfused with ^{13}C-25(OH)D_3 compared to control unperfused samples, suggesting that vitamin D is being taken up into the placental tissue. However the perfused samples do show a lot of variation in *CYP24A1* expression. This variation may be due to a number of factors, including genetic and epigenetic variation between participants, maternal 25(OH)D concentration, BMI, calcium levels and ethnicity (Novakovic et al., 2009, Mazahery and von Hurst, 2015). Unfortunately this data about our participants is not available to us in this study.

3.4.2 Placental transfer of 25(OH)D_3

Unlabelled 25(OH)D_3 was primarily present in the maternal perfusate, with only a small amount present in the fetal circulation. The peak in maternal output of 25(OH)D_3 at 30 min, with declining output thereafter suggests that this is endogenous 25(OH)D_3 that was present in the tissue before the start of the experiment. The greater output of 25(OH)D_3 in the maternal compared to fetal circulation suggests that 25(OH)D_3 present in the placenta is primarily transferred back to the maternal circulation, with a small amount of transfer to the fetal circulation.

The loss of labelled ^{13}C-25(OH)D_3 in the maternal circulation at most time points in this experiment, shown through a decrease in the percentage of the stock value in the maternal perfusate, suggests placental uptake of the ^{13}C-25(OH)D_3. The presence of 102% of the maternal stock ^{13}C-25(OH)D_3 in the maternal perfusate at 120 min, in addition to 7% in the fetal perfusate at 120 min, suggest that there is a pool of placental ^{13}C-25(OH)D_3 available. ^{13}C-25(OH)D_3 has displaced endogenous 25(OH)D_3 in this pool by 120 min, and therefore more ^{13}C-25(OH)D_3 was able to leave the placenta in the maternal and fetal perfusate than was entering in the stock at this time point.

^{13}C-25(OH)D_3 from the maternal stock was identified in the fetal perfusate, demonstrating placental transfer of 25(OH)D_3 from the maternal to the fetal circulation. This is consistent with a study in the rat placenta (Liu and Hewison, 2011), in which 25(OH)D_3 was transferred across the placenta into the fetal perfusate. Whilst the concentration of ^{13}C-25(OH)D_3 in the fetal perfusate was low at 9-10 pmol/min, this is the output of a single cotyledon. The placenta has an average of 20 cotyledons (Benirschke et al., 2006), allowing us to estimate a transfer of 20 times this value, suggesting a transfer of 180-200 pmol/min ^{13}C-25(OH)D_3 to the fetal circulation. Transfer of 25(OH)D_3 at a rate of 180-200 pmol/min into the fixed volume of the fetal circulation would allow for a build-up in concentration of 25(OH)D_3 over time to physiologically active levels.

In the fetal perfusate the increasing levels of ^{13}C-25(OH)D_3, alongside decreasing unlabelled 25(OH)D_3 with time again suggests that there is a pool of placental 25(OH)D_3, which is being replaced with labelled ^{13}C-25(OH)D_3 as the experiment progresses. The consistent transfer of 7-8% of the maternal stock into the fetal perfusate from 2-5 h suggests that a steady state is achieved, and that any further ^{13}C-25(OH)D_3 which is not present in the maternal or fetal perfusate at these times must be either metabolised or stored in the placenta.

3.4.3 Placental Vitamin D metabolism

^{13}C-24,25(OH)$_2D_3$ identified in this experiment is a downstream metabolite of the ^{13}C-25(OH)D_3 present in the maternal stock, and therefore demonstrated placental metabolism of 25(OH)D_3 by the enzyme CYP24A1. ^{13}C-24,25(OH)$_2D_3$ was identified in both the maternal and fetal perfusate, demonstrating that 24,25(OH)$_2D_3$ produced in the placenta is transferred to both the maternal and fetal circulations. As ^{13}C-24,25(OH)$_2D_3$ was transferred to the maternal circulation at a greater rate than fetal circulation, this suggests that transfer of ^{13}C-24,25(OH)$_2D_3$ to the maternal circulation may limit transfer to the fetal circulation.

The metabolites 25(OH)D_2, 3-epi-25(OH)D_3 and 24,25(OH)$_2D_3$ were also measured by LCMS in this dataset. The concentration of 25(OH)D_2, 3-epi-25(OH)D_3 and 24,25(OH)$_2D_3$ in the perfusate samples was close to or below the limit of quantification at all time points, resulting in negative values and large variation. Due to these samples being measured close to or below the limit of quantification it is not possible to draw conclusions regarding fluctuations in the concentration over the course of the experiment.

As 1,25(OH)$_2D_3$ was unable to be measured by LCMS, it is not possible to distinguish between ^{13}C-1,25(OH)$_2D_3$ and 1,25(OH)$_2D_3$ in this dataset. The presence of 1,25(OH)$_2D_3$ in the fetal perfusate demonstrates that 1,25(OH)$_2D_3$ is transported from the placenta into the fetal circulation. The decrease in 1,25(OH)$_2D_3$ in the maternal perfusate between 30 and 60 min likely

represents endogenous 1,25$(OH)_2D_3$ being transported out of the placental tissue into the maternal perfusate. The increased output of 1,25$(OH)_2D_3$ in the maternal perfusate after 60 min and in the fetal perfusate after 180 min suggest that metabolism of 25$(OH)D_3$ to 1,25$(OH)_2D_3$ by the enzyme CYP27B1 is taking place, as other endogenous vitamin D metabolites appear to have cleared from the system by these later time points, and output in the fetal circulation is rising. This is supported by the increase in *CYP24A1* gene expression in ^{13}C-25$(OH)D_3$ perfused placental tissue. Increased *CYP24A1* gene expression suggests an increase in the hydroxylation of 25$(OH)D_3$ to 1,25$(OH)_2D_3$ within the placenta, as *CYP24A1* expression is induced by the action of 1,25$(OH)_2D_3$ activated VDR-RXRα on the VDRE present in its promoter.

This study also supports the previous study in human placentas (Ron et al., 1984) which suggested that 1,25$(OH)_2D_3$ crosses the placenta to the fetal circulation, however we also observed substantial 25$(OH)D_3$ transfer and metabolism which the previous study suggested was not the case. Placental production of 1,25$(OH)_2D_3$ and transfer to the maternal circulation will contribute to the increased maternal 1,25$(OH)_2D_3$ levels observed during pregnancy, although increased activity of CYP27B1 in the maternal kidney is thought to be the primary source of increased 1,25$(OH)_2D_3$ (Christakos et al., 2013, Karras et al., 2017). Placental metabolism of 25$(OH)D_3$ and transfer of metabolites to both the mother and fetus both regulates vitamin D actions within the placenta, as well as supporting appropriate vitamin D levels in the maternal and fetal circulations.

3.4.4 Does metabolism indicate placental regulation of transfer?

The consistent transfer of 7-8% (9-10 pmol/min) of the maternal stock ^{13}C-25$(OH)D_3$ from the maternal circulation to the fetal circulations between 60 – 300 min suggests that either the transfer capability of the placenta is saturated at this level, or that transfer is being regulated at this level. To investigate whether placental transfer of 25$(OH)D_3$ is saturated at a rate of 9-10 pmol/min, or whether it is regulated at this level placental perfusions could be carried out at a range of 25$(OH)D_3$ concentrations. Perfusion with a range of lower 25$(OH)D_3$ concentrations would allow us to plot the curve of increasing transfer with increasing concentration and identify the point at which placental transfer of 25$(OH)D_3$ becomes saturated.

The metabolism of ^{13}C-25$(OH)D_3$ to ^{13}C-24,25$(OH)_2D_3$ within the placenta suggests that the placenta may be regulating the activity of ^{13}C-25$(OH)D_3$ within the placental tissue. However this metabolism of ^{13}C-25$(OH)D_3$ may also regulate the pool of both ^{13}C-25$(OH)D_3$ and ^{13}C-24,25$(OH)_2D_3$ available for transfer to the fetus and the mother. The increasing production of ^{13}C-24,25$(OH)_2D_3$ with time suggests that metabolism is regulating transfer by limiting the increase in

^{13}C-25(OH)D_3 available for transfer to the fetus. Release of ^{13}C-24,25$(OH)_2D_3$ into the maternal circulation may limit transfer to the fetal circulation.

Understanding the metabolism of vitamin D within the placenta will allow us to better understand the actions of vitamin D on the tissue, and if metabolism is a mechanism regulating transfer.

3.5 Limitations

A limitation of this study is that the levels of vitamin D metabolites in the mother's circulation before delivery of the placenta are unknown. The pool of endogenous vitamin D in the placenta at the start of the experiment may affect the amount of transfer and metabolism of the ^{13}C-25(OH)D_3 which we measured, and therefore variation between patients may contribute to variation in the levels measured between experiments. However, our data indicate that by time point 120 min this endogenous pool has been metabolised or transferred and the later time points are representing net transfer and metabolism of the labelled 25(OH)D.

A number of factors are documented to affect an individual's ability to respond to 25(OH)D_3, including present 25(OH)D_3 concentration, BMI, calcium intake and ethnicity (Mazahery and von Hurst, 2015). Information on these factors is not known about our participants, and therefore how they alter placental uptake and response to 25(OH)D_3 in this experiment is not known.

Due to the difficulties in obtaining fresh placental tissue that is suitably undamaged from delivery the number of samples for this experiment is limited, but clearly demonstrate that metabolism and transfer of 25(OH)D_3 occurs. Given that it is known that vitamin D metabolism is affected by a number of factors, a higher sample number would allow us to better determine how the amount and rate of transfer of vitamin D metabolites observed here are reflected in the general population. When measuring *CYP24A1* gene expression levels, perfused tissue (n = 5) was compared to unmatched, unperfused placental tissue (n = 10), due to the timing and complexity of the placental perfusion methodology.

The current methodologies available for measuring vitamin D metabolites are limited due to available expertise/facilities and assay validation requirements for different sample types and metabolite concentration. Currently the approved techniques for measures in plasma are LCMS for 25(OH)D and ELIZA for 1,25$(OH)_2$D as recommended by the UK National Vitamin D External Quality Assurance Scheme. Although LCMS is the gold standard technique it was currently not possible to measure 1,25$(OH)_2D_3$ in this manner. Unfortunately we are therefore unable to distinguish between ^{13}C-1,25$(OH)_2D_3$ and 1,25$(OH)_2D_3$ in this experiment, and therefore unable to determine what proportion of the 1,25$(OH)_2D_3$ measured is a direct metabolite of ^{13}C-25(OH)D_3. We can however assume the proportion based on the 1,25(OH)D transfer profile compared to the labelled and unlabelled transfer profiles of the other metabolites.

3.6 Future work

In this study we have measured vitamin D metabolites in the maternal and fetal perfusate samples at various time points when perfused with 30 nmol/l ^{13}C-25(OH)D_3. Although it is not possible to sample the tissue at time points throughout the experiment, measuring the vitamin D metabolites present in the tissue at the end of the experiment will allow us to better understand what metabolism of the ^{13}C-25(OH)D_3 has occurred in the tissue. Measuring vitamin D metabolites present in the tissue of the placenta may give a better indication of whether placental vitamin D metabolism is a mechanism regulating transfer of vitamin D to the fetus.

It was not determined in this experiment whether 1,25(OH)$_2D_3$ from the maternal circulation is taken up by the placenta and transferred to the fetus. Understanding whether it is maternal 1,25(OH)$_2D_3$, or locally synthesised 1,25(OH)$_2D_3$ that is primarily transferred to the fetus will allow us to better understand the role of placental vitamin D metabolism in regulating vitamin D transfer to the fetus. This could be carried out by perfusing *ex vivo* placental cotyledons with a labelled 1,25(OH)$_2D_3$ as has been carried out with labelled 25(OH)D_3 in this experiment.

3.7 Conclusions

Vitamin D must pass from the maternal circulation to the fetal circulation during pregnancy. Placental transfer of vitamin D metabolites is summarised in Figure 3-6.Here we have shown that the metabolites $25(OH)D_3$, $1,25(OH)_2D_3$ and $24,25(OH)_2D_3$ are transferred from the placenta into the fetal circulation. We have shown that a continuous supply of 9-10 pmol/min $25(OH)D_3$ is transferred to the fetal circulation over a period of 3 h, suggesting a steady supply to the fetus. We have demonstrated that $1,25(OH)_2D_3$ is transferred from the placenta into the maternal circulation, contributing to maternal $1,25(OH)_2D_3$ levels. We have also demonstrated placental metabolism of $25(OH)D_3$ to $24,25(OH)_2D_3$, and observed transfer of $24,25(OH)_2D_3$ to both the maternal and fetal circulations. Transfer of maternal $25(OH)D_3$ across the placenta to the fetus may underlie the association between maternal $25(OH)D_3$ and fetal growth. A sufficient maternal $25(OH)D_3$ supply may be necessary for enough $25(OH)D_3$ to transferred across the placenta to meet fetal demands. Placental metabolism of $25(OH)D_3$ may be a mechanism by which it regulates placenta activity and rate of transfer to the fetus.

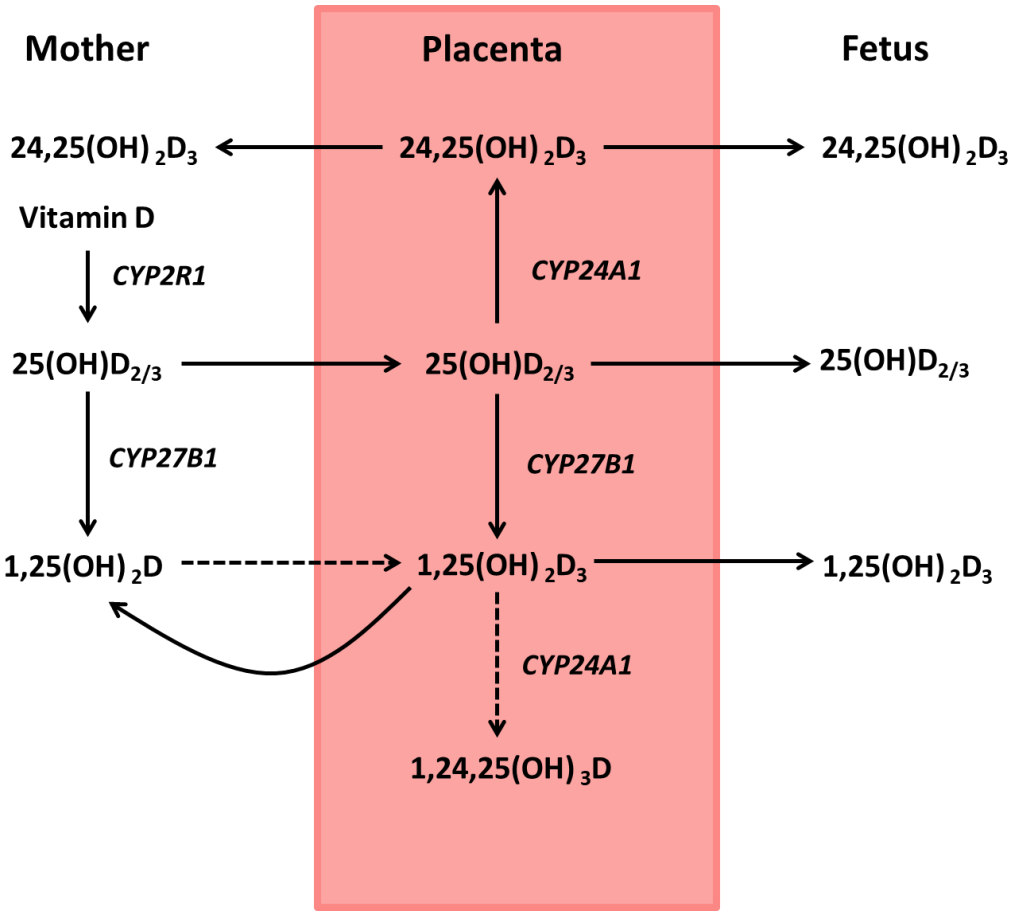

Figure 3-6 ***Placental vitamin D metabolism.*** *Solid arrows show pathways demonstrated in this study. Dashed arrows show hypothesised pathways.*

Chapter 4 Vitamin D induced changes in placental DNA methylation, RNA and protein expression

4.1 Introduction

The transfer of vitamin D from the maternal circulation to the fetus is important, but vitamin D does more than simply pass through the placenta, it also acts upon the placental tissue, potentially changing its function.

$1,25(OH)_2D$ binds to the VDR in the cytoplasm of target cells, which then moves into the nucleus and forms a heterodimer with RXR. The $1,25(OH)_2D$ bound VDR-RXR complex binds to VDREs in the promoters of vitamin D responsive genes, inducing or inhibiting gene transcription. $1,25(OH)_2D$ therefore acts at the transcriptional level to alter gene expression (Molnar, 2014). Maternal vitamin D levels are associated with mRNA expression levels of genes within the placenta such as amino acid transporters (Cleal et al., 2015, Chen et al., 2016), angiogenic biomarkers (Schulz et al., 2017b), calbindins (Halhali et al., 2010) and innate immune markers (Longtine et al., 2017). However whether these changes in mRNA expression result in subsequent protein expression changes has been less well investigated.

Associations have been observed between maternal $25(OH)D_3$ deficiency and poor fetal outcomes, such as reduced fetal growth, poorer bone health and an increased risk of childhood obesity (Harvey et al., 2014a, Crozier et al., 2012), but $1,25(OH)_2D$ is rarely measured. Effects of maternal $25(OH)D_3$ deficiency on the placenta may contribute to the poor fetal outcomes. Maternal $25(OH)D_3$ deficiency in pregnancy has been associated with an increased chance of developing pregnancy complications such as preeclampsia, gestational diabetes mellitus and preterm labour (Dovnik and Mujezinovi, 2018). It is possible the effects of vitamin D on the placenta play a causative role in the development of pregnancy complications. Maternal $25(OH)D_3$ and vitamin D binding protein levels relate to amino acid transporter gene expression within the placenta, which are also associated with effects on fetal growth (Cleal et al., 2015, Day et al., 2015, Chen et al., 2016). $1,25(OH)_2D$ action via the VDR to alter transcription underlies some of its effects within the placenta, however as not all affected genes have a VDRE present in their promoter, other mechanisms of action must be taking place.

Alterations to placental epigenetic processes, such as miRNA expression, DNA methylation and histone modifications in response to vitamin D may be another mechanism by which vitamin D alters gene expression and subsequently placental function during pregnancy. $25(OH)D_3$ and $1,25(OH)D_3$ have been observed to alter epigenetic mechanisms in tissues such as the liver, cord blood and prostate cells, so it is likely that vitamin D also acts at the epigenetic level in the placenta (Xue et al., 2016, Junge et al., 2016, Singh et al., 2015). However vitamin D induced changes to the placental epigenome have not yet been observed.

$25(OH)D_3$ has been observed to alter DNA methylation in human cord blood, mouse liver and mouse germline cells (Junge et al., 2016, Xue et al., 2016, Doig et al., 2013). $1,25(OH)_2D_3$ has been observed to alter histone methylation/acetylation in bone marrow stromal cells, mesenchymal stem cells and colon cancer cells (Fu et al., 2013, Meyer et al., 2014, Pereira et al., 2011). $1,25(OH)_2D_3$ has been observed to alter miRNA expression in cancerous prostate cells (Singh et al., 2015). Observed $25(OH)D_3$ induced DNA methylation changes and $1,25(OH)_2D_3$ induced miRNA expression changes occurred after a long period of vitamin D exposure, but changes to histone methylation were seen after 3 h of exposure to $1,25(OH)_2D_3$ (Meyer et al., 2014). Vitamin D may have short term effects on placental epigenetics by inducing short term transient changes to placental gene expression in response to fetal signals or altered maternal environment, for example changing demands of the fetus throughout gestation. However it may also have longer term effects on placental gene expression. Vitamin D may cause stable alterations to placental epigenetic factors, in response to the maternal environment. For example maternal vitamin D levels may reflect maternal nutrient reserves more generally, with a mother who has a poor quality diet and poor body composition likely to also have low vitamin D levels. Lower vitamin D levels could indicate lower maternal nutrient reserves and mediate a reduction in placental transfer of nutrients, allowing the mother to support the entire pregnancy.

Understanding how vitamin D alters placental DNA methylation, RNA and protein expression is therefore necessary to understanding how vitamin D affects placental function. Vitamin D may be acting to alter transcription of epigenetic factors such as DNA methyltransferases (DNMTs), to modify histone protein activity or to alter DNA methylation, as depicted in Figure 4-1. Understanding how vitamin D acts within the placenta may allow us to understand how vitamin D deficiency affects placental function. This in turn may allow us to understand what treatment gives optimal health outcomes for pregnant women deficient in vitamin D.

4.1.1 Aims

1. To investigate how short term $25(OH)D_3$ treatment alters DNA methylation, mRNA and protein expression in term villous tissue.

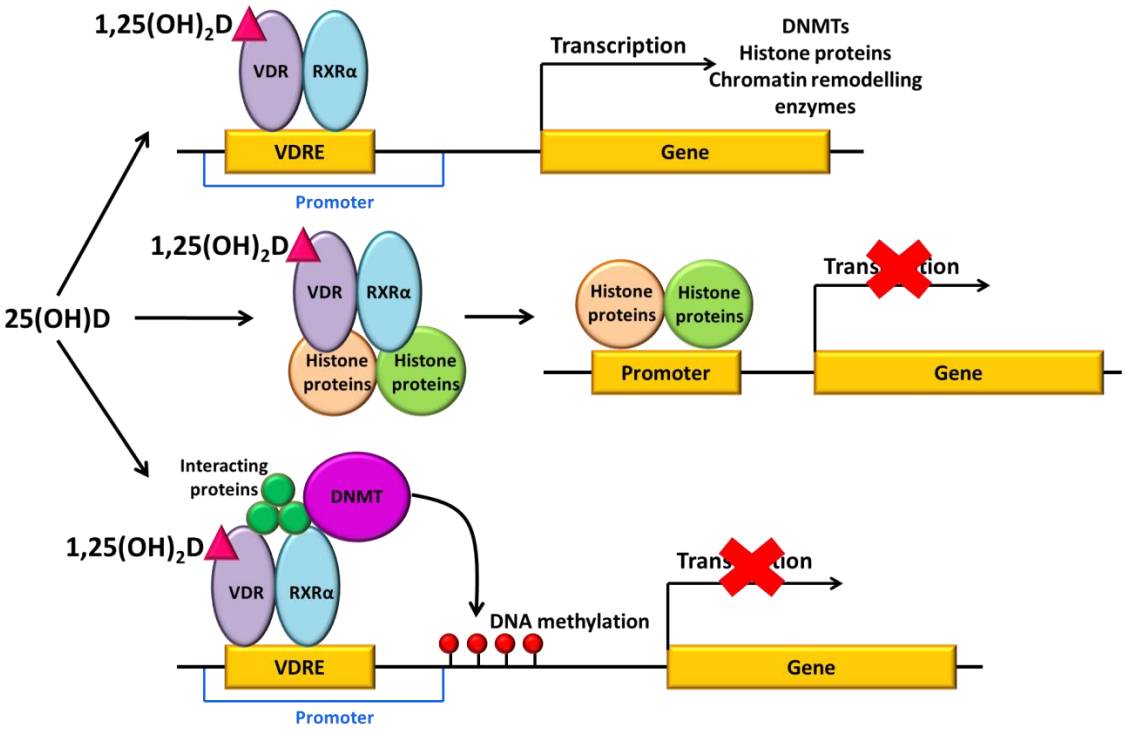

Figure 4-1 ***Proposed mechanisms of action of 1,25(OH)$_2$D within the placenta.*** *1,25(OH)$_2$D interacts with the VDR, allowing it to form a complex with RXRα and interact with VDREs, enhancing or repressing transcription of genes involved in epigenetic remodelling. 1,25(OH)$_2$D may modify histone proteins, altering how they interact with DNA and subsequently blocking or allowing access of transcription factors to the DNA altering expression. 1,25(OH)$_2$D activated VDR/RXRα may recruit DNA methyl transferases (DNMTs) to the DNA, altering DNA methylation and subsequently blocking or allowing access of transcription factors to the DNA altering expression.*

4.2 Methods

4.2.1 Placental collection

Term human placentas were collected within 30 min of delivery as described in Chapter 2.2.1, from women who had healthy, uncomplicated pregnancies. Tissue was transported to the laboratory as quickly as possible for experimentation.

4.2.2 Placental fragment culture

Placental fragments were cultured as described in Chapter 2.4 by Dr Claire Simner (Simner, 2015). 10 mg villous tissue fragments were incubated in Tyrode's buffer (see Table 2-2), with 20 µmol 25(OH)D_3 (dissolved in ethanol) and 0.7 mmol/l BSA or ethanol control with 0.7 mmol/l BSA at 37°C for 8 h (n = 8). At 8 h the buffer was removed, fragments washed in Tyrode's buffer and snap frozen on dry ice. Fragments were stored at -80°C.

4.2.3 DNA extraction

DNA was extracted from snap frozen villous tissue fragments that had been stored at -80°C as described in Chapter 2.9.2 using the Qiagen DNeasy blood and tissue kit. Fragments in triplicate were lysed in 20 µl proteinase K and 180 µl buffer ATL at 56°C for 3 h. Ethanol was used to precipitate the DNA in the solution, and DNA was then selectively bound to a DNeasy mini spin column. Contaminants are washed and then the DNA was eluted from the column in buffer AE (10 mM Tris-Cl, 0.5 mmol EDTA, pH 9.0). The quantity and integrity of total DNA was confirmed by Nanodrop 1000 Spectrophotometer and agarose gel electrophoresis, as described in Chapter 2.9.4 and 2.9.5.

4.2.4 RNA extraction

RNA was extracted from snap frozen villous tissue fragments that had been stored at -80°C as described in Chapter 2.9.3 using the Qiagen miRNeasy mini kit. Fragments in triplicate were homogenised in QIAzol Lysis Reagent. The Qiagen miRNeasy mini kit was used to extract RNA from homogenate. Chloroform was used to separate RNA from DNA and protein, with RNA selectively bound to a spin column. Contaminates were washed away and then the RNA was eluted from the column in RNAse free water. The quantity and integrity of total RNA was confirmed by Nanodrop 1000 Spectrophotometer and agarose gel electrophoresis, as described in Chapter 2.9.4 and 2.9.5.

4.2.5 Illumina 850K DNA methylation array

DNA methylation at over 850,000 CpG sites throughout the genome was analysed using an Illumina EPIC array, as described in Chapter 2.10.1. Briefly DNA was bisulphite converted, amplified and then the methylation status of individual CpGs was determined using Illumina Infinium Bead Chip assays (n = 8 per treatment group).

4.2.6 RNA sequencing

RNA expression was investigated using HiSeq 2x 50 bp paired-end sequencing on an Illumina platform, as described in Chapter 2.10.2. Briefly cDNA synthesis was carried out using the Illumina TruSeq Stranded mRNA sample preparation kit, and the resulting library quantified, normalised and bound to a flow cell. Sequences were determined via the addition of fluorescently labelled nucleotides. Poor quality reads were removed and sequences were aligned to the human transcriptome (n = 4 per treatment group).

4.2.7 Proteomics

Protein expression was determined using LCMS as described in Chapter 2.10.3. Briefly samples were homogenised, sonicated and peptides isolated. Peptides were separated using high-pH reversed-phase (RP) chromatography, and the resulting fractions LCMS analysed with low-pH RP capillary chromatography and nanospray ionization FT-MS (n = 4 per treatment group).

4.2.8 Statistical analysis

<u>Methylation data</u>

Methylation data as β-values were normalised and differentially methylated CpGs identified by Dr Faisel Rezwan. Data were not normally distributed so non-parametric testing was used. A Wilcoxon signed-rank test with control verses vitamin D treated was used. Data were initially filtered by me to a probability of 5%, and mapped to pathways using Toppgene (Division of Bioinformatics, Cincinnati Children's Hospital Medical Centre). Data were then further filtered to a probability of 1% and biological pathway analysis carried out using GREAT V3.0.0 (http://great.stanford.edu/public/html/index.php, Bejerano Lab, Stanford University) by Dr Christopher Bell.

RNA expression data

Raw data were analysed by Dr Cory White. Briefly data were mapped to hg38 (Ensemble, March 2017), filtered and normalised as described in Chapter 2.14.2, and differential expression determined using EdgeR (Robinson et al., 2010). Data were filtered to a B&H FDR corrected probability of 5%. Genes with increased and those with decreased expression with vitamin D treatment were mapped to biological pathways using Toppgene (Division of Bioinformatics, Cincinnati Children's Hospital Medical Centre). Pathways accepted with a minimum hit count of 4 and B&H FDR corrected q value of ≤ 0.05.

Proteomic data

Differential expression of peptides with vitamin D treatment was determined by Dr Spiros Garbis and Dr Antigoni Manousopoulou. Permutation testing was carried out in which 3 out of 4 permutations with a probability of 5% was accepted as differentially expressed. Genes with altered protein expression were mapped to biological pathways using MetaCore (Clarivate; USA).

4.3 Results

In order to establish the effects of short term 25(OH)D_3 incubation on DNA methylation, RNA expression and protein expression, placental fragments were incubated with 20 µmol 25(OH)D_3 plus BSA for 8 h.

4.3.1 Methylation array

To determine whether 25(OH)D_3 treatment altered DNA methylation in placental villous fragments the Illumina EPIC array was carried out.

Due to the large number of measures carried out in this array, and the small sample size (n = 8), it was not possible to analyse this dataset at the FDR level without loss of all significance. Significance has therefore been accepted as $p < 0.05$ for DNA methylation data in this study. To strengthen the results of this array pyrosequencing could be carried out on a subset of the CpG sites investigated to validate the results.

Of the over 850000 CpG sites measured in this array, 33676 sites had significantly altered methylation (excluding control median = 0, $p \leq 0.05$). Of these 17439 sites contained significantly increased methylation and 16237 sites contained significantly decreased methylation.

Altered CpG sites mapped to a total of 13096 genes, with 8890 genes containing one or more sites of increased methylation, 7816 genes containing one or more sites of decreased methylation, and 3609 genes containing at least one site of increased and one of decreased methylation.

CpG sites were mapped in relation to their corresponding CpG island, and allocated to whether they are in the north shelf, north shore, island, south shore, south shelf or other, as shown in Figure 4-3. As depicted in Figure 4-2, the north shelf was defined as 2-4 kb upstream of the CpG island, north shore 0-2 kb upstream, south shore 0-2 kb downstream, south shelf 2-4 kb and other as over 4 kb up or downstream of the island.

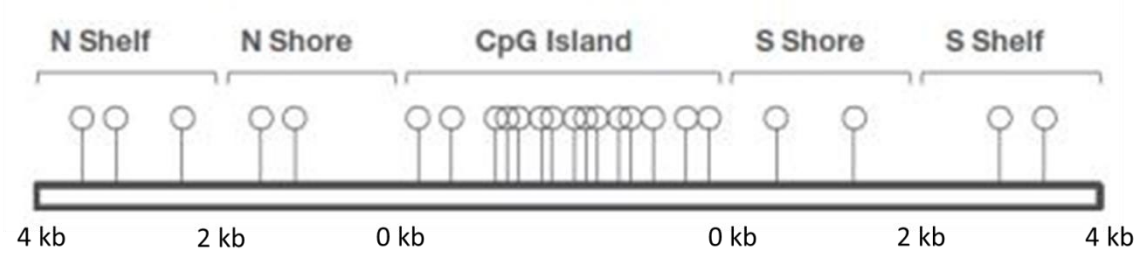

Figure 4-2 ***DNA methylation location in relation to CpG islands***. *CpG sites are described according to their nearest CpG island, with distance from CpG site measured in kilo bases (kb).Adapted from University of Bonn Medical Centre; www.lifeandbrain.com/content/uploads/2018/03/Genomics.pdf*

Altered methylation was observed across the chromosomes, as shown in Figure 4-4. The X and Y chromosomes were not included in this study, as they were not available on the Illumina 850K methylation array platform used in this study.

Genes containing altered methylation were mapped to biological pathways using the software GREAT (www.great.stanford.edu), as seen in Figure 4-5. Full pathways data is presented in Appendix A.

A number of genes directly associated with vitamin D uptake, metabolism and activity were found to contain sites of altered DNA methylation with short term 25(OH)D_3 treatment, as shown in Table 4-1. These include *CYP24A1* (cytochrome P450 enzyme 25-hydroxylase), *VDR* (vitamin D receptor), *RXRα* (retinoid X receptor alpha), *RXRβ* (retinoid X receptor beta), *LRP2* (megalin) and *CUBN* (cubilin).

We do not know what a change in the methylation level of a specific CpG site will have on transcription of an associated gene, as this is affected by numerous factors such as chromatin structure and location of transcription factor binding. However increased DNA methylation within the promoter or enhancer generally reflects a reduction in gene expression, due to inhibition of transcription factor binding. In some cases this can also lead to inhibition if blocking the binding of a repressive transcription factor. Methylation within the gene body is thought to relate to increased gene expression. In our data the direction of change to DNA methylation in line with the location within the gene sequence can be taken as an indicator for the affect it will have on expression of the associated gene. We also do not know the magnitude of any effect of altered DNA methylation at a specific CpG site on transcription of the associated gene.

Sinclair *et al* demonstrated that a maternal dietary change resulted in a DNA methylation change of 4% in the ovine fetal liver, and that this methylation change was associated with altered outcomes in the offspring (Sinclair et al., 2007). In line with the fact that 1% of CpG islands display

altered DNA methylation within human tissues with age (Tra et al., 2002), and <3.4% of loci vary between primary tumors and their normal tissue counter parts (Plass and Smiraglia, 2006), this represents a degree of difference expected to have a marked biological significance.

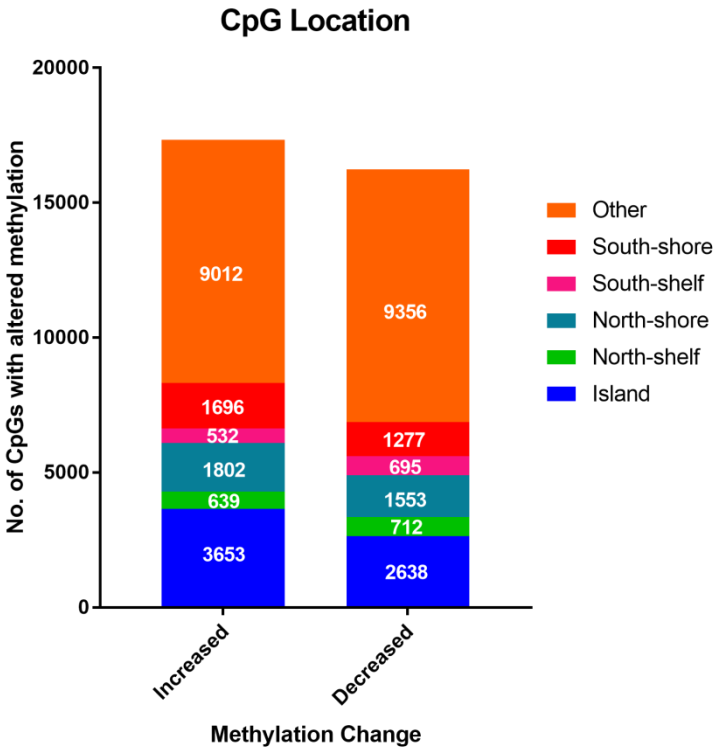

Figure 4-3 ***Genomic location of CpG sites*** *CpG sites containing altered methylation were mapped to their corresponding CpG island.*

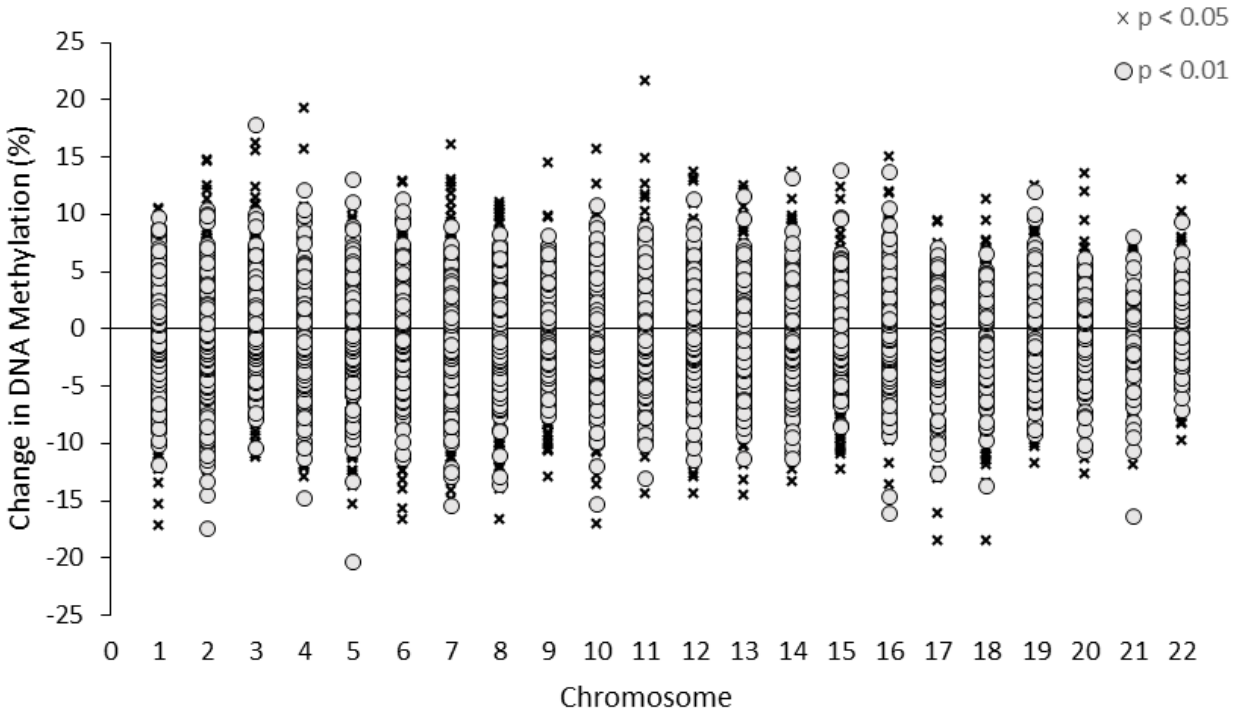

Figure 4-4 ***DNA methylation percentage change*** *CpG DNA methylation percent change mapped to chromosomal location.*

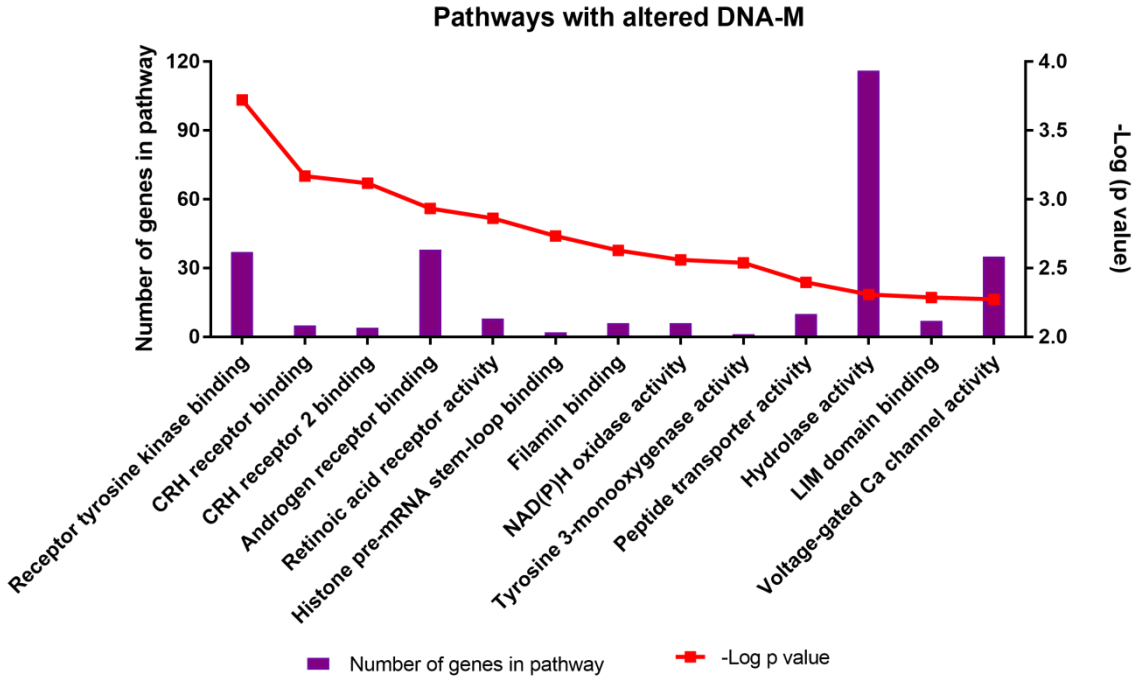

Figure 4-5 ***Pathways with altered DNA methylation in response to 25(OH)D_3 treatment*** *Pathways that were significantly altered mapped to sites with clusters of altered DNA methylation (DNA-M). Pathways identified using GREAT (www.great.stanford.edu), and adjusted for array bias. Significance displayed as –Log p value.*

Table 4-1 *CpG sites with altered methylation status in genes of the vitamin D pathway.*

Gene	Altered CpG	Fold change
CYP2R1	-	-
CYP27B1	-	-
CYP24A1	cg13646093	-0.0663
DBP	-	-
VDR	cg10195011	0.1960
	cg03137447	-0.1314
	cg06369854	-0.3806
	cg14311020	-0.3832
RXRα (NR2B1)	cg09800519	0.1221
	cg13689699	0.0215
	cg02059519	-0.0125
	cg15266275	-0.0240
	cg14051721	-0.0401
	cg10984912	-0.0592
RXRβ (NR2B2)	cg22320183	0.0772
	cg24252536	0.0430
	cg09993092	-0.3912
RXRγ (NR2B3)	-	-
LRP2	cg17328451	0.0357
	cg25554917	-0.1807
	cg24606651	-0.4695
CUBN	cg07823663	0.2355
	cg26276014	0.0549
	cg12317505	0.0323
	cg16709412	-0.0223

Cg = CpG site ID number

4.3.2 RNA sequencing

To determine whether 25(OH)D_3 treatment altered RNA expression in placental villous fragments HiSeq 2x 50 bp paired-end sequencing on an Illumina platform was carried out.

Of the 15065 sequences identified in this experiment, 493 were differentially expressed using a 5% FDR. Of these, 358 had increased expression and 135 had decreased expression.

Genes with altered mRNA expression were mapped to biological pathways using the software ToppGene (www.toppgene.cchmc.org, Division of Biomedical Informatics, Cincinnati Children's Hospital Medical Center, Cincinnati), as seen in Figure 4-6. Pathways accepted with a minimum hit count of 4 and B&H FDR corrected q value of ≤ 0.05. A total of 10 pathways with increased and 12 pathways with decreased RNA expression were identified. Full pathways data is presented in Appendix A.

All differentially expressed genes were displayed in a heatmap, as shown in Figure 4-7. This indicates a significantly different expression profile in 25(OH)D_3 treated placentas compared to control.

Differential expression of genes directly associated with vitamin D uptake, metabolism and activity are displayed in Table 4-2. *CYP24A1, VDR, RXRα* and *LRP2* had significantly altered expression ($p \leq 0.05$) with 25(OH)D_3 treatment, although only *CYP24A1* was still significant with a FDR of 5%.

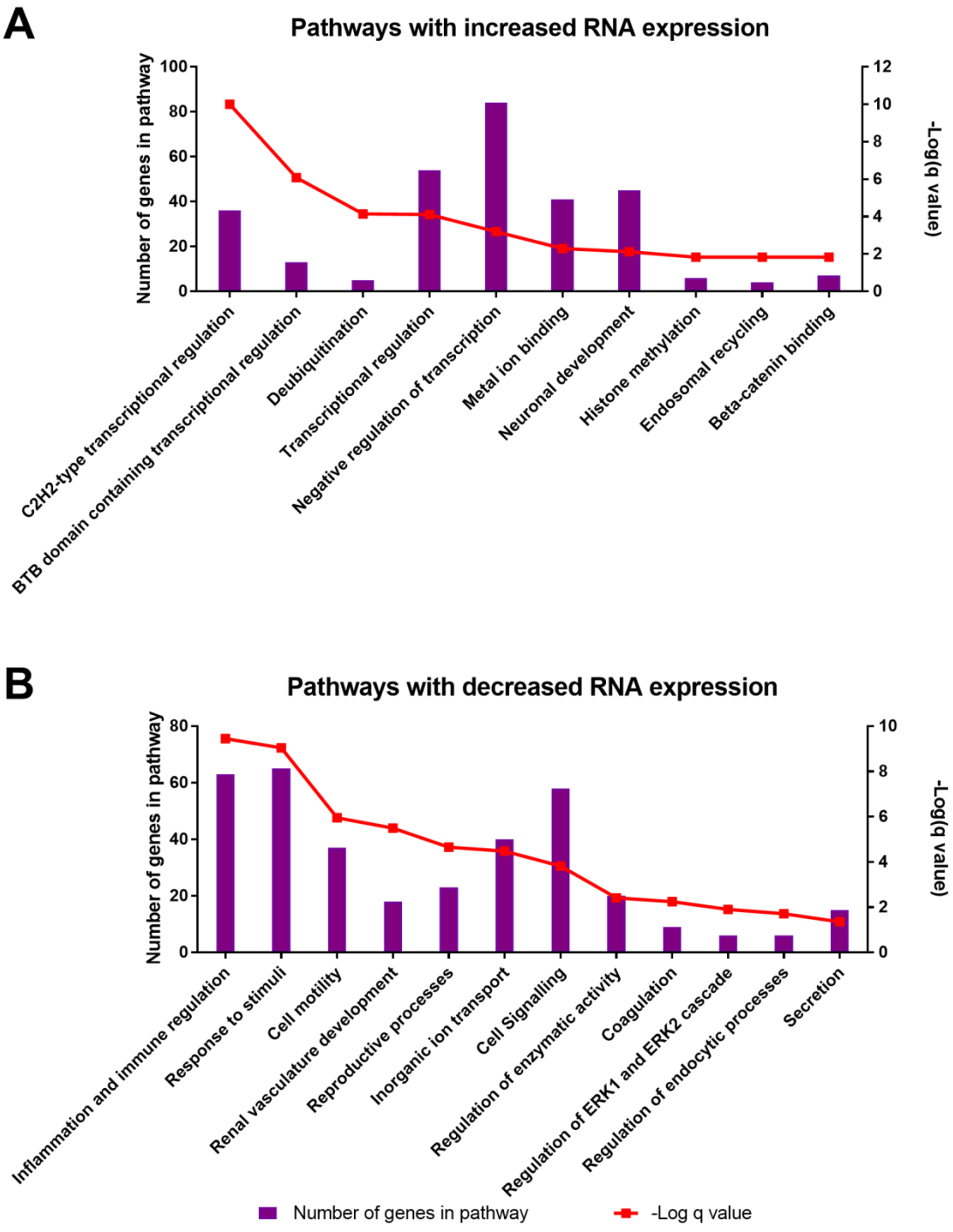

Figure 4-6 ***Pathways with altered RNA expression in response to 25(OH)D_3 treatment***
Significantly altered pathways of increased (A) or decreased (B) RNA expression. Pathways identified using ToppGene and significance displayed as –Log B&H FDR corrected q value.

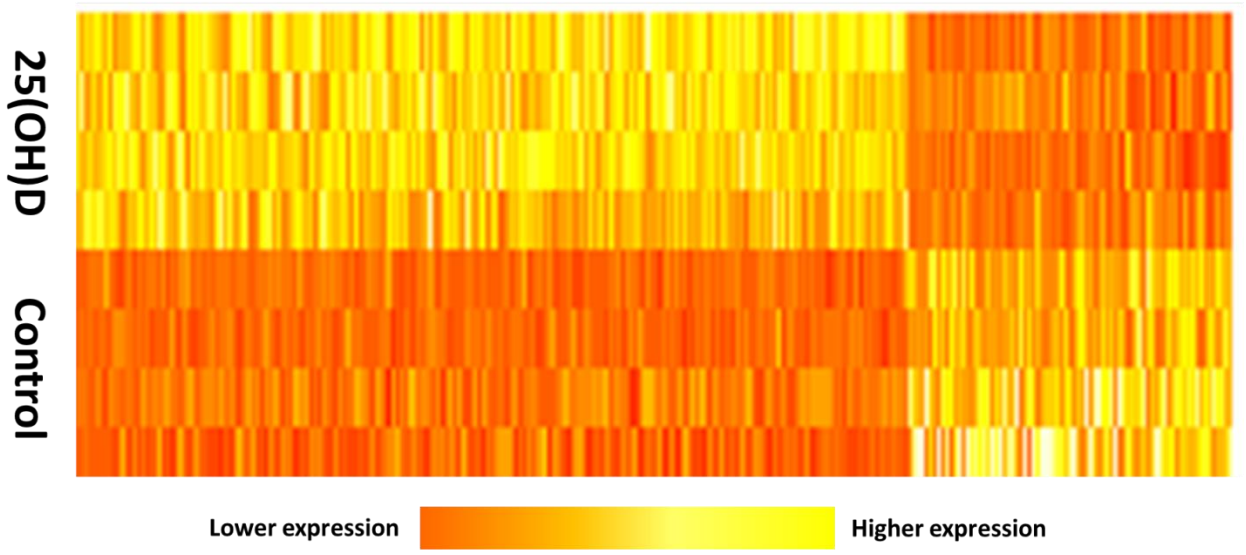

Figure 4-7 ***Differentially expressed genes with 25(OH)D$_3$ treatment*** *A heat map of differentially expressed genes (z-scores), showing distinctly altered gene expression with 25(OH)D treatment.*

Table 4-2 *Differential expression of RNA from genes of the Vitamin D pathway.*

Gene	Lg2 Fold change
CYP2R1	0.237
CYP27B1	-0.215
CYP24A1	4.407#*
DBP	0.653
VDR	0.560#
RXRα (NR2B1)	0.500#
RXRβ (NR2B2)	-0.026
RXRγ (NR2B3)	-0.094
LRP2	0.725#
CUBN	0.033

# indicates $p \leq 0.05$, * indicated FDR corrected $p \leq 0.05$.

4.3.3 Proteomics

To determine whether 25(OH)D$_3$ treatment altered protein expression in placental villous fragments LCMS analysis of the proteins in the tissue was carried out.

25(OH)D$_3$ treatment resulted in 246 differentially expressed proteins being identified (3 out of 4 permutations), of which 192 had increased expression and 54 decreased expression.

Additionally 98 methylated, 67 phosphorylated and 9 acetylated differentially expressed proteins were also identified (paired permutation testing, $p < 0.05$).

Genes with altered protein expression were mapped to biological pathways using the software MetaCore (Clarivate; USA), as seen in Figure 4-8. Pathways accepted with a minimum hit count of 4 and B&H FDR corrected q value of ≤ 0.05. A total of 10 pathways with altered protein expression were identified. Full pathways data is presented in Appendix A.

Proteins associated with vitamin D uptake (megalin, cubilin), metabolism (25-hydroxylase, 1-α-hydroxylase, 24-hydroxylase) and activity (RXR, VDR, DBP) were not identified using this technique.

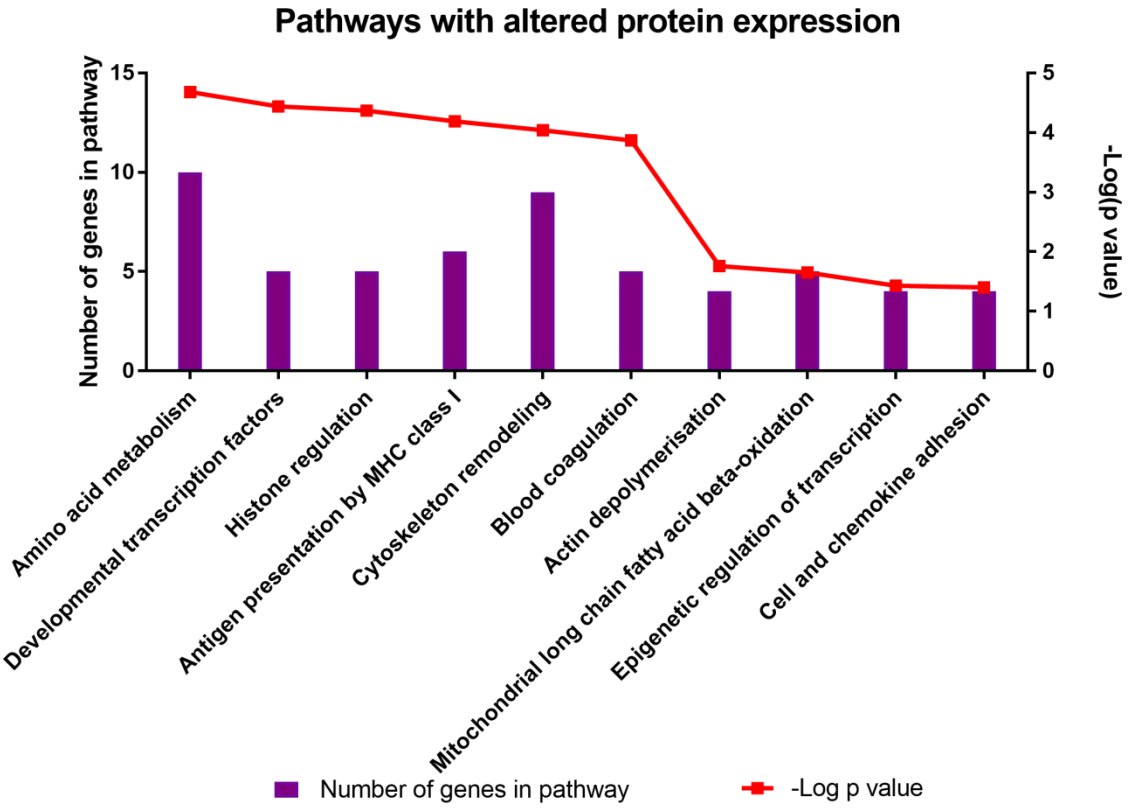

Figure 4-8 ***Pathways with altered protein expression in response to 25(OH)D_3 treatment***
Significantly altered pathways from genes mapped to sites of altered protein expression. Pathways identified using MetaCore and displayed as –Log p value.

4.3.4 Combined analysis

A total of 13096 genes ($p \leq 0.05$) mapped to sites of altered DNA methylation, 494 genes (FDR ≤ 0.05) had altered RNA expression, and 246 genes (3 out of 4 permutations) had altered protein expression. Aligned gene data is displayed in Figure 4-9. When the altered genes from each dataset are aligned, 253 contain both altered DNA methylation and RNA expression, 145 contain both altered DNA methylation and protein expression, and six contain both altered RNA

expression and protein expression. Overall, six genes contained altered DNA methylation, RNA and protein expression with 25(OH)D_3 treatment. Data on these genes is displayed in Table 4-3.

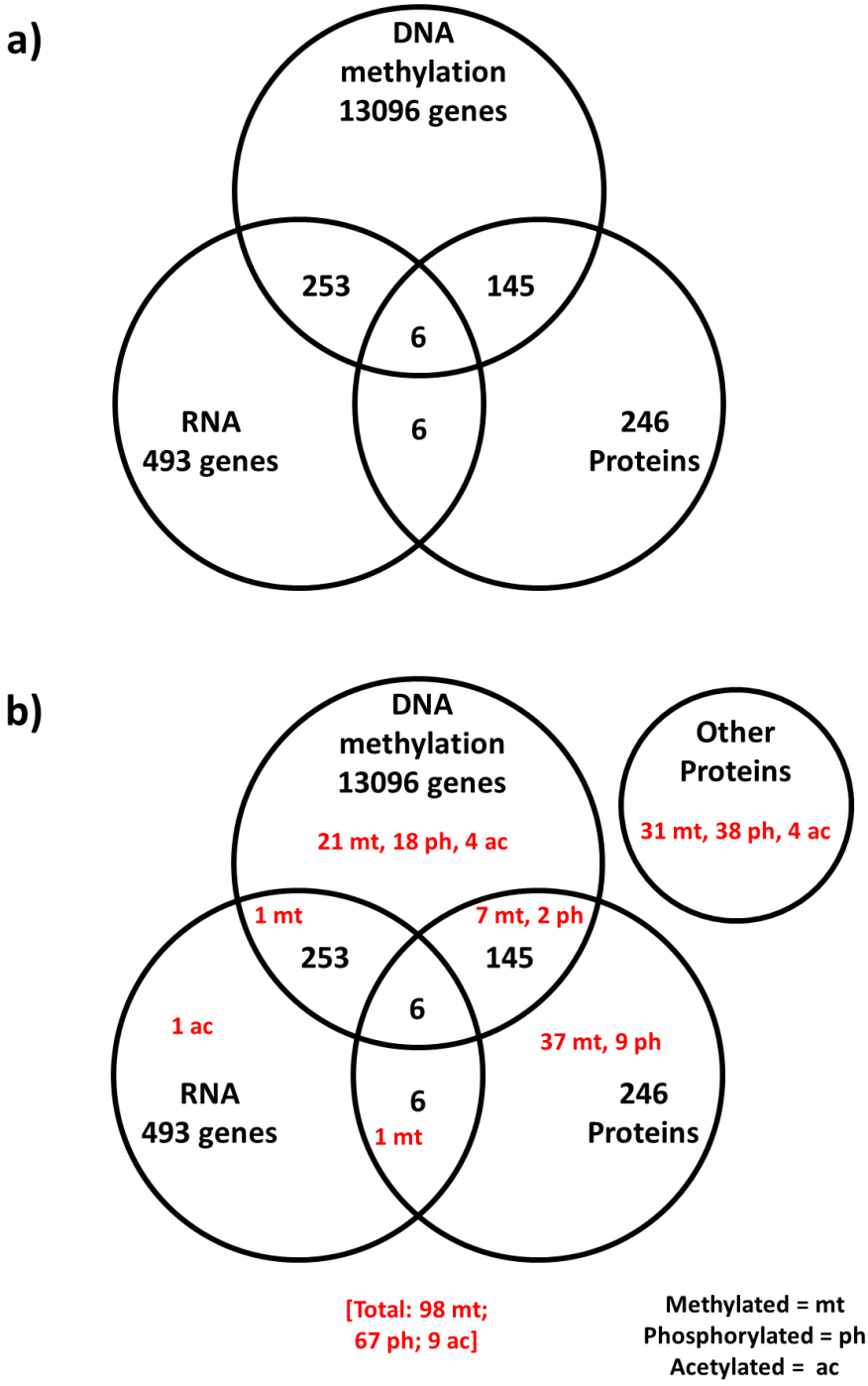

Figure 4-9 ***Alignment of DNA methylation, RNA and protein expression data a)*** *Aligned genes containing altered DNA methylation, RNA expression and protein expression.* ***b)*** *Aligned genes containing altered DNA methylation, RNA expression and protein expression with modified proteins overlaid in red.*

Table 4-3 *Gene containing altered DNA methylation, RNA expression and protein expression. All data significant at p ≤ 0.05 (DNA methylation), FDR ≤ 0.05 (RNA expression) and 3 out of 4 permutations (protein expression).*

	DNA methylation		**RNA**	**Protein**
Gene	**CpG**	**Fold change**	**Log Fold change**	**Log2 Fold change**
AHDC1	cg21455485	0.629	0.980	1.175
	cg11697038	0.060		
	cg13920090	0.047		
	cg02576395	0.026		
PLEKGH2	cg17860186	0.148	-0.732	-0.638
	cg03115281	0.031		
	cg06427718	-0.026		
CDRT1	cg27178956	0.042	1.291	0.768
	cg24324600	-0.082		
ENDOU	cg10675780	0.211	1.122	-0.446
	cg02744604	-0.017		
HIVEP2	cg15798191	0.027	0.943	0.480
	cg09659869	-0.022		
KIAA1522	cg00251405	0.107	0.785	-0.333
	cg06786238	0.049		

Cg = CpG site ID number

Genes identified as containing both altered DNA methylation and protein expression were mapped to biological pathways using the software Toppgene (www.toppgene.cchmc.org, Division of Biomedical Informatics, Cincinnati Children's Hospital Medical Center, Cincinnati), as seen in Figure 4-10. Pathways accepted with a minimum hit count of 4 and B&H FDR corrected q value of ≤ 0.05. Full pathways data is presented in Appendix A.

Genes identified as containing both altered DNA methylation and RNA expression were mapped to biological pathways using the software Toppgene (www.toppgene.cchmc.org, Division of Biomedical Informatics, Cincinnati Children's Hospital Medical Center, Cincinnati), as seen in Figure 4-11. Owing to the low number of pathways identified when corrected for FDR, significance was accepted as $p < 0.05$ and a minimum hit count of 10. Full pathways data is presented in Appendix A.

Owing to only six genes containing both altered RNA expression and protein expression pathway analysis was not carried out for these.

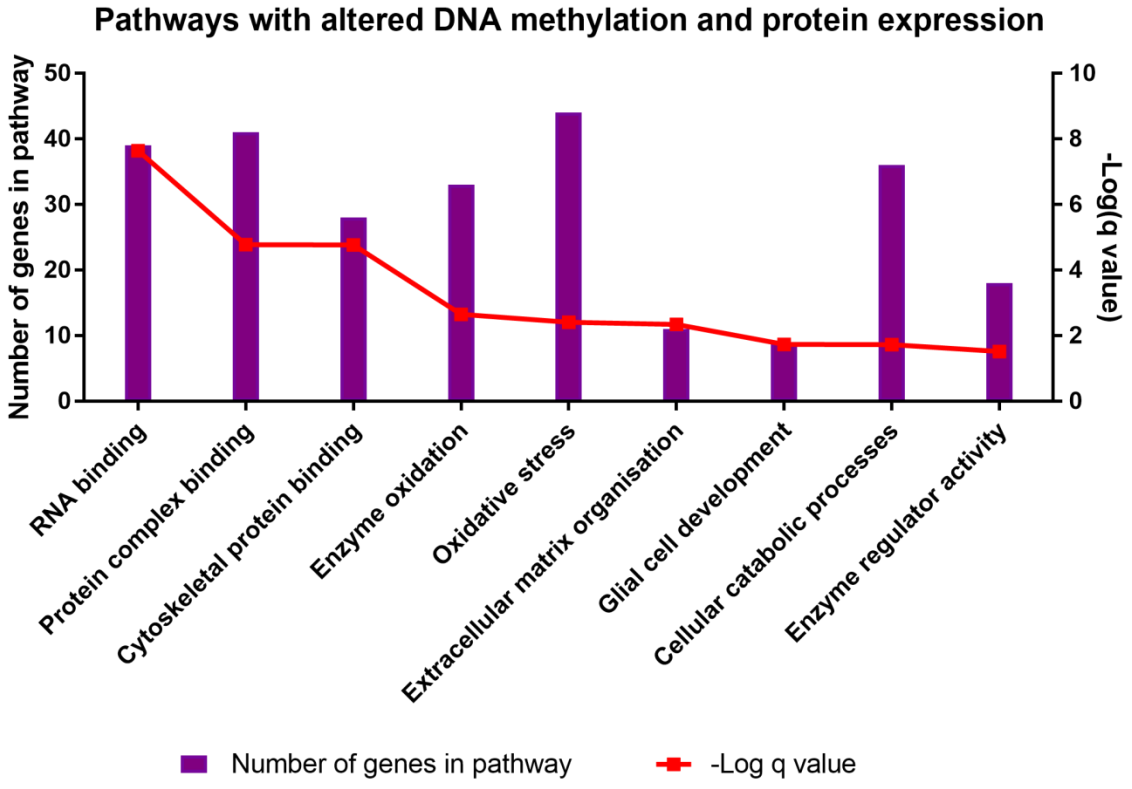

Figure 4-10 ***Pathways with altered DNA methylation and protein expression with 25(OH)D_3 treatment*** *Pathways identified using ToppGene and significance displayed as –Log B&H FDR corrected q value.*

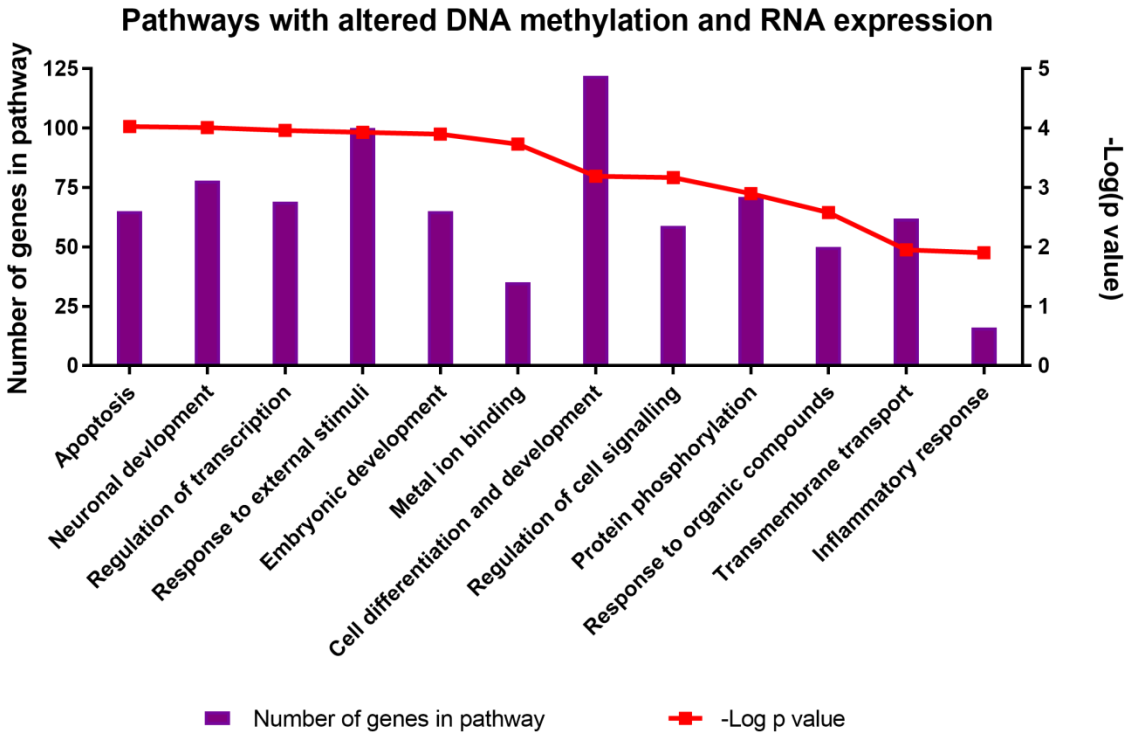

Figure 4-11 ***Pathways with altered DNA methylation and RNA expression with 25(OH)D_3 treatment*** *Pathways identified using ToppGene and significance displayed as –Log p value.*

4.4 Discussion

This study demonstrated that short term 25(OH)D_3 treatment can alter DNA methylation, RNA expression and protein expression in term *ex vivo* human placenta. These changes map to biological pathways within the placenta that could impact on growth and development. This suggests that maternal vitamin D status could impact placental function and therefore fetal development.

4.4.1 DNA methylation

This study has demonstrated that an 8 h treatment of 25(OH)D_3 alters placental DNA methylation across the genome. This rapid effect of 25(OH)D_3 on DNA methylation is supported by a previous study in a human prostate cell line observing altered DNA methylation with 1,25$(OH)_2D_3$ treatment within 4 h (Doig et al., 2013).

A large proportion of the altered CpG sites (48% of increased and 42% of decreased), were identified within a CpG island or its shores/shelves. CpG islands are predominantly found in transcriptional start sites, with around 70% of promoters containing a CpG island (Deaton and Bird, 2011). This suggests that the alterations to DNA methylation observed in this study may be acting to alter expression of the relevant genes. Increased methylation within CpG islands represses transcription by inhibiting access of the transcriptional machinery to the DNA, and decreased methylation allows greater access. Therefore the pattern of these changes within the tissue is important for understanding what effect this altered DNA methylation will be having.

Biological Pathways

Genes containing altered methylation were mapped to pathways using the software GREAT (www.great.stanford.edu), as this accounts for clusters of alterations, which may have greater biological significance.

25(OH)D_3 treatment altered pathways of corticotropin-releasing hormone (CRH) receptor binding, altering methylation in the genes *CRH, GNAO1, UCN1, UCN2* and *UCN3*. This pathway shows a decrease in DNA methylation across the affected genes, suggesting an upregulation of their expression. CRH, UCN1, 2 and 3 all act on their target cells by binding the cell surface CRH receptors CRH-R1 and CRH-R2 (Dautzenberga et al., 2001, Vitale et al., 2016). To my knowledge no previous studies have identified changes to DNA methylation in CRH or the UCN genes in the placenta with vitamin D treatment. The placenta produces CRH during pregnancy, with maternal levels increasing up to 10000 times the normal non-pregnant levels. CRH plays a role in regulating

uterine contraction and placental glucose transfer (Thomson, 2013), with CRH treatment causing increased expression of the glucose transporter GLUT1 in syncytiotrophoblast cells (Gao et al., 2012). Glucose transfer to the fetus is important for fetal growth. Reduced DNA methylation of CRH in the presence of vitamin D may therefore induce greater glucose transfer and thus increase fetal growth. CRH is thought to play a role in the timing of labour, with high levels of CRH associated with pre-term delivery (Grammatopoulos, 2007). Low vitamin D levels have also been suggested to be associated with pre-term delivery, and published data suggests that vitamin D and CRH levels are linked (Wang et al., 2018a). Wang *et al* suggested that vitamin D stimulates transcription of miRNAs that inhibit CRH, and thus high vitamin D levels could supress CRH levels. However our DNA methylation data here suggests that vitamin D may act to increase CRH expression, by decreasing its DNA methylation. The outcomes of these studies may differ as Wang *et al* studied a primary cytotrophoblast cell model and did not treat with vitamin D, whereas we used whole tissue and treated with $25(OH)D_3$.

Another pathway containing altered DNA methylation with $25(OH)D_3$ treatment is retinoic acid receptor activity. Methylation was altered in the genes *ESRRG, PRAM1, RARα, RARβ, RARγ, RXRα,* and *RXRβ.* ESRRG (estrogen related receptor gamma) is a member of the estrogen receptor related family, and mediates transcriptional regulation in response to estrogen binding (Kim et al., 2011). PRAM1 (PML-RARA Regulated Adaptor Molecule 1) is thought be involved in myeloid differentiation and integrin signalling. PRAM1 expression is inhibited by PML-RARα, a complex of promyelocytic leukaemia (PML) and the retinoic acid receptor (RARα) (Clemens et al., 2004). RAR and RXR are both families of transcriptional regulators that form a heterodimer (RAR-RXR) and interact with DNA, inducing transcription (Samarut and Rochette-Egly, 2012). There was an overall increase in the DNA methylation of genes in this pathway, with the exception of *RXRα*, which displayed an overall decrease. This suggests that vitamin D may be acting to reduce expression of genes in the retinoic acid receptor pathway, potentially through its action with RXRα, which decreases expression of other members of the pathway.

DNA methylation was increased with $25(OH)D_3$ treatment in genes of the histone pre-mRNA stem loop binding pathway, *SLBP* and *ESI1*. SLBP (stem-loop binding protein) plays a role in allowing histone mRNAs to move to the cytoplasm for translation, thus allowing expression of histone proteins (Gunjan et al., 2005, Dominski et al., 2003). ESI1 (exoribonuclease 1) on the other hand degrades histone mRNAs, reducing histone protein expression (Yang et al., 2006). Increased methylation, suggesting decreased expression of *SLBP*, could reduce the transfer of histone mRNAs to the cytoplasm for translation. Increased *ESI1* DNA methylation suggests a reduction in the degradation of histone mRNAs, potentially increasing histone protein expression. If there is a reduction in histone mRNA transfer to the cytoplasm then *ESI1* may not need to be expressed, as

the histone mRNA may not be present in quantities that warrant its degradation. Therefore *ESI1* DNA methylation may be a downstream effect of *SLBP* methylation. Alterations to histone protein expression and thus chromatin structure with 25(OH)D_3 treatment could significantly alter RNA expression in the placenta.

The pathway of voltage gated calcium channel activity was altered with 25(OH)D_3 treatment. Voltage gated calcium channels are composed of pore forming α1 subunits, and various auxiliary proteins (Dolphin, 2016). In this study eight of the 10 isoforms of the *CACNA1* genes, which encode for the pore forming α1 subunits, contained altered DNA methylation with vitamin D treatment. There was an overall decrease in DNA methylation, suggesting an increase in *CACNA1* gene expression. However increased DNA methylation was observed in the auxiliary protein gene families, *CACNA2D1* and *CACNG.* During pregnancy calcium must be transferred to the fetus, and the majority of calcium uptake into the placenta is via voltage independent calcium channels (Moreau et al., 2002). However voltage gated calcium channels do play a role in vasoconstriction within the placenta (Jakoubek et al., 2006). The auxiliary genes target the channel pore proteins to the cell membrane, and act to regulate their activity (Dolphin, 2016). Therefore vitamin D may be acting to increase the placentas ability to undergo calcium mediated vasoconstriction by increasing the availability of channel pore proteins, without causing vasoconstriction due to the decrease in auxiliary protein expression, in a DNA methylation mediated manor.

4.4.2 RNA expression

This study demonstrated that an 8 h treatment of 25(OH)D_3 alters the expression of a number of genes at the RNA level. This rapid response to vitamin D exposure suggests an effect of vitamin D on placental function.

Biological pathways – Increased expression

Four pathways of transcriptional regulation had increased RNA expression, C2H2-type transcriptional regulation, BTB domain containing transcriptional regulation, transcriptional regulation and negative regulation of transcription. These pathways contain upregulation of the transcription factor gene families *ZNF, ZBTB,* and *SOX*, as well as a number of additional transcription factors such as *TSP1, BACH2* and *TBX20* (Lambert et al., 2018). Transcription factors in these families reportedly target developmental pathways including fertility, limb patterning and nervous system development and genes of the immune system (Schmitges et al., 2016, Siggs and Beutler, 2012, She and Yang, 2015). Poor maternal vitamin D levels during pregnancy have been associated with an increased risk of developing schizophrenia in later life, suggesting a role of

vitamin D in fetal brain development (Eyles et al., 2018). 25(OH)D_3 treatment may therefore be affecting the regulation of gene expression of a wide range of genes in the placenta, with a particular target towards those involved in immunity and nervous system development.

25(OH)D_3 treatment altered a pathway of deubiquitination, increasing the RNA expression of five deubiquitinases, *OTUD7B, YOD1, OTULIN, OTUD3, VCPIP1*. *OTUD7B, YOD1* and *OTULIN* regulate the noncanonical NF-κB pathway, which plays an important role in inflammation and immune regulation, including lymphoid organogenesis and B-cell maintenance (Hu et al., 2013, Schimmack et al., 2017, Damgaard et al., 2016). *OTUD3* however is involved in regulating tumor suppression (Yuan et al., 2015), and *VCIP1* is thought to play a role in the reassembly of golgi fragments after mitosis (Wang et al., 2004). This suggests that vitamin D may be acting to regulate inflammation and immune function within the placenta by modulating the actions of deubiquitinases on the NF-κB pathway.

Histone methyltransferases in the pathway of histone methylation had increased expression with 25(OH)D_3 treatment. *ASH1L* and *NSD1* both methylate H3K36 (An et al., 2007, Qiao et al., 2010). *KMT2C* and *KMT2D*, genes of the same family, both methylate H3K4 (Froimchuk et al., 2017). *BPTF* is not a histone methyltransferase, but binds to H3K4me3 marks on histone tails (Morrison et al., 2018). *DPF2* is also not a histone methyltransferase, but binds to acetylated H3 and H4 histone tails (Hubera et al., 2017). Vitamin D may be acting to modify chromatin structure and the accessibility of genes to transcription factors by altering histone methylation. Binding of the proteins BPTF and DPF2 to histone tails also alters the ability of other histone modifiers to interact with the tails. Therefore vitamin D may be acting to modify gene expression by the action of histone methyltransferases and histone tail binding proteins on chromatin, repressing or allowing transcription to occur. DNA methylation changes were also observed in genes which act to regulate histone protein expression.

A pathway of endosomal recycling was upregulated with 25(OH)D_3 treatment, upregulating the expression of the genes *SYDE2, PCLO, RAB11FIP1* and *RAB11FIP5*. The upregulated genes all play roles in in cytoskeletal remodelling, cell migration, localising machinery for endocytosis, endosomal recycling, targeting receptors to the recycling pathway (Lo et al., 2017, Fenster and Garner, 2002, Jin and Goldenring, 2006, Schonteich et al., 2008). Collectively the upregulation of these genes suggest that vitamin D plays a role in increasing endosomal recycling within the placenta. This may be a result of increased uptake of vitamin D into the cell via an active endocytic mechanism.

Biological pathways – Decreased expression

A pathway of inflammation and immune regulation showed decreased RNA expression with 25(OH)D_3 treatment. Decreased expression was observed in the genes encoding for a number of interleukins (*IL24, IL32*), interleukin family receptors (*IL1R2, IL1RL1, IL36RN, IL2RG, IL3RA*), tumour necrosis factors (*TNFAIP6, TNFRSF11B*), IgG receptors (*FCGR3A, FCGR3B*), and chemokines (*CCL2, CCL4, CCL4L2*). Interleukins, tumour necrosis factors and chemokines are all cytokines, stimulating a response in their target cells. During pregnancy maternal-fetal immune tolerance must be maintained, whilst still being able to mount an appropriate inflammatory response to a pathogenic insult (Tamblyn et al., 2015). A reduction in the expression cytokine receptors in response to 25(OH)D_3 treatment may reduce the cells ability to generate an inflammatory response in the presence of cytokines. The reduction in expression of various cytokines, in addition to the reduction in the expression of cytokine receptors, may suggest that vitamin D is acting to modulate the immune system towards a tolerant environment.

A broad pathway of response to stimuli had decreased RNA expression with 25(OH)D_3 treatment. Reduced RNA expression was observed in a number of genes associated with inflammation and immune regulation (including *IL24, IL32, CXCL10* and *ACOD1*) as well as calcium binding protein and proteases. A recent study in human bronchial epithelial cells demonstrated a reduction in *IL24* expression when incubated with 1,25(OH)D_3 (Pfeffer et al., 2018). Reduction in the expression of this collection of genes suggests a change in the responsiveness of the placenta to its environmental signals, in particular to signals of the immune system.

25(OH)D_3 treatment reduced the RNA expression of a pathway of inorganic ion transporters, including the genes *MCHR1, STEAP4, SCAMP5, MMP3* and *NNAT*. *MCHR1 and NNAT* regulate calcium channel expression and calcium flux in cells, particularly during brain development (Saito et al., 2013, Pitale et al., 2016). *MMP3* plays an important role in trophoblast invasion into the endometrium, allowing for remodelling of the vasculature and blood flow to the placenta (Husslein et al., 2009). Inorganic ions such as calcium are involved in cell signalling and in regulating pathways of activity. Vitamin D may be acting to modulate placental activity by altering the composition of inorganic ions within the placental cells. DNA methylation was also altered in genes altering voltage-gated calcium channel activity.

A pathway of regulation of endocytic processes had reduced RNA expression with 25(OH)D_3 treatment, affecting the genes *OLFM4, DKK1, SCAMP5, PTX3, CCL2* and *C4BPB*. Within these genes there is overlap with those identified in the downregulated inflammation and immune regulation pathways, as well as further immune related roles. This suggests that vitamin

D is acting to affect placental inflammation and immune regulation through altering the regulation of endocytic processes that are involved in inflammatory processes.

4.4.3 Protein expression

This study demonstrates that an 8 h 25(OH)D_3 treatment alters the placental proteome, suggesting an effect of vitamin D on placental function and activity at the protein level.

Biological pathways

The 8 h 25(OH)D_3 treatment altered a pathway of amino acid metabolism. Previous studies have demonstrated altered RNA expression of amino acid transporters with vitamin D in both a cohort study (Cleal et al., 2015) and in primary cultured trophoblast cells (Chen et al., 2016). The results of these studies suggest vitamin D can alter the amount and type of amino acids being transferred to the fetus. Here we show that the expression of a number of enzymes involved in the metabolism of amino acids is also altered, including *ACAT1, FAH* and *AOC3*. These changes to the expression of amino acid metabolisers suggest that vitamin D may be acting to alter the type and amount of amino acids present in the placenta. In turn, this could alter the availability of amino acids for use by the placenta or for transfer to the fetus, which could affect fetal growth.

A number of pathways affecting transcription were also altered with 8 h 25(OH)D_3 treatment, including developmental transcription factors, histone regulation and epigenetic regulation of transcription. Altered expression of transcription factors may act on specific genes or gene families to alter their expression, potentially altering placental function. Alterations to the expression of the histone proteins identified in these pathways (*H2BFM, HIST2H2AC, HMGB1, HIST1H4A, HIST1H1B*), may alter transcription more globally, by altering how accessible sections of DNA are to transcription factors. Increased expression of histone proteins will inhibit transcription by allowing DNA to condense, becoming inaccessible to transcription factors, and vice versa with decreased histone protein expression. Vitamin D may therefore be acting to alter transcription within the placenta through a number of mechanisms. Alterations to histone protein activity were observed at both the DNA methylation and RNA expression levels.

A pathway of antigen presentation by MHC class 1 was altered with 8 h 25(OH)D_3 treatment. The altered proteins HSP90B1, PSME2, TPP2, CANX, PSMB2 and ERAP2 showed a general decrease in expression, demonstrating a downregulation of this pathway. Antigen presentation by MHC class 1 molecules plays a role in inducing both innate and adaptive responses in the placenta (Reeves and James, 2017). A downregulation of the proteins present in

this pathway could therefore suggest a change in placental immune function towards a less reactive, more tolerant environment. A number of pathways of immune activity were also altered at the RNA expression level.

The 8 h 25(OH)D_3 treatment altered pathways of cytoskeleton remodelling and actin depolymerisation. Remodelling of the cytoskeleton, occurs with a number of cellular processes including cell migration, cell division and endocytic uptake processes. Alterations to the expression of proteins in these pathways with vitamin D treatment suggests that that vitamin D may be acting on one or more of these cellular processes by its interaction with the cytoskeleton. Alterations to pathways of endocytosis were also observed to be altered at the RNA expression level.

4.4.4 Overall expression

The majority of studies investigating the effects of vitamin D on a tissue only look at the effects of vitamin D at one or two levels (Junge et al., 2016, Castellano-Castillo et al., 2019). Here we have investigated the effects of vitamin D treatment on placental tissue at three levels, DNA methylation, gene expression and protein expression. This has allowed us to investigate whether changes in DNA methylation or gene expression are leading to downstream changes in protein expression.

Vitamin D metabolic pathway

Altered DNA methylation and RNA expression was observed at sites within genes of the vitamin D metabolic pathway. Unfortunately within this study proteins of the vitamin D metabolic pathway were not identified. This may be due to low expression levels, but is also likely a result of the technique used to identify proteins present. LCMS requires unique fragments of the proteins to be present after fragmentation. This therefore excludes proteins which do not contain unique, identifiable fragments, thus not giving us a complete picture of the proteome.

CYP24A1, the 25-hydroxylase enzyme responsible for the inactivation of 25(OH)D and 1,25$(OH)_2$D, had decreased methylation at one CpG site. RNA expression was increased, with a log 4.41 fold change. *CYP24A1* is a vitamin D responsive gene, with increased expression occurring in the presence of vitamin D. This helps enable the tight regulation of 1,25$(OH)_2$D, with increased levels causing increased breakdown. Therefore a reduction in DNA methylation here may play a role in increasing the expression of *CYP24A1* in the presence of vitamin D. A previous study demonstrating that individuals with less DNA methylation in *CYP24A1* had a reduced response to vitamin D supplementation, likely due to increased breakdown, supports our findings of decreased *CYP24A1* methylation (Zhou et al., 2014).

VDR, which forms a complex with *RXRα* in the presence of 1,25$(OH)_2$D, contained one site of increased and three sites of decreased DNA methylation. RNA expression was increased, with a log 0.56 fold change. A number of studies have demonstrated that changes in *VDR* promoter DNA methylation cause changes to its expression (Fetahu et al., 2014). The overall decrease in DNA methylation observed here may therefore underlie the increase in expression of *VDR* in response to 25$(OH)D_3$ treatment. Increasing the pool of VDR available for 1,25$(OH)_2$D to bind to may allow for increased action of the vitamin D.

RXRα, which acts in complex with *VDR* in the presence of 1,25$(OH)_2$D, contains two increased and four decreased sites of DNA methylation. RNA expression was increased, with a log 0.5 fold change. Once again the overall decrease in DNA methylation observed in *RXRα* may underlie the greater expression of *RXRα* in response to 25$(OH)D_3$ treatment, suggesting a greater pool of *RXRα* available for 1,25$(OH)_2$D to bind. *RXRβ*, an isoform of *RXRα*, contains two sites of increased and one site of decreased DNA methylation, and *RXRγ* did not contain any sites of altered DNA methylation. RNA expression was decreased in *RXRβ* and *RXRγ*, with a negative log 0.03 and 0.09 fold change respectively. This overall increase in methylation and decrease in expression of RXRβ and RXRγ, although small, may reflect the preference for RXRα binding to VDR in the presence of 1,25$(OH)_2$D.

LRP2 (megalin) contained one site of increased and one site of decreased DNA methylation, and had a log 0.73 fold change increase in RNA expression. *CUBN* (cubilin), contained three sites of increased and one site of decreased DNA methylation, and had a negative log 0.03 fold change decrease in expression. Collectively megalin and cubilin mediate uptake of 25(OH)D into the renal proximal tubules of the kidneys (Nykjaer et al., 2001), and this may also be a method of uptake into the placenta. The lack of directional change to *LRP2* DNA methylation suggests this methylation may not be underlying the increase in RNA expression. The overall increase in *CUBN* methylation might underlie the small decrease in its RNA expression. If 25(OH)D does enter the placenta via megalin/cubilin mediated uptake then a decrease in *CUBN* expression could limit the cells exposure, regulating it's response to vitamin D.

Biological pathways

When looking at the pathways with altered DNA methylation, RNA expression and protein expression with vitamin D treatment collectively, a number of similar pathways arise at more than one level of expression.

Alterations to histone protein expression or activity were identified in the DNA methylation, RNA expression and protein expression data. Collectively this suggests that vitamin D

is acting to alter the expression and activity of histone proteins. Histone proteins play a role in controlling how accessible sections of DNA are to other interacting proteins, such as transcription factors. Regulation of the expression and activity of histone proteins may therefore be a mechanism by which vitamin D regulates other cellular functions.

Pathways of altered transcriptional regulation were identified in both the RNA expression and protein expression data. A pathway of regulation of transcription was also identified when analysing genes containing both altered DNA methylation and RNA expression. Collectively this suggests that vitamin D is acting to alter a number of pathways of transcriptional regulation within the cells. The action of vitamin D to change histone protein expression and activity described above may be one mechanism through which vitamin D achieves these transcriptional regulation changes.

Pathways altering inorganic ion channels were identified in both the DNA methylation and RNA expression data. A reduction in the methylation of genes that form voltage gated calcium channel pore proteins suggests an increased sensitivity of the placenta to calcium mediated vasoconstriction, whilst decreased RNA expression of inorganic ion transporters suggests a reduction in the ability of the cell to perform inorganic ion mediated signalling and pathway transduction. The decrease in responsiveness to inorganic ions observed with the RNA expression data may be in response to an increased ability of the placenta to take up calcium through voltage gated calcium channels.

A pathway of endosomal recycling had increased RNA expression with vitamin D treatment. Within this pathway a number of genes involved in cytoskeletal binding and remodelling, important for bringing relevant proteins into place at the cell surface, were altered. Similar pathways were also identified in the protein expression data, and when analysing genes containing both altered DNA methylation and protein expression. Here a further pathway of transmembrane transport was also identified. Collectively these suggest that vitamin D is acting to mediate endosomal uptake and recycling through remodelling of the cytoskeleton. Unpublished data from within our laboratory suggests that vitamin D is taken up into the placenta in an endocytosis mediated manner. These changes to cytoskeletal remodelling and increased endocytic recycling may therefore reflect the increase in uptake of vitamin D into the cell.

Pathways affecting inflammation and immune regulation were identified in both the RNA and protein expression data. A pathway of inflammatory response was also identified when genes containing both altered DNA methylation and RNA expression were analysed. Collectively this suggests that vitamin D may be acting to modulate the placental immune environment. Immune changes are necessary for successful pregnancy to prevent rejection of the fetus, however the

mother must still be able to respond appropriately to incoming pathogens. This data suggests that vitamin D may be acting to promote an immune tolerant environment, consistent with the effect of vitamin D on the immune system (Prietl et al., 2013).

4.5 Limitations

This section of research has a number of limitations. First is the small sample size used in all three techniques, with DNA methylation having an n of 8 and both the RNA sequencing and LCMS proteomics having an n of 4 per treatment group. This is due to both the practicalities of obtaining fresh human placental samples, in addition to the expensive nature of these techniques. In this dataset, there was a trade-off between the number of samples that could be investigated, and the techniques used. For example using pyrosequencing to measure DNA methylation, qRT-PCR to measure RNA expression and western blotting to measure protein expression would have been cheaper than using the array based methods presented here. This would have meant a larger number of samples could have been investigated. However a much smaller number of DNA methylation sites, RNAs and proteins could have been investigated and these targets would be selected by us. Using a DNA methylation array, RNA sequencing and LCMS proteomics allowed us to investigate changes across the genome, and identify unexpected changes to genes of which we had no prior knowledge. The use of matched control and treated samples from the same patients strengthens this dataset in regards to sample size.

There is a limitation to measuring DNA methylation using the Infinium® MethylationEPIC array. Whilst this array provides coverage of 95% of CpG islands, > 850K CpGs and 99% RefSeq promoters, CpG sites with potentially important functions are still not measured. Therefore potentially important changes in the DNA methylation at these sites could be missed.

Another limitation is that only mRNA was investigated in this study. Other RNAs, including many long and small non-coding RNAs, were excluded from the study due to the methods used, which selected for polyadenylated RNA (mRNA). It is well known that other RNAs, such as miRNAs, piwi-interacting RNAs, and transfer RNAs play important roles in the functioning of a cell (Umu et al., 2018). Therefore information on these RNAs was not obtained, and it is plausible given the changes seen to mRNA expression with vitamin D treatment that changes may also be seen in other RNA types.

LCMS requires unique protein fragments to be detected in order for a protein to be identified, as if the fragment is common to many proteins, it is not possible to determine which it originated from. Therefore the use of LCMS creates a limitation in this study, as proteins were likely present that were not detectable by this technique.

Given the small sample size in this study, and the large number of measures being made, it was not possible to analyse all of the data at the FDR level. The DNA methylation data and

proteomics was not analysed using FDR as all significance was lost. B&H FDR corrected q values were used when possible to ensure data were stringently analysed.

In this study whole villous tissue fragment were used, meaning multiple cell types were analysed including cytotrophoblast, syncytiotrophoblast, endothelial cells, blood cells, macrophages, fibroblasts and smooth muscle cells (Huppertz, 2008). Therefore it is not possible to conclude in what cell types the changes observed occurred. Changes that occurred in less abundant cell types, such as immune cells, may have been diminished by analysing in conjunction with more abundant cell types such as cytotrophoblast cells.

4.6 Future work

The data generated in this study raise a number of further questions, some of which will be investigated further throughout this thesis, including:

1. What placental cell types do the observed DNA methylation, RNA and protein expression changes occur in?
2. Are the same RNA expression changes observed when measured by RNA sequencing as when measured using qRT-PCR?

These questions are further addressed in Chapter 5 of this thesis.

The mechanism through which vitamin D acts to alter placental DNA methylation is unknown. Further studies could begin to address this by looking at where vitamin D and associated proteins are interacting with the DNA. This can be carried out using Chromatin Immunoprecipitation, followed by sequencing of the DNA (ChIP-Seq). A recent study looked at where the VDR binds DNA in human primary cultured syncytiotrophoblast cells (Wang et al., 2018a), and a similar method could be used to identify sites of binding close to our altered sites of DNA methylation. It would also then be possible to identify if DNA methyltransferases are bound to the VDR in any complexes that are pulled down. Overlaying the VDR DNA binding data by Wang *et al* with our array data may allow us to identify where changes observed in our array datasets occur by VDR-RXRα mediated transcriptional activation, and where other epigenetically mediated mechanism may be acting.

Investigation of other types of RNA could provide further information on how vitamin D acts to alter the transcriptome. Other types of RNAs, such as small non-coding RNAs play a number of roles in the functioning of a cell, and therefore information on how their expression is affected by vitamin D could provide further clarity to how vitamin D alters the transcriptome. This could again be carried out using a genome wide sequencing method.

The use of LCMS to investigate changes to the proteome with vitamin D treatment undoubtedly meant that certain proteins were present but not identified, due to the lack of unique peptides. Therefore to investigate proteins of interest that were not identified here further, a more specific technique such as western blotting could be used. As no proteins of the vitamin D pathway were identified it would be particularly interesting to see if the RNA expression changes observed matched any subsequent protein expression changes. A number of other interesting genes were identified to have altered RNA expression but no protein was identified, and these could also be investigated in this manner.

4.7 Conclusions

Vitamin D is known to affect transcription through its interaction with the VDR-RXRα complex, which then binds VDREs and induces transcription in vitamin D responsive genes. Data presented here suggest vitamin D is also acting to alter transcription via an epigenetic mediated mechanism, by altering DNA methylation, as shown in Figure 4-12. A number of genes have previously been identified to have altered RNA expression in the placenta with vitamin D treatment. Here we identify many novel genes whose altered expression with vitamin D treatment has not previously been described. We have also identified a number of novel proteins with altered expression with vitamin D treatment, information on which is lacking in the current literature. Pathway analysis of these datasets has demonstrated consistent themes to the changes with vitamin D treatment. This suggests vitamin D is acting to alter placental function, regulating transcription, histone expression, ion channel activity, endocytosis and immune regulation within the placenta.

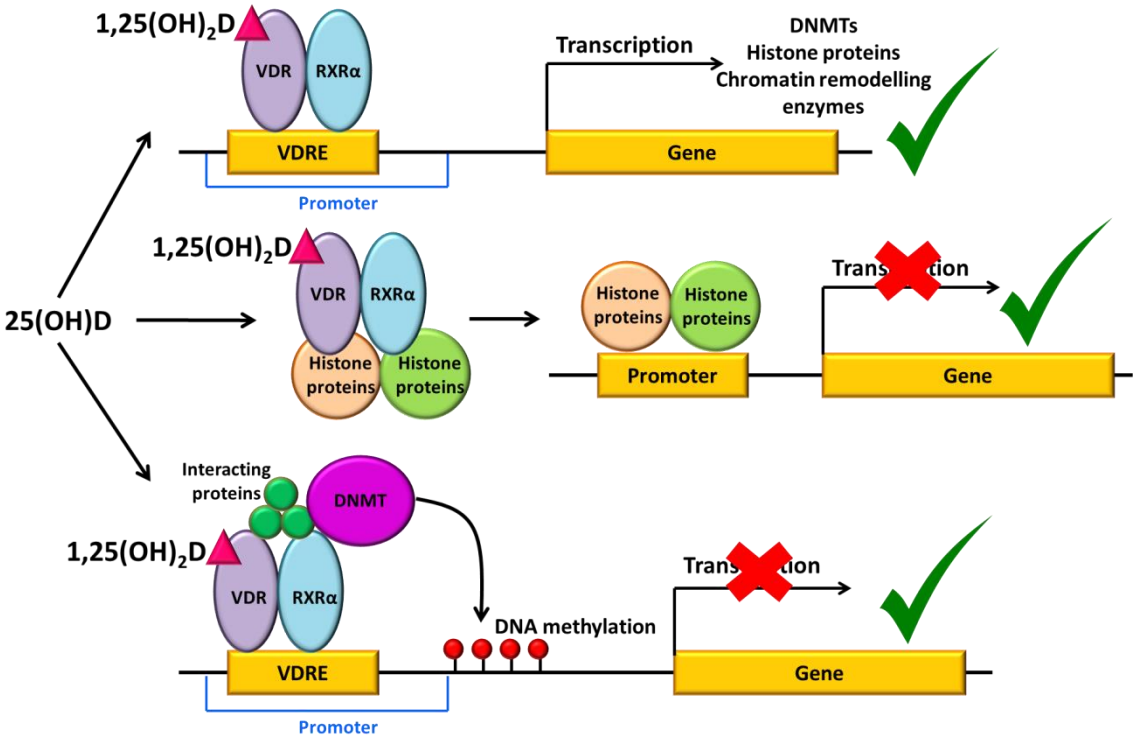

Figure 4-12 ***Mechanisms of action of 1,25(OH)$_2$D within the placenta.*** *1,25(OH)$_2$D can enhance or repress transcription of genes involved in epigenetic remodelling. 1,25(OH)$_2$D may modify histone protein activity, altering how they interact with DNA and subsequently blocking or allowing access of transcription factors to the DNA altering expression. 1,25(OH)$_2$D alters DNA methylation.*

Chapter 5 Vitamin D induced changes to the placental transcriptome and epigenome

5.1 Introduction

Vitamin D treatment is associated with changes in human placental gene expression, including the expression of amino acid transporters (Cleal et al., 2015, Chen et al., 2016), calbindins (Halhali et al., 2010), immune genes (Longtine et al., 2017) and angiogenic markers (Schulz et al., 2017a). In Chapter 4 data was presented also showing changes to placental gene expression with vitamin D treatment, and suggesting that these changes may be regulated in an epigenetic manner. In this chapter I investigate further some of the observations from Chapter 4, investigating where changes may occur within the placenta, duration of vitamin D exposure and whether DNA or histone methylation underlies functional changes with vitamin D treatment.

The syncytiotrophoblast is the primary barrier in the human placenta, separating maternal blood from the fetal vasculature (Cleal and Lewis, 2016). The syncytiotrophoblast plays an important role in the regulation of transfer of nutrients from the maternal to the fetal circulation. Nutrients have been observed to act on the placental syncytiotrophoblast to alter placental function, for example, vitamin D acts on the syncytiotrophoblast to alter system A amino acid transporter function (Chen et al., 2016). However there are many other cell types within the placenta, as shown in Figure 5-1, such as epithelial cells, fibroblasts and immune cells upon which nutrients may act to exert an effect on placental function (Huppertz, 2008). It is not clear whether the changes observed in Chapter 4 are occurring in the syncytiotrophoblast, in another specific cell type, or in multiple cell types within the placenta.

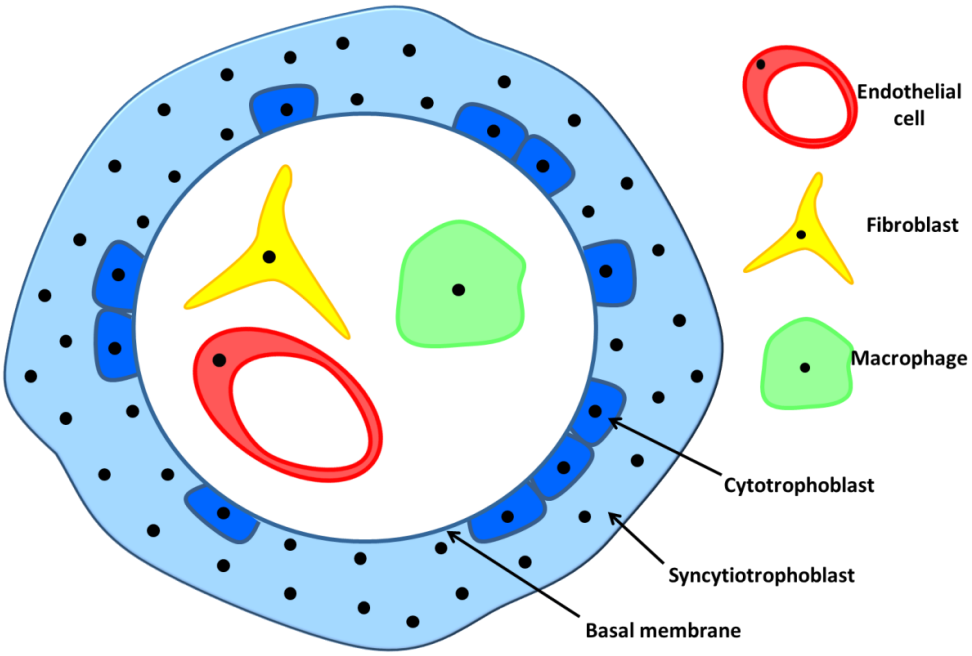

Figure 5-1 ***A diagram of a human term placental villi.*** *Cross section of a terminal villi showing placental cell types that may be present. Vitamin D may act differently on different cell types within the placenta.*

Epigenetic mechanisms such as DNA methylation and histone modification may underlie changes to placental gene expression. Increased DNA methylation inhibits transcription by inhibiting transcriptional machinery from accessing the DNA, or by binding proteins that recruit transcriptional repressors (Moore et al., 2013). Methyl groups are added to cytosine residues at CpG sites by members of the DNA methyltransferase (DNMT) family, producing 5-methylcytosine. Dnmt3a and Dnmt3b add *de-novo* methyl groups and DNMT1 adds methyl groups to hemimethylated DNA (Moore et al., 2013). DNA methyltransferases may be acting to alter placental DNA methylation in response to vitamin D treatment, either by changes in their expression or changes in their activity.

Histone N-terminal tails undergo methylation, acetylation, phosphorylation and ubiquitinylation at specific nucleotides, which can interact with chromatin changing its structure, as shown in Figure 5-2. Histone modification mediated changes to chromatin structure can subsequently alter gene expression, by altering the accessibility of DNA to the transcriptional machinery. Data presented in Chapter 4 suggests alterations to histone protein expression and the expression of histone modifying proteins with vitamin D treatment. However it is not known whether these changes result in changes to histone protein modifications and whether they occur with long term exposure (Cutter and Hayes, 2015, Nelissen et al., 2011).

Understanding where in the placenta vitamin D is acting, and how the changes underlying altered placental function occur, will allow us to better understand the role vitamin D plays in healthy fetal development. This in turn may allow us to better understand how to approach treatment for pregnant mother deficient in vitamin D.

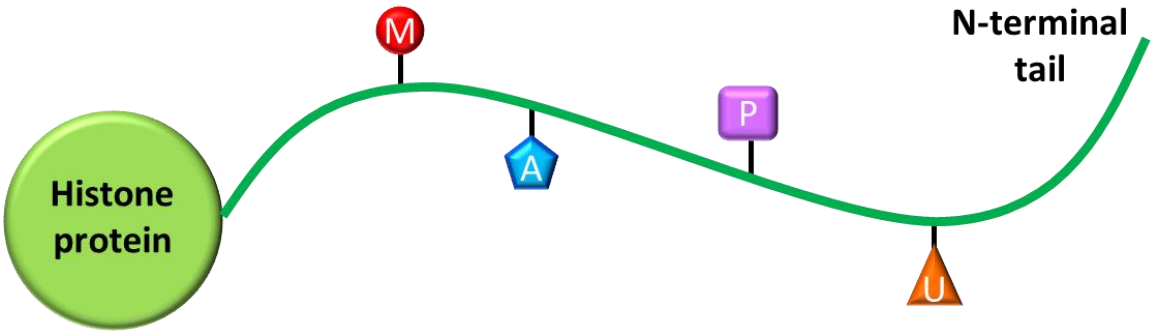

Figure 5-2 ***Histone modifications.*** *The N-terminal tails of histone proteins may undergo methylation (M), acetylation (A), phosphorylation (P) or ubiquitination (U).*

5.1.1 Aims

1. To investigate the effects of vitamin D on the mRNA expression of genes of interest in human placental syncytiotrophoblast and fragment culture models.
2. To investigate how DNA methylation and histone modifications may underlie changes in gene expression in response to vitamin D in human placenta.

5.2 Methods

5.2.1 Cohort studies

Cohort studies were utilised to investigate the effects of long term exposure to cholecalciferol supplementation on placental DNA methylation and histone modifications.

Maternal Vitamin D and Osteoporosis Study

The Maternal Vitamin D Osteoporosis Study (MAVIDOS) was a randomised double-blind trial investigating whether supplementing mothers with vitamin D during pregnancy results in offspring having a higher bone mass at birth, as described in Chapter 2.1.1. Briefly women were recruited at around 12 weeks of pregnancy and their serum 25(OH)D levels measured. If they had a serum concentration of 25(OH)D between 25 – 100 nmol/l they were randomly assigned to once daily oral supplementation of 1000 IU cholecalciferol or matched placebo (Bilcare GCS Ltd). At birth placental tissue was collected by Dr Claire Simner as described in Chapter 2.2.2.

Southampton Pregnancy Intervention for the Next Generation

The Southampton Pregnancy Intervention for the Next Generation (SPRING) is a randomised controlled trial investigating two different interventions, a healthy conversation skills intervention and cholecalciferol supplementation, as described in Chapter 2.1.2. Briefly women were recruited at 8 – 12 weeks of pregnancy and randomised to receive either healthy conversation skills support or control, and once daily oral supplement of 1000 IU cholecalciferol or a matched placebo (Sharp Clinical Services Ltd, UK). At birth placental tissue was collected as described in Chapter 2.2.2.

5.2.2 Placental collection

General collection

Term human placentas were collected within 30 min of delivery as described in Chapter 2.2.1, from women who had healthy, uncomplicated pregnancies. Tissue was transported to the laboratory as quickly as possible for villous fragment culture (n = 5) or primary cytotrophoblast cell isolation (n = 5).

Cohort studies

Term human placenta samples were collected within 30 min from the MAVIDOS study (n = 74), or as soon as possible after delivery in the SPRING study (n = 94), as described in Chapter 2.2.2. Briefly ten 0.5 cm^3 villous tissue samples were cut from the placenta using a random sampling grid, and snap frozen in liquid nitrogen. Samples were stored at -80°C prior to RNA extraction (only if collected within 30 min of delivery), DNA extraction or histone protein extraction.

5.2.3 Primary cytotrophoblast cell isolation

Cytotrophoblast cells were isolated from fresh placental tissue as described in Chapter 2.5.1. Briefly the umbilical cord, membranes, decidua and chorionic plate were removed. The remaining villous tissue was minced and visible vessels, blood clots and gritty tissue removed. Tissue was strained through sterile gauze, and placed in a conical flask with a digestion solution of HBSS, DNase and trypsin. Tissue was incubated in the digestion solution for 30 min at 37 °C in a shaking water bath, and then the supernatant was collected. The supernatant contained single cells that had been digested out of the tissue. The digestion process was repeated a further two times. Supernatant was layered over NCS, and centrifuged to pellet cells. Pellets were resuspended in DMEM, combined and centrifuged again to create one cell pellet. The pellet was resuspended in DMEM, and layered over a Percoll gradient. The Percoll gradient was centrifuged, separating the cells based on density. Bands containing cytotrophoblast cells were collected.

5.2.4 Cytotrophoblast cell counting

Cytotrophoblast cells were counted as described in Chapter 2.5.3. Briefly cells removed from the Percoll gradient as described above were diluted and cells between 6 - 19 µm in diameter were counted on a Beckman Coulter Z1 Particle Counter. A range of sizes were counted that fell within that expected for cytotrophoblast cells (Yabe et al., 2016), as the cells size and shape varies with development and interaction with its neighbouring cells. The dilution was then accounted for to determine the number of cells obtained.

5.2.5 Cytotrophoblast cell culture

Cytotrophoblast cells were cultured as described in Chapter 2.5.2. Briefly cells were plated at a density of 3 x 10^6 cells per 32 mm diameter well of a 6 well plate, with 2 ml of culture media. At 18 h after plating, and every 24 h thereafter, media was removed and replaced with 2 ml fresh culture media. A sample of the removed media was stored at -20°C for hCG analysis. At 66 h, a

selection of the culture wells had 25(OH)D_3 added to a final concentration of 20 µM and cultured for a period of 24 h before collection at 90 h. At either 18 h or 90 h media was removed and cells washed in PBS. Cells were either fixed in methanol, or scraped into the appropriate medium for DNA or RNA extraction.

5.2.6 β-human Chorionic Gonadotrophin quantification

β-hCG produced by cultured cytotrophoblast cells and released into the culture media was measured using a β-hCG ELISA Kit as described in Chapter 2.8. This is an ELISA that works via the 'sandwich principle', in which β-hCG binds to a bound antibody on the plate, and is detected with an anti-β-hCG antibody conjugated to horseradish peroxidase. Culture media samples containing greater amounts of β-hCG therefore generated a greater colour change from the horseradish peroxidase, which was detected using a plate reader.

5.2.7 Cytotrophoblast staining and imaging

Fixed cytotrophoblast cells were stained and imaged as described in Chapter 2.11. Briefly cells were washed in PBS, blocked with BSA and incubated overnight at 4°C with 1/100 mouse anti-human Desmoplakin antibody. Cells were washed and incubated for 2 h at RT with 1/250 DAPI + 1/500 goat anti-mouse Alexa Fluor 568. Cells were again washed and stored under PBS at 4°C until imaging on a Lecia SP8 confocal microscope.

5.2.8 Fragment culture

Placental fragments were cultured as described in Chapter 2.4. 10 mg villous tissue fragments were incubated in Tyrode's buffer (see Table 2-2), with 20 µmol 25(OH)D_3 (dissolved in ethanol) + 0.7 mmol/l BSA, ethanol control with 0.7 mmol/l BSA, 20 µmol 25(OH)D_3 + 9 µmol DBP or ethanol control + 9 µmol DBP at 37°C for 8 h (n = 5). At 8 h the buffer was removed, fragments washed in Tyrode's buffer and snap frozen on dry ice. Fragments were stored at -80°C.

5.2.9 DNA extraction

DNA was extracted from 25(OH)D_3 treated villous tissue fragments, 25(OH)D_3 treated cytotrophoblasts, MAVIDOS placental tissue and SPRING placental tissue using the Qiagen DNeasy blood and tissue kit, as described in Chapter 2.9.2. Cells/tissue were lysed in 20 µl proteinase K and 180 µl buffer ATL at 56°C for 3 h. Ethanol was used to precipitate the DNA in the solution, and DNA was then selectively bound to a DNeasy mini spin column. Contaminants are washed and then the DNA was eluted from the column in buffer AE (10 mmol Tris-Cl, 0.5 mmol EDTA, pH 9.0).

The quantity and integrity of total DNA was confirmed by Nanodrop 1000 Spectrophotometer and agarose gel electrophoresis, as described in Chapter 2.9.4 and 2.9.5.

5.2.10 RNA extraction

RNA was extracted from villous tissue fragments, cytotrophoblasts and MAVIDOS placental tissue using the using the Qiagen miRNeasy mini kit, as described in Chapter 2.9.3. Chloroform is used to separate RNA from DNA and protein, and RNA is selectively bound to a spin column. Contaminants are removed and then the RNA is eluted from the column in RNAse free water. The quantity and integrity of total RNA was confirmed by Nanodrop 1000 Spectrophotometer and agarose gel electrophoresis, as described in Chapter 2.9.4 and 2.9.5.

5.2.11 Histone protein extraction

Histones were extracted from villous tissue fragments and SPRING placental samples using the EpiQuik^{TM} total histone extraction kit (Epigentek, USA), as described in Chapter 2.12.1. Briefly 30 mg of tissue was disaggregated with 0.5 ml pre-lysis buffer in a Dounce homogeniser. The homogenised mixture was centrifuged at 1000 rpm for 1 min at 4°C, and supernatant discarded. The pellet was resuspended in 200 µl lysis buffer and incubated on ice for 30 min, then centrifuged at 12000 rpm for 5 min at 4°C. 60 µl of balance-DTT buffer was added to the supernatant, containing acid soluble proteins, and proteins stored at -80°C.

5.2.12 Histone protein quantification

Histone protein concentration was measured using the Pierce^{TM} BCA protein assay, as described in Chapter 2.12.1. Briefly 25 µl of standard or sample was added to a plate with 200 µl of working reagent, mixed and incubated for 30 min at 37°C. Absorbance was measured at 562 nm on a plate reader and concentration determined with a standard curve.

5.2.13 Histone methylation/acetylation measures

Measurement of histone methylation/acetylation at specific marks was carried out using purified histone proteins obtained as described in Chapter 2.12.1 and using the EpiQuik^{TM} Global Methyl/Acetyl Histone Quantification Colourimetric Kits (Epigentik), as described in Chapter 2.12.2. 50 µl of standard control or 300 ng histone extract was added to each well of the plate with 50 µl antibody buffer. Samples were covered, mixed and incubated at RT for 2 h. Samples were removed and wells washed three times with 150 µl of wash buffer. 50 µl detection antibody was added and incubated for 1 h at RT on an orbital shaker, then wells washed again. 100 µl of

colour developer was added and incubated in the dark at RT for 2-10 min until a medium blue colour was reached. 50 µl stop solution was added and absorbance at 450 nm was measured on a plate reader within 2-15 mi. The amount of the methylation/acetylation mark was determined with a standard curve.

5.2.14 Reverse transcription

To convert RNA to cDNA samples underwent reverse transcription as described in Chapter 2.9.6. Total RNA (12 µg) was reverse transcribed with 250 ng random hexamer primers, 100 units M-MLV reverse transcriptase, 25 units recombinant RNasin ribonuclease inhibitor and 0.5 mmol/L PCR nucleotuide mix in a final reaction volume of 12.5 µl in 1x MMLV reaction buffer. PCR conditions were 37 °C for 60 min then 95 °C for 10 min. Each sample was reverse transcribed individually at the same time to reduce variation. A standard curve, NECs and CVs were also reverse transcribed in the same batch.

5.2.15 Quantitative real-time polymerase chain reaction

Gene expression was measured using qRT-PCR as described in Chapter 2.9.7. mRNA expression was measured using Roche UPL assays. HKGs, (as previously selected using geNorm analysis) were also measured using a Primer Design Perfect Probe assay, with primers as described in Table 2-7. Gene of interest primer sequences are displayed in Table 5-1. UPL qRT-PCR cycling conditions were 95°C for 10 min; 45 cycles of 95°C for 10 s, 60°C for 30 s and 72°C for 1 s; 50°C for 30 s, with data collection at the 72°C step. Perfect Probe HKG qRT-PCR cycling conditions were 95°C for 10 min; 50 cycles of 95°C for 10 s, 50°C for 30 s and 72°C for 15 s; 50°C for 30 s, with data collection at the 50°C step. For each qRT-PCR assay, samples (4 ng) were run alongside a standard curve, CV controls, NECs and NTCs in triplicate. Cp values were determined by the second derivative method and were converted to DNA concentration using a standard curve as described in Chapter 2.9.7. Expression levels of genes of interest were normalised to the geometric mean of the HKGs for each sample.

Table 5-1 *Primers and probes used for qRT-PCR.*

Gene	Accession number	Primer sequence (5'-3')	UPL number	Amplicon (bp)
AHDC1	NM_001029882.3	F: CCCCAGGACACCTCTCTACC R: CATTTAATTCTTCATACCAATCCTTG	38	449-468 499-524
ASCT1	NM_001193493.1 NM_003038.4	F: TTTGCGACAGCATTTGCTAC R: GCACTTCATCATAGAGGGAAGC	78	1189-1248 1289-1348
ASCT2	NM_001145144.1 NM_001145145.1 NM_005628.2	F: GAGGAATATCACCGGAACCA R: AGGATGTTCATCCCCTCCA	43	114-179 304-369
CDRT1	NM_001282540.1 NM_006382.3	F: TGCAACCCCAAATTACTGCT R: GATGTCTTGATTGAGCCCTGA	74	622-641 694-714
CRH	NM_000756.3	F: GGCAGGGCCCTATGATTTA R: CGCTCTCTTGACAGCTCGAT	68	44-62 86-105
CYP24A1	NM_000782.4	F: GAAAGAATTGTATGCTGCTGTCA R: CACATTAGACTGTTTGCTGTCGT	78	1337-1359 1386-1408
CYP27B1	NM-000785.3	F: CGCAGCTGTATGGGGAGA R: CACCTCAAAATGTGTTAGGATCTG	53	1509-1526 1563-1586
DNMT1	NM_001379.3 NM_001130823.2 NM_001318731.1 NM_001318730.1	F: GGGAAATGTAAAGCCTGCAA R: GGCCATATTGGGACACCTC	87	2229-2248 2303-2321
DNMT3B	NM_006892.3 NM_175848.1 NM_175849.1 NM_175850.2 NM_001207055.1 NM_001207056.1	F: CGATGGCTATCAGTCTTACTGC R: CAGGCACTCCACACAGAAAC	74	1734-1755 1414-1833
EZH2	NM_001203247.1 NM_15299.2 NM_004456.4 NM_001203249.1 NM_001203248.1	F: GACTGGCGAAGAGCTGTTTT R: TCTTTCGATGCCGACATACTT	64	2344-2363 2396-2416
HIVEP2	NM_006734.3	F: CGGCAAGCTTACATCATCAA R: AGGACGCATCAGGTTTCATC	38	5888-5907 5930-5949
KMT2D	NM_003482.3	F: GGGGGTATGGCACTACCTG R: TTGGGCCAGAGCTGTATTAAG	64	10978-10996 11017-11037
LAT1	NM_003486.5	F: GTGGAAAAACAAGCCCAAGT R: GCATGAGCTTCTGACACAGG	25	1503-1573
PLEKHG2	NM_022835.2	F: TCCCCTAGGATTCTCTGAAGC R: GGAGGACCCACACCAAATAA	76	5746-5766 5807-5826
RNASE7	NM_032572.3	F: GAAGACCAAGCGCAAAGC R: AGCAGAAGGGGGCAGAAT	63	201-218 278-295

RXRα	NM_002957.4	F: ACATGCAGATGGACAAGACG R: TCGAGAGCCCTTGGAGT	26	1238-1257 1298-1315
TXNIP	NM_006472.4	F: AACATCCCTGATACCCCAGA R: TCTCCAATCGGTGATCTTCA	52	1308-1327 1358-1377
VEGF	NM_001017536.1 NM_000376.2 NM_001017535.1	F: TCTGTGACCCTAGAGCTGTCC R: TCCTCAGAGGTGAGGTCTCTG	43	1197-1217 1304-1324
VDR	NM_001017536.1 NM_000376.2 NM_001017535.1	F: TCTGTGACCCTAGAGCTGTCC R: TCCTCAGAGGTGAGGTCTCTG	43	1197-1217 304-1324

UPL = Universal probe library, bp = base pairs, F = Forward, R = reverse

5.2.16 Pyrosequencing

DNA samples extracted from villous tissue fragments, cytotrophoblasts, MAVIDOS placental tissue and SPRING placental tissue underwent pyrosequencing at 13 CpG sites as described in Chapter 2.13. 13 CpG sites in the promoter of RXRα were analysed as described in Table 5-2. Briefly, 1 µg DNA samples were bisulphite converted using the EZ-96 DNA Methylation-Gold Kit, amplified using PCR then sequenced on the PyroMark workstation.

Table 5-2 *RXRα CpG site locations*

CpG	Distance from transcription start site	Chromosome	Genome coordinates hg38
0	-2693	9	134323882
1	-2686	9	134323889
2	-2682	9	134323893
3	-2673	9	134323902
4	-2649	9	134323926
5	-2642	9	134323933
6	-2554	9	134324021
7	-2465	9	134324110
8	-2406	9	134324169
9	-2391	9	134324184
10	-2387	9	134324188
11	-2385	9	134324190
12	-2357	9	134324218

5.2.17 Data analysis

Gene expression

Gene expression was measured using qRT-PCR, as described in Section 5.2.15. qRT-PCR data were normalised to HKG expression, and is presented as relative expression to HKG. Expression was tested for normal distribution, and in this chapter all gene expression data was normally distributed. Data from these experiments required the comparison of two paired groups (samples from matched placentas); control and vitamin D treated, were analysed using a paired Student's t-test. Data presented as mean ± SEM.

Histone methylation/acetylation marks

The concentration of histone methylation/acetylation marks in villous tissue fragments and SPRING placental samples was measured as described in Section 5.2.13. Expression was tested for normal distribution, and if not normally distributed log transformed and re-tested. Fragment samples were matched between treatment groups and therefore analysed by a paired Student's t-test. SPRING samples were unmatched and therefore analysed by independent Student's t-test. Data presented as mean ± SEM.

DNA methylation

DNA methylation at CpG sites within the RXRα promoter were measured by pyrosequencing, as described in Section 5.2.16. Expression was tested for normal distribution, and if not normally distributed log transformed and re-tested. Cytotrophoblast and fragment samples were matched between treatment groups and therefore analysed by a paired Student's t-test. MAVIDOS and SPRING samples were unmatched and therefore analysed by independent Student's t-test. Data presented as mean ± SEM.

MAVIDOS data

MAVIDOS data were analysed by linear regression by Medical Research Council Lifecourse Epidemiology Unit statistician Stefania D'Angelo. All outcomes were tested for normal distribution, and if not normally distributed log transformed and re-tested. Associations between maternal metabolite concentrations and placental DNA methylation were analysed with metabolite concentration as the predictor, and adjusted for season of delivery. Data were adjusted for season of delivery due to seasonal variations in sunlight exposure altering vitamin D metabolism. Associations between placental DNA methylation and mRNA expression were analysed with DNA methylation as the predictor, and adjusted for treatment group, sex and gestational age. Data were adjusted for treatment group to see independent effects of DNA

methylation on gene expression, adjusted for sex to account for sex-specific differences in gene expression and adjusted for gestational age to account for changes in placental gene expression throughout gestation. The β-value gives the amount of change in the outcome with one unit change in the predictor. Data are presented as β-values.

5.3 Results

To determine the effects of short term 25(OH)D_3 treatment on the RNA expression of genes of interest identified from our array analysis whole villous tissue and cultured primary cytotrophoblast cells were investigated.

5.3.1 Syncytialisation of cytotrophoblast cells

Healthy cytotrophoblast cells should spontaneously begin to syncytialise in culture, joining together forming large multinucleate cells. Two methods were used to determine if this had occurred, imaging and β-hCG analysis. Imaging the nuclei and surface of the cell allows you to see whether the cell is multinucleate, and thus whether syncytialisation of the cells has occurred. Measuring the β-hCG content of the media also provides a measure of syncytialisation as the syncytiotrophoblast cells produce β-hCG.

Increasing levels of β-hCG production was observed with time of culture, as seen in Figure 5-3. Average β-hCG levels in the 90 h culture media were 413.13 mIU/ml. Syncytialisation of cultured cells was observed as shown in Figure 5-4.

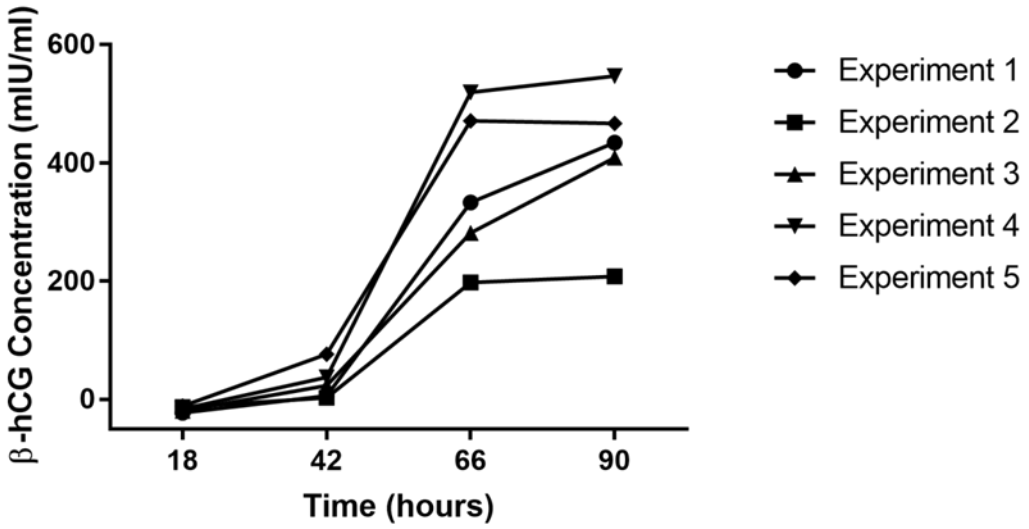

Figure 5-3 ***Cytotrophoblast β-hCG production.*** *β-hCG levels in the culture media of cultured primary cytotrophoblast cells.*

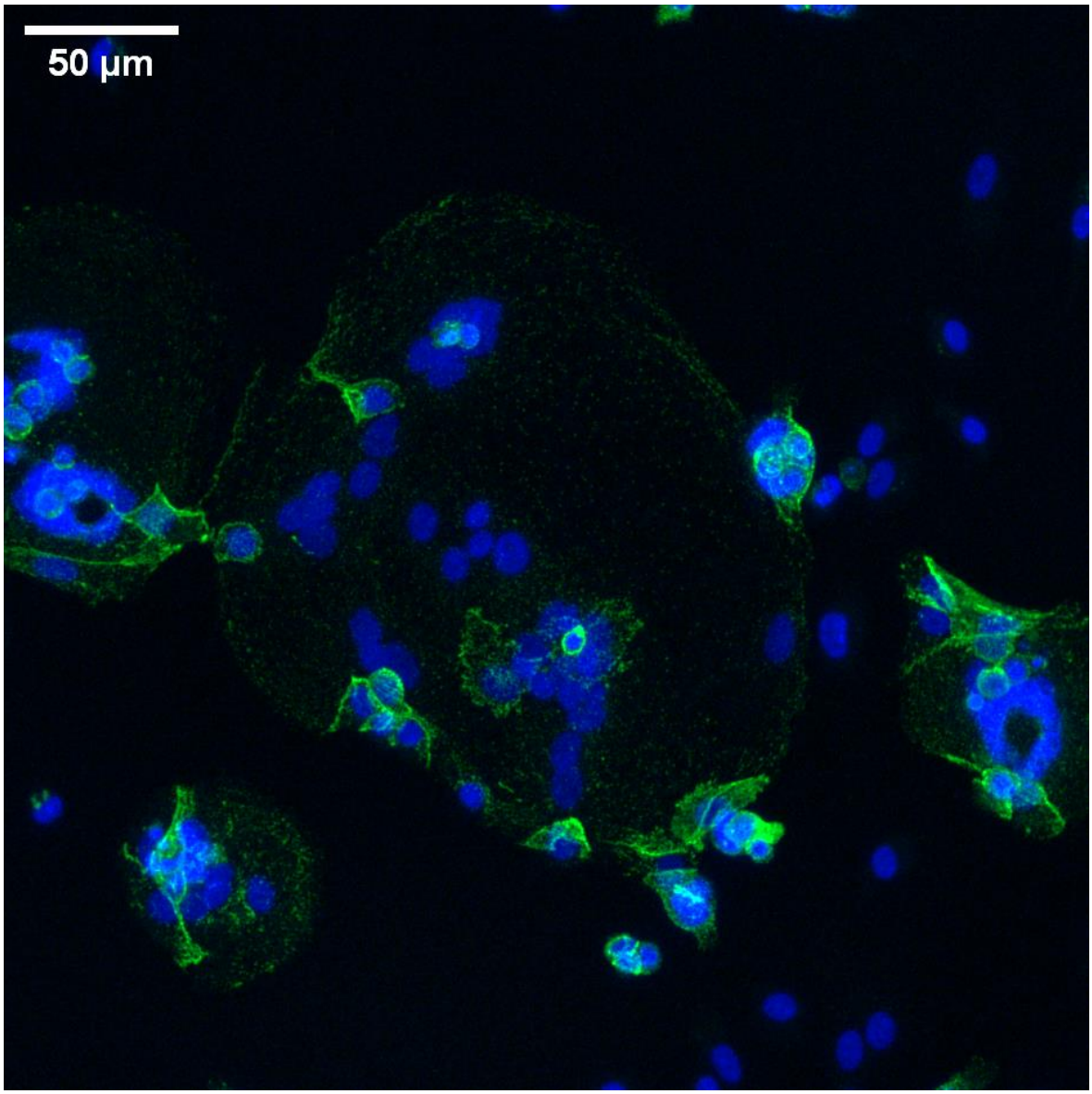

Figure 5-4 ***Confocal image of cultured cytotrophoblast cells.*** *Representative confocal microscopy image of cytotrophoblast cells cultured for 90 h and stained with DAPI (blue; nuclei) and desmoplakin (green), present on the cell surface. Multiple nuclei within a single cell demonstrate syncytialisation has occurred.*

5.3.2 Gene expression data

Vitamin D pathway genes

Genes of the vitamin D pathway, *CYP27B1, CYP24A1, VDR* and *RXRα* were analysed for changes in mRNA expression in both cytotrophoblast and villous fragment tissue, with effect of both length of cell culture and 25(OH)D_3 treatment investigated.

Untreated cytotrophoblast samples cultured for 90 h had reduced mRNA expression of the genes *CYP27B1* and *CYP24A1* compared to 18 h of culture, whereas VDR and RXRα showed no significant difference (n = 5; Figure 5-5, Table 5-3). 25(OH)D_3 treated cytotrophoblast samples cultured for 90 h had increased mRNA expression of *CYP24A1* and decreased expression of *RXRα*

mRNA compared to untreated cytotrophoblast samples cultured for 90 h, with no effect on *CYP27B1* and *VDR* mRNA (n = 8; Figure 5-6, Table 5-3).

In placental fragments, 25(OH)D_3 + BSA treatment increased *CYP24A1* mRNA expression, but did not affect the expression of *CYP27B1*, *RXRα* or *VDR* (n = 5; Figure 5-7, Table 5-3). In 25(OH)D_3 + DBP treated fragments there was no significant change in *CYP24A1*, *CYP27B1*, *RXRα* or *VDR* expression (n = 4; Figure 5-7, Table 5-3).

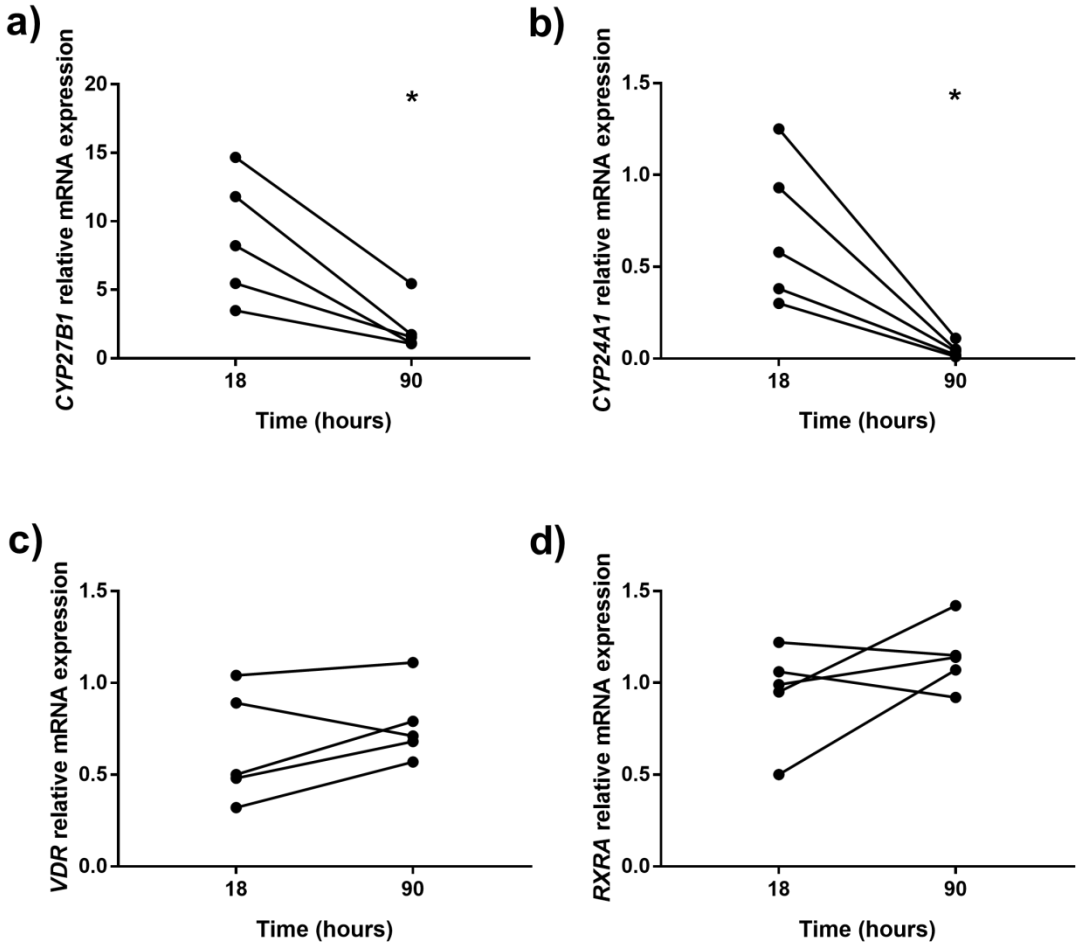

Figure 5-5 ***Vitamin D related gene expression in cytotrophoblast cells.*** *Vitamin D related genes mRNA expression relative to HKG in cytotrophoblast cells cultured for 18 h or 90 h.* ***a)*** *CYP27B1 relative mRNA expression.* ***b)*** *CYP24A1 relative mRNA expression.* ***c)*** *VDR relative mRNA expression.* ***d)*** *RXRα relative mRNA expression. Data analysed by paired Student's t-test. n = 5.* $p < 0.05$ *indicates 90 h significantly different to 18 h.*

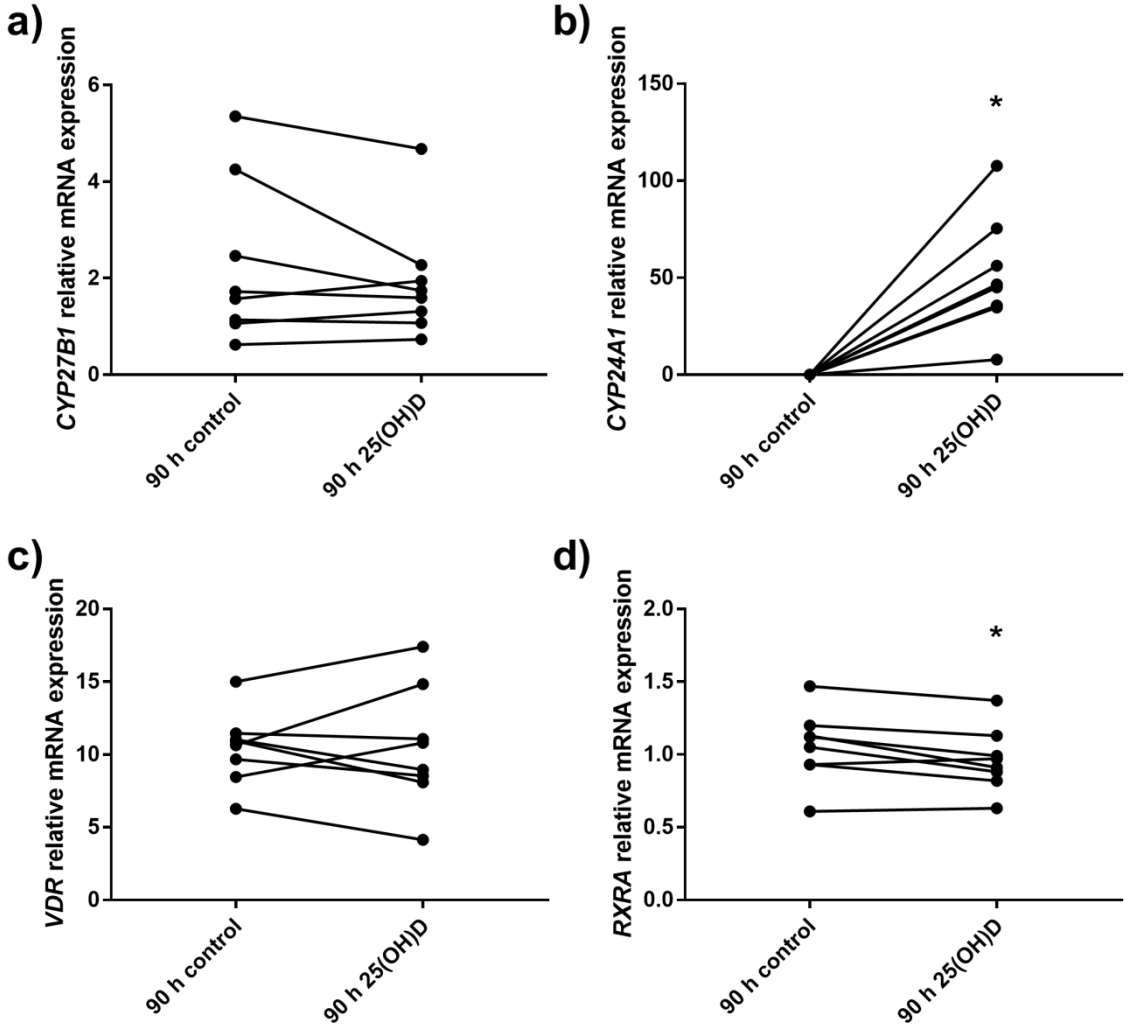

Figure 5-6 ***Vitamin D related gene expression in 25(OH)D_3 treated cytotrophoblast cells.*** *Vitamin D related genes mRNA expression relative to HKG in cytotrophoblast cells cultured for 90 h with no treatment (90 h control) or with a 25(OH)D_3 treatment (90 h 25(OH)D) for the final 24 h of culture.* ***a)*** *CYP27B1 relative mRNA expression.* ***b)*** *CYP24A1 relative mRNA expression.* ***c)*** *VDR relative mRNA expression.* ***d)*** *RXRα relative mRNA expression. Data analysed by paired Student's t-test. n = 8.* $p < 0.05$ *indicates 90 h 25(OH)D significantly different to 90 h control.*

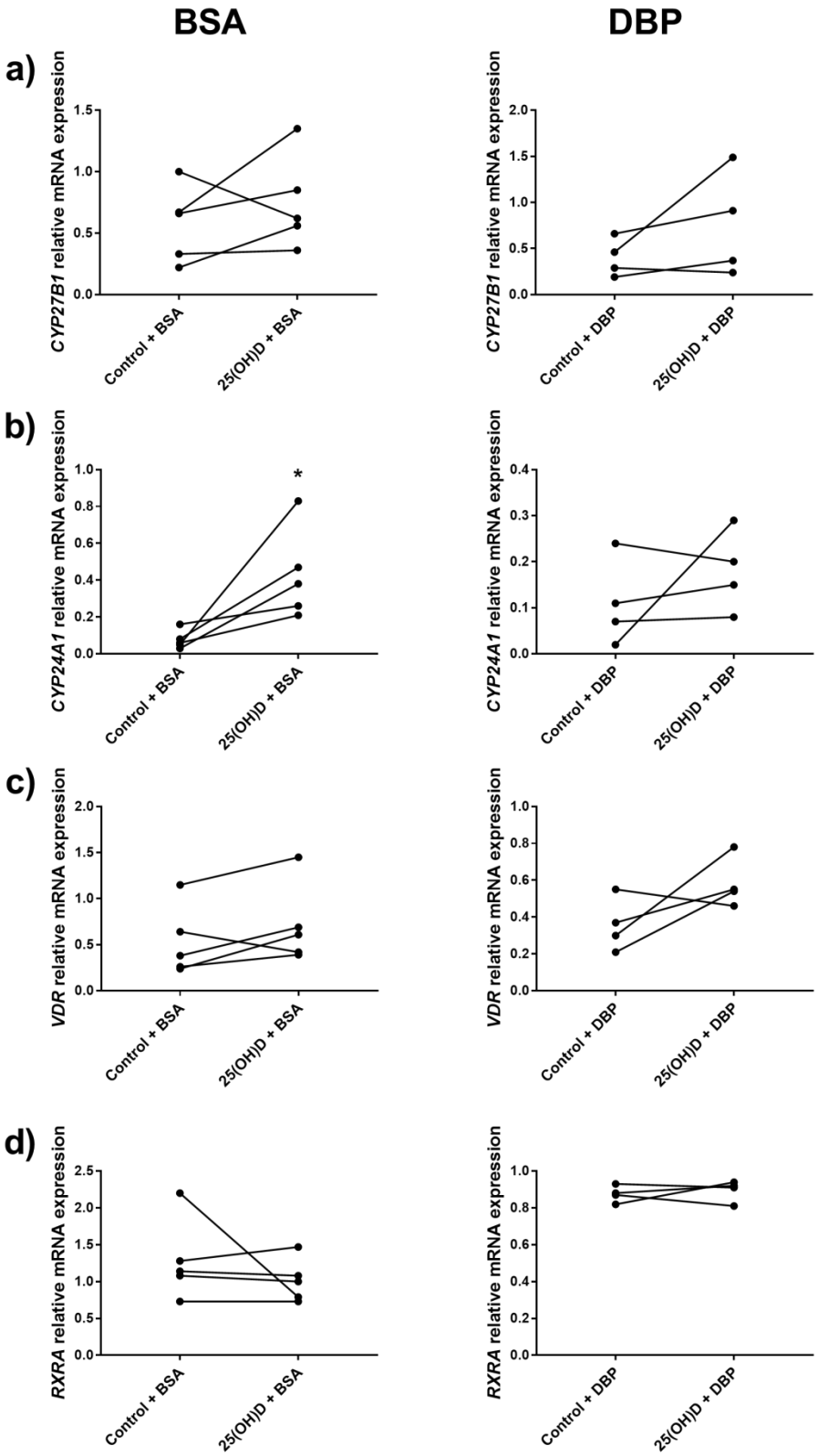

Figure 5-7 ***Vitamin D related gene expression in fragments.*** *Vitamin D related genes mRNA expression relative to HKG in fragment samples treated with Control + BSA vs 25(OH)D + BSA (n = 5) or Control + DBP vs 25(OH)D + DBP (n = 4).* ***a)*** *CYP27B1 relative mRNA expression.* ***b)*** *CYP24A1 relative mRNA expression.* ***c)*** *VDR relative mRNA expression.* ***d)*** *RXRα relative mRNA expression. Data analysed by paired Student's t-test.* p < 0.05 indicates 25(OH)D treated is significantly different to control.*

Table 5-3 *Vitamin D related gene expression*

	Cytotrophoblast		Fragments	
Gene	**90 h vs 18 h**	**Control vs 25(OH)D_3**	**Control vs 25(OH)D_3 + BSA**	**Control vs 25(OH)D_3 + DBP**
CYP27B1	↓ p = 0.012	⇔ p = 0.232	⇔p = 0.385	⇔p = 0.232
CYP24A1	↓ p = 0.016	↑ p = 0.002	↑p = 0.044	⇔p = 0.376
VDR	⇔p = 0.212	⇔p = 0.958	⇔p = 0.171	⇔p = 0.162
RXRα	⇔p = 0.238	↓p = 0.021	⇔p = 0.396	⇔p = 0.644

↑↓⇔ = direction of gene expression change; increased, decreased or no change respectively.

Genes of interest

A selection of genes that displayed vitamin D induced changes in Chapter 4 were selected for further investigation in the cytotrophoblast and fragment samples. The genes selected were *AHDC1, CDRT1, CRH, DNMT1, DNMT3B, EZH2, HIVEP2, KMT2D, PLEKHG2* and *RNASE7*.

Cytotrophoblast changes with duration of culture

CDRT1, DNMT3B, HIVEP2 and *RNASE7* all showed a significant decrease in expression at 90 h of culture compared to 18 h. *PLEKHG2* showed a significant increase in expression at 90 h of culture compared to 18 h. *AHDC1, CRH, DNMT1*and *EZH2* showed no significant change in expression with duration of culture. *KMT2D* was not measured in these samples. Data is displayed in Figure 5-8 and Table 5-4.

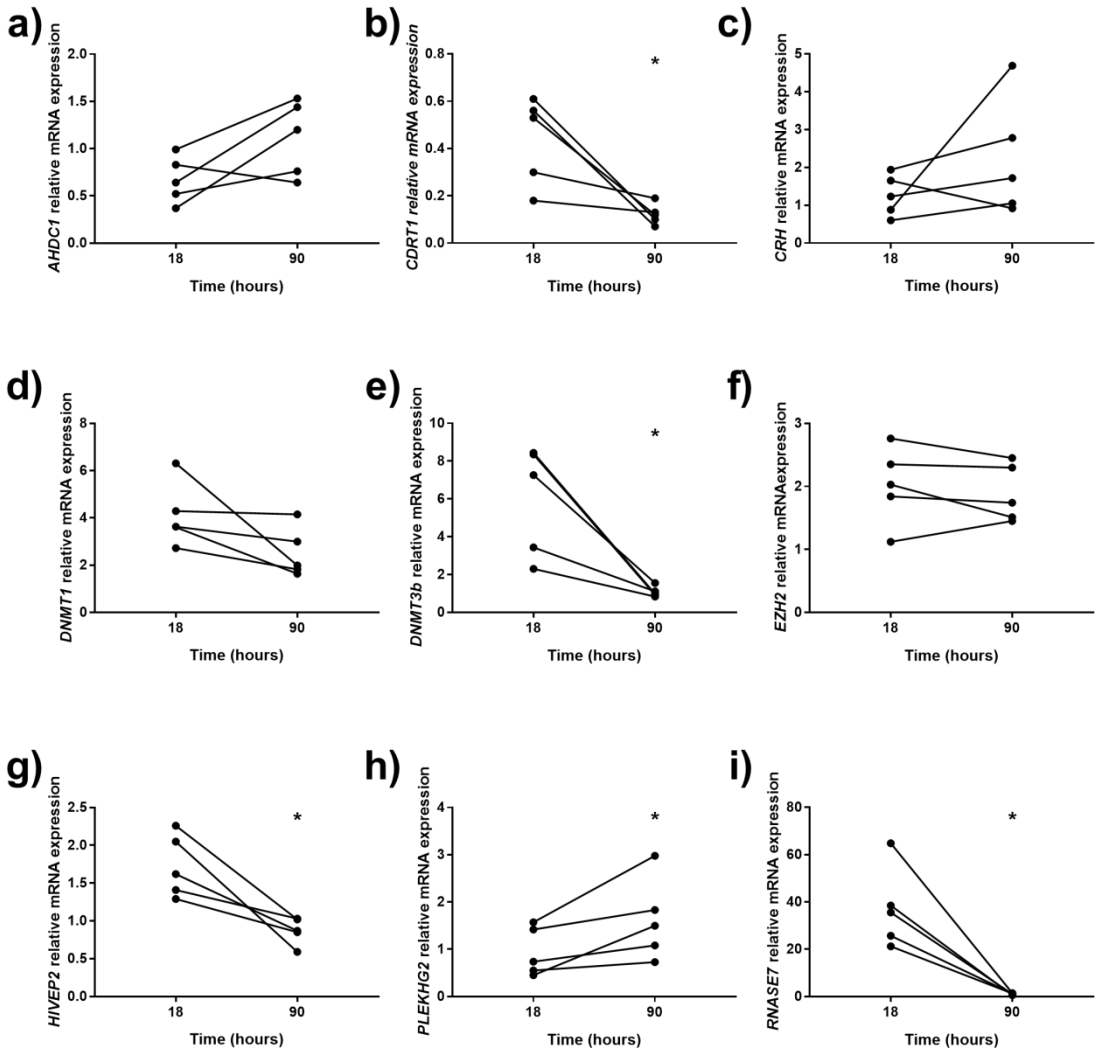

Figure 5-8 ***Gene expression in cytotrophoblast cells.*** *mRNA expression of genes of interest relative to HKG in cytotrophoblast cells cultured for 18 h or 90 h.* ***a)*** *HIVEP2 relative mRNA expression.* ***b)*** *EZH2 relative mRNA expression.* ***c)*** *PLEKHG2 relative mRNA expression.* ***d)*** *RNASE7 relative mRNA expression.* ***e)*** *DNMT1 relative mRNA expression.* ***f)*** *DNMT3b relative mRNA expression.* ***g)*** *CRH relative mRNA expression.* ***h)*** *CDRT1 relative mRNA expression.* ***i)*** *AHDC1 relative mRNA expression. n = 8. Data analysed by paired Student's t-test.* $p < 0.05$ indicates 90 h significantly different to 18 h.*

Cytotrophoblast changes with vitamin D treatment

HIVEP2 showed a significant increase in mRNA expression with 25(OH)D_3 treatment. *RNASE7* showed a significant decrease in expression with 25(OH)D_3 treatment. *AHDC1, CRH, CDRT1, DNMT1, DNMT3B* and *PLEKHG2* showed no significant change in expression with 25(OH)D_3 treatment. *KMT2D* was not measured in these samples. Data is displayed in Figure 5-9 and Table 5-4.

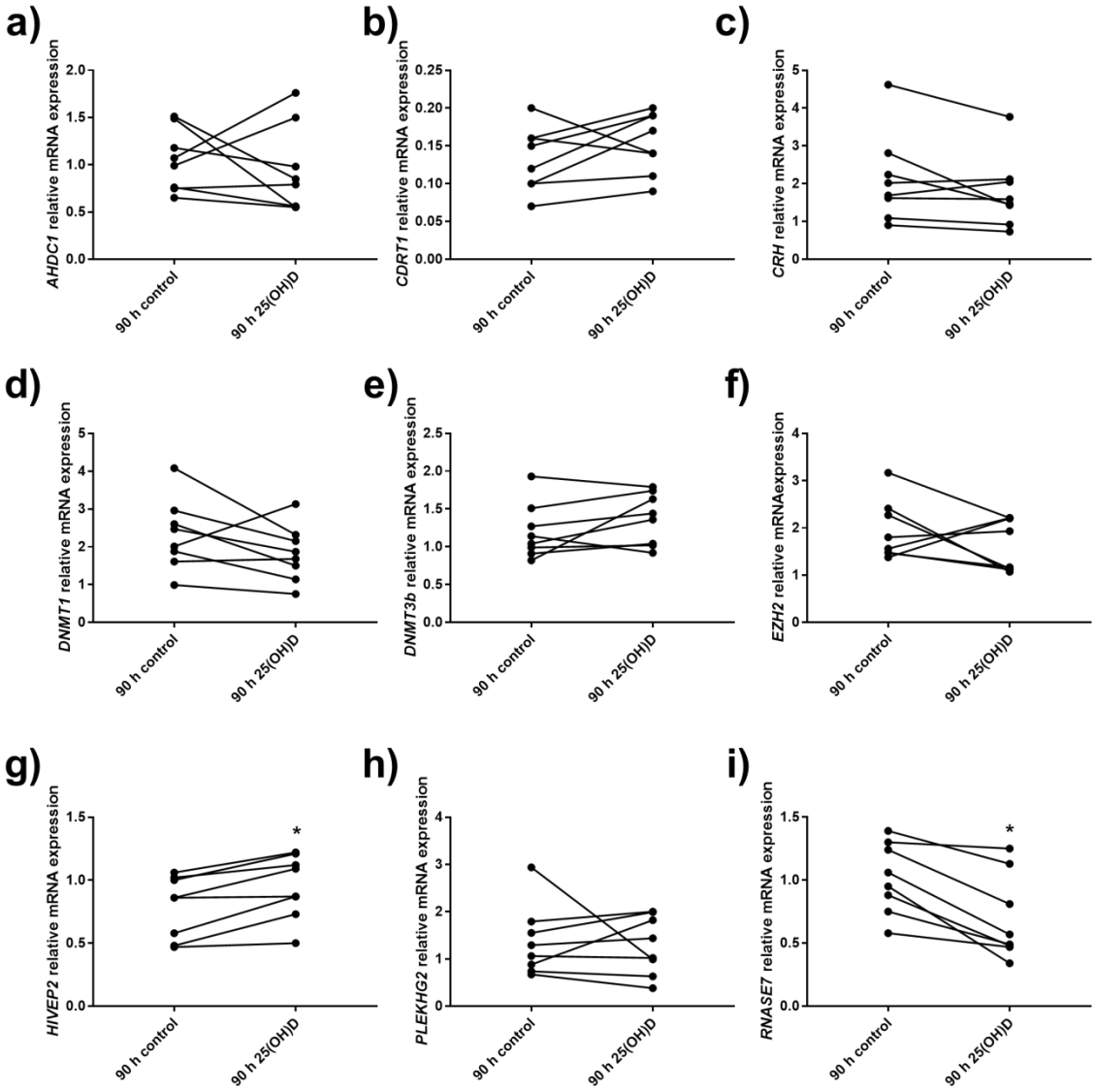

Figure 5-9 ***Gene expression in 25(OH)D_3 treated cytotrophoblast cells.*** *mRNA expression of genes of interest relative to HKG in cytotrophoblast cells cultured for 90 h with and without 25(OH)D_3 treatment.* ***a)*** *HIVEP2 relative mRNA expression.* ***b)*** *EZH2 relative mRNA expression.* ***c)*** *PLEKHG2 relative mRNA expression.* ***d)*** *RNASE7 relative mRNA expression.* ***e)*** *DNMT1 relative mRNA expression.* ***f)*** *DNMT3b relative mRNA expression.* ***g)*** *CRH relative mRNA expression.* ***h)*** *CDRT1 relative mRNA expression.* ***i)*** *AHDC1 relative mRNA expression. n = 8. Data analysed by paired Student's t-test. * p < 0.05 indicates 90 h 25(OH)D is significantly different to 90 h control.*

Fragment changes with vitamin D treatment

25(OH)D_3 + BSA and 25(OH)D_3 + DBP treated fragment sample gene expression data is displayed in Figures 5-10 and 5-11 and Table 5-4. 25(OH)D_3 + BSA treatment significantly altered *CDRT1* and *RNASE7* gene expression in villous tissue fragments. 25(OH)D_3 + DBP treatment significantly altered *AHDC1, CDRT1, DNMT1, EZH2, HIVEP2, PLEKHG2* and *RNASE7* gene expression in villous tissue fragments.

RNASE7 expression was significantly increased with 25(OH)D_3 + BSA treatment, and *CDRT1* expression significantly decreased. *AHDC1, DNMT1, EZH2, HIVEP2* and *RNASE7* had increased expression and *CDRT1* and *PLEKHG2* had significantly decreased expression with 25(OH)D_3 + DBP treatment.

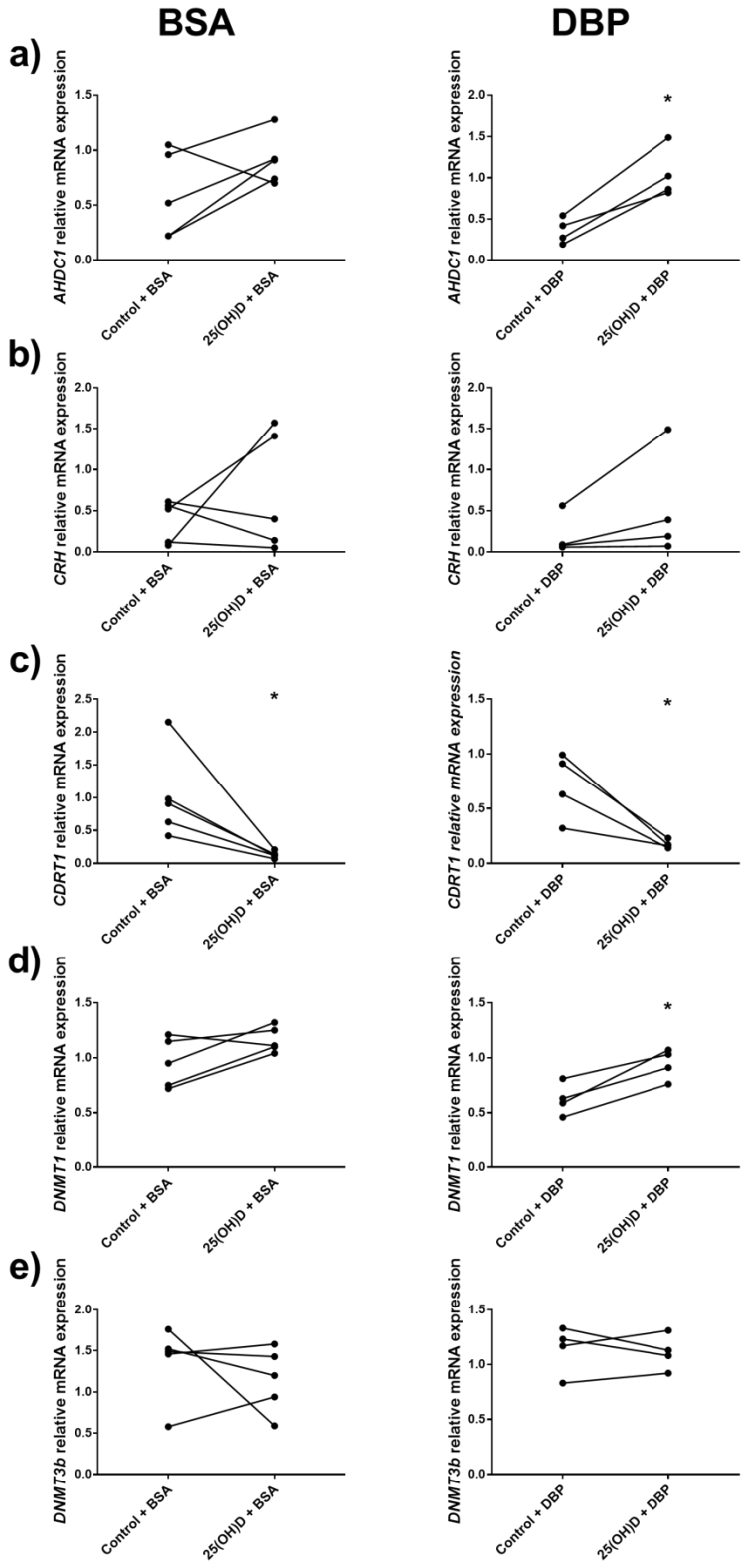

Figure 5-10 ***Gene expression in fragments (1).*** *mRNA expression of genes of interest relative to HKG in fragment samples treated with Control + BSA vs 25(OH)D + BSA (n = 5) or Control + DBP vs 25(OH)D + DBP (n = 4).* ***a)*** *AHDC1 relative mRNA expression.* ***b)*** *CDRT1 relative mRNA expression.* ***c)*** *CRH relative mRNA expression.* ***d)*** *DNMT1 relative mRNA expression.* ***e)*** *DNMT3B relative mRNA expression. Data analysed by paired Student's t-test.* $p < 0.05$ indicates 25(OH)D treated is significantly different to control.*

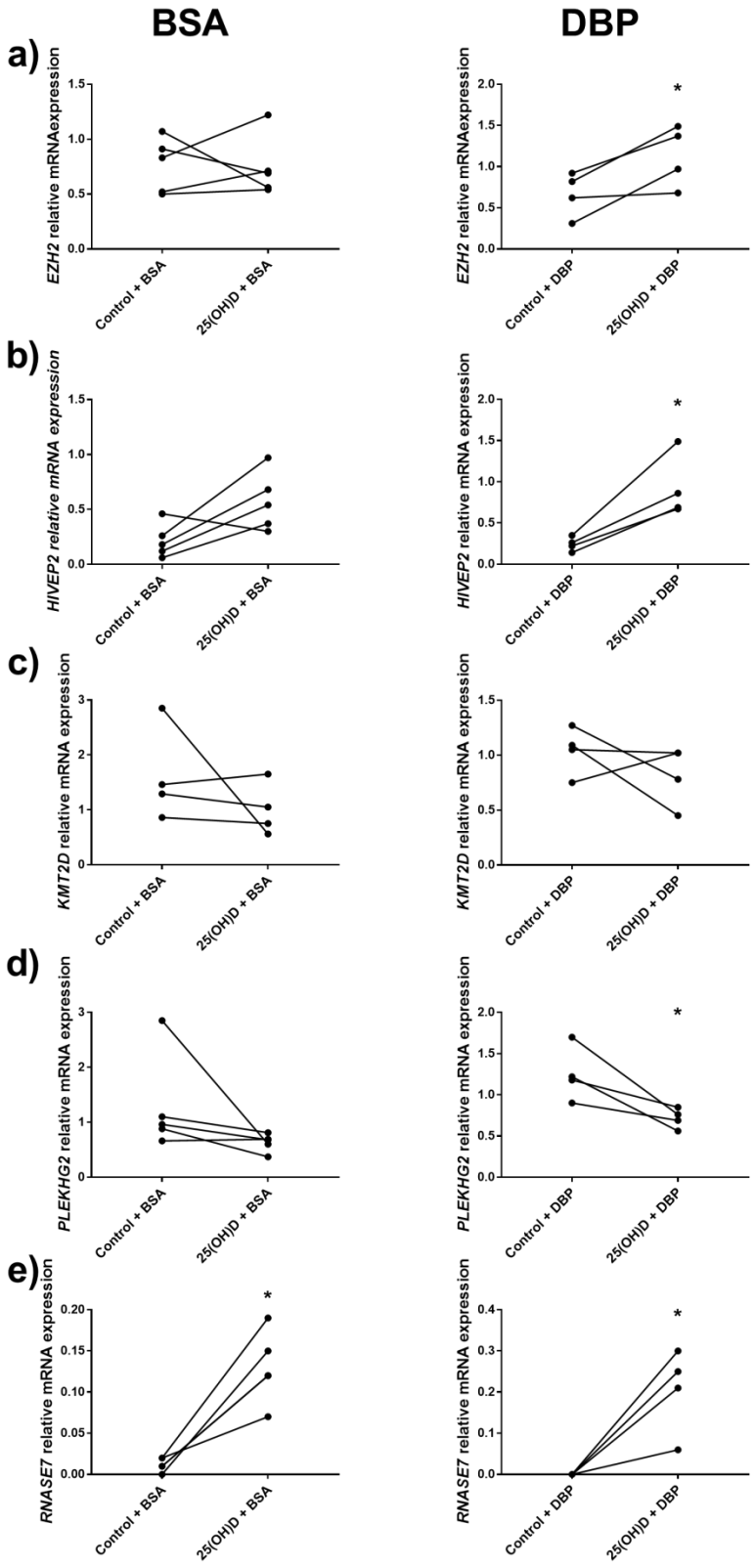

Figure 5-11 ***Gene expression in fragments (2).*** *mRNA expression of genes of interest relative to HKG in fragment samples treated with Control + BSA vs 25(OH)D + BSA (n = 5) or Control + DBP vs 25(OH)D + DBP (n = 4).* ***a)*** *EZH2 relative mRNA expression.* ***b)*** *HIVEP2 relative mRNA expression.* ***c)*** *KMT2D relative mRNA expression.* ***d)*** *PLEKHG2 relative mRNA expression.* ***e)*** *RNASE7 relative mRNA expression. Data analysed by paired Student's t-test.* $* p < 0.05$ *indicates 25(OH)D treated is significantly different to control.*

Table 5-4 *mRNA expression of genes of interest in cytotrophoblast and fragment samples.*

	Cytotrophoblast		Fragments	
Gene	**90 h vs 18 h**	**Control vs 25(OH)D_3**	**Control vs 25(OH)D_3 + BSA**	**Control vs 25(OH)D_3 + DBP**
HIVEP2	↓ p = 0.016	↑ p = 0.003	⇔ p = 0.068	↑ p = 0.022
EZH2	⇔ p = 0.412	⇔ p = 0.311	⇔ p = 0.891	↑ p = 0.049
PLEKHG2	↑ p = 0.045	⇔ p = 0.793	⇔ p = 0.179	↓ p = 0.047
RNASE7	↓ p = 0.009	↓ p = 0.002	↑ p = 0.003	↑ p = 0.031
DNMT1	⇔ p = 0.100	⇔ p = 0.136	⇔ p = 0.078	↑ p = 0.011
DNMT3b	↓ p = 0.018	⇔ p = 0.182	⇔ p = 0.459	⇔ p = 0.739
CRH	⇔ p = 0.269	⇔ p = 0.117	⇔ p = 0.411	⇔ p = 0.202
CDRT1	↓ p = 0.032	⇔ p = 0.219	↓ p = 0.034	↓ p = 0.033
AHDC1	⇔ p = 0.081	⇔ p = 0.592	⇔ p = 0.152	↑ p = 0.009
KMT2D	-	-	⇔ p = 0.359	⇔ p = 0.367

- Indicates no measures were made.

↑↓⇔ = direction of gene expression change; increased, decreased or no change respectively.

5.3.3 Histone analysis

<u>25(OH)D_3 treated fragments</u>

The amount of the histone methylation marks H3K4me3 and H3K27me3 was measured in 25(OH)D_3 + BSA treated fragments, as shown in Figure 5-12. Unfortunately due to the generation of a poor standard curve, it was not possible to determine the concentration of H3K4me3. However as absorbance values were obtained, these were analysed to determine if there was a difference in the absorbance of treated vs untreated samples. H3K4me3 showed no difference in absorbance at 450 nm between 25(OH)D_3 + BSA treated vs untreated samples (p = 0.687). H3K27me3 showed no difference in concentration between 25(OH)D_3 + BSA treated vs untreated samples (p = 0.315).

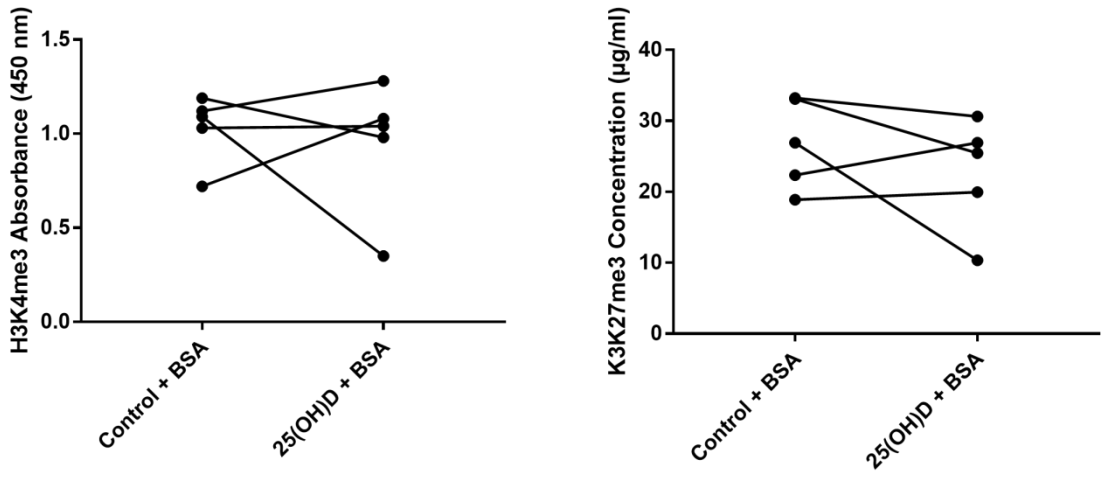

Figure 5-12 ***Histone modification in fragments.*** *Histone methylation mark measures in 25(OH)D_3 treated fragment samples. Treatment groups: Control + BSA or 25(OH)D + BSA (n = 5 per treatment group). H3K4me3 absorbance at 450 nm. H3K27me3 concentration (µg/ml). Data analysed by paired Student's t-test.*

SPRING placental samples

The amount of the histone methylation mark H3K27me3 and acetylated H3K27 (H3K27ac) was measured in placental samples from the SPRING study, as shown in Figure 5-13. SPRING placenta samples are currently still blinded and therefore have been analysed as group 1 vs group 2. Treatment groups are either 400 (placebo) or 1000 IU cholecalciferol daily from 14 weeks gestation. There was no significant difference in the amount of H3K27me3 (p = 0.914) or H3K27ac (p = 0.620) between treatment groups. The amount of H3K27me3 measured showed a large amount of variability, likely as result of being present in quantities close to the limit of detection of 0.2 µg/ml for this kit.

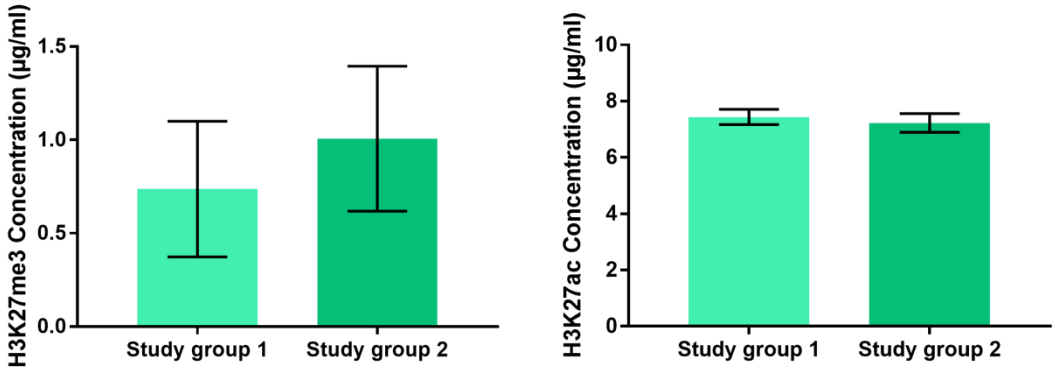

Figure 5-13 ***Histone modification modifications in SPRING placental samples.*** *Treatment groups blinded 400 IU vs 1000 IU cholecalciferol daily. H3K27me3 (n = 27 group 1, n = 29 group 2) and total acetylation of H3K27 (H3K27ac; n = 42 group 1, n = 38 group 2) in µg/ml. Data analysed by independent Student's t-test and displayed as mean ± SEM.*

5.3.4 RXRα DNA methylation

DNA methylation was measured at 13 CpG sites (CpG0-12) present upstream of the RXRα transcriptional start site by pyrosequencing in cytotrophoblast, fragment, MAVIDOS and SPRING samples.

25(OH)D_3 treated cytotrophoblast samples

Cytotrophoblast samples cultured for 90 h and treated with 25(OH)D_3 showed no difference in DNA methylation at any of the 13 CpG sites when compared to control treated cytotrophoblast samples. Data is displayed in Figure 5-14 and p values presented in Appendix B.

25(OH)D_3 treated fragment samples

Fragment samples treated with 25(OH)D_3 + BSA showed no difference in DNA methylation at any of the 13 CpG sites when compared to control treated fragment samples (n = 8 per treatment group). Data is displayed in Figure 5-15 and p values presented in Appendix B.

MAVIDOS samples

MAVIDOS treatment groups are either 400 (control/placebo) or 1000 IU cholecalciferol daily from 14 weeks gestation. MAVIDOS RXRα DNA methylation data is displayed in Figure 5-16 and p values presented in Appendix B. CpG6 showed a significant increase in DNA methylation with 1000 IU cholecalciferol daily treatment ($p = 0.035$), with a mean increase of 4.7% DNA methylation. This degree of DNA methylation change has previously been demonstrated to be able to alter gene expression and to be associated with developmental outcome changes, as discussed in section 4.3.1 (Simner et al., 2017, Harvey et al., 2014b). There was no significant difference in DNA methylation at any of the other CpG sites analysed between treatment groups.

SPRING samples

SPRING RXRα DNA methylation data is displayed in Figure 5-17 and p values presented in Appendix B. SPRING placenta samples are currently still blinded and therefore have been analysed as group 1 vs group 2. Treatment groups are either 400 (placebo) or 1000 IU cholecalciferol daily from 14 weeks gestation. There was no significant difference in DNA methylation at any of the 13 CpG sites analysed between treatment groups.

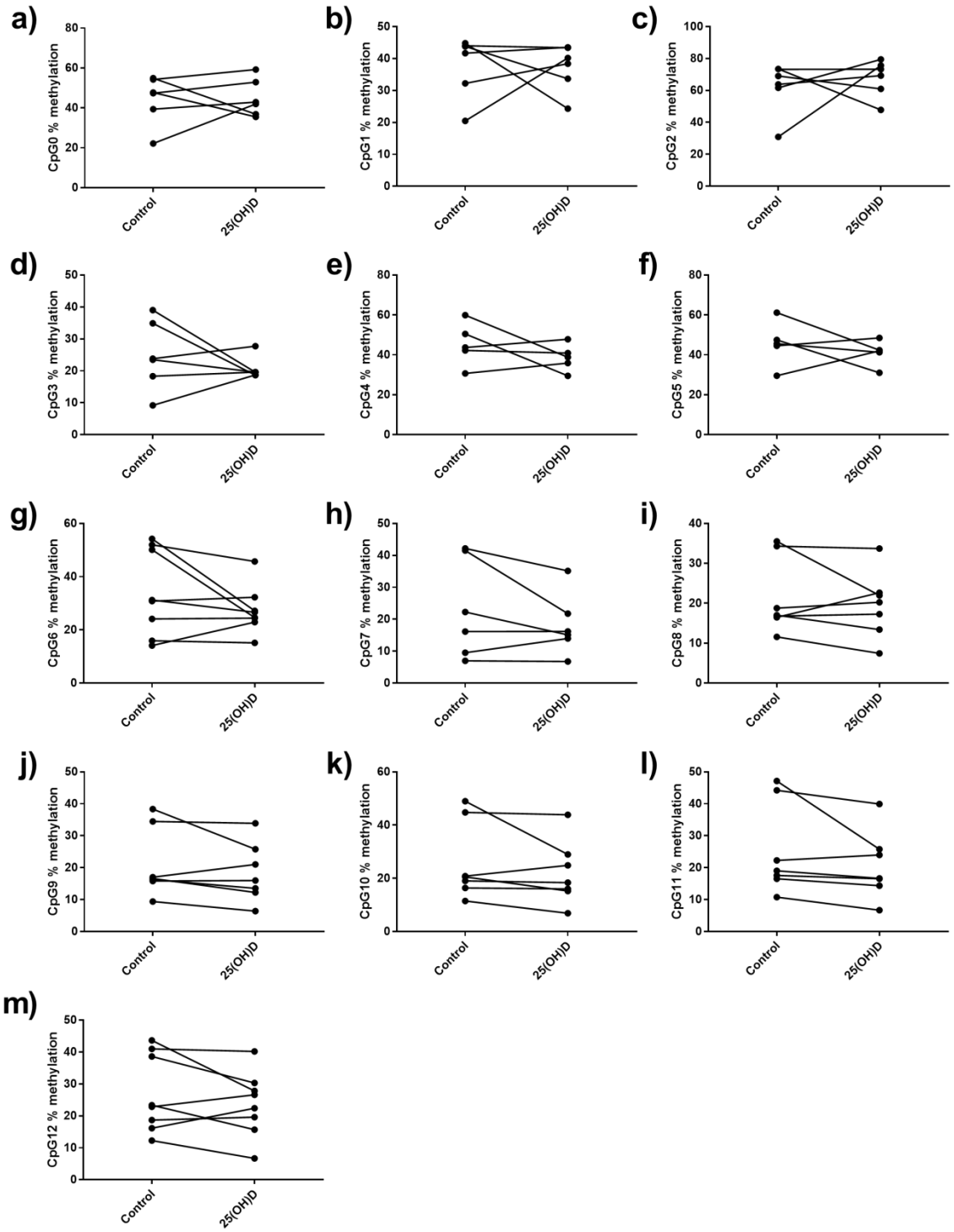

Figure 5-14 ***RXRα DNA methylation in cytotrophoblast cells.*** *Percentage DNA methylation at sites CpG0-12 of the gene RXRα in 25(OH)D_3 treated cytotrophoblast cells.* ***a)*** *CpG0,* ***b)*** *CpG1,* ***c)*** *CpG2,* ***d)*** *CpG3,* ***e)*** *CpG4,* ***f)*** *CpG5,* ***g)*** *CpG6,* ***h)*** *CpG7,* ***i)*** *CpG8,* ***j)*** *CpG9,* ***k)*** *CpG10,* ***l)*** *CpG11,* ***m)*** *CpG12.Data analysed by paired Student's t-test. n = 5 - 8 per treatment group.*

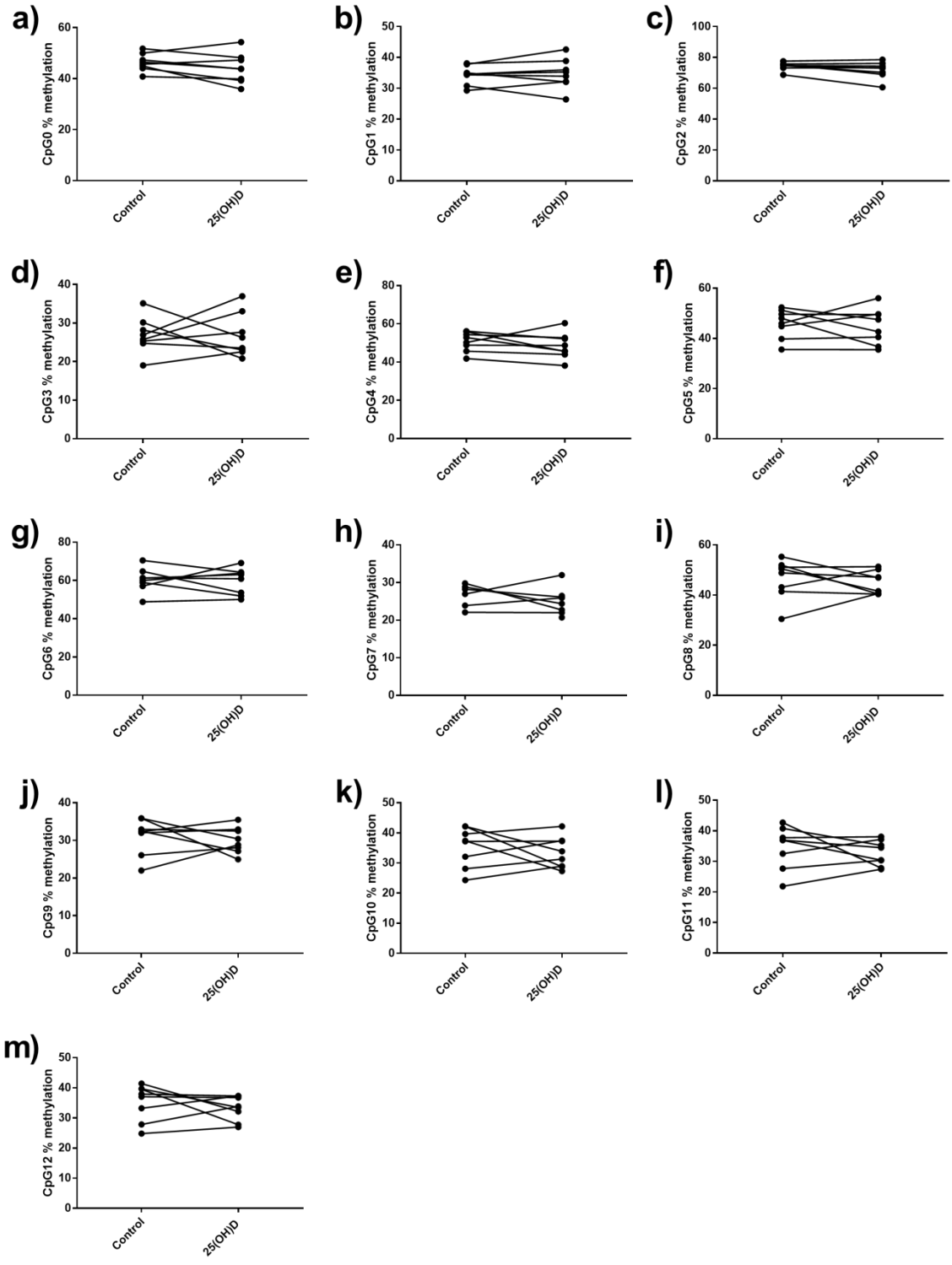

Figure 5-15 ***RXRα DNA methylation in fragments.*** *Percentage DNA methylation at sites CpG0-12 of the gene RXRα in 25(OH)D_3 treated villous fragments.* ***a)*** *CpG0,* ***b)*** *CpG1,* ***c)*** *CpG2,* ***d)*** *CpG3,* ***e)*** *CpG4,* ***f)*** *CpG5,* ***g)*** *CpG6,* ***h)*** *CpG7,* ***i)*** *CpG8,* ***j)*** *CpG9,* ***k)*** *CpG10,* ***l)*** *CpG11,* ***m)*** *CpG12.Data analysed by paired Student's t-test. n = 6 - 8 per treatment group.*

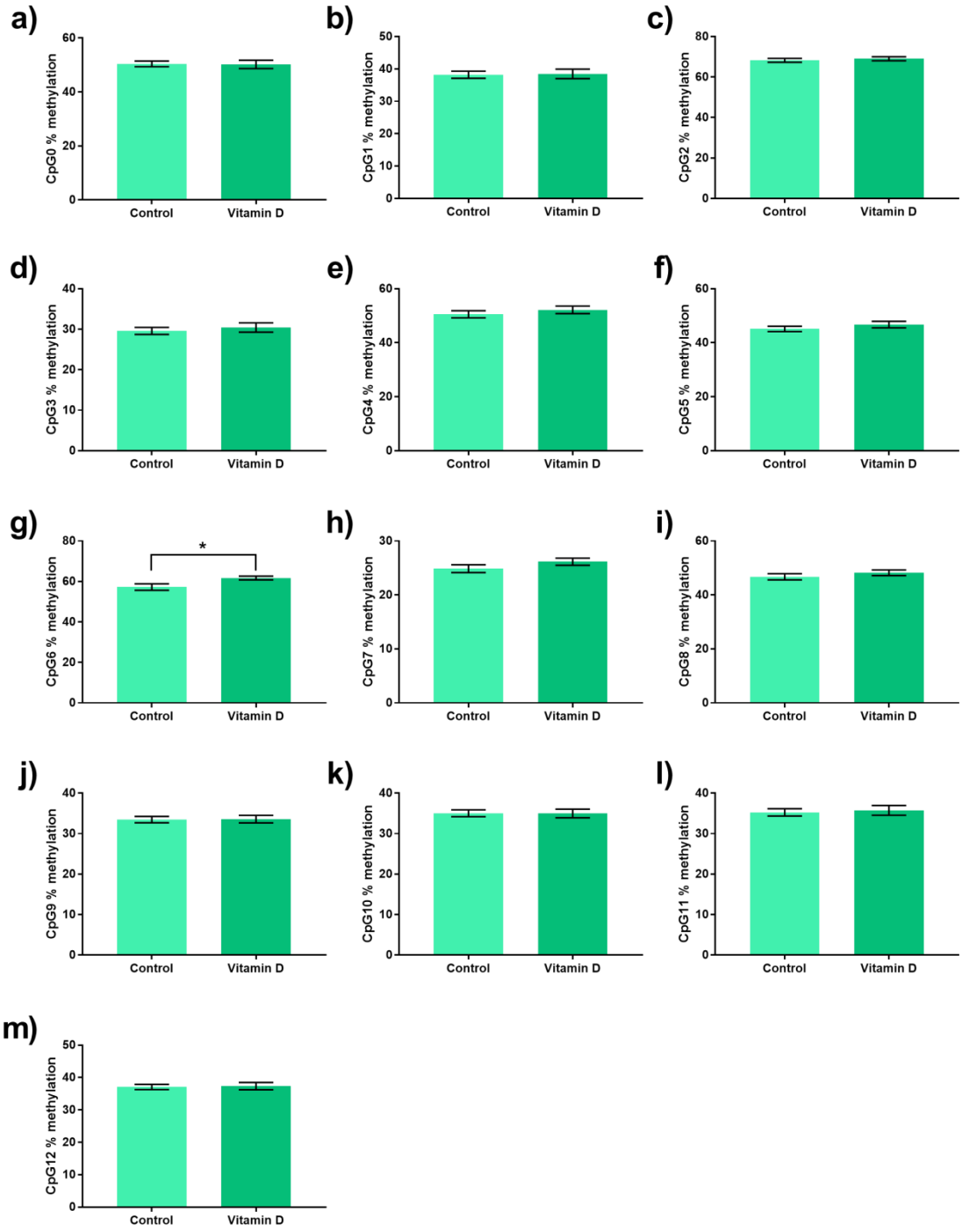

Figure 5-16 ***RXRα DNA methylation in MAVIDOS placental samples.*** *Percentage DNA methylation at sites CpG0-12 of the gene RXRα in MAVIDOS study samples.* ***a)*** *CpG0,* ***b)*** *CpG1,* ***c)*** *CpG2,* ***d)*** *CpG3,* ***e)*** *CpG4,* ***f)*** *CpG5,* ***g)*** *CpG6,* ***h)*** *CpG7,* ***i)*** *CpG8,* ***j)*** *CpG9,* ***k)*** *CpG10,* ***l)*** *CpG11,* ***m)*** *CpG12.Data analysed by independent Student's t-test and displayed as mean ± SEM. n = 28 - 41 control, n = 22 - 33 25(OH)D treatment.*

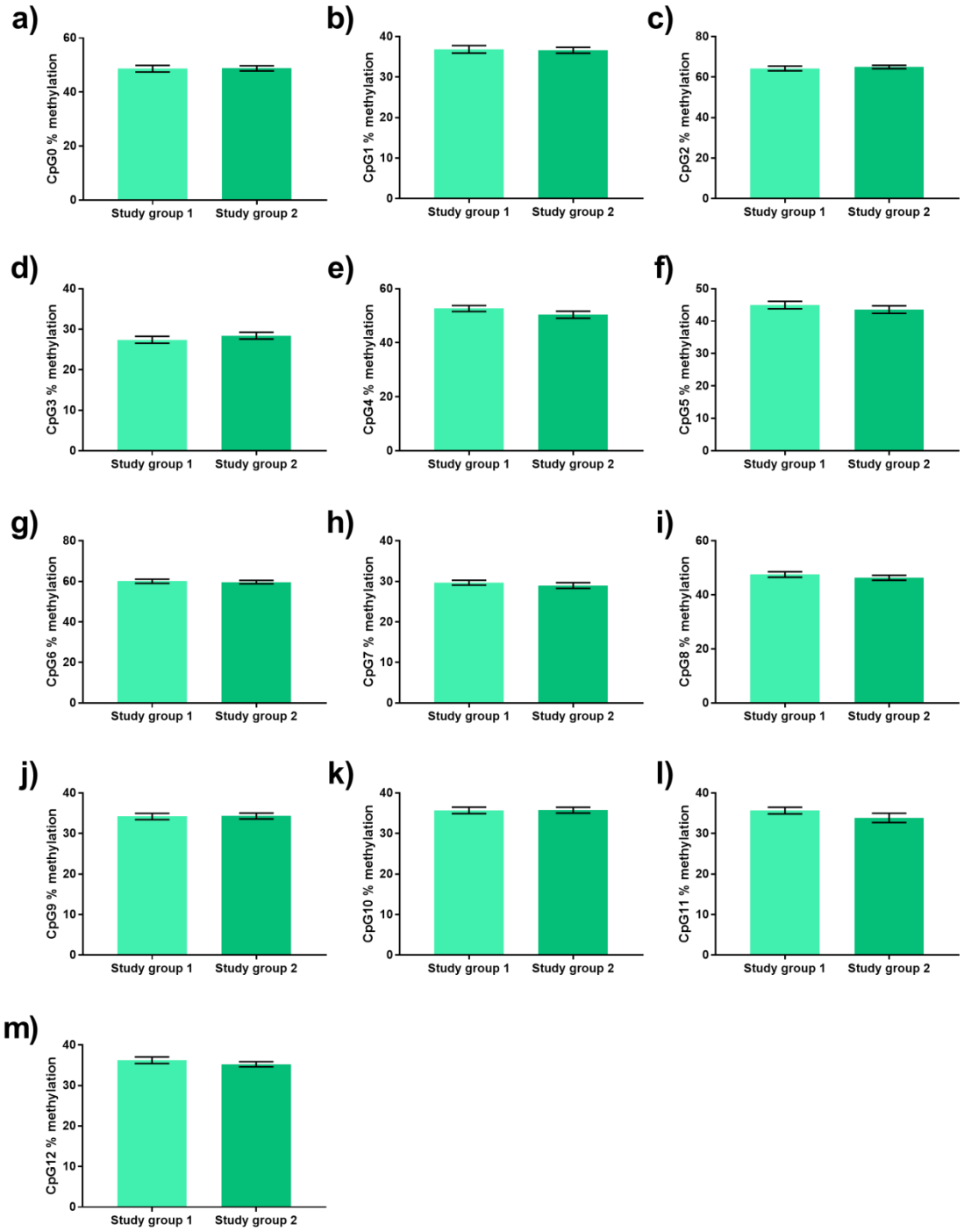

Figure 5-17 ***RXRα DNA methylation in SPRING placental samples.*** *Percentage DNA methylation at sites CpG0-12 of the gene RXRα in SPRING study samples.* ***a)*** *CpG0,* ***b)*** *CpG1,* ***c)*** *CpG2,* ***d)*** *CpG3,* ***e)*** *CpG4,* ***f)*** *CpG5,* ***g)*** *CpG6,* ***h)*** *CpG7,* ***i)*** *CpG8,* ***j)*** *CpG9,* ***k)*** *CpG10,* ***l)*** *CpG11,* ***m)*** *CpG12.Data analysed by independent Student's t-test and displayed as mean ± SEM. n = 33 - 47 control, n = 34 - 47 25(OH)D treatment.*

5.3.5 RXRα DNA methylation and MAVIDOS outcomes

Associations between RXRα DNA methylation and other outcomes from the MAVIDOS study were investigated.

Vitamin D associated metabolites and placental RXRα DNA methylation

Maternal 25(OH)D_3 status at 14 weeks gestation was not associated with DNA methylation at any of the 13 RXRα CpG sites investigated in this study. At 34 weeks gestation, an association between increased maternal 25(OH)D_3 concentration and decreased placental DNA methylation at CpG0 was observed, adjusted for season of birth. 34 week 25(OH)D_3 concentration was not associated with placental DNA methylation at any other CpG site. Data is displayed in Table 5-5.

Increased maternal calcium status at 14 weeks gestation was associated with decreased placental DNA methylation at CpG4 and CpG5. No other associations between 14 week calcium and placental DNA methylation were observed. Increased maternal calcium concentration at 34 weeks gestation was associated with decreased placental DNA methylation at CpG7. No other associations between 34 week calcium and placental DNA methylation were observed. Data is displayed in Table 5-5.

Maternal albumin concentration at 14 weeks gestation was not associated with placental DNA methylation at any of the 13 RXRα CpG sites investigated in this study. Increased maternal albumin concentration at 34 weeks gestation was associated with increased placental DNA methylation at CpG2. No other associations between 34 week albumin and placental DNA methylation were observed. Data is displayed in Table 5-5.

Table 5-5 *Associations between placental RXRα DNA methylation and pregnancy 25(OH)D_3, calcium and albumin status in MAVIDOS study participants .*

		25(OH)D_3 (nmol/L)		Calcium (mmol/L)		Albumin (g/L)	
RXRα		**14 weeks gestation**	**34 weeks gestation**	**14 weeks gestation**	**34 weeks gestation**	**14 weeks gestation**	**34 weeks gestation**
CpG0	β	0.012	**-0.089***	-2.636	-10.970	0.112	0.471
	p	0.807	**0.048**	0.816	0.334	0.766	0.479
	n	57	**46**	57	46	57	46
CpG1	β	0.064	-0.050	-9.014	-3.926	0.095	0.756
	p	0.120	0.165	0.365	0.702	0.774	0.205
	n	58	47	58	47	58	47
CpG2	β	0.013	-0.040	3.095	3.307	0.498	**1.156***
	p	0.766	0.248	0.765	0.747	0.141	**0.046**
	n	60	49	60	49	60	**49**
CpG3	β	0.014	-0.031	-4.748	-10.602	-0.103	0.448
	p	0.722	0.344	0.626	0.272	0.749	0.421
	n	60	49	60	49	60	49
CpG4	β	0.030	0.047	**-30.891***	-24.48	-0.200	-0.413
	p	0.621	0.316	**0.027**	0.056	0.670	0.617
	n	54	46	**54**	46	54	46
CpG5	β	0.076	0.027	**-25.578***	-10.375	0.073	-0.915
	p	0.115	0.500	**0.022**	0.360	0.850	0.787
	n	55	46	**55**	46	55	46
CpG6	β	-0.020	0.149	-4.543	-9.624	0.277	-2.358
	p	0.818	0.061	0.836	0.671	0.701	0.071
	n	67	55	67	55	67	55
CpG7	β	-0.010	0.033	-12.667	**-13.48***	-0.226	-0.210
	p	0.736	0.182	0.071	**0.050**	0.330	0.608
	n	67	55	67	**55**	67	55
CpG8	β	0.072	0.040	0.188	-5.457	-0.254	-0.757
	p	0.099	0.278	0.986	0.596	0.474	0.207
	n	66	55	66	55	66	55
CpG9	β	0.044	-0.013	-3.494	0.609	-0.313	-0.0374
	p	0.201	0.640	0.678	0.938	0.258	0.407
	n	66	54	65	54	65	54
CpG10	β	0.042	-0.010	3.308	-6.067	-4.201	-0.491
	p	0.276	0.767	0.737	0.515	0.198	0.375
	n	58	49	58	49	58	49
CpG11	β	0.032	-0.001	3.219	-11.485	-0.529	-0.729
	p	0.465	0.979	0.768	0.243	0.142	0.209
	n	59	50	59	50	59	50
CpG12	β	0.027	0.006	-2.43	-9.520	-0.395	-0.678
	p	0.488	0.863	0.798	0.294	0.218	0.213
	n	65	54	65	54	65	54

Significant results ($p < 0.05$) are highlighted in bold and marked with *

Placental RXRα DNA methylation and gene expression

Associations between placental RXRα DNA methylation and placental gene expression of vitamin D related genes were investigated. Data is adjusted for treatment group, sex and gestational age, and displayed in Table 5-6.

Increased expression of *VDR* was associated with decreased DNA methylation at CpG8. Increased expression of *CYP27B1* was associated with decreased DNA methylation at CpG6. Increased expression of *CYP24A1* was associated with decreased DNA methylation at CpG8. Expression of *RXRα, LRP2* (megalin) or *CUBN* (cubilin) were not associated with DNA methylation at any CpG site.

Table 5-6 *Associations between RXRα DNA methylation and placental gene expression.*

		Gene expression					
RXRα		***VDR***	***RXRα***	***CYP27B1***	***CYP24A1***	***LRP2***	***CUBN***
CpG0	β	-0.001	0.001	0.015	-0.022	-0.010	-0.010
	p	0.955	0.907	0.024	0.255	0.438	0.583
	n	57	56	57	57	57	57
CpG1	β	0.020	0.007	0.022	-0.026	-0.015	-0.006
	p	0.243	0.377	0.128	0.252	0.280	0.774
	n	58	57	58	58	58	58
CpG2	β	0.007	0.002	0.009	-0.003	-0.004	0.010
	p	0.691	0.759	0.505	0.906	0.776	0.614
	n	60	59	60	60	60	60
CpG3	β	-0.006	0.007	0.006	-0.016	-0.003	-0.016
	p	0.731	0.368	0.657	0.474	0.833	0.434
	n	60	59	60	60	60	60
CpG4	β	-0.010	0.005	0.010	-0.014	0.007	0.020
	p	0.427	0.444	0.061	0.544	0.492	0.191
	n	53	52	53	53	53	53
CpG5	β	-0.015	-0.001	0.001	-0.039	0.000	0.001
	p	0.333	0.878	0.804	0.169	0.983	0.969
	n	54	53	54	53	54	54
CpG6	β	-0.005	-0.005	**-0.013***	-0.017	0.006	-0.008
	p	0.389	0.160	**0.016**	0.117	0.289	0.302
	n	68	67	**67**	68	68	68
CpG7	β	-0.003	-0.009	-0.003	0.013	0.001	0.025
	p	0.898	0.341	0.854	0.706	0.928	0.300
	n	68	67	68	68	68	68
CpG8	β	**-0.027***	-0.007	-0.011	**-0.048***	-0.008	0.002
	p	**0.013**	0.332	0.280	**0.038**	0.441	0.881
	n	**66**	66	67	**66**	67	67
CpG9	β	-0.014	-0.004	-0.011	-0.052	-0.019	0.012
	p	0.451	0.672	0.443	0.081	0.179	0.560
	n	66	65	66	66	66	66
CpG10	β	-0.015	-0.011	-0.018	-0.017	-0.019	0.001
	p	0.396	0.175	0.172	0.449	0.143	0.964
	n	59	58	59	59	59	59
CpG11	β	-0.006	-0.003	-0.009	-0.006	-0.013	-0.001
	p	0.682	0.738	0.463	0.756	0.269	0.992
	n	60	59	60	60	60	60
CpG12	β	-0.017	-0.011	-0.001	-0.032	-0.015	0.002
	p	0.262	0.148	0.924	0.206	0.234	0.914
	n	66	65	66	66	66	66

Significant results ($p < 0.05$) are highlighted in bold and marked with *

5.4 Discussion

This study has demonstrated that 25(OH)D_3 treatment can alter gene expression in villous fragment tissue and isolated cytotrophoblast cells. Changes were not observed in histone protein methylation/acetylation. Changes to RXRα DNA methylation was observed in placentas from the MAVIDOS study.

5.4.1 Gene expression

The expression of selected vitamin D pathway genes and genes of interest from data displayed in Chapter 4 were investigated in isolated cytotrophoblast cells and villous fragment tissue. Cytotrophoblast cells were investigated between 18 h and 90 h of culture without treatment, during which time the cells undergo syncytialisation, and at 90 h with and without 24 h 20 µmol 25(OH)D_3 treatment. Villous fragment samples were investigated with 8 h 20 µmol 25(OH)D_3 + 0.7 mmol/l BSA vs ethanol control with 0.7 mmol/l BSA, equivalent to those investigated in Chapter 4, or 8 h 20 µmol 25(OH)D_3 + 9 µmol DBP vs ethanol control + 9 µmol DBP, more closely representing physiological conditions.

Vitamin D pathway genes

CYP27B1 (25-hydroxyvitamin D 1α-hydroxylase) is the cytochrome P450 enzyme responsible for the hydroxylation of 25(OH)D to 1,25$(OH)_2D_3$ (Jones et al., 2014). Expression of *CYP27B1* within the placenta allows for local production of active 1,25$(OH)_2D_3$ within placental tissue, and contributes to the elevated maternal 1,25$(OH)_2D_3$ levels experienced during pregnancy (Novakovic et al., 2009). The decrease in expression of *CYP27B1* between 18 h and 90 h of untreated culture suggests a decrease in *CYP27B1* mediated hydroxylation of 25(OH)D_3 in the syncytiotrophoblast layer. In all 25(OH)D_3 treated samples; cytotrophoblasts, 25(OH)D_3 + BSA treated and 25(OH)D_3 + DBP treated fragments there was no change in *CYP27B1* gene expression, suggesting that *CYP27B1* does not respond to increased presence of 25(OH)D_3 in the syncytiotrophoblast. Collectively this suggests that *CYP27B1* does not upregulate metabolism of 25(OH)D_3 in response to increased 25(OH)D_3 concentration.

CYP24A1 (25-hydroxylase) is a vitamin D responsive gene containing a VDRE in it's promoter, responsible for the hydroxylation and inactivation of 25(OH)D_3 and 1,25$(OH)_2D_3$ (Jones et al., 2014). *CYP24A1* is expressed within placental tissue, and allows for regulation of local 1,25(OH)D_3 levels (Novakovic et al., 2009). Expression of *CYP24A1* in isolated cytotrophoblast cells decreased from 18 h to 90 h of culture as the cells syncytialised, but increased with 25(OH)D_3

treatment at 90 h. *CYP24A1* expression also increased in 25(OH)D_3 + BSA fragment samples, but there was no change in 25(OH)D_3 + DBP treated fragment samples. This suggests that in the syntiotrophoblast metabolic inactivation of 25(OH)D_3 and 1,25(OH)$_2D_3$ by *CYP24A1* is decreased, which could underlie the increased 1,25(OH)$_2D_3$ present in pregnant women and ensure a local supply of these metabolites are available for supply to the fetus. Increased expression of *CYP24A1* in the presence of 25(OH)D_3 treated cytotrophoblasts and 25(OH)D_3 + BSA treated fragments suggests that the placenta may be acting to limit the local concentration of 25(OH)D_3 and 1,25(OH)D_3 regulating their effects both on the placental tissue and availability for transfer to the fetus. In the 25(OH)D_3 + DBP treated fragment samples three of the four samples investigated displayed an increase in expression with treatment, whilst one sample displayed a decrease. This increase in *CYP24A1* gene expression with vitamin D treatment is consistent with the increase observed in fragments in Chapter 4, and in published data (Shenga et al., 2019).

RXRα (retinoid X receptor alpha) forms a heterodimer with 1,25(OH)$_2D_3$ activated VDR, forming a complex that can interact with VDREs in the DNA, altering expression of vitamin D responsive genes (Orlov et al., 2012, Christakos et al., 2016). No change in the expression of *RXRα* was identified in cytotrophoblasts with syncytialisation during culture from 18 h to 90 h, but there was a small significant decrease in expression with 25(OH)D_3 treatment in the syncytialised cells. No change in expression was identified in either 25(OH)D_3 + BSA or 25(OH)D_3 + DBP treated fragment samples. There was no significant change in *VDR* expression in cytotrophoblast cells cultured for 18 h vs 90 h, 25(OH)D_3 treated cytotrophoblast cells, or in fragments treated with either 25(OH)D_3 + BSA or 25(OH)D_3 + DBP. This suggests that the ability of the placental tissue to respond to vitamin D by altering gene expression is not altered with the addition of 25(OH)D_3, and therefore any changes to gene expression in response to treatment must either utilise the VDR and RXRα already present, or utilises another mechanism. Other mechanisms could include alterations to placental DNA methylation or histone protein expression that could make genes more or less accessible to transcription factors, as suggested in Chapter 4.

Gene expression during syncytialisation

As cytotrophoblast cells syncytialise they undergo changes in both structure and function, becoming a large multinucleate cell layer responsible for regulating the transfer of nutrients to the fetus. The gene *PLEKHG2* (Pleckstrin Homology and RhoGEF Domain Containing G2), is a Rho guanidine exchange factor (RhoGEF) responsible for activating RhoGTPases, which in turn plays a role in the rearrangement of the actin cytoskeleton (Edvardson et al., 2016). *PLEKHG2* had increased expression between 18 h and 90 h of culture, as syncytialisation occurred. This increase

in *PLEKHG2* expression likely reflects the cytoskeletal changes that occur during the process of syncytialisation, allowing the cells to change shape and merge into multinucleate cells.

As syncytialisation occurred there was a decrease in the expression of the genes *CDRT1* (CMT1A Duplicated Region Transcript 1), *DNMT3b* (DNA Methyltransferase 3 Beta), *HIVEP2* (human immunodeficiency virus type I enhancer binding protein 2) and *RNASE7* (Ribonuclease A Family Member 7). Decreased expression of *HIVEP2*, a transcription factor, and *DNMT3b*, a *de novo* DNA methyltransferase, suggest a down regulation in transcription in the syncytiotrophoblast compared to cytotrophoblast cells (Steinfeld et al., 2016, Moore et al., 2013). Greater levels of transcription in the cytotrophoblast may be due to the cells actively changing as they locate neighbouring cells and prepare to syncytialise, compared to the syncytiotrophoblast cells that are in a relatively steady state. A decrease in *CDRT1* expression, a gene involved in the demyelination of peripheral nerves, suggests that it's function within the syncytiotrophoblast is not needed (Berciano et al., 2010). Decreased *RNASE7* expression in the syncytiotrophoblast, an antimicrobial peptide that acts to downregulate Th2 cytokine production from T-cells, suggests a change towards a more immune tolerant environment compared to cytotrophoblast. The syncytiotrophoblast, tissue of fetal origin, comes into contact with maternal blood, and thus the promotion of an immune tolerant environment by vitamin D here may help prevent inappropriate immune responses occurring.

The effect of vitamin D on syncytialisation was unfortunately not investigated in this study. Vitamin D supplementation in pregnancy studies have shown different outcomes when the supplementation was started later in pregnancy compared to those that start in the first trimester, suggesting that vitamin D may play an important role early in pregnancy when the syncytiotrophoblast layer is developing (Cooper et al., 2016, Vaziri et al., 2016). It would therefore be interesting to investigate if vitamin D has any effect on syncytialisation. The effect of vitamin D on syncytialisation could be investigated by treating cytotrophoblast cells with 25(OH)D_3 as they syncytialise and measuring changes in the rate of syncytialisation (hCG production and imaging) and gene expression changes (qRT-PCR).

<u>25(OH)D_3 mediated gene expression changes in the syncytiotrophoblast</u>

25(OH)D_3 treatment of the syncytiotrophoblast resulted in an increase in *HIVEP2* expression, and a decrease in *RNASE7* expression. Increased *HIVEP2* expression may be a result of vitamin D acting to alter gene expression in the placenta via its interaction with the VDR-RXRα complex. Altered gene expression in response to vitamin D may mediate an increase in the expression of transcription factors, such as *HIVEP2*, to allow for this. Decreased expression of the antimicrobial peptide *RNASE7* may reduce the ability of the syncytiotrophoblast to respond to an

immune threat. There is a balance that must be maintained in the placenta between immune tolerance, to allow the fetus to not be rejected by the mother, and immune reactivity, to respond appropriately to pathogens and environmental threats to protect the fetus. In Chapter 4 we identified altered gene pathways of inflammation and immune regulation with vitamin D treatment. This data further supports the role of vitamin D in the syncytiotrophoblast, acting to promote an immune tolerant environment in the placenta.

Vitamin D treatment caused no obvious observable differences to the degree of syncytialisation, cell viability or rate of apoptosis during the 24 h of treatment; however these factors were not measured. Measuring the effect of vitamin D on these outcomes could allow us to determine how vitamin D affects the health of the cells, and if this is a mechanism by which vitamin D may function within the placenta. Effects of vitamin D on the degree of syncytialisation could be determined by comparing hCG production between treated and untreated cells. Effects of vitamin D on cell viability and rate of apoptosis could be investigated by staining with a viability dye such as trypan blue and imaging the cells.

<u>25(OH)D_3 mediated gene expression changes in placental villous fragments</u>

Villous fragment samples were treated with 25(OH)D_3 + BSA or 25(OH)D_3 + DBP for a period of 8 h. In the BSA treated samples there was increased expression of *RNASE7*, and decreased expression of *CDRT1*. This expression pattern was also seen in the DBP treated samples, with the addition of increased *AHDC1* (AT-Hook DNA Binding Motif Containing 1), *DNMT1* (DNA methyltransferase 1), *EZH2* (Enhancer of Zeste 2 Polycomb Repressive Complex 2 Subunit), and *HIVEP2* expression and decreased *PLEKHG2* expression. The change in the expression levels of more genes with 25(OH)D_3 + DBP compared to 25(OH)D_3 + BSA suggests that the presence of DBP may be required to observe the full effects of vitamin D. Vitamin D mediated effects may therefore be being missed in some studies, as BSA is primarily used as the binding protein in experimental conditions due to it being cost-effective and readily available.

Increased expression of *AHDC1* (a DNA binding protein), *DNMT1* (methyaltes hemimethylated DNA produced during semi conservative DNA replication), and *HIVEP2* (a transcription factor) all suggest an increased in transcriptional activity with 25(OH)D_3 + DBP treatment (García-Acero and Acosta, 2017, Moore et al., 2013, Steinfeld et al., 2016). This is consistent with the alterations to pathways of transcriptional regulation observed with vitamin D treatment in Chapter 4, and suggests that vitamin D is a factor that acts to alter transcriptional regulation within the placenta. Changes in transcriptional regulation may be a mechanism by which vitamin D acts to alter placental function, by altering the expression of genes or sets of genes with a particular activity. Increased expression of *EZH2*, which acts to catalyse the

trimethylation of lysine 27 on histone 3 (H3K27me3), suggests that vitamin D treatment may act to alter histone methylation in the placenta (Christofides et al., 2016). Altering histone methylation may be another mechanism by which vitamin D acts to alter transcriptional regulation, by changing the availability of a particular section of DNA to transcription factors. Altered histone methylation with vitamin D treatment is again supported by the data presented in Chapter 4 which showed changes in pathways of histone regulation.

Both $25(OH)D_3$ + BSA and $25(OH)D_3$ + DBP treated fragments displayed an increase in *RNASE7* expression, however $25(OH)D_3$ treated syncytiotrophoblast cells showed decreased expression. The difference in the expression of *RNASE7* with vitamin D treatment likely results from the fragment samples consisting of mixed-cell type tissue, compared to the single cell type present in the syncytiotrophoblast samples. $25(OH)D_3$ may act differently upon the different cell types, resulting in a different change in *RNASE7* expression. In the syncytiotrophoblast $25(OH)D_3$ appeared to promote a more immune tolerant environment with decreased *RNASE7* expression, whereas in the fragment samples the increased expression suggests promotion of a more immune reactive environment. This may be due to the action of $25(OH)D_3$ immune cells such as macrophages within the placenta, which play an important role in protecting the fetus from the maternal environment. Investigating other cell types within the placenta such as macrophages and fibroblasts individually would allow us to investigate how cell type is affecting gene expression here further.

$25(OH)D_3$ + BSA and $25(OH)D_3$ + DBP treated fragments both displayed a decrease in the expression of *CDRT1* with vitamin D treatment. *CDRT1* plays a role in the demyelination of peripheral nerves, but its role within the placenta is less clear (Berciano et al., 2010). This decrease in *CDRT1* expression was not observed in $25(OH)D_3$ treated syncytiotrophoblast cells, suggesting that this change in expression does not occur in the syncytiotrophoblast cells. Decreased *PLECKHG2* expression in $25(OH)D_3$ + DBP treated fragments suggest that vitamin D is acting to limit actin remodelling within the tissue (Edvardson et al., 2016). Again this change in *PLECKHG2* expression was not observed in $25(OH)D_3$ treated syncytiotrophoblast, suggesting that it is another placental cell type, such as an immune cell, fibroblast or endothelial cell type in which this change occurs.

5.4.2 Histone modifications

Epigenetic histone modifications such as histone methylation and acetylation marks suggested to be altered in Chapter 4 were investigated in villous fragments and SPRING placenta samples. No change to the amount of H3K4me3, H3K27me3 or H3K27ac was identified between treatment groups in this study, suggesting that vitamin D is not altering the expression of these

marks in the placenta. Histone modifications act to alter gene transcription by altering how histone proteins interact with the DNA, condensing or releasing the chromatin structure. Whilst it is possible that vitamin D metabolites may act to alter other histone marks, this data suggests that altering histone modifications is not a mechanism by which vitamin D alters gene expression within the placenta.

5.4.3 RXRα DNA methylation

The methylation status at 13 CpG sites present in the promoter of RXRα were investigated in 25(OH)D_3 treated cytotrophoblast samples, 25(OH)D_3 + BSA treated fragments samples and in placentas from the MAVIDOS and SPRING studies. In Chapter 4 data presented showed altered methylation at six other RXRα CpG sites in fragments treated with 25(OH)D_3 + BSA. This data is consistent with that seen in the MAVIDOS trial, in which methylation of CpGs 2, 3 ,4 and 5 of RXRα in the umbilical cord were significantly altered between treatment groups (Curtis et al., 2019). Altered RXRα DNA methylation may be of clinical importance, as demonstrated by a study utilising the SWS cohort, which identified an association between umbilical cord RXRα DNA methylation and bone mineral content at age 4 years (Harvey et al., 2014b).

Short term 25(OH)D_3 treatment of cytotrophoblasts and villous fragments

In this study 24 h 25(OH)D_3 treatment of cytotrophoblast cells, and 8 h treatment of villous fragments resulted in no changes to the methylation status of the 13 CpG sites investigated, suggesting short term 25(OH)D_3 treatment does not alter RXRα DNA methylation. This is supported by very small or no changes in RXRα gene expression observed. However this is not consistent with the fragment data presented in chapter 4 in which alternative CpG sites in the promoter of RXRα had altered methylation with an 8 h 25(OH)D_3 treatment.

Long term cholecalciferol treatment

In this study daily 1000 IU cholecalciferol supplementation from 14 weeks gestation increased DNA methylation at RXRα CpG6 in MAVIDOS samples, but no changes were observed at any other CpG site in MAVIDOS or SPRING samples. As supplementation in MAVIDOS and SPRING was consistent, it would be reasonable to expect changes observed in MAVIDOS to also be observed in SPRING samples. Alteration to CpG6 DNA methylation in MAVIDOS placentas is also not consistent with that seen in MAVIDOS umbilical cords (Curtis et al., 2019). This suggests that although significant, altered DNA methylation at CpG6 in MAVIDOS placentas may not be a true finding, and further investigation would be required to confirm this result. Data presented in this

chapter is therefore not conclusive as to whether long term 1000 IU daily cholecalciferol treatment alters RXRα DNA methylation in the placenta.

RXRα DNA methylation and MAVIDOS outcomes

In the MAVIDOS study we observed altered RXRα CpG DNA methylation in the placenta associated with maternal early pregnancy calcium and late pregnancy $25(OH)D_3$, albumin and calcium levels. This suggests that $25(OH)D_3$ and related metabolites in the maternal environment are able to alter RXRα DNA methylation in the placenta. RXRα DNA methylation was associated with the expression of *VDR, CYP24A1* and *CYP27B1*, genes which play a role in regulating the metabolism and activity of vitamin D metabolites within the placenta. This data suggests that RXRα DNA methylation may play a role in modifying gene expression, which could alter placental function. Placental function changes may underlie the altered offspring outcomes observed with maternal $25(OH)D_3$ deficiency. This hypothesis is supported by MAVIDOS data presented in Appendix C, which identifies associations between placental gene expression and offspring body composition outcomes at birth and four years of age. The genes *ASCT1, ASCT2, CYP24A1, CYP27B1, LAT1, LRP2, TXNIP* and *VEGF* were associated with body composition outcomes including birth weight, fat mass, bone mineral density, bone mineral content and bone area.

Overall relationships

In this chapter we have observed few changes to RXRα DNA methylation with vitamin D treatment, but an association between late pregnancy $25(OH)D_3$ concentration and RXRα DNA methylation. This suggests that it may be the circulating amount of $25(OH)D_3$, as opposed to cholecalciferol treatment itself, that acts to alter RXRα DNA methylation and potentially function.

5.5 Limitations

There are limitations to the data presented here in this study. Firstly the number of primary cytotrophoblast samples investigated is limited due to experimental difficulties. Isolating cytotrophoblast cells from the mix of cell types present in the placenta is a time consuming process that is detrimental to the health of the placental cells. This process therefore requires the placenta to be obtained quickly after delivery, to be processed in an efficient manner, and for cells to be successfully separated to obtain enough healthy cytotrophoblast cells for culture. This does however provide us with matched samples of a single cell type, providing valuable genetic data that is not influenced by composition of tissue or differences between participants. Some gene expression data in this study is possibly confounded by single anomalous samples, and therefore obtaining a higher sample number may improve confidence in the results.

Whilst obtaining data on isolated primary cytotrophoblast cells is useful for identifying the cell type in which gene expression and DNA methylation changes have occurred, other cell types also need to be investigated. For example a number of possible changes to the expression of gene involved in immune functions were identified in Chapter 4, it is likely these changes primarily occurred in immune cells within the placenta, but this was not investigated here.

In this study we investigated three histone marks suggested to be modified in Chapter 4, however there is a large number of histone modifications than can act to alter gene expression. It is therefore not possible to definitively conclude that altered histone marks are not underlying altered gene expression with 25(OH)D_3 treatment. Here we also investigated total changes to histone marks, where as it is more likely that changes may occur locally at a specific region in the DNA.

Whilst pyrosequencing is considered the gold standard for measuring DNA methylation, it does limit the number of CpG sites that can be investigated. Therefore only a limited number of RXRα CpG sites have been investigated in cytotrophoblast, MAVIDOS and SPRING samples. These CpG sites also do not match to those observed to be altered in Chapter 4. Unfortunately due to the sequence location of the CpG sites investigated in Chapter 4 it was not possible to design specific primers for them to be suitable for pyrosequencing. It has therefore not been possible to determine if the RXRα CpG sites altered in 25(OH)D_3 treated fragments in Chapter 4 were also altered with long term treatment in MAVIDOS and SPRING samples.

5.6 Future work

To further investigate the cell type in which changes to placental gene expression and DNA methylation occur, other placental cell types need to be investigated. To do so the protocol for isolating cytotrophoblast samples from the placenta needs to be modified and optimised for other specific cell types. Cell types of particular interest include macrophages and fibroblasts. Investigating gene expression in a larger number of cytotrophoblast samples would also increase our confidence in this dataset.

Specific histone proteins of interest could be investigated to see if they are interacting in regions of DNA which show gene expression changes with vitamin D treatment in the placenta. To do so Chromatin Immunoprecipitation targeting specific histone proteins, followed by sequencing of the DNA (ChIP-Seq), could be carried out. This could help identify a mechanism by which vitamin D is altering placental gene expression.

Investigating the RXRα associated CpG sites that were altered in 25(OH)D_3 + BSA treated villous fragments in Chapter 4 in the MAVIDOS and SPRING placenta samples would allow us to investigate whether these CpG sites may be of clinical importance. Altered RXRα DNA methylation in the umbilical cord has previously been identified to be associated with bone outcomes in the offspring (Harvey et al., 2014b). The presence of Wharton's jelly in the umbilical cord makes DNA extraction more difficult compared to in placental samples. Finding biomarkers in the placenta that potentially relate to future health outcomes therefore makes their use clinically more feasible.

Altered protein expression was identified in 25(OH)D_3 + BSA treated placental fragment samples in Chapter 4, but protein expression changes were not always consistent with gene expression changes. Measuring the expression of proteins of interest in cytotrophoblast, MAVIDOS and SPRING placental samples may therefore provide a fuller picture of the changes induced by vitamin D treatment. This could be carried out by Western blotting to avoid proteins of interest not being measured due to them containing no unique fragment, as is the case when using LCMS.

5.7 Conclusions

Vitamin D metabolites are known to alter the expression of specific genes within the placenta. Here we show that short term $25(OH)D_3$ treatment results in altered placental expression of a number of novel genes. Gene expression changes are dependent upon placental cell type, with $25(OH)D_3$ treated cytotrophoblast cells displaying different gene expression changes to villous fragments. Modification of epigenetic histone marks may not be a mechanism by which vitamin D metabolites alter placental gene expression, although further study is needed to confirm this. DNA methylation of RXRα, which plays an important role in $1,25(OH)_2D_3$ transcriptional activity, is not altered at any of the 13 CpG sites investigated here by short term $25(OH)D_3$ or long term cholecalciferol treatment.

Chapter 6 General discussion

6.1 Overview

This study investigated the metabolism of vitamin D within the human placenta, and how vitamin D metabolites act upon the placental tissue. Maternal $25(OH)D_3$ levels have been associated with fetal growth, implicating maternal $25(OH)D_3$ in the immediate and lifelong health of the offspring. To reach the fetus vitamin D metabolites must be transferred across the placenta, but data suggests that vitamin D metabolites are also acting upon the placental tissue itself. Data presented in this thesis suggests that $25(OH)D_3$ is metabolised within the placenta, with metabolites passed to both the maternal and fetal circulations. Short term treatment with $25(OH)D_3$ alters placental gene expression, protein expression and DNA methylation in pathways that affect key placental functions, with some changes occurring in the syncytiotrophoblast layer. Long term cholecalciferol treatment altered RXRα DNA methylation at one CpG site in the MAVIDOS study, although this was not seen in short term $25(OH)D_3$ treated samples, suggesting the duration of exposure and metabolites used in treatment may effects how vitamin D acts upon the placenta.

Data presented in Chapter 3 demonstrated that in *ex vivo* perfused placental cotyledons $25(OH)D_3$ is metabolised to $24,25(OH)_2D_3$ and $1,25(OH)_2D_3$, with metabolites transferred to both maternal and fetal circulations. The observation that placental derived $1,25(OH)_2D_3$ is transferred to the mother suggests that the placenta is contributing to pregnancy induced increased maternal $1,25(OH)_2D_3$ levels and potentially regulating vitamin D transfer to the fetus.

Data presented in Chapter 4 demonstrated that short term exposure of placental villous fragments to $25(OH)D_3$ altered placental DNA methylation, demonstrating mediated placental epigenetic changes, a mechanism by which it may alter placental function. $25(OH)D_3$ treated fragments also displayed altered gene and protein expression in pathways of transcriptional regulation, histone expression and immune activity, suggesting altered placental function.

Changes observed in $25(OH)D_3$ treated villous fragments were also observed in treated syncytiotrophoblast cells in Chapter 5, suggesting this is the cell type in which some of these changes occur. In the MAVIDOS study maternal 34 week $25(OH)D_3$ levels were associated with placental RXRα DNA methylation, and RXRα DNA methylation was associated placental gene expression, suggesting maternal $25(OH)D_3$ affects placental transcription in an epigenetically regulated manner.

In this chapter I will briefly summarise the findings of this thesis, discussing how findings may relate to each other and the implications these may have for future research.

6.2 Placental metabolism and transfer of $25(OH)D_3$

6.2.1 Placental metabolism of $25(OH)D_3$

Perfusion of *ex vivo* placental cotyledons with ^{13}C-$25(OH)D_3$ in the maternal circulation allowed me to identify if direct metabolism of the ^{13}C-$25(OH)D_3$ was occurring. By identifying the presence of downstream metabolites with a ^{13}C label attached in the perfusate, I could confirm that the downstream metabolite was a product of the original ^{13}C-$25(OH)D_3$. Placental metabolism of vitamin D is displayed in Figure 6-1. In this study I identified the presence of ^{13}C-$24,25(OH)_2D_3$ in the maternal and fetal perfusate, demonstrating that the placenta metabolises $25(OH)D_3$. The data also suggested metabolism of $25(OH)D_3$ to $1,25(OH)_2D_3$ was occurring within the tissue, but as I was unable to distinguish between ^{13}C-$1,25(OH)_2D_3$ and $1,25(OH)_2D_3$, I am unable to confirm that this direct metabolism is taking place. Metabolism of $25(OH)D_3$ within the placenta does suggest that the placenta may be regulating the actions of vitamin D, both in its transfer to the fetal circulation and the actions it exerts on the placental tissue itself.

- **The placenta metabolises $25(OH)D_3$ to $24,25(OH)_2D_3$ and $1,25(OH)_2D_3$. Placental metabolism of $25(OH)D_3$ may be a mechanism by which the placenta regulates transfer and actions of vitamin D.**

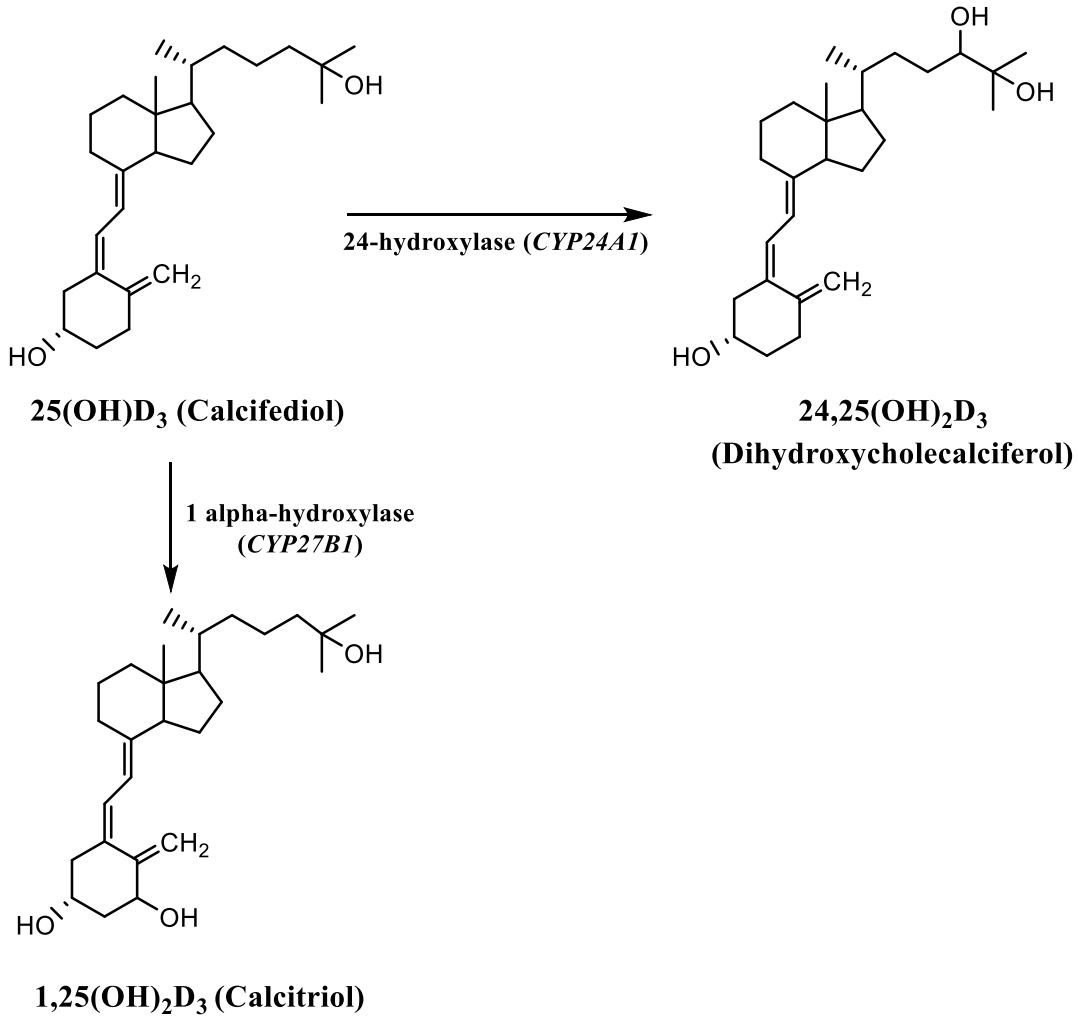

Figure 6-1 ***Metabolism of 25(OH)D_3 within the human placenta.*** *25(OH)D_3 undergoes hydroxylation to 24,25(OH)$_2D_3$ and 1,25(OH)$_2D_3$ within the human placenta.*

6.2.2 Transfer of vitamin D metabolites to the fetus

Transfer of vitamin D from the maternal to the fetal circulation is necessary to meet fetal demands during gestation. Studies in rat and human models have provided conflicting data regarding the type of vitamin D that crosses the placenta to the fetus (Liu and Hewison, 2011, Ron et al., 1984). In addition the human study had a number of experimental limitations which make the results difficult to interpret. In the current study I perfused *ex vivo* placental cotyledons with ^{13}C-25(OH)D_3, and demonstrated direct transfer of ^{13}C-25(OH)D_3 from the maternal to the fetal circulation, as shown in Figure 6-2. I have also demonstrated transfer of ^{13}C-24,25(OH)$_2D_3$ and 1,25(OH)$_2D_3$ from the placenta to the fetal circulation for the first time, showing that multiple vitamin D metabolites are passed to the fetus. Transfer of vitamin D metabolites into the fetal circulation allows them to be utilised by the fetus, potentially affecting fetal growth and development.

$1,25(OH)_2D_3$ is the primary metabolically active vitamin D metabolite, and transfer to the fetal circulation brings $1,25(OH)_2D_3$ into contact with the fetus, where it could potentially act to alter fetal development. $25(OH)D_3$ transferred into the fetal circulation may exert non-genomic effects in the fetus, and also act to regulate levels of $1,25(OH)_2D_3$ through hydroxylation of $25(OH)D_3$ by *CYP27B1* expressed in the fetal kidneys. The associations previously observed between reduced maternal $25(OH)D_3$ during pregnancy and offspring bone health may be mediated by insufficient vitamin D transfer to the fetus (Javaid et al., 2006). Low fetal $25(OH)D_3$ or $1,25(OH)_2D_3$ may not allow for sufficient action of $1,25(OH)_2D_3$ on the developing intestinal epithelium to produce calcium channels necessary for dietary calcium uptake. This may predispose the infant to reduced dietary calcium uptake in early life, which may contribute to the reduced bone mineral content observed in later childhood. The data presented in this thesis demonstrates that multiple vitamin D metabolites are able to act directly on the fetus during development.

- **The vitamin D metabolites $25(OH)D_3$, $1,25(OH)_2D_3$ and $24,25(OH)_2D_3$ are transferred across the placenta to the fetal circulation, where they may interact with the fetus during development.**

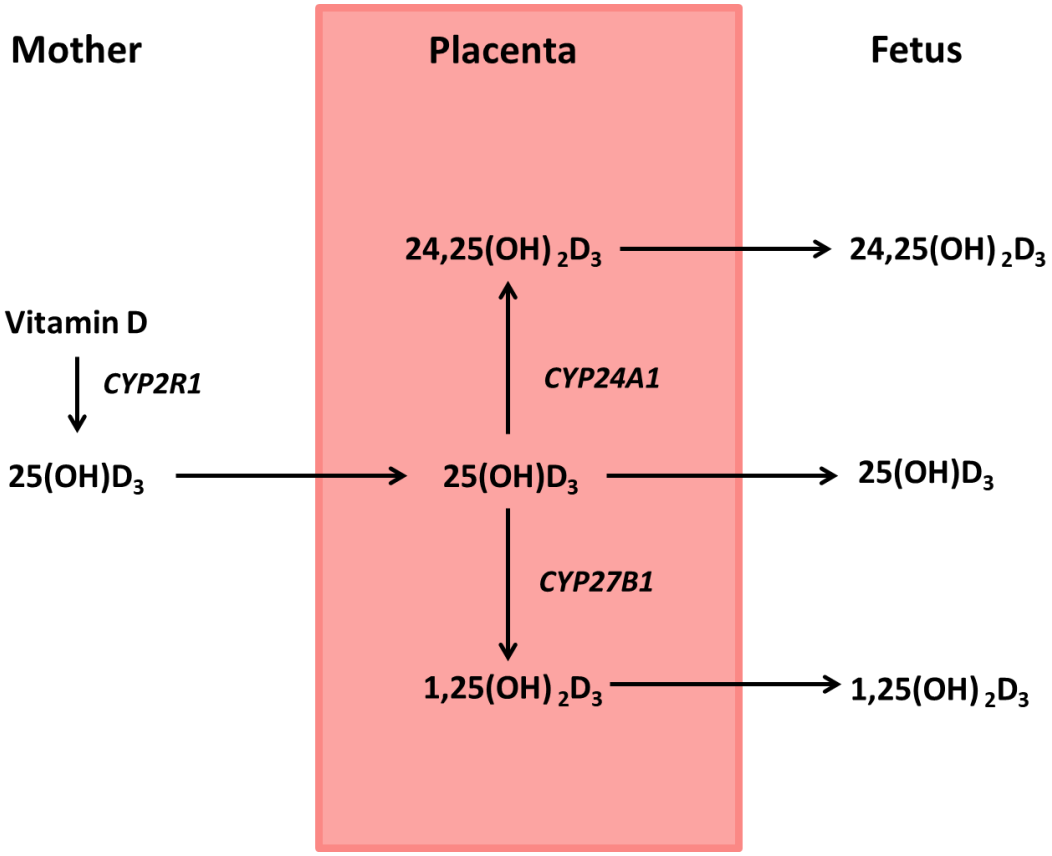

Figure 6-2 ***Transfer of vitamin D to the fetal circulation.*** *$25(OH)D_3$ from the maternal circulation is taken up in to the placenta and transferred across to the fetal circulation. The metabolites of $25(OH)D_3$, $24,25(OH)_2D_3$ and $1,25(OH)_2D_3$ are also transferred from the placental tissue into the fetal circulation.*

6.2.3 Transfer of vitamin D metabolites to the mother

The primary source of vitamin D for the placenta is from the maternal circulation, however this study demonstrates that placental metabolism creates alternative metabolites of vitamin D which are transferred back to the maternal circulation. In this study I observed transfer of $25(OH)D_3$ (unlabelled endogenous vitamin D released from the tissue), ^{13}C-$24,25(OH)_2D_3$ and $1,25(OH)_2D_3$ from the placenta into the maternal circulation, as shown in Figure 6-3. Transfer of vitamin D metabolites from the placenta to the maternal circulation will alter the pool of vitamin D metabolites available in the mother, and allow them to act upon on maternal tissues. The levels of $1,25(OH)_2D_3$ in maternal serum increase up to two and a half times the normal pre-pregnant levels during pregnancy, which is thought to occur due to increased synthesis in the kidneys rather than decreased breakdown (Besta et al., 2019, Karras et al., 2017). The findings of this study raise the question as to what proportion of the increase in maternal $1,25(OH)_2D_3$ levels is due to placental metabolism. Placental metabolism of $1,25(OH)_2D_3$ and transfer to maternal circulation may act to increase maternal dietary calcium uptake necessary for both maternal and fetal health.

- **The vitamin D metabolites $25(OH)D_3$, $1,25(OH)_2D_3$ and $24,25(OH)_2D_3$ are transferred from the placenta to the maternal circulation, where they may act upon maternal tissues and alter the composition of the maternal pool of vitamin D metabolites.**

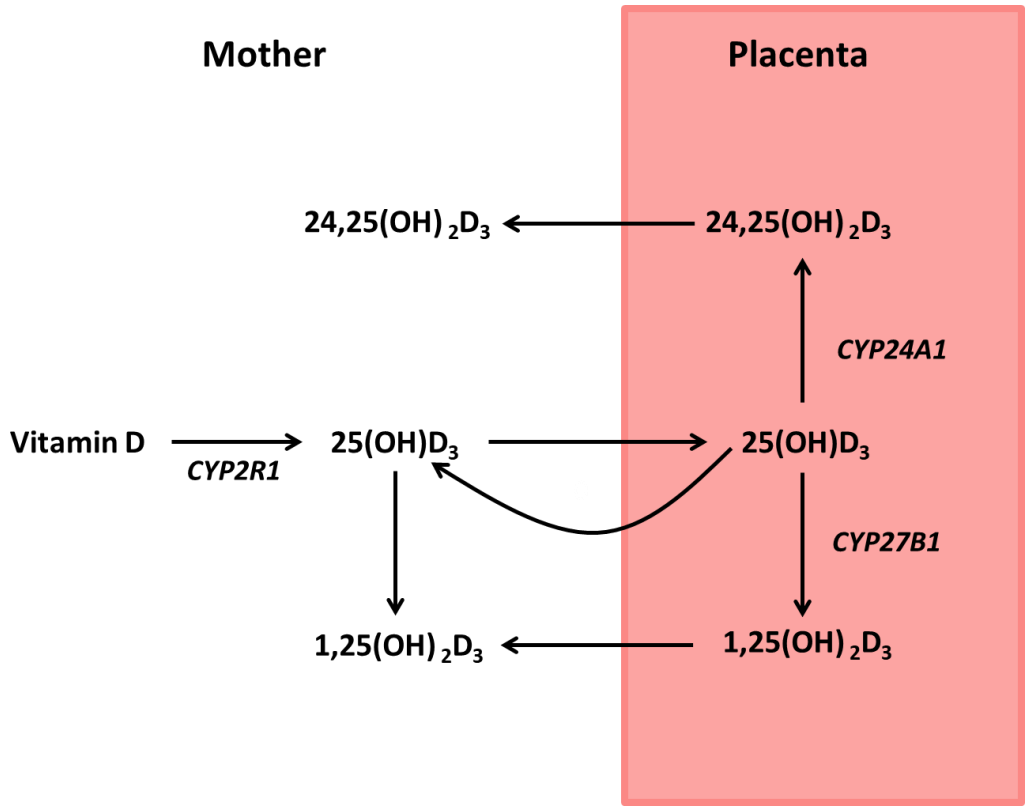

Figure 6-3 ***Transfer of vitamin D to the maternal circulation.*** *$25(OH)D_3$ from the maternal circulation is taken up in to the placenta and undergoes metabolism to$24,25(OH)_2D_3$ and $1,25(OH)_2D_3$. The metabolites of $25(OH)D_3$, $24,25(OH)_2D_3$ and $1,25(OH)_2D_3$ are transferred from the placental tissue into the maternal circulation.*

6.2.4 Summary

In this study I aimed to investigate how $25(OH)D_3$ is metabolised within the placenta and what vitamin D metabolites are transferred to the fetal and maternal circulations. Here we demonstrate that $25(OH)D_3$ is metabolised to $24,25(OH)_2D_3$ and $1,25(OH)_2D_3$, and that all three metabolites are transferred from the placenta into the fetal circulation, where they may interact with fetal tissues. We also demonstrated that $25(OH)D_3$, $24,25(OH)_2D_3$ and $1,25(OH)_2D_3$ are transferred from the placenta to the maternal circulation. Metabolism of $25(OH)D_3$ within the placenta and transfer of these metabolites to the mother will alter the maternal pool of vitamin D metabolites. Transfer of placental derived $1,25(OH)_2D_3$ into maternal circulation will contribute to the pregnancy induced rise in maternal $1,25(OH)_2D_3$ levels, supporting maternal functions.

6.3 Vitamin D links to fetal and maternal outcomes

The transfer of vitamin D metabolites from the placenta to the maternal and fetal circulations may alter maternal and fetal outcomes.

6.3.1 Offspring outcomes

In chapter 3 I demonstrated transfer of the metabolites $25(OH)D_3$, $1,25(OH)_2D_3$ and $24,25(OH)_2D_3$ from the placenta to the fetal circulation, where they may interact with the fetus. The availability of vitamin D metabolites in the fetus may alter the development of tissues by altering transcriptional regulation and gene expression. As discussed in Chapter 5 we have observed associations between the actions of vitamin D in the placenta and offspring body composition at birth and 4 years of age. Increased *CYP24A1* gene expression, a $1,25(OH)_2D_3$ responsive gene, was associated with increased placental weight, birth weight, fat mass, bone mineral content and bone area at birth, suggesting a strong relationship between *CYP24A1* expression in the placenta and body composition at birth. Increased placental *CYP27B1* expression was associated with reduced bone mineral density and bone mineral content at 4 years of age, suggesting that the effects of placental gene expression persist into childhood. Collectively this data indicates that maternal $25(OH)D_3$ mediated alterations to placental gene expression could subsequently change fetal development in a manner that leads to a different body composition at birth and in childhood.

- **Maternal $25(OH)D_3$ exposure alters placental gene expression. Placental gene expression is associated with body composition at birth and 4 years of age.**

6.3.2 Effects of placental vitamin D on the mother

$1,25(OH)_2D_3$ plays an important role in calcium homeostasis, increasing dietary calcium uptake. During pregnancy calcium uptake must increase in the mother to meet fetal demand without detriment to her own bone health. Fetal calcium requirements increase throughout pregnancy, with fetal calcium deposition peaking at around 350 mg/day in the third trimester (Hacker et al., 2012). Placental production and release of $1,25(OH)_2D_3$ into the maternal circulation observed in this study may contribute to the increased dietary calcium uptake during pregnancy. Increased calcium uptake in turn may support the heath of the mother by maintaining sufficient plasma calcium levels, minimising bone resorption and reducing her later life risk of

osteoporosis. It may also ensure sufficient calcium is available for transfer to the fetus, supporting healthy bone development in the offspring.

Vitamin D metabolites released from the placenta into the maternal circulation may also play a role in maintaining maternal glucose homeostasis. $1,25(OH)_2D_3$ reportedly acts on pancreatic β-cells to regulate insulin secretion, and insufficient maternal $25(OH)D_3$ is considered a risk factor for insulin resistance (Kaushal and Magon, 2013). $1,25(OH)_2D_3$ released from the placenta into the maternal circulation may therefore play a role in ensuring maternal glucose levels are maintained in an appropriate range, which will also support healthy fetal growth via placental glucose transfer to the fetus. Insufficient placental hydroxylation of $25(OH)D_3$ to $1,25(OH)_2D_3$ and release to the maternal circulation may be one mechanism that underlies the observed links between insufficient maternal $25(OH)D_3$ concentrations and GDM (Zhang et al., 2018, Ede et al., 2019).

- **Placental derived $1,25(OH)_2D_3$ in the maternal circulation may increase intestinal calcium uptake and support glucose homeostasis necessary for maternal and fetal health.**

6.3.3 Summary

Transfer of vitamin D from the placenta to the maternal and fetal circulations, in addition to the actions of vitamin D on the placental tissue, may alter maternal and fetal outcomes. Placental gene expression of vitamin D responsive genes is associated with bone outcomes at birth and 4 years of age, demonstrating lasting effects of maternal vitamin D on offspring outcomes. Placental derived $1,25(OH)_2D_3$ in the maternal circulation supports the increased dietary calcium uptake required during pregnancy, supporting the health of both the mother and the fetus.

6.4 Effects of vitamin D on the human placenta

6.4.1 Vitamin D induced changes to placental gene and protein expression

The expression pattern of genes and proteins in the placenta determines its functional capabilities, and therefore influences the transfer of nutrients necessary for healthy fetal growth. Treatment of villous fragments with $25(OH)D_3$ for 8 h resulted in changes to both RNA and protein expression, in pathways of transcriptional regulation, histone modifications, immune functions, amino acid metabolism and inorganic ion transport. Changes to gene and protein expression in these pathways could alter placental function, and subsequent fetal development. Select genes of interest identified in the array based measures were also altered in cultured syncytiotrophoblast cells, suggesting them vitamin D is acting in the main maternal-fetal barrier to alter placental function.

Regulation of transcription allows for sets of genes to be expressed or silenced in response to environmental stimuli. Alterations to numerous pathways of transcriptional regulation at both the RNA and protein expression level suggest that $25(OH)D_3$ is acting to regulate the expression of placenta functions. These may in turn alter fetal growth and development. One method of transcriptional regulation is the modification of histone proteins, altering how they interact with DNA and thus allowing or inhibiting access of transcription factors to the DNA. Decreased *HIVEP2* expression in syncytiotrophoblast with 24 h of $25(OH)D_3$ treatment demonstrates that some of the transcriptional regulator changes are occurring in the barrier separating the maternal and fetal circulations. Altered RNA and protein expression of factors that can alter epigenetic regulation of gene expression, such as histone modifying proteins, may be a mechanism by which vitamin D alters the placental epigenome.

$25(OH)D_3$ and $1,25(OH)_2D_3$ have previously been observed to alter amino acid transporter gene expression within the human placenta (Cleal et al., 2015, Chen et al., 2016). Amino acids are the building blocks of new proteins, and are required by the developing fetus. In this study I observed alterations to the expression of proteins involved in amino acid metabolism, which could alter the composition of the pool of amino acids available for transfer to the fetus. Inorganic ions are also required by the growing fetus, and the expression of genes involved in their transfer across the placenta was also altered in this study. Altered amino acid metabolism and inorganic ion transport could both alter the transfer of nutrients required for growth by the fetus across the placenta. These changes may contribute to the association between maternal $25(OH)D_3$ levels and fetal growth observed.

- **25(OH)D_3 alters RNA and protein expression in the human placenta. Altered RNA and proteins map to pathways that could underlie the associations observed between maternal 25(OH)D_3 levels and fetal growth. Some vitamin D induced changes in gene expression occur in the syncytiotrophoblast cells.**

6.4.2 Vitamin D alters placental epigenetics

Epigenetic factors such as DNA methylation are important determinants of placental function, and are able to influence fetal growth and development. For example, maternal tobacco smoking decreases placental DNA methylation in the *CYP1A1* gene, increasing its expression, allowing it to detoxify harmful compounds and protect the fetus (Suter et al., 2010). I have identified vitamin D induced changes to placental DNA methylation in this study, which to my knowledge is the first time this has been observed. An 8 h 25(OH)D_3 treatment in villous fragments resulted in altered DNA methylation in gene pathways of CRH receptor binding, retinoid acid receptor activity, histone pre-mRNA processing and voltage gated calcium channel activity, potentially affecting placental function. Changes to RXRα DNA methylation in 25(OH)D_3 treated villous fragments were identified when measured by a 850K methylation array, but the CpG sites measured by pyrosequencing were not altered. No changes to placental RXRα DNA methylation were identified with short term 25(OH)D_3 treatment of syncytiotrophoblast, or with long term cholecalciferol treatment in the SPRING study. However, maternal 34 week serum 25(OH)D_3 levels in the MAVIDOS study were associated with placental RXRα DNA methylation. Collectively this suggests that it is actual 25(OH)D_3 concentration, as opposed to cholecalciferol treatment, that alters RXRα DNA methylation in the placenta. Decreased RXRα DNA methylation in MAVIDOS placentas was associated with increased expression of the genes *VDR, CYP27B1* and *CYP24A1*, suggesting epigenetically mediated alterations to vitamin D related gene expression. Altered RXRα expression or activity in response to altered DNA methylation may in turn affect the expression or activity of other genes containing VDREs.

The placental DNA methylation changes with 25(OH)D_3 observed in this study could contribute to the association between maternal serum 25(OH)D_3 levels and fetal growth. Altered DNA methylation in the pathway of CRH receptor binding with 25(OH)D_3 treatment may alter the placentas ability to transport glucose. Indeed, CRH treatment has been observed to increase GLUT1 expression in syncytiotrophoblast cells, increasing the ability of the cells to transport glucose (Gao et al., 2012). As glucose is an important nutrient for fetal growth, altered CRH receptor binding activity could underlie the association between poor maternal 25(OH)D_3 levels

and fetal growth. Changes to DNA methylation in genes of the voltage gated calcium channel proteins may also contribute to the association between maternal $25(OH)D_3$ levels and fetal growth. Voltage gated calcium channel expression alters the placentas ability to undergo vasoconstriction (Jakoubek et al., 2006), with constriction of placental vessels inhibiting nutrient transfer, a process which can inhibit fetal growth.

Changes in the DNA methylation of members of the retinoid acid receptor pathway could alter the activity of RXRα, potentially altering the ability of $1,25(OH)_2D_3$ to interact with DNA and effect transcription. Altered DNA methylation in genes involved in the processing of histone protein pre-mRNA could alter histone protein activity, changing chromatin structure and altering gene expression. Changes to retinoid acid receptor and histone pre-mRNA processing DNA methylation may therefore be a mechanism by which vitamin D regulates its activity within the placenta. In addition to DNA methylation changes in genes involved in histone protein processing and histone protein modification, these genes also contained both altered RNA and protein expression. The histone marks investigated in this study were not altered with 8h $25(OH)D_3$ treatment or long term cholecalciferol treatment. However, these were measured at the global level, and it is more likely that any changes would have occurred locally, acting to alter histone activity at specific regions of the DNA.

Metabolism of $25(OH)D_3$ to $1,25(OH)_2D_3$ may allow for vitamin D to alter placental DNA methylation, as shown in Figure 6-4. $1,25(OH)_2D_3$ activated VDR-RXRα interacts with VDREs in the promoter of vitamin D responsive genes. It then recruits interacting proteins, with enhance or repress transcription of that gene. $1,25(OH)_2D_3$ activated VDR-RXRα may recruit DNMTs or TET proteins to the DNA, where they act to alter DNA methylation.

- **$25(OH)D_3$ can alter placental DNA methylation. Altered DNA methylation maps to pathways the could underlie the associations observed between maternal $25(OH)D_3$ levels and fetal growth.**

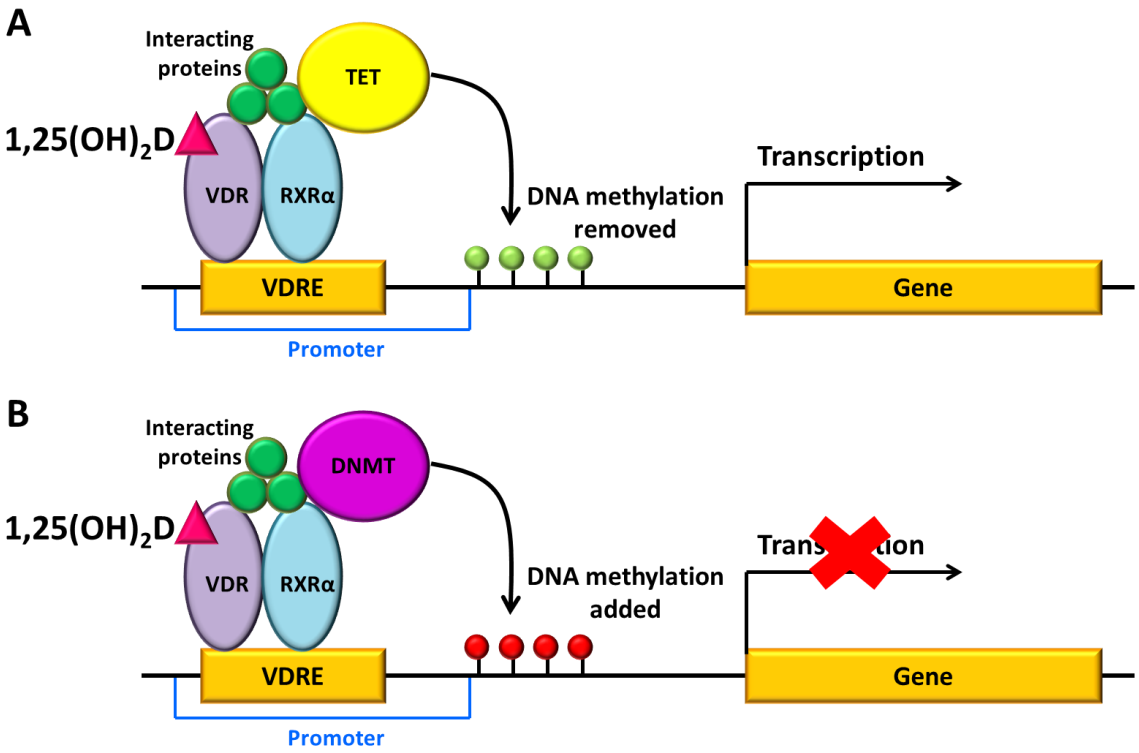

Figure 6-4 ***Vitamin D mediated changes in DNA methylation.*** *$25(OH)D_3$ undergoes hydroxylation to $1,25(OH)_2D_3$ within the placenta. $1,25(OH)_2D_3$ interacts with the VDR, allowing it to form a complex with RXRα and interact with vitamin D receptor elements (VDREs), where it recruits proteins that enhance or repress transcription of the downstream gene.* ***A)*** *TET may be recruited to the DNA, where it acts to remove DNA methylation marks.* ***B)*** *DNA methyl transferases (DNMTs) may be recruited to the DNA, where they act to introduce new methylation marks on to the DNA.*

6.4.3 Short term versus long term effects of vitamin D on the placenta

Changes to DNA methylation at 13 CpG sites associated with RXRα in response to short term 8 h $25(OH)D_3$ treatment in villous fragments and long term cholecalciferol treatment in MAVIDOS and SPRING were investigated using pyrosequencing. The only change to RXRα DNA methylation was an increase in DNA methylation at CpG6 in MAVIDOS with 1000 IU cholecalciferol treatment. Altered DNA methylation at CpG6 was not observed in SPRING, despite participants receiving the same 1000 IU cholecalciferol treatment. This data suggests that short term $25(OH)D_3$ treatment does not alter RXRα DNA methylation, but the data on long term cholecalciferol treatment is less conclusive. Placental RXRα DNA methylation in MAVIDOS is not consistent with that seen in the MAVIDOS umbilical cords, although both tissues are of fetal origin (Curtis et al., 2019). The placenta is exposed to maternal vitamin D, whereas the umbilical cord is only exposed to vitamin D that reaches the fetal circulation. Therefore, the changes in the placenta likely reflect maternal $25(OH)D_3$ status, compared to fetal $25(OH)D_3$ status in the umbilical cords.

The amount of the histone methylation mark H3K27me3 was measured in both short term 8 h 25(OH)D_3 treatment in villous fragments and long term cholecalciferol treated SPRING study samples. There was no change in the amount of H3K27me3 between treatment groups in either the 8 h 25(OH)D_3 treated villous fragments or long term cholecalciferol treated SPRING placental samples, suggesting that neither 25(OH)D_3 or cholecalciferol alter the expression of H3K27me3 in the placenta.

As few changes were observed with 25(OH)D_3 or cholecalciferol treatment in these studies it is difficult to conclude whether there are differences between short and long term vitamin D treatment in the placenta. Future studies could look to address this by investigating the differences between gene expression, which have been observed to be altered by both short and long term treatment.

- **No difference in the effect of short term 25(OH)D_3 compared to long term cholecalciferol treatment on the placenta were observed in this study.**

6.4.4 Summary

25(OH)D_3 has been observed to act upon the placental tissue, altering DNA methylation, RNA and protein expression in pathways that may alter placental function. 25(OH)D_3 alters RXRα DNA methylation, which may in turn alter gene expression associated with altered body composition at birth and in childhood. 25(OH)D_3 also alters DNA methylation, RNA and protein expression of factors involved in histone protein activity, a potential mechanism by which 25(OH)D_3 may alter placental function. Altered RNA and protein expression of pathways of transcriptional regulation, amino acid metabolism and inorganic ion transport in response to 25(OH)D_3 treatment may underlie associations between maternal 25(OH)D_3 and fetal growth. Unfortunately in this study the data collected was not sufficient to determine if short term 25(OH)D_3 treatment results in the same or different changes to placental DNA methylation as long term cholecalciferol treatment.

6.5 Vitamin D and pregnancy overall

The data presented in this thesis contributes to the overall field investigating the role of vitamin D in pregnancy. Here I will discuss how my data relates to some of the questions and challenges within the field.

6.5.1 Future directions of vitamin D pregnancy research

An important question in vitamin D pregnancy research is what are the mechanisms underlying how vitamin D acts upon the placenta? Data presented in this thesis has demonstrated both direct and indirect effects of vitamin D on placental tissue, through changes to DNA methylation and gene expression in response to vitamin D treatment. While we have a reasonably clear understanding of how $1,25(OH)_2D_3$ activated VDR-RXRα complexes interact with VDREs in the promotors of genes to alter gene expression, the mechanisms by which vitamin D alters placental DNA methylation for example are less clear. Pathway analysis of the array data also suggested further indirect effects of vitamin D on the placenta, by changes to the expression of histone protein modifiers. The extent to which indirect compared to direct effects of vitamin D on the placenta act to alter placental function is not understood.

Another important question in vitamin D pregnancy research is how the results we see with short term *ex vivo* $25(OH)D_3$ or $1,25(OH)_2D_3$ treatment of placental tissue in the laboratory relate to the physiological outcomes for pregnant women, with or without cholecalciferol supplementation. A small amount of data presented in this thesis suggests that DNA methylation may be altered differently in $25(OH)D_3$ treated tissue compared to long term cholecalciferol treatment, but this needs to be investigated further. Targets identified in short term *ex vivo* treatment studies could be investigated in samples from supplementation cohort studies or cohort studies with maternal vitamin D levels measured to further the clinical relevance of this research.

6.5.2 Stage of gestation and vitamin D

All placental samples used in this study were taken from term deliveries. However, both the anatomy and the functional capabilities of the placenta change throughout gestation to meet the changing demands of the fetus. It is therefore likely that vitamin D may act differently on the placenta depending on the stage of gestation, and gene expression data presented in this thesis supports this. In this study we observed different gene expression in cytotrophoblast, syncytiotrophoblast, and villous fragment samples. Earlier in gestation there is a greater amount

of cytotrophoblast cells compared to syncytiotrophoblast, but as gestation progresses the number of cytotrophoblast cells decreases while the amount of syncytiotrophoblast increases, altering the composition of the placenta (Huppertz, 2008). If vitamin D affects different placental cells in a different manner as our data suggests, then it is likely to elicit a different response earlier in gestation compared to later. Investigating samples at a range of gestations from women with known vitamin D levels could allow us to investigate this.

6.5.3 Should pregnant women supplement with vitamin D?

Most studies report high levels of vitamin D deficiency and insufficiency during pregnancy. For example in the MAVIDOS study 6% of screened participants had deficient 25(OH)D levels (<25 nmol/l; subsequently excluded from study), and 61% of eligible participants had insufficient 25(OH)D levels (<50 nmol/l) (Cooper et al., 2016). Cholecalciferol supplementation has been demonstrated as a suitable way to raise 25(OH)D levels in pregnant women, and as such the National Institute for health and Care Excellence (NICE) recommends daily supplementation with 400 IU cholecalciferol. Supplementation with higher levels of cholecalciferol have been suggested to have beneficial effects, and much higher levels have been safely given to pregnant women (Karamali et al., 2015). However there are risks associated with taking too high a dose of vitamin D, particularly when that dose is taken frequently over an extended period of time. Too much vitamin D supplementation can lead to hypervitaminosis D and hypercalcaemia, which may lead to irreversible deposition of calcium in soft tissues (Shea and Berg, 2017).

Whilst it is possible to obtain sufficient levels of vitamin D through diet and sunlight exposure alone, this is increasingly difficult for many people due to poor dietary intake and lifestyles that involve little sunlight exposure. Supplementation is a useful tool to combat poor vitamin D levels, but factors such as dietary intake, sunlight exposure and amount of cholecalciferol should be considered before beginning supplementation.

6.5.4 Challenges in studying vitamin D

A number of factors provide challenges when studying the role of vitamin D in pregnancy and the placenta. For example an individual's current 25(OH)D_3 levels, BMI, calcium intake, calcium concentration and ethnicity are all documented to affect their response to vitamin D treatment (Mazahery and von Hurst, 2015), but often not enough information is known about study participants to control for these. Variation in the DNA methylation of *CYP24A1* also affects its ability to respond to vitamin D treatment, but again the DNA methylation in placental samples is rarely investigated (Novakovic et al., 2009). A lack of information on these confounding factors can make it difficult to discern true effects of vitamin D on placental tissue.

In this thesis data was presented demonstrating that the placenta metabolises vitamin D. While 1,25$(OH)_2D_3$ is the primary active form of vitamin D, action of other vitamin D metabolites has also been observed (Lou et al., 2010, Molnar et al., 2011). When investigating the effects of vitamin D within the placenta, it can be difficult to distinguish which metabolite is causing an effect, as the metabolite you are treating with may be metabolised into another, and endogenous metabolites may be present. This is another factor which makes understanding the mechanisms of vitamin D action difficult.

Vitamin D has indirect effects on the placenta, and it is important to consider these when investigating vitamin D in pregnancy. For example a number of studies have associated maternal vitamin D with fetal bone development (Javaid et al., 2006, Mahon et al., 2010, Cooper et al., 2016), but whether changes observed are a direct result of higher vitamin D levels, or due to a subsequent increase in calcium uptake is less well investigated. It is therefore important to consider the mechanisms underlying observed changes with vitamin D treatment.

6.6 Limitations

We know maternal factors such as BMI and ethnicity effect an individual's response to $25(OH)D_3$ (Mazahery and von Hurst, 2015), therefore increasing the sample size of some experiments in this thesis, or obtaining more detailed patient history, could allow me to more fully understand the actions of $25(OH)D_3$ on the placenta.

Perfusion of the placenta with ^{13}C-$25(OH)D_3$ allowed me to directly observe its metabolism by identifying the production of ^{13}C-labelled metabolites in the perfusate. However due to limitations of the LCMS technique used to measure these it has not been possible to measure ^{13}C-$1,25(OH)_2D_3$ in the perfusate samples, meaning I am not able to directly confirm metabolism of $25(OH)D_3$ to $1,25(OH)_2D_3$ within the placenta.

Unfortunately in our proteomics data no vitamin D pathway proteins were identified, again due to limitations of the LCMS technique used which requires sufficient unique fragments of proteins to be measured for identification. Therefore I was unable to investigate differences in the expression of proteins of the vitamin D pathway in response to 8 h $25(OH)D_3$ treatment in villous fragment samples.

Array based analysis carried out in Chapter 4 gives us DNA methylation, RNA and protein expression based upon whole villous tissue, which contains multiple cell types. This data may therefore over represent more abundant cell types and diminish changes seen in less abundant cell types. It is also not possible to determine what cell types any changes are occurring in. Gene expression in primary cultured cytotrophoblast cells was investigated, but numerous other cells types are present in the placenta. Therefore I have not determined what cells in the placenta are affected by the changes observed.

The SPRING study is presently still recruiting participants, and thus the grouping of participants is still blinded, and limited outcome data is available. Both MAVIDOS and SPRING participants were given the same placebo or 1000 IU cholecalciferol treatment from 14 weeks gestation, and therefore it may be possible to combine the datasets, giving us a greater sample size to analyse. Combining MAVIDOS and SPRING datasets may be particularly useful when investigating offspring outcomes, due to the reduced number of participants that have both placental and body composition measures.

The RXRα CpG sites measured in the 850K Illumina EPIC array do not match the RXRα CpG sites that were able to be measured by pyrosequencing. It was therefore not possible to compare whether the RXRα CpG sites with altered DNA methylation in villous fragments measured using

the Illumina EPIC array were also altered in cultured syncytiotrophoblast cells or in MAVIDOS or SPRING placental samples. As such I have been unable to determine the cell type in which the RXRα DNA methylation changes occur, or if there are difference between 8 h 25(OH)D_3 treatment and long term cholecalciferol treatment.

6.7 Future directions

To continue analysis of the ^{13}C-25(OH)D_3 placental perfusions measurement of ^{13}C-1,25$(OH)_2D_3$ is being pursued, but results were not available in time to be included in this thesis. Perfusate samples will be analysed in the laboratory of Professor Martin Hewison, whom has previously demonstrated the ability to measure 1,25$(OH)_2D_3$ using LCMS (Hassan-Smith et al., 2017). Vitamin D metabolites in the perfused placental tissue will also be measured by LCMS by Professor Hewison. A further line of investigation in the perfusate from the ^{13}C-25(OH)D_3 perfused placental experiments would be to use metabolomics on the perfusate to identify novel effects of vitamin D on the placental metabolome. Gene expression data in this thesis and previous studies (Cleal et al., 2015, Chen et al., 2016) suggest that vitamin D metabolites act to alter placental amino acid metabolism and transport. Measurement of the amino acids present in the perfusate at time points throughout the experiment by LCMS could identify amino acids whose transfer is increased in the presence of 25(OH)D_3, and may be important for fetal growth.

The effects of 25(OH)D_3 on the placenta may be mediated by proteins of the vitamin D pathway, such as DBP which is associated with the expression of amino acid transporters (Cleal et al., 2015). Therefore, measurement of the expression of vitamin D pathway protein in villous fragments would allow us to better understand if 25(OH)D_3 alters the expression of these proteins, which may be important for the actions of 25(OH)D_3 on the placental tissue. This could be carried out by western blotting to identify specific proteins.

To investigate whether short term 25(OH)D_3 treatment effects the placenta differently to long term cholecalciferol treatment DNA methylation and gene expression in the MAVIDOS and SPRING samples could be investigated and compared to that seen in our villous fragment samples. The 850K Illumina EPIC array and RNA sequencing could be used on the cohort study samples to ensure that the data is comparable to the villous fragment data. In the literature short term 25(OH)D_3 treatment is primarily used to investigate the effect of vitamin D on the placenta, whereas cholecalciferol supplementation is primarily used by pregnant women. Understanding if 25(OH)D_3 and cholecalciferol elicit similar effects on the placenta will allow us to better determine if the effects of 25(OH)D_3 treatment seen on the placenta in the laboratory is comparable to supplementing a pregnant woman.

In this study I observed 1,25$(OH)_2D_3$ transfer from the placenta to the maternal circulation, suggesting the placenta plays a role in the pregnancy induced rising maternal 1,25$(OH)_2D_3$ levels. As expression of *CYP24A1* is highly altered by the presence of 1,25$(OH)_2D_3$ in the placenta, it would be interesting to investigate whether placental *CYP24A1* expression was associated with

$1,25(OH)_2D_3$ levels in the mother during late pregnancy. This could be carried out by measuring $1,25(OH)_2D_3$ in the 34 week blood samples taken from MAVIDOS participants, and comparing to the *CYP24A1* gene expression measure made by Dr Claire Simner (Simner, 2015).

ChIP-seq could be a useful technique by which the mechanism that $1,25(OH)_2D_3$ alters gene expression could be investigated. Treating cultured primary cytotrophoblast cells with $25(OH)D_3$ or $1,25(OH)_2D_3$ followed by ChIP-seq targeting the VDR or histone proteins of interest will allow for the identification of where $1,25(OH)_2D_3$ is interacting with DNA in the placenta. This will allow me to identify if $1,25(OH)_2D_3$ activated VDR interacts with DNA in regions that do not contain a VDRE, and if $1,25(OH)_2D_3$ interacts with histone proteins potentially altering gene expression in an epigenetic manner.

Plans are in place to follow up children born to the SPRING study in a manner similar to those born to the MAVIDOS study. This will allow me to continue to investigate the role of vitamin D induced changes in placental DNA methylation in gene expression on offspring body composition at birth and throughout childhood.

6.8 Implications

This study has demonstrated that the metabolites $25(OH)D_3$, $1,25(OH)_2D_3$ and $24,25(OH)_2D_3$ are transferred from the placenta to both the mother and the fetus. The placenta may regulate the transfer and activity of $25(OH)D_3$ via metabolism, with potential downstream effects on both maternal and fetal health. Placental transfer of vitamin D to the fetus has long been considered to be important for fetal health. Here I have shown that the primary active metabolite of vitamin D, $1,25(OH)_2D_3$, in addition to the primary circulating form of, $25(OH)D_3$ are both transferred to fetal circulation, and are thus available for use by the fetus. This may allow the fetus to regulate the effects of vitamin D by metabolism of $25(OH)D_3$, and also indicates that non-genomic actions of $25(OH)D_3$ on the fetus are possible. Unexpectedly I also observed $1,25(OH)_2D_3$ transfer from the placenta to the mother, indicating the placenta plays a role in contributing to the increased $1,25(OH)_2D_3$ levels in maternal circulation during pregnancy. Raised maternal $1,25(OH)_2D_3$ concentration is important to ensuring the mother can absorb sufficient dietary calcium in the intestine to meet fetal demand, without sourcing the calcium from her skeletal system. Therefore the placenta may also be acting to support maternal health.

$25(OH)D_3$ altered placental DNA methylation, RNA and protein expression in pathways that may underlie the observed associations between maternal $25(OH)D_3$ and fetal growth and bone health (Javaid et al., 2006, Harvey et al., 2014a). Altered amino acid metabolism and transfer in the presence of sufficient maternal $25(OH)D_3$ may optimise amino acid transfer to the fetus, supporting fetal growth. Increased calcium transfer to the fetus as a result of both increased maternal uptake and altered placental transfer will support fetal growth and bone development. The DOHaD hypothesis states that *in utero* physiological changes a fetus undergoes can have later life impacts on the health of the offspring. The data presented here suggests that increased maternal $25(OH)D_3$ concentrations may increase calcium transfer to the fetus, promoting healthy bone development *in utero* and at birth. This in turn may allow the offspring to develop a higher peak bone mass and reduce the risk of osteoporosis in later life, as shown in Figure 6-5. Babies born smaller are also at an increased risk of a number of other later life health complications such as cardiovascular diseases, and therefore vitamin D mediated effects on fetal growth may also mitigate the risks associated with these.

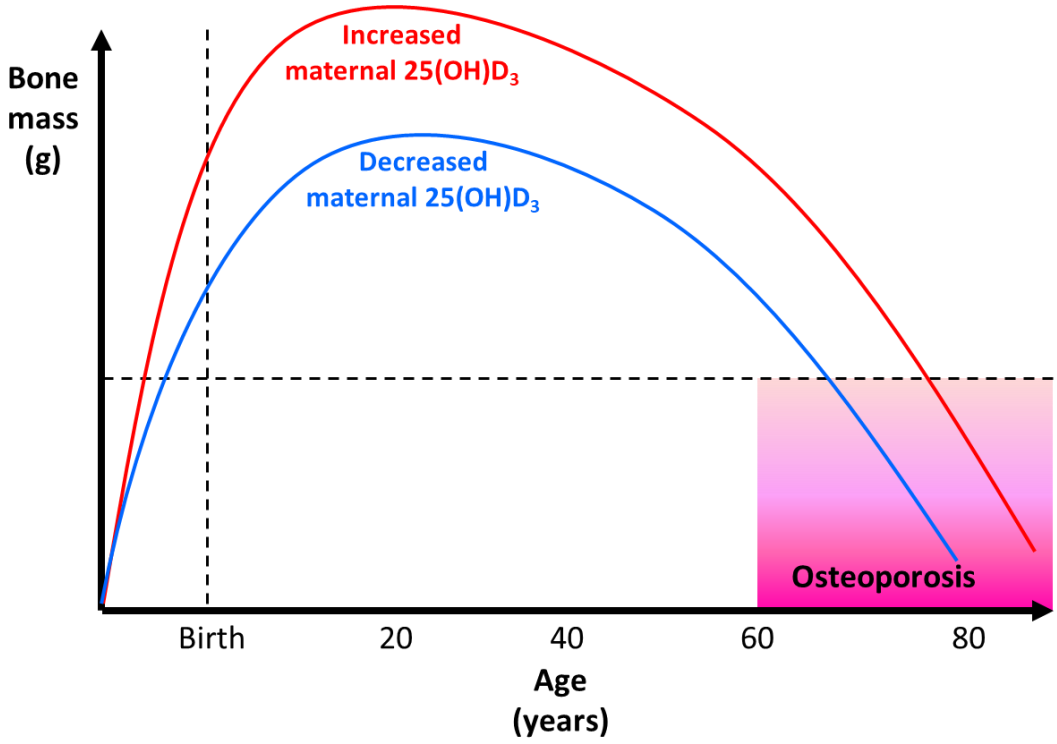

Figure 6-5 ***Relationship between vitamin D, bone mass and osteoporosis****. Placental exposure to maternal 25(OH)D_3 may impact upon bone development. Increased placental exposure and response to 25(OH)D_3 may increase fetal bone mass, setting the offspring on a path to achieving a higher peak bone mass and reducing the risk of developing osteoporosis in later life.*

Results of this study demonstrate that 25(OH)D_3 acts to alter placental DNA methylation, a mechanism by which it may act to alter placental function. DNA methylation can be altered by factors such as diet, body composition and ethnicity, all factors which also alter an individual's response to vitamin D. An interaction between the effects of 25(OH)D_3 and these factors on DNA methylation may explain why observed effects of 25(OH)D_3 on pregnancy outcomes are not always consistent (Harvey et al., 2014a). DNA methylation is however modifiable, and therefore a personalised approach to supplementation may allow for improved pregnancy outcomes.

Associations between *CYP24A1* placental gene expression and body composition at birth and 4 years of age in the MAVIDOS study suggest that placental gene expression could be used to identify children with poorer bone health. Identifying children at risk of later life poor bone health may allow for early intervention to improve outcomes. The placenta, as a waste product after birth, could be investigated for use as a cost effective, non-invasive predictor of bone health in later life.

6.9 Summary

In summary the aims of this thesis were addressed by investigating placental vitamin D metabolism in an *ex vivo* isolated perfused placental cotyledon model, determining that 25(OH)D_3 is metabolised and its metabolites are transferred to the maternal and fetal circulations. Changes to placental villous fragment DNA methylation, RNA and protein expression were identified after 8 h exposure to 25(OH)D_3, and these changes relate to pathways which may alter placental function and subsequent fetal growth. Genes of interest from villous fragment studies were investigated in primary cytotrophoblast cells, identifying changes that may occur in the syncytiotrophoblast layer. DNA methylation data was collected for both the MAVIDOS and SPRING studies, and related to placental gene expression and offspring outcomes in MAVIDOS, with SPRING data to follow with completion of the first stage of the study. The data presented in this thesis is summarised in Figure 6-6.

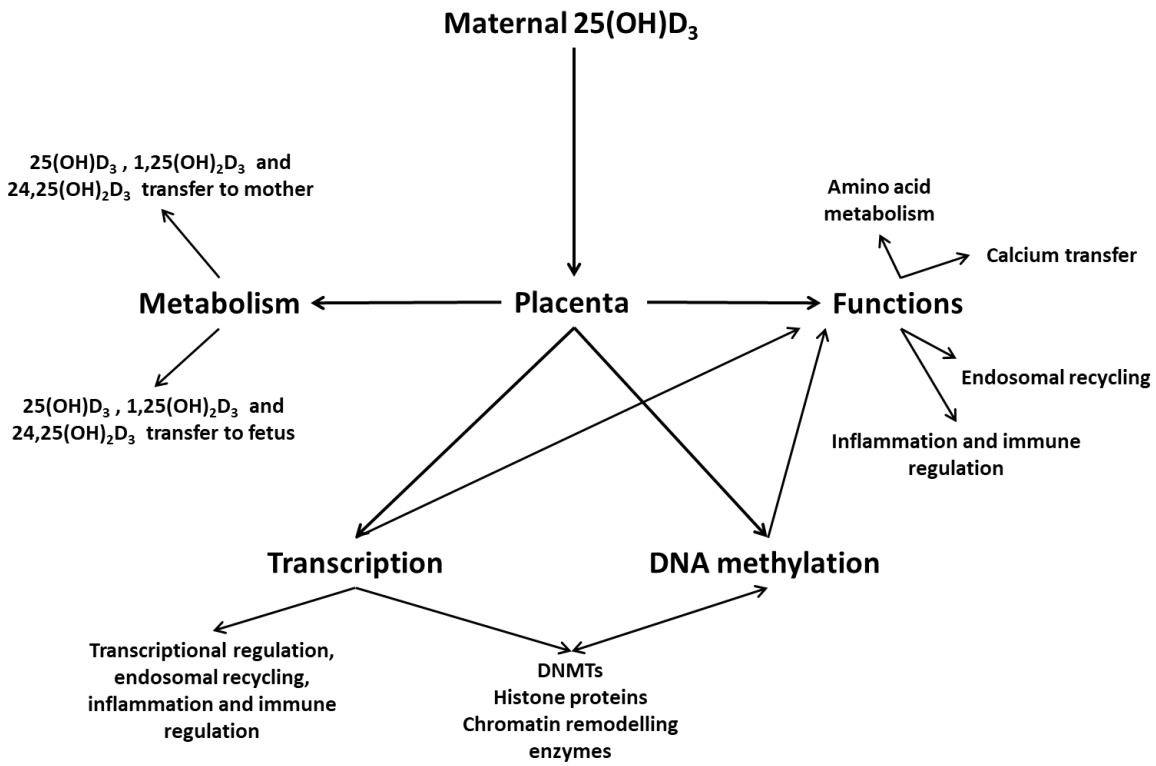

Figure 6-6 ***A summary of the effects of maternal 25(OH)D_3 on the placenta.*** *25(OH)D_3 is metabolised within the placenta, and alters transcription, DNA methylation and placental function in a manner which may impact upon fetal growth and development.*

Appendix A Full pathways of altered DNA methylation, RNA expression and protein expression

Below are tables containing the full datasets of genes for pathways of altered DNA methylation, RNA expression and protein expression, as described in Chapter 4.

A.1 DNA methylation

Table 6-1 *Pathways of altered DNA methylation.*

Pathway	Altered Genes	P value
Receptor tyrosine kinase binding	ACKR6,ANGPT1,ANGPT2,ANGPT4,ARHGEF16,DOCK4,DOK2,ELMO2,FRS2,GAB2,GAS6,GNB2L1,NRG1,NRG3,PIK3R1,PIK3R2,PTPN1,PTPN11,PTPN2,SH2B2,SHC4,SOCS5	**<0.001**
Corticotropin-releasing hormone receptor binding	CRH,GNAO1,UCN,UCN2,UCN3	**<0.001**
Corticotropin-releasing hormone receptor 2 binding	CRH,UCN,UCN2,UCN3	**<0.001**
Androgen receptor binding	CALR,CCNE1,CDK7,CTNNB1,DAXX,EP300,FHL2,FOXH1,GRIP1,KDM1A,KDM3A,KDM4C,NRIP1,PIAS1,PPARGC1A,PRKCB,PRPF6,RAN,RNF4,RNF6,TCF21,TGFB1I1,TRIM68,WIPI1	**0.0012**
Retinoic acid receptor activity	PRAM1,RARA,RARB,RARG,RXRA,RXRB,RXRG	**0.0014**
Histone pre-mRNA stem-loop binding	ERI1,SLBP	**0.0018**
Filamin binding	FAM101B,FBLIM1,MICALL2,NEBL,PDLIM2,TMEM67	**0.0024**
NAD(P)H oxidase activity	CYB5R4,DUOX1,DUOX2,NOX4,TXNRD1	**0.0027**
Tyrosine 3-monooxygenase activity	TH	**0.0029**
Peptide transporter activity	ABCB10,CDH17,DISP1,ENSG00000250264,SLC15A1,TAP1,TAP2,TAPBP	**0.0040**
Hydrolase activity, acting on carbon-nitrogen (but not peptide) bonds		**0.0049**
LIM domain binding	ACTN2,LDB2,RIPK2,RPH3AL	**0.0051**
Voltage-gated calcium channel activity	CACNA1A,CACNA1B,CACNA1C,CACNA1E,CACNA1G,CACNA1H,CACNA1I,CACNA1S,CACNA2D1,CACNA2D2,CACNG3,CACNG4,CACNG5,CACNG7,GAS6,GRM7,ITGAV,NCS1,OPRM1,RYR1,TPCN2	**0.0053**

A.2 Increased RNA expression

Table 6-2 *Pathways of increased RNA expression.*

Pathway	Altered Genes	Q value
C2H2-type transcriptional regulation	SP4, ZNF609, ZNF142, HIVEP1, ZBTB16, HIVEP2, ZBTB43, TRPS1, ZBTB41, ZNF699, ZXDA, SALL1, GLI3, ZNF286B, PLAG1, ZNF81, ZFP69B, ZNF844, ZNF823, ZNF652, ZKSCAN2, PRDM4, ZNF850, ZXDB, ZNF503, ZBTB34, ZBTB44, ZNF106, KLF7, RBAK, ZBTB10, ZNF808, ZNF721, ZNF749, ZFP92, ZNF669	**<0.001**
BTB domain containing transcriptional regulation	KLHL24, ZBTB16, KLHL28, BACH2, ZBTB43, KBTBD8, ZBTB41, KLHL11, ZBTB34, ZBTB44, KLHL15, ZBTB10, GAN	**<0.001**
Deubiquitination	OTUD7B, YOD1, OTULIN, OTUD3, VCPIP1	**<0.001**
Transcriptional regulation	SOX4, SOX12, ZBTB16, TRPS1, ASH1L, SERTAD2, ISL1, SIX4, ZXDA, JMY, BPTF, HOXB9, SALL1, GLI3, MED12L, LBH, PLAG1, IRF2BPL, MLLT11, TBX20, TET3, HMBOX1, FOXO3, CAMK4, NSD1, HIPK2, REL, PPARA, REST, TEF, RFX3, CREBBP, CREB5, KMT2D, KLF7, RORA, CTH, PBX3, NFAT5, EP300, PROX1, HIVEP1, HIVEP2, BACH2, ZNF704, DPF2, ARHGAP35, SP4, KIAA1958, ZKSCAN2, BEND3, IRF2BP1, TFCP2L1, RYBP	**<0.001**
Negative regulation of transcription	SOX4, SOX12, SP4, HIVEP1, ZBTB16, IRF2BP1, CDK12, BACH2, TRPS1, ASH1L, ISL1, SIX4, ACVR2B, GDF9, JMY, OTUD7B, BPTF, TFCP2L1, HOXB9, NEO1, SALL1, GLI3, MED12L, KIAA1958, PLAG1, IRF2BPL, TBX20, TET3, FNIP2, FOXO3, ZNF704, NSD1, HIPK2, BEND3, REL, ZKSCAN2, PPARA, REST, XPO1, ARHGAP35, TEF, ATXN1L, RFX3, CREBBP, CREB5, RYBP, KMT2D, KLF7, CBX6, ZBTB10, RORA, PBX3, NFAT5, EP300, CBX8, PROX1, BCL7A, NKRF, OTULIN, AGO3, RBM15B, HMBOX1, ADGRG3, MEX3D, PRDM4, ZNF503, CPEB4, RBAK, SAMD4A, NF2, SOGA1 FBP1, HIVEP2, ZNF699, ZXDA, TULP4, ZNF286B, ZNF81, ZFP69B, CBL, ZNF808, ZNF669, DPF2, KMT2C	**<0.001**
Metal ion binding	ZSWIM3, GALNT3, MYCBP2, CYP24A1, TRPS1, ASH1L, ISL1, RNF43, MEX3C, OTUD7B, TXNRD1, ZCCHC14, BPTF, KMT2C, SCD, TRIM63, ENDOU, MICAL3, MMP9, TRIM36, PDLIM2, MEX3B, MEX3D, AOC2, NSD1, DPF2, PPARA, ADAM32, CBL, PRDM4, CREBBP, MSL2, RYBP, KMT2D, KLF7, RBAK, PRKCG, RORA, LONRF2, RNF24, EP300	**0.0051**
Neuronal development	EPHB3, SOX4, MYCBP2, MARK1, MBP, ISL1, SIX4, WNK1, SOCS7, XYLT1, NEO1, ADRA2B, NRXN3, SALL1, SSH1, NF2, FMN1, GLI3, HS6ST1, NECTIN1, PLAG1, TBX20, POMK, CNR1, CHST3, FOXO3, CCSAP, HIPK2, NLGN1, REST, ARHGAP35, OPHN1, NKD1, CELSR3, CELSR2, KLF7, SIPA1L1, PAK3, BLOC1S3, RORA, LTA, MARK2, PBX3, EP300, PROX1	**0.0075**
Histone methylation	ASH1L, BPTF, KMT2C, NSD1, DPF2, KMT2D	**0.0146**
Endosomal recycling	SYDE2, PCLO, RAB11FIP1, RAB11FIP5	**0.0146**
Beta-catenin binding	SALL1, NF2, GLI3, MED12L, FOXO3, RORA, EP300	**0.0147**

A.3 Decreased RNA expression

Table 6-3 *Pathways of decreased RNA expression.*

Pathway	Altered Genes	Q value
Inflammation and immune regulation	IL24, CXCL10, PDGFB, GBP2, C5AR2, SERPINB7, OLFM4, ACOD1, S100A8, ITGB3, FCGR3A, IL1R2, IL32, CYP1A1, C8orf4, LCN2, CD177, GPR4, FOLR2, PPBP, S100A12, IL36RN, CCL4L2, FCGR3B, IL1RL1, CCL2, C3AR1, C1QA, PSG3, IGSF6, SCAMP5, IL2RG, LTF, C4BPB, CCL4, CSF2, RNASE7, GGTA1P, PTX3, SERPINB2, IL3RA, LY86, ALOX5AP, UCP2, TNFRSF11B, F2RL3, CXCL11, FCMR, TNFAIP6, TSPAN2, FOSL1, TFPI2, PMCH, CD163L1, SPRR3, F2RL2, IGFBP4, XAF1, MX2, TSLP, HBG1, MMP3, LILRA5	**<0.001**
Response to stimuli	IL24, PDGFB, CYP1A1, CXCL10, PRSS23, S100A12, FOSL1, ACOD1, SERPINB7, IL32, S100A16, TNFRSF11B, C5AR2, ITGB3, RNASE7, C1QA, PTX3, CH25H, IL36RN, MCHR1, PPBP, LCN2, STC1, ACTC1, FOLR2, CCL2, LTF, GJB2, GBP2, IL1R2, MMP3, S100A8, CCL4, WNT9A, SERPINB2, FCGR3B, HAS1, TNFAIP6, MMP10, HBG1, MED24, CD163L1, TNNT2, CXCL11, MMP19, OLFM4, C8orf4, UCP2, ALOX5AP, DNER, CITED4, MX2, CYTL1, ESM1, C3AR1, CSF2, IL1RL1, FCGR3A, LY86, C4BPB, DKK1, IGFBP4, TSLP, NNAT, PMCH	**<0.001**
Cell motility	IL24, PDGFB, FOLR2, C5AR2, CXCL10, CD177, ABI3, DNER, PPBP, ITGB3, CCL2, OLFM4, S100A8, GGTA1P, CCL4, DKK1, STC1, S100A12, FCGR3B, CXCL11, PSG2, FCGR3A, PTX3, C3AR1, LY6K, SCAMP5, HAS1, MMP19, FOSL1, NDRG4, MMP3, CD163L1, TNFAIP6, C4BPB, ACTC1, MMP10, TNNT2	**<0.001**
Renal vasculature development	SERPINB7, GPR4, CXCL10, PDGFB, ESM1, ITGB3, WNT9A, SH2D2A, C3AR1, CCL2, ACTC1, CYTL1, STC1, FOSL1, MMP19, DKK1, TNNT2, NDRG4	**<0.001**
Reproductive processes	REC8, VMP1, CYP1A1, PDGFB, PSG2, PSG3, PSG4, STC1, FOSL1, ACOD1, PI3, GJB2, CSF2, UCP2, CCL2, LY6K, HAS1, FST, MMP19, PMCH, IGSF6, SIRPB2, MPZL2	**<0.001**
Inorganic ion transport	MCHR1, PDGFB, C8orf4, F2RL3, STEAP4, OLFM4, CXCL10, LCN2, ACOD1, ITGB3, C5AR2, S100A8, CSF2, STC1, TNFRSF11B, F2RL2, CXCL11, LTF, IL36RN, C3AR1, CCL2, UCP2, DKK1, IGFBP4, CCL4, PMCH, IL1R2, SCAMP5, PTX3, IL1RL1, SERPINB2, MMP3, FST, NNAT, NDRG4, C4BPB, FCMR, TNNT2, MX2, TNFAIP6	**<0.001**
Cell Signalling	IL24, PDGFB, GPR4, CXCL10, SERPINB7, C5AR2, F2RL3, GBP2, ESM1, FOLR2, WNT9A, IL1R2, SH2D2A, PPBP, MAP3K7CL, TFPI2, ITGB3, CCL2, C3AR1, C8orf4, TNFRSF11B, IL36RN, DKK1, MMP3, C4BPB, CSF2, OLFM4, STC1, IGFBP4, UCP2, CCL4, MMP10, FCMR, F2RL2, ACOD1, S100A12, S100A8, CXCL11, MMP19, MED24, PI3, IL2RG, PMCH, PLEKHG2, IL3RA, XAF1, FCGR3A, FOSL1, SERPINB2, IL1RL1, FCGR3B, NDRG4, LTF, LY86, MPZL2, MX2, EMP3, NNAT	**<0.001**
Regulation of enzymatic activity	IL24, SERPINB7, PDGFB, TFPI2, WNT9A, PLEKHG2, S100A8, PI3, CSF2, PTX3, SERPINB2, CCL2, CCL4, LTF, TNNT2, IL2RG, IL3RA, FCMR, IL1R2, C4BPB	**0.0039**
Coagulation	PDGFB, CD177, F2RL3, TFPI2, F2RL2, ITGB3, SERPINB2, C4BPB, HBG1	**0.0056**
Regulation of ERK1 and ERK2	PDGFB, C5AR2, ITGB3, CCL2, CCL4, NDRG4	**0.0126**

cascade		
Regulation of endocytic processes	OLFM4, DKK1, SCAMP5, PTX3, CCL2, C4BPB	**0.0194**
Secretion	VMP1, PDGFB, C5AR2, PPBP, ITGB3, STC1, S100A8, S100A12, CSF2, IL36RN, SCAMP5, IL1R2, UCP2, IL1RL1, NNAT	**0.0439**

A.4 Protein expression

Table 6-4 *Pathways of altered protein expression.*

Pathway	Altered Genes	P value
Amino acid metabolism	ACAT1, HADHA, FAH, ACAA1, MIF, HADHB, AOC3, ODO2, ODO1, AL1B1	**<0.001**
Developmental transcription factors	KRT19, SERPINA1, ALB, CPSM, KRT7	**<0.001**
Histone regulation	H2BFM, HIST2H2AC, HMGB1, HIST1H4A, HIST1H1B	**<0.001**
Antigen presentation by MHC class I	HSP90B1, PSME2, TPP2, CANX, PSMB2, ERAP2	**<0.001**
Cytoskeleton remodelling	KRT1, KRT19, EPPK1, VIM, KRT7, DSTN, CFL1, TPM1, COL4A2	**<0.001**
Blood coagulation	SERPINC1, SERPINE2, SERPINA1, FGB, F13A1	**<0.001**
Actin depolymerisation	DSTN, CFL1, MSN	**0.0174**
Mitochondrial long chain fatty acid beta-oxidation	HADHA, ACAT1, CPT-1A, HADHB	**0.0222**
Epigenetic regulation of transcription	HIST2H2AC, H2BFM, HIST1H4A, HIST1H1B	**0.0371**
Cell and chemokine adhesion	SERPINE2, MSN, CFL1, COL4A2	**0.0402**

A.5 Altered DNA methylation and RNA expression

Table 6-5 *Pathways of altered DNA methylation and RNA expression.*

Pathway	Altered Genes	P value
Apoptosis	SOX4, ZBTB16, KIF1B, TRPS1, ACTC1, ISL1, JMY, GLI3, UCP2, PHLPP1, CCL2, MLLT11, MMP9, LY86, CNR1, FNIP2, DUSP6, WNT9A, HIPK2, DPF2, PLEKHG2, ACVR1C, LCN2, CBL, TNFRSF11B, RYBP, CSF2, CPEB4, SERPINB2, PRKCG, CTH, XAF1, LTF, PDGFB, ASH1L, SERTAD2, CYTL1, BPTF, SALL1, MED12L, PLAG1, TET3, FOXK1, HMBOX1, CAMK4, NSD1, PPARA, TEF, CREB5, KHDRBS3, KLF7, RORA, PBX3, PROX1, ITGB3, TXNRD1, NEO1, GPR75, CYP1A1, PSG4, STOX2, GJB2, TFCP2L1, ADRA2B, ENDOU	**<0.001**
Neuronal development	EPHB3, SOX4, PDGFB, MYCBP2, MARK1, MBP, DNER, ISL1, WNK1, SOCS7, XYLT1, NEO1, ADRA2B, NRXN3, SALL1, SSH1, NF2, FMN1, GLI3, HS6ST1, CCL2, PLAG1, NNAT, CNR1, CHST3, WNT9A, HIPK2, NLGN1, ARHGAP35, TSPAN2, NKD1, KLF7, SIPA1L1, BLOC1S3, RORA, MARK2, PBX3, NDRG4, PROX1, PDE4D, ABI3, ITGB3, JMY, GNA12, MMP9, ADGRG3, CD177, CMTM4, FOLR2, ACVR1C, TNFAIP6, HAS1, GAB1, TRPS1, ACTC1, NEB, TXNRD1, GPR4, COL12A1, DUSP6, PPARA, TNNT2, CLSTN2, PDXP, MLLT11, MEX3B, FNIP2, HMBOX1, LCN2, CBL, CSF2, KIRREL1, MICAL3, ICAM4, ATXN1L, TNFRSF11B, EXOC8, SH3PXD2B	**<0.001**
Regulation of transcription	SOX4, SP4, ZBTB16, HIVEP1, IRF2BP1, PDGFB, CDK12, BACH2, TRPS1, ASH1L, ISL1, CYTL1, JMY, OTUD7B, BPTF, TFCP2L1, NEO1, SALL1, GLI3, MED12L, PLAG1, FST, TET3, FOXK1, FNIP2, ZNF704, NSD1, HIPK2, BEND3, ZKSCAN2, PPARA, ARHGAP35, TEF, ATXN1L, CREB5, RYBP, KLF7, CBX6, RORA, PBX3, CBX8, PROX1, IL1R2, C4BPB, HMBOX1, ADGRG3, MEX3D, ZNF503, CPEB4, RBAK, AMD4A, SERTAD2, ACTC1, ITGB3, MLLT11, CAMK4, LCN2, CSF2, KHDRBS3, CTH, LTF, NF2, HIVEP2, DPF2, ZNF713, ZNF699, TULP4, CBL	**<0.001**
Response to external stimuli	PDGFB, ASH1L, ISL1, SOCS6, RNF43, SOCS7, OTUD7B, XYLT1, YOD1, SALL1, NF2, IL1R2, GLI3, UCP2, PHLPP1, CCL2, C4BPB, MMP9, FST, ADGRG3, DUSP6, HIPK2, PPARA, ARHGAP35, CBL, CSF2, IL36RN, NKD1, IGFBP4, SPRY4, SERPINB2, RORA, CTH, LTF, TNFAIP6, NDRG4, PDE4D, CDK12, MAP3K7CL, ITGB3, JMY, ADRA2B, GNA12, DNMBP, NLGN1, PLEKHG2, TNFRSF11B, SIPA1L1, GAB1, IL32, DNER, CYTL1, NEO1, NRXN3, ENDOU, MARCH1, CMTM4, ICAM4, WNT9A, AAK1, NSD1, ACVR1C, ZNF106, TSLP, PROX1, SCD, CD163L1, RNASE7, C1QA, LY86, ALOX5AP, CNR1, CHST3, AP1S3, CAMK4, FOLR2, LCN2, TSPAN2, XAF1, MX2, SOX4, TRPS1, MLLT11, CYP1A1, BPTF, PR4, CD177, F2RL3, TFPI2, BLOC1S3, PRKCG, HBG1, SSH1, PDXP, TRIM63, SOGA1, CPEB4, HAS1, EXOC8, EPHB3	**<0.001**
Embryonic development	SOX4, TANC2, CYP1A1, ZBTB16, PDGFB, KIF1B, ISL1, ITGB3, TXNRD1, BPTF, STOX2, SALL1, NF2, GLI3, HS6ST1, GNA12, MMP9, TET3, COL12A1, DUSP6, WNT9A, NSD1, HIPK2, ARHGAP35, ACVR1C, NKD1, NDRG4, GAB1, PROX1, EPHB3, SERPINB7, PDE4D, CLSTN2, ADRA2B, NRXN3, CCL2, PLAG1, FST, CNR1, NLGN1, ATXN1L, RORA, CTH, LTF, MARK2, CBX8, TRPS1, ACTC1, GPR4, PPARA, SH3PXD2B, TNNT2, FMN1,	**<0.001**

	CYTL1, KMT2C, CLCN2, BLOC1S3, TFCP2L1, SCD, UCP2, PSG4, GJB2, ENDOU, REC8	
Metal ion binding	CYP1A1, MYCBP2, CYP24A1, TRPS1, ASH1L, ISL1, RNF43, OTUD7B, TXNRD1, ZCCHC14, BPTF, KMT2C, SCD, TRIM63, ENDOU, MICAL3, MMP9, MARCH1, PDLIM2, MEX3B, MEX3D, NSD1, PPARA, DPF2, LCN2, CBL, RYBP, KLF7, RBAK, PRKCG, RORA, XAF1, LTF, LONRF2, HBG1	**<0.001**
Cell differentiation and development	EPHB3, SERPINB7, ZBTB16, PDGFB, TRPS1, MBP, CLSTN2, ISL1, ITGB3, XYLT1, ADRA2B, NRXN3, SALL1, SSH1, NF2, GLI3, PHLPP1, CCL2, PLAG1, MMP9, FST, CNR1, GPR4, CAMK4, DUSP6, WNT9A, HIPK2, NLGN1, ARHGAP35, ACVR1C, ATXN1L, TNFRSF11B, NKD1, SIPA1L1, CTH, LTF, MARK2, NDRG4, PROX1, HIVEP1, IRF2BP1, BACH2, OTUD7B, BPTF, TFCP2L1, FOXK1, FNIP2, HMBOX1, ADGRG3, MEX3D, NSD1, BEND3, PPARA, RYBP, SOGA1, CBX6, CPEB4, RBAK, ZBTB10, CBX8, SAMD4A, SOX4, ASH1L, SERTAD2, CYTL1, JMY, MED12L, MLLT11, TET3, TEF, CREB5, CSF2, KLF7, RORA, PBX3, KHDRBS3, PRKCG, SH3PXD2B, ABCG1, PDE4D, EXTL3, SOCS6, SOCS7, KMT2C, FMN1, SCD, IGFBP4, WNK1, IL1R2, C4BPB, TFPI2, SPRY4, SERPINB2, KIRREL1, TSPAN2, STON2, MPZL2, HS6ST1, CHST6, PGM2L1, GGTA1P, MGAT3, MGAT5, DHDH, PYGM, CHST3, GALNT10, SLC5A3, HAS1, ACTC1, TNNT2, GAB1, COL12A1, GNA12, CD177, F2RL3, BLOC1S3, HBG1, OCLN, DNER, NEB, NEO1	**<0.001**
Regulation of cell signalling	ASH1L, ISL1, SOCS6, RNF43, SOCS7, OTUD7B, ADRA2B, SALL1, NF2, IL1R2, GLI3, UCP2, PHLPP1, MMP9, FST, ADGRG3, DUSP6, HIPK2, ARHGAP35, ACVR1C, RAB11FIP1, CBL, CSF2, IL36RN, NKD1, IGFBP4, SPRY4, RORA, CTH, LTF, NDRG4, SOX4, PDGFB, TRPS1, MAP3K7CL, CLSTN2, ITGB3, NEO1, CCL2, MLLT11, NNAT, LY86, WNT9A, AAK1, NLGN1, TNFRSF11B, GAB1, KIF1B, MBP, CHRNA5, GJB2, NRXN3, C1QA, CNR1, CAMK4, SIPA1L1, STON2, PRKCG, TNFAIP6	**<0.001**
Protein phosphorylation	EPHB3, PDE4D, ABI3, PDGFB, MARK1, CDK12, ASH1L, MAP3K7CL, ISL1, SOCS6, WNK1, STK35, ITGB3, SOCS7, ADRA2B, NF2, PHLPP1, CCL2, MMP9, MEX3B, FNIP2, CAMK4, DUSP6, AAK1, NSD1, HIPK2, ACVR1C, TNFRSF11B, CSF2, IGFBP4, MOB1B, SPRY4, KIRREL1, PRKCG, LTF, MARK2, NDRG4, ALPK2, GAB1, PROX1, SOX4, PPARA, SERPINB7, MYCBP2, YOD1, IL1R2, C4BPB, TFPI2, MEX3D, WNT9A, CPEB4, SERPINB2, SAMD4A, GTF3C4, KMT2C, TET3, BEND3, FKBPL, CTH, CBX8, PGM2L1, ZBTB16, KLHL28, BACH2, RNF43, TULP4, TRIM63, MARCH1, VCPIP1, CBL	**0.0013**
Response to organic compounds	SOX4, CYP1A1, PDE4D, PDGFB, CYP24A1, MBP, ACTC1, SOCS7, TXNRD1, GJB2, SSH1, SCD, UCP2, PDXP, TRIM63, CCL2, PYGM, NNAT, LY86, CNR1, FOLR2, WNT9A, PPARA, ACVR1C, LCN2, TNFRSF11B, ZNF106, CSF2, SOGA1, CPEB4, RORA, LTF, CBX8, GAB1, ISL1, ITGB3, CHRNA5, BPTF, NEO1, GLI3, FST, DUSP6, HIPK2, CBL, ABCG1, PRKCG, HAS1, MMP9, EXOC8, PROX1	**0.0026**
Transmembrane transport	SOX4, PDE4D, PDGFB, ISL1, WNK1, ITGB3, YOD1, NEO1, ADRA2B, KCNA3, CLCN2, IL1R2, GLI3, UCP2, SCN4A, CCL2, C4BPB, NNAT, MMP9, MEX3B, CNR1, F2RL3, CAMK4, AAK1, NLGN1, PPARA, ACVR1C, RAB11FIP1, CBL, ABCG1, IL36RN, STON2, KCNK5, PRKCG, TNNT2, NDRG4, MX2, EPHB3, ABI3,	**0.0113**

	MYCBP2, MARK1, KIF1B, DNER, ACTC1, NEB, JMY, SOCS7, NRXN3, NF2, GNA12, CHST3, ADGRG3, CD177, FOLR2, NKD1, KLF7, BLOC1S3, TNFAIP6, MARK2, HAS1, GAB1, PROX1	
Inflammatory response	ASH1L, ISL1, IL1R2, CCL2, C4BPB, LY86, ALOX5AP, CNR1, CAMK4, FOLR2, PPARA, TSPAN2, TNFRSF11B, IGFBP4, RORA, TNFAIP6	**0.0126**

A.6 Altered DNA methylation and protein expression

Table 6-6 *Pathways of altered DNA methylation and protein expression.*

Pathway	Altered genes	P value
RNA binding	MRPS31, VIM, RPL32, EPPK1, SRSF7, MAP4, RSL1D1, ANXA1, EIF1B, PSMA1, CANX, PSMA6, APEX1, HMGB1, IFI16, ADARB1, TFAM, HNRNPAB, TUFM, PDIA4, U2AF1, PARP1, LONP1, TRAP1, PSIP1, UBE2L3, HIST1H4A, P4HB, H1F0, MACF1, COL14A1, ENDOU, SLC25A11, HADHB, CKAP4, DEK, RPL9, RPL18, ATP5F1C	**<0.001**
Protein complex binding	VIM, EPS8L2, MYH10, IQGAP2, MAP4, KRT19, SYNM, LAMA5, APEX1, LAMB2, MYO1B, H2AFY, CPS1, PFKP, FANCM, TFAM, SRPRB, HP1BP3, PARP1, FBN1, PSIP1, CD9, P4HB, H1F0, MACF1, COL14A1, HADHB, MRPS31, TPM1, TPM4, COL4A2, KRT1, RPL32, ANXA1, LAMA2, PRELP, SLC25A13, SLC25A11, AGRN, RPL9, RPL18	**<0.001**
Cytoskeletal protein binding	TPM1, TPM4, SYNPO2, EPS8L2, MYH10, IQGAP2, MAP4, SYNM, PACSIN3, MYO1B, MIB2, GSN, SLC4A1, XIRP2, LMOD1, MACF1, PALLD, NOS3, CNN1, VIM, KRT19, ANXA1, PRKAR1A, EPHA5, LMCD1, PARP1, COL14A1, AGRN	**<0.001**
Enzyme oxidation	ACADS, KRT19, TNC, ANXA1, APEX1, HMGB1, CPS1, GSTP1, PARP1, LONP1, SERPINA1, FBN1, UBE2L3, PGRMC2, TSPO, PRKAR1A, AKR1B1, NOS3, EPHA5, SPTLC3, TP53I3, IDH2, OGDH, CBR4, ACBD4, HADHB, SERPINE2, PRELP, SERPINC1, AGRN, TFAM, CDC37, DLST	**<0.001**
Oxidative stress	KRT1, PSAP, LMCD1, RSL1D1, ANXA1, PSMA1, PSMA4, PSMA6, APEX1, HMGB1, IFI16, FAM13B, GSN, CDC37, GSTP1, U2AF1, PARP1, TRAP1, AP2M1, SERPINE2, P4HB, HPX, TSPO, SERPINC1, DEK, SCARA3, NOS3, STOM, TPM1, MYH10, TNC, ROCR, LAMB2, F13A1, SERPINA1, CD9, PRKAR1A, MACF1, SLC4A1, LONP1, PSIP1, AKR1B1, CPS1, SLC25A13	**<0.001**
Extracellular matrix organisation	COL4A2, COL6A2, COL6A3, TNC, LAMA2, LAMA5, LAMB2, GSN, FBN1, COL14A1, AGRN	**<0.001**
Gliogenesis	VIM, ANXA1, LAMA2, LAMB2, GSN, GSTP1, SERPINE2, CD9, TSPO	**<0.001**
Cellular catabolic processes	RPL32, PSAP, ACADS, PSMA1, PSMA4, PSMA6, USP43, PACSIN3, HMGB1, CUL7, CPS1, CPT1A, IFI16, OGDH, CRAT, FAH, U2AF1, LONP1, UBE2L3, USP42, ERAP2, PRELP, H1F0, TSPO, DLST, HADHB, NOS3, RPL9, RPL18, PFKP, SERPINE2, CTSD, AGRN, CANX, AP2M1, MARCH1	**<0.001**
Enzyme regulator activity	COL6A3, GAPVD1, PSAP, IQGAP2, ANXA1, HMGB1, H2AFY, FAM13B, B3GAT3, DC37, GSTP1, SERPINA1, SERPINE2, UBE2L3, SGSM2, PRKAR1A, SERPINC1, AGRN	**<0.001**

Appendix B Significance of altered RXRα DNA methylation

Statistical data of the RXRα DNA methylation measured in Chapter 5.

B.1 Cytotrophoblast

Table 6-7 DNA methylation at sites CpG0-12 of the gene RXRα in 25(OH)D_3 treated cytotrophoblast samples. Significance displayed as independent t test p value.

CpG site	P value
0	0.919
1	0.921
2	0.584
3	0.419
4	0.311
5	0.480
6	0.184
7	0.214
8	0.433
9	0.209
10	0.223
11	0.144
12	0.277

B.2 Fragment

Table 6-8 DNA methylation at sites CpG0-12 of the gene RXRα in 25(OH)D_3 treated fragment samples. Significance displayed as independent t test p value.

CpG site	P value
0	0.149
1	0.744
2	0.085
3	0.948
4	0.311
5	0.656
6	0.788
7	0.566
8	0.544
9	0.587
10	0.471
11	0.434
12	0.413

B.3 MAVIDOS

Table 6-9 DNA methylation at sites CpG0-12 of the gene RXRα in 25(OH)D_3 MAVIDOS placental samples. Significance displayed as independent t test p value. Si*gnificant values highlighted in* bold and marked with *.

CpG site	P value
0	0.836
1	0.927
2	0.602
3	0.552
4	0.411
5	0.369
6	**0.035***
7	0.213
8	0.440
9	0.884
10	0.881
11	0.824
12	0.935

B.4 SPRING

Table 6-10 DNA methylation at sites CpG0-12 of the gene RXRα in 25(OH)D_3 SPRING placental samples. Significance displayed as independent t test p value.

CpG site	P value
0	0.942
1	0.857
2	0.626
3	0.386
4	0.185
5	0.394
6	0.742
7	0.438
8	0.376
9	0.901
10	0.949
11	0.207
12	0.349

Appendix C MAVIDOS outcomes

Associations between MAVIDOS placental gene expression and offspring outcomes. Data discussed in Chapter 5.

C.1 Placental gene expression and birth outcomes

Table 6-11 Associations between placental gene expression and birth outcomes in the MAVIDOS study.

Gene name		Placental weight (g)	Birth weight (g)	Fat mass (g)	Lean mass (g)	Bone mineral density (g/cm^2)	Bone mineral content (g)	Bone area (cm^2)
ASCT1	β	**-57.568***	-80.048	-0.141	-45.800	-0.004	-3.684	-12.442
	p	**0.019**	0.482	0.565	0.611	0.466	0.185	0.149
	n	**67**	51	51	51	51	51	51
ASCT2	β	-6.331	-44.561	0.184	-92.867	0.002	1.289	0.442
	p	0.874	0.770	0.573	0.438	0.727	0.730	0.970
	n	68	51	51	51	51	51	51
CUBN	β	-20.453	-44.183	0.043	-54.141	0.002	0.253	-2.270
	p	0.185	0.650	0.838	0.480	0.578	0.916	0.759
	n	68	51	51	51	51	51	51
CYP24A1	β	**29.384***	**128.798***	**0.227***	57.597	0.002	**3.483***	**11.74***
	p	**0.008**	**0.006**	**0.029**	0.136	0.455	**0.001**	**0.000**
	n	**67**	**51**	**51**	51	51	**51**	**51**
CYP27B1	β	-40.557	38.501	0.292	-17.733	0.000	0.717	2.778
	p	0.068	0.719	0.200	0.834	0.940	0.785	0.347
	n	68	51	51	51	51	51	51
LAT1	β	-4.354	-114.596	-0.324	-38.303	**-0.009***	-4.118	-7.076
	p	0.818	0.197	0.087	0.587	**0.012**	0.057	0.297
	n	68	51	51	51	**51**	51	51
LRP2	β	**59.319**	143.318	0.206	139.497	0.006	4.536	13.632
	p	**0.009**	0.227	0.419	0.135	0.276	0.118	0.130
	n	**67**	51	51	51	51	51	51
RXRα	β	-37.227	-109.528	-0.660	33.179	-0.013	-4.587	-5.609
	p	0.291	0.539	0.080	0.814	0.080	0.293	0.680
	n	68	51	51	51	51	51	51
TXNIP	β	**-74.705***	-68.305	0.101	-94.272	0.003	0.410	-3.320
	p	**0.019**	0.637	0.746	0.407	0.580	0.908	0.763
	n	**67**	51	51	51	51	51	51
VDR	β	-31.400	-112.973	0.306	-181.400	-0.002	-1.322	-4.821
	p	0.078	0.386	0.272	0.074	0.718	0.681	0.628
	n	68	51	51	51	51	51	51
VEGF	β	**-32.659**	-148.470	-0.234	-91.855	-0.002	-2.670	-0.743
	p	**0.040**	0.079	0.200	0.171	0.514	0.202	0.132
	n	**67**	51	51	51	51	51	51

Significant results ($p < 0.05$) are highlighted in bold and marked with *

Adjusted for gestation, sex and treatment group

C.2 Placental gene expression and 4 year outcomes

Table 6-12 Associations between placental gene expression and 4 year old childhood outcomes in the MAVIDOS study.

Gene name		Bone mineral density (g/cm^2)	Bone mineral content (g)	Bone area (cm^2)
ASCT1	β	-0.012	-13.181	-3.366
	p	0.319	0.417	0.828
	n	33	33	33
ASCT2	β	-0.015	-42.603	**-50.335***
	p	0.423	0.089	**0.043**
	n	33	33	**33**
CUBN	β	-0.008	-11.457	-4.729
	p	0.477	0.433	0.734
	n	33	33	33
CYP24A1	β	-0.000	1.947	4.174
	p	0.994	0.849	0.668
	n	33	33	33
CYP27B1	β	**-0.035***	**-35.439***	1.468
	p	**0.001**	**0.028**	0.929
	n	**33**	**33**	33
LAT1	β	-0.005	-6.781	-6.064
	p	0.619	0.599	0.626
	n	33	33	33
LRP2	β	0.008	7.401	-1.027
	p	0.493	0.653	0.948
	n	33	33	33
RXRα	β	0.019	15.845	-5.959
	p	0.363	0.586	0.829
	n	33	33	33
TXNIP	β	**-0.032***	**-45.501***	-23.527
	p	**0.042**	**0.040**	0.284
	n	**33**	**33**	33
VDR	β	-0.009	-10.905	-2.557
	p	0.465	0.525	0.876
	n	33	33	33
VEGF	β	0.004	-1.208	-8.160
	p	0.651	0.914	0.438
	n	33	33	33

Significant results ($p < 0.05$) are highlighted in bold and marked with *

Adjusted for gestation, sex and treatment group

Appendix D Abstracts

D.1 Abstracts

- 25(OH)D_3 treatment alters DNA methylation in the human placenta. Ashley. B, Simner. C, Lillycrop. K, Harvey. N, Lewis. R, Cleal. J
  (Southampton Medical and Health research Conference, 2017)
- Short term vitamin D exposure alters methylation status of term placental villi. Ashley. B, Simner. C, Rezwan. FI, Holloway. JW, Lillycrop. K, Harvey. N, Lewis. RM, Cleal. JK
  (International Federation of Placenta Associations, 2017)
- 25(OH)D_3 treatment alters DNA methylation and RNA expression in the human placenta. Ashley. B, Simner. C, Rezwan. FI, Holloway. JW, Lillycrop. K, Harvey. N, Lewis. R, Cleal. J
  (Southampton Medical and Health research Conference, 2018)
- 25(OH)D_3 treatment alters DNA methylation, RNA expression and protein expression in human term placenta. Ashley. B, Simner. C, Rezwan. FI, White. CH, Manousopoulou. A, Holloway. JW, Garbis. S, Lewis. RM, Harvey. NC, Cleal. JK
  (Cambridge Trophoblast Research, 2018)
- 25(OH)D_3 treatment alters DNA methylation, RNA expression and protein expression in human term placenta. Ashley. B, Simner. C, Rezwan. FI, White. CH, Manousopoulou. A, Holloway. JW, Garbis. S, Lewis. RM, Harvey, NC, Cleal. JK
  (International Federation of Placenta Associations, 2018)

Appendix E Publications

ORIGINAL ARTICLE

JBMR®

Gestational Vitamin D Supplementation Leads to Reduced Perinatal RXRA DNA Methylation: Results From the MAVIDOS Trial

Elizabeth M Curtis,[1*] Nevena Krstic,[2*] Eloïse Cook,[2*] Stefania D'Angelo,[1] Sarah R Crozier,[1] Rebecca J Moon,[1,3] Robert Murray,[2] Emma Garratt,[2] Paula Costello,[2] Jane Cleal,[2] Brogan Ashley,[2] Nicholas J Bishop,[4] Stephen Kennedy,[5] Aris T Papageorghiou,[5] Inez Schoenmakers,[6,7] Robert Fraser,[8] Saurabh V Gandhi,[8] Ann Prentice,[6] M Kassim Javaid,[9] Hazel M Inskip,[1,10] Keith M Godfrey,[1,10] Christopher G Bell,[1,2] Karen A Lillycrop,[2†] Cyrus Cooper,[1,9,10†] Nicholas C Harvey[1,10†], and the MAVIDOS Trial Group

[1]MRC Lifecourse Epidemiology Unit, University of Southampton, UK
[2]Institute of Developmental Sciences, University of Southampton, UK
[3]Paediatric Endocrinology, University Hospitals Southampton NHS Foundation Trust, Southampton, UK
[4]Academic Unit of Child Health, Sheffield Children's Hospital, University of Sheffield, Sheffield, UK
[5]Nuffield Department of Obstetrics and Gynaecology, John Radcliffe Hospital, University of Oxford, Oxford, UK
[6]MRC Elsie Widdowson Laboratory, Cambridge, UK
[7]Department of Medicine, Faculty of Medicine and Health Sciences, University of East Anglia, Norwich, UK
[8]Sheffield Hospitals NHS Trust, (University of Sheffield,), Sheffield, UK
[9]NIHR Oxford Biomedical Research Centre, University of Oxford, Oxford, UK
[10]NIHR Southampton Biomedical Research Centre, University of Southampton and University Hospital Southampton NHS Foundation Trust, Southampton, UK

ABSTRACT

We have previously demonstrated inverse associations between maternal 25(OH)-vitamin D status and perinatal DNA methylation at the retinoid-X-receptor-alpha *(RXRA)* locus and between *RXRA* methylation and offspring bone mass. In this study, we used an existing randomized trial to test the hypothesis that maternal gestational vitamin D supplementation would lead to reduced perinatal *RXRA* locus DNA methylation. The Maternal Vitamin D Osteoporosis Study (MAVIDOS) was a multicenter, double-blind, randomized, placebo-controlled trial of 1000 IU/day cholecalciferol or matched placebo from 14 weeks' gestation until delivery. Umbilical cord (fetal) tissue was collected at birth and frozen at −80°C ($n = 453$). Pyrosequencing was used to undertake DNA methylation analysis at 10 CpG sites within the *RXRA* locus (identified previously). *T* tests were used to assess differences between treatment groups in methylation at the three most representative CpG sites. Overall, methylation levels were significantly lower in the umbilical cord from offspring of cholecalciferol-supplemented mothers, reaching statistical significance at four CpG sites, represented by CpG5: mean difference in % methylation between the supplemented and placebo groups was −1.98% (95% CI, −3.65 to −0.32, $p = 0.02$). ENCODE (Encyclopedia of DNA Elements) evidence supports the functionality of this locus with strong DNase hypersensitivity and enhancer chromatin within biologically relevant cell types including osteoblasts. Enrichment of the enhancer-related H3K4me1 histone mark is also seen in this region, as are binding sites for a range of transcription factors with roles in cell proliferation, response to stress, and growth factors. Our findings are consistent with previous observational results and provide new evidence that maternal gestational supplementation with cholecalciferol leads to altered perinatal epigenetic marking, informing mechanistic understanding of early life mechanisms related to maternal vitamin D status, epigenetic marks, and bone development. © 2018 The Authors. *Journal of Bone and Mineral Research* Published by Wiley Periodicals Inc.

KEY WORDS: EPIGENETIC; METHYLATION; RXRA; VITAMIN D; OSTEOPOROSIS; EPIDEMIOLOGY

Received in original form May 11, 2018; revised form October 10, 2018; accepted October 6, 2018. Accepted manuscript online October 15, 2018.

Address correspondence to: Professor Cyrus Cooper, MRC Lifecourse Epidemiology Unit, University of Southampton, Southampton General Hospital, Southampton, SO16 6YD, UK. E-mail: cc@mrc.soton.ac.uk

Additional information: MAVIDOS Trial Group: Nigel K Arden, Andrew Carr, Michael Clynes, Elaine M Dennison, Richard Eastell, M Zulf Mughal, David M Reid, Sian M Robinson

*EMC, NK, and EC are joint first authors.
†KAL, CC, and NCH are joint senior authors.

International Standard Randomized Controlled Trial Registry: ISRCTN: 82927713; European Clinical Trials Database: EudraCT 2007-001716-23. Maternal Gestational Vitamin D Supplementation and Offspring Bone Health.

Additional Supporting Information may be found in the online version of this article.

Journal of Bone and Mineral Research, Vol. 34, No. 2, February 2019, pp 231–240
DOI: 10.1002/jbmr.3603

Introduction

It is becoming increasingly recognized that environmental factors acting through epigenetic mechanisms induce persistent changes in gene expression, leading to differences in phenotype.[1,2] Various examples of such epigenetic mechanisms have come from the natural world, and also from experimental animal studies. For example, altered pregnancy diet in rats has been shown to lead to modification of DNA methylation, gene expression, and phenotype in the offspring.[1–4] Evidence for the relevance of such mechanisms in human disease is increasing; we have recently documented associations between perinatal DNA methylation at particular loci and bone phenotype in the offspring.[5,6] We previously demonstrated that methylation at the cyclin-dependent kinase inhibitor 2A (*CDKN2A*)[6] and retinoid-X-receptor-alpha (*RXRA*)[5] loci in umbilical cord DNA was associated with offspring bone mass in childhood in the Southampton Women's Survey (SWS) mother–offspring cohort. RXRA is an essential part of vitamin D signaling, forming a heterodimer with the vitamin D receptor in the nuclear action of $1,25(OH)_2$-vitamin D. We reasoned that this latter observation might be of key relevance to our demonstrations of associations between maternal 25(OH)-vitamin D status in pregnancy and offspring bone mass,[7–9] together with our finding of a positive effect of maternal vitamin D supplementation during pregnancy on neonatal bone mass for winter births (when background 25(OH)-vitamin D concentrations are lowest).[10] In the SWS, methylation at one CpG site upstream of the *RXRA* promoter was associated with a marker of maternal pregnancy 25(OH)-vitamin D status, with greater 25(OH)-vitamin D status associated with lower *RXRA* promoter methylation.[5] Clearly, causation cannot be concluded from an observational study; therefore, we hypothesized, in the setting of the Maternal Vitamin D Osteoporosis Study (MAVIDOS) randomized, double-blind, placebo-controlled trial of vitamin D supplementation in pregnancy,[10] that this intervention would lead to reduced *RXRA* DNA methylation in umbilical cord tissue at birth compared with placebo.

Participants and Methods

Participants: The Maternal Vitamin D Osteoporosis Study

We analyzed *RXRA* DNA methylation data from the MAVIDOS study, a multicenter, double-blind, randomized, placebo-controlled trial of vitamin D supplementation in pregnancy, in which the primary outcome was neonatal bone mass. The study methods and primary findings have been published previously.[10,11] The study was approved by the Southampton and South West Hampshire Research Ethics Committee. MAVIDOS was registered prospectively (International Standard Randomised Controlled Trial Registry: ISRCTN 82927713; European Clinical Trials Database: EudraCT 2007-001716-23) with full approval from the UK Medicines and Healthcare Products Regulatory Agency. Written informed consent was obtained from all participants.

Women attending one of three UK hospitals (University Hospital Southampton NHS Foundation Trust, Southampton; Oxford University Hospitals NHS Foundation Trust, Oxford; Sheffield Hospitals NHS Trust, University of Sheffield, Sheffield) for early pregnancy ultrasound screening (11 to 14 weeks' gestation) between October 6, 2008 and February 11, 2014 were invited to participate in the study.[10,11] Inclusion criteria were age over 18 years, singleton pregnancy, and gestation less than 17 weeks based on last menstrual period and ultrasound measurements. Exclusion criteria included women with known metabolic bone disease, renal stones, hyperparathyroidism or hypercalciuria, those taking medication known to interfere with fetal growth, fetal anomalies on ultrasonography, and women already using >400 IU/day vitamin D supplementation. A screening blood sample was obtained and analyzed on the local NHS platform [all three hospitals participate in the DEQAS (Vitamin D External Quality Assessment Scheme); http://www.deqas.org/]; women with 25(OH)D between 25 and 100 nmol/L and serum calcium <2.75 mmol/L were eligible to enroll in the study.

Participants were randomized to receive either cholecalciferol 1000 IU/day or matched placebo [Merck KGaA, Darmstadt, Germany)/Sharp Clinical Services (previously DHP-Bilcare), Crickhowell, UK], from before 17 weeks' gestation until delivery. Packs of study treatment were randomly assigned in a 1:1 ratio by Sharp Clinical Services using a computer-generated sequence in randomly permuted blocks of 10, starting randomly midway through the block, and sequentially numbered, before delivery to the study sites, and then were dispensed in order by each study pharmacist. The study medication was provided in a blister pack in a single box containing all medication for the whole pregnancy. The participants, those providing antenatal and intrapartum care, and all field researchers involved in data collection and sample analysis were blinded to the intervention. All participants received standard antenatal care, and could continue self-administration of dietary supplements containing up to 400 IU/day vitamin D.

Maternal assessments during pregnancy

The participants attended the research center for a detailed assessment of diet (including supplement use), lifestyle (smoking, physical activity participation, employment), and health (past medical history, current medication use) using interviewer-led questionnaires both prior to commencing the study medication, and again at 34-weeks' gestation. Ethnicity was reported by the participant and categorized as white or non-white.

Assessment of 25(OH)D status

A nonfasted venous blood sample was obtained on the day that the study medication was dispensed and also at 34-weeks' gestation; serum was stored at −80°C. 25(OH)D was assessed by chemiluminescent assay (liaison automated platform; DiaSorin, Stillwater, MN, USA). All samples were analyzed in a single batch at the end of the study at MRC Human Nutrition Research, Cambridge, UK. Details of assay performance and quality control through participation in the DEQAS, US National Institute of Standards and Technology (NIST), and the UK National External Quality Assessment Service (NEQAS) are given elsewhere.[12,13]

Neonatal DXA

All neonates underwent DXA assessment at whole-body minus head and lumbar spine sites (Hologic Discovery, Hologic Inc, Bedford, MA, USA, or GE-Lunar iDXA, GE-Lunar, Madison, WI, USA, with neonatal software) within 2 weeks of birth. The current analysis uses the whole-body minus head measures. The infant was undressed, clothed in a standard towel, fed, and pacified before the assessment. Each instrument underwent daily quality control with cross-calibration between sites. The total radiation dose was

estimated to be 0 · 04 mSv, equivalent to about 7-days' exposure to background radiation in the UK. All DXA images were reviewed for movement artifacts and quality by two operators (NCH and RJM), who were blinded to treatment allocation.

Umbilical cord DNA extraction

Immediately following delivery, a 5- to 10-cm segment was cut from the midportion of each cord, flushed with saline to remove fetal blood, flash-frozen in liquid nitrogen, and stored at −80°C until required for DNA isolation. Genomic DNA was isolated from frozen archived umbilical cord tissue by classical proteinase K digestion and phenol:chloroform extraction.

Quantitative DNA methylation analysis and pyrosequencing

The region of interest is in close proximity of the *RXRA* gene locus, 2252 base pairs upstream from the transcriptional start site. It contains 12 CpG dinucleotides (chr9: 137215735 to 137216064, human genome hg19/GRCh37 build; Supplementary Fig. 1). We used sodium bisulfite targeted pyrosequencing (Pyromark MD; QIAGEN, Hilden, Germany; https://www.qiagen.com/fi/resources/technologies/pyrosequencing-resource-center/technology-overview/)[14] to carry out in-depth analysis of the methylation status of 10 out of 12 CpGs within the previously identified differentially methylated region of *RXRA* in umbilical cords. Pyrosequencing was not performed on CpG 6 and CpG 7 [at genomic coordinates (hg19) chr9 137215867 and 137215956, respectively] for sample conservation purposes because of their distance from other CpGs (therefore requiring separate amplicons), as shown in Supplementary Fig. 1. Inter- and intraplate controls were added to each plate as a control for inter- and intraplate variability, and 0% and 100% methylation controls were run to ensure that the full range of methylation could be detected. The genomic coordinates for the *RXRA* CpG sites are provided in Supplementary Table 1.

Statistical analysis

Women who had delivered a liveborn infant and babies who had umbilical cord *RXRA* pyrosequencing analysis were included in the analysis. All outcomes were assessed for normality via visual inspection of histograms. Percentage DNA methylation at all *RXRA* CpGs analyzed was normally distributed, except at CpG 1 and CpG 3. Characteristics of the women in the two treatment arms were compared using *t* tests, and Mann-Whitney *U* and χ^2 tests for normally distributed, non-normally distributed, and categorical variables, respectively. Characteristics of the MAVIDOS babies (boys versus girls) for whom neonatal DXA and *RXRA* methylation data were available were also compared. Neonatal DXA indices were whole-body minus head bone area (BA), BMC, and areal bone mineral density (aBMD). Continuous child characteristics were summarized using mean (SD) or median (interquartile range [IQR]). Categorical variables were summarized using percentages. Differences in continuous variables between boys and girls were tested using *t* tests or Mann-Whitney *U* tests where appropriate. All participants were analyzed by the group to which they were originally randomized. Differences in *RXRA* DNA methylation between the two treatment groups were compared using *t* tests or Mann-Whitney *U* tests for normally distributed and non-normally distributed variables, respectively. *RXRA* methylation was Fisher-Yates transformed to SDs. Separate linear regression analyses were carried out to analyze the difference in methylation between the treatment groups. We analyzed the interaction between treatment group, *RXRA* methylation, and season of birth because of previously described seasonal variations in 25(OH)D concentrations reported in many previous studies. To ensure adequate sample sizes, we defined season of birth as a binary variable using the UK Meteorological Office classification, combining winter (December to February) with spring (March to May) to give an overall "winter" variable (December to May), and summer (June to August) with autumn (September to November) to give an overall "summer" variable (June to November). To explore associations between *RXRA* methylation and bone outcomes, linear regression analyses were carried out, adjusted for treatment group and sex where appropriate.

Based on previous findings, we recognized that there was likely to be colinearity between the individual exposures and outcomes,[5,6] so we undertook a data reduction approach by investigating clustering of the CpG methylation.[6] Our approach was appropriate given the relatively small number of tests in our analysis, compared with larger scale genome-wide associations studies, for which methods such as Bonferroni or the Benjamini-Hochberg/false discovery rate corrections for multiple testing would be appropriate.[15] Previous studies have shown that where clusters of differential CpGs can be identified, they are more likely to be of functional relevance than are individual CpG changes.[16] By investigating the correlation between methylation at each of the individual CpG sites (Supplementary Table 2) and calculating the median absolute deviation (MAD) from the median for each site (Supplementary Table 3), we grouped the CpG sites into three clusters (CpG 1 to CpG 5, CpG 8 to CpG 11, CpG 12), with each cluster represented by the site with the highest MAD score (ie, the site with the greatest variability within the cluster): CpG sites 5, 11, and 12, respectively. For completeness, we also used the Simes' modification of the Bonferroni method to undertake a *p*-value correction on the analyses, using the Stata "qqvalue" command (StataCorp, College Station, TX, USA), which is similar to the "p.adjust" command in R https://www.rdocumentation.org/packages/stats/versions/3.1.1/topics/p.adjust. These are presented as *q* values in the relevant results Tables 2, 3 and Supplementary Table 4.

Further biological support for this clustering was provided by exploration of the ENCODE data,[17] demonstrating distinct DNase I hypersensitivity sites at either end of the differentially methylated region, and discrete grouping of transcription factor binding. All analyses were performed in Stata v14 (StataCorp). A p value of <0.05 was considered statistically significant.

Results

Characteristics of participants

There were 965 women (85%) who remained in the study until delivery (Fig. 1).[10] There were 486 live births in the control group and 479 in the cholecalciferol group, of which 228 and 225 umbilical cords, respectively, underwent pyrosequencing of the *RXRA* region of interest. Seventy-eight babies for whom pyrosequencing results were available did not have a useable DXA scan (43 randomized to placebo, 35 to cholecalciferol), leaving 375 babies with *RXRA* methylation analyses, DXA outcomes, and the relevant maternal information. Of the 453 women included in the initial analysis, the mean age at delivery was 30.9 (SD 5.2) years in the placebo group and 30.7 (SD 5.1) years in the cholecalciferol supplemented group. Baseline characteristics of women in the placebo and cholecalciferol

Appendix E

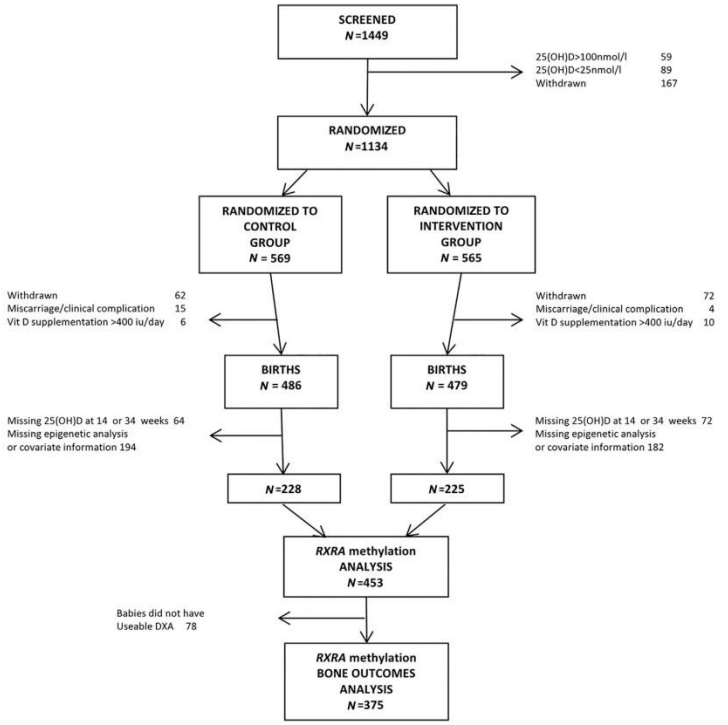

Fig. 1. MAVIDOS trial consort diagram.

groups at randomization were similar (Table 1A). Neonatal DXA whole-body minus head bone measurements were available for 202 boys (91 born to mothers randomized to placebo, 111 to cholecalciferol) and 173 girls (94 born to mothers randomized to placebo, 79 to cholecalciferol; Table 1B). A χ^2 test demonstrated no difference in the sex distribution of the treatment groups. There was no difference in gestational age between the boys and girls. As would be expected, boys had a greater average whole-body minus head bone mineral content (g) and bone area (cm^2) than girls. In this subset of the MAVIDOS trial population, no differences in gestational age or whole-body minus head DXA outcomes were observed in the babies by maternal randomization group to placebo or 1000 IU cholecalciferol (Table 1C).

Cholecalciferol supplementation and perinatal RXRA methylation

Percentage methylation at the *RXRA* differentially methylated region (DMR) varied greatly across the 10 CpG sites measured, for example, ranging from 29.0% to 81.4% at CpG 5 (mean 47.7%, SD 9.0%; Supplementary Table 1). However, percentage methylation tended to be lower in the cholecalciferol-supplemented group than in the placebo group (Fig. 2). At CpG 5 (representing CpG 1 to CpG 5), mean (SD) percentage methylation was 46.7% (8.2%) in the cholecalciferol group and 48.7% (9.7%) in the placebo group (mean difference −1.98 percentage points, $p = 0.02$). Although percentage methylation at both CpG 11 (representing CpG 8 to CpG 11) and CpG 12 was lower in cholecalciferol than placebo group births, these differences were not statistically significant (Table 2 and Supplementary Table 4). We observed no consistent associations between maternal 25(OH)D status at 34 weeks, or change in 25(OH)D from early to late pregnancy, and RXRA methylation in umbilical cord tissue across the cohort. However, there was evidence of an interaction between change in 25(OH)D between 14- and 34-weeks' gestation 25(OH)D and treatment allocation to cholecalciferol or placebo on RXRA methylation at CpG 11 ($p = 0.022$).

Interactions between season of birth, treatment group, and percentage DNA methylation at *RXRA*

Greater increases in maternal 25(OH)D status were seen in summer (June to November) than in winter (December to May) births; the increase in 25(OH)D during pregnancy was more than double in the women giving birth in summer. In summer births, mean (SD) change in 25(OH)D between 14- and 34-weeks' gestation was 8.1 (16.0) nmol/L in the placebo group ($n = 124$), and 28.0 (19.8) nmol/L in the vitamin D supplemented group ($n = 127$). In winter births, mean (SD) change in 25(OH)D

Table 1A. Baseline Characteristics of the Randomly Assigned Pregnant Women Included in the Analysis

	n	*Placebo (N = 228)*	*Cholecalciferol 1000 IU/day (N = 225)*
Mean (SD) or median (IQR)			
Age (years)	427	30.9 (5.2)	30.7 (5.1)
Height (cm)	423	166.4 (6.3)	165.3 (6.1)
Weight (kg)	427	73.6 (13.1)	71.6 (14.1)
Pregnancy weight gain (kg)	415	9.4 (3.6)	9.7 (3.5)
BMI (kg/m^2)†	423	25.7 (23.0,29.7)	24.9 (22.4,28.8)
Sum of skinfold thickness (mm)	360	81.9 (27.0)	78.3 (29.1)
25(OH)D at 14 weeks (nmol/L)	445	45.1 (16.2)	44.4 (15.2)
25(OH)D at 34 weeks (nmol/L)	432	42.8 (20.0)	66.3 (19.8)
n (%)			
Nulliparous	427	99 (46.3)	91 (42.7)
Educational qualification > A level	423	156 (74.3)	163 (76.5)
Current smoker	426	16 (7.5)	12 (5.7)
Strenuous exercise ≥ once a week	390	22 (11.3)	32 (16.4)

Values are *n* (%), mean (SD), or median (interquartile range [IQR]). P difference 25(OH)D at 34 weeks, cholecalciferol supplemented versus placebo group, $p < 0.001$.

Table 1B. Whole-Body Minus Head DXA Characteristics of the MAVIDOS Babies by Sex for Whom DXA and RXRA Methylation Data Are Available

	Boys ($n = 202$)	Girls ($n = 173$)	*p* difference between boys and girls
Gestational age (weeks)	40.2 (1.3)	40.1 (1.4)	0.22
BA (cm^2)	306.5 (34.8)	295.8 (33.8)	0.003
BMC (g)	63.1 (10.7)	59.9 (10.5)	0.004
aBMD (g/cm^2)	0.205 (0.018)	0.202 (0.020)	0.100

p values <0.05 are in bold.
BA = bone area; BMC = bone mineral content; aBMD = areal bone mineral density.

Table 1C. Whole-Body Minus Head DXA Characteristics of the MAVIDOS Babies by Maternal Randomization Group for Whom DXA and *RXRA* Methylation Data Are Available

	Placebo ($N = 185$)	Cholecalciferol 1000 IU/day ($N = 190$)	*p* difference between maternal randomization group
Gestational age (weeks)	40.1 (1.4)	40.2 (1.2)	0.23
BA (cm^2)	299.4 (36.7)	303.6 (32.6)	0.24
BMC (g)	61.2 (10.9)	62.0 (10.6)	0.46
aBMD (g/cm^2)	0.204 (0.019)	0.203 (0.019)	0.93

p values <0.05 are in bold.
BA = bone area; BMC = bone mineral content; aBMD = areal bone mineral density.

between 14- and 34-weeks' gestation was −15.0 (17.6) nmol/L in the placebo group ($n = 103$), and 13.6 (22.6) nmol/L in the vitamin D supplemented group ($n = 95$).

There was evidence of statistically significant interactions for the outcome of *RXRA* methylation between treatment allocation (cholecalciferol versus placebo) and season of birth (at all three representative CpGs: CpG 5, $p = 0.02$; CpG 11, $p = 0.009$; and CpG 12 $p = 0.01$). The effect of treatment group on *RXRA* methylation appeared greater in summer than winter births (Table 3). In summer births, there was a difference in percentage methylation at *RXRA* CpG 5, CpG 11, and CpG 12 between treatment groups ranging from −3.69% at CpG 5 ($p = 0.001$), to −2.38% at CpG 11 ($p = 0.01$), and −2.13% at CpG 12 ($p = 0.005$), but the differences between groups were nonsignificant for winter births. This interaction persisted after adjustment for potential differences in maternal characteristics between the season groups (maternal BMI and skinfold thickness), and for other factors known to influence methylation (offspring sex and maternal smoking).

RXRA methylation and offspring bone indices measured by DXA

In the population as a whole, there were modest positive associations between *RXRA* methylation at CpG 5 and offspring whole-body minus head BA, BMC, and aBMD (Table 4). However, on stratification according to treatment allocation, associations were noted in the placebo, but not the cholecalciferol

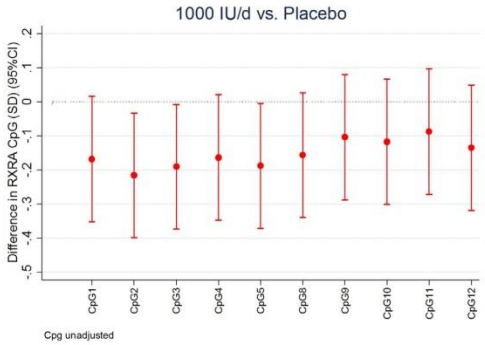

Fig. 2. Difference in *RXRA* DNA methylation at each CpG site between cholecalciferol 1000 IU/day supplemented group and placebo group (expressed as SDs). Each bar is the outcome of a separate linear regression (mean difference and 95% CI).

Table 2. RXRA DNA Methylation in Cholecalciferol 1000 IU/day Supplemented and Placebo Groups

	n	*% methylation Cholecalciferol 1000 IU/day*	*% methylation Placebo*	*Mean diff. % methylation*	*95% CI*	*p difference*	*q difference*
RXRA CpG 5	447	46.7 (8.2)	48.7 (9.7)	**−1.98**	**−3.65, −0.32**	**0.02**	**0.06**
RXRA CpG 11	446	58.3 (7.5)	58.9 (8.1)	−0.67	−2.12, 0.78	0.36	0.36
RXRA CpG 12	446	66.1 (5.8)	66.9 (6.6)	−0.84	−1.99, 0.31	0.15	0.225

CpG 5 represents CpG 1 to CpG 5; CpG 11 represents CpG 8 to CpG 11. *p* values < 0.05 are in bold. q values were obtained using the Simes method. Difference in methylation = mean (cholecalciferol 1000 IU/day) − mean (placebo).

Table 3. RXRA DNA Methylation in Cholecalciferol 1000 IU/day Supplemented and Placebo Groups, Stratified by Season: Winter Births (December to May) and Summer Births (June to November)

	Winter births (Dec to May)				*Summer births (June to Nov)*			
CpG	Mean diff. % methylation	95% CI	*p*	q	Mean diff. % methylation	95% CI	*p*	q
RXRA CpG 5	0.27	(−2.27, 2.82)	0.83	0.83	**−3.69**	**(−5.92,−1.45)**	**0.001**	**0.004**
RXRA CpG 11	1.51	(−0.73, 3.76)	0.18	0.55	**−2.38**	**(−4.29,−0.47)**	**0.02**	**0.01**
RXRA CpG 12	0.79	(−1.00, 2.58)	0.38	0.58	**−2.13**	**(−3.60,−0.65)**	**0.005**	**0.007**

Difference in methylation = mean (cholecalciferol 1000 IU/day) − mean (placebo). *p* values <0.05 are in bold. q values were obtained using the Simes method.

supplemented groups, as documented in Fig. 3. In the placebo group (red bars in Fig. 3), *RXRA* methylation at CpG 11 was positively associated with BA ($\beta = 6.96$ cm^2 per 10% increase in methylation, $p = 0.05$). There was also a tendency towards positive associations between methylation and BA at CpG 5 and CpG 12. Furthermore, again in the placebo group, methylation at CpG 5 and CpG 11 was positively associated with offspring BMC (at CpG 5, $\beta = 1.75$g per 10% increase in methylation, $p = 0.03$; at CpG 11, $\beta = 2.34$g per 10% increase in methylation, $p = 0.02$). Conversely, in the cholecalciferol-supplemented group (blue bars in Fig. 3), no statistically significant associations were found between methylation at CpG 5, CpG 11, and CpG 12 and offspring neonatal DXA bone outcomes (Supplementary Table 5).

ENCODE functional analysis

The DMR itself resides within the upstream CpG island shore region (within 2 kb) of the *RXRA* 5′CpG island. ENCODE consortium data were interrogated for functional evidence within this location.[17] This investigation revealed that the region of interest within the *RXRA* locus contains a cluster of DNase I hypersensitive sites (DHS, a general regulatory marker, often found within regulatory elements such as promoters and enhancers[18]), identified in 84 cell lines out of 125 (see Supplementary Fig. 2, with examples from the chorion and osteoblast cell lines highlighted). Furthermore, significant enrichment of the enhancer-related H3K4me1 histone mark

Table 4. Relationships Between Perinatal Methylation in Umbilical Cord at CpG Sites Within the RXRA Region of Interest and Bone Indices at Birth (Measured by DXA, Whole Body Minus Head)

	BA, (cm^2)		BMC, (g)		aBMD, (g/cm^2)	
RXRA CpG	β (95% CI)	*p*	β (95% CI)	*p*	β (95% CI)	*p*
CpG 5	**4.18 (0.16, 8.20)**	**0.04**	**1.50 (0.27, 2.74)**	**0.02**	**0.002 (0.000, 0.004)**	**0.05**
CpG 11	2.77 (−1.93, 7.48)	0.25	0.84 (−0.61, 2.30)	0.26	0.001 (−0.002, 0.004)	0.47
CpG 12	2.85 (−3.19, 8.88)	0.35	0.62 (−1.25, 2.49)	0.52	0.000 (−0.003, 0.003)	0.91

Associations are adjusted for sex and treatment group. β coefficients and 95% CIs have been multiplied by 10 and therefore represent the change associated with a 10% increase in methylation. *p* values <0.05 are in bold.
BA = bone area; BMC = bone mineral content; aBMD = areal bone mineral density.

across a range of tissue types was found both across and within 250 bp of the DMR (Supplementary Fig. 2). Enhancer loci may show dynamic DNA methylation indicative of transcription factor interaction within these functional regions.[19] Consistent with this, genome segmentations from ENCODE (displaying chromatin state segmentations from six cell lines) predict weak enhancer activity or an open chromatin *cis* regulatory element at the *RXRA* DMR (yellow region in Supplementary Fig. 2) at the *RXRA* DMR. Finally, ENCODE transcription factor binding data demonstrate significant binding within the *RXRA* DMR. The numbers of transcription factor binding sites found at the *RXRA* DMR in the ENCODE database vary between cell types. For example, in the cell line, MCF-7, which is highly responsive to estrogen and TSH,[20] three transcription factors bind with high affinity at the *RXRA* DMR (MYC, CTCF, and POL2RA). In summary, these findings suggest the *RXRA* DMR as a region of significant functional activity across a range of cell types, with evidence of strong DNAse I hypersensitivity sites, weak enhancer or *cis* regulatory element activity, and transcription factor binding.

RXRA methylation and gene expression in vitamin D-treated placental villous fragments

To experimentally investigate the influence of vitamin D on *RXRA* methylation in perinatal tissue (placenta), we collected six placentas from healthy term pregnancies, outside the MAVIDOS trial (with full ethics approval, REC 11/sc/0323), within 30 min of delivery. Placental villous fragments were cultured in buffered solution with or without 20 μM 25-hydroxyvitamin D [25(OH)D] (for detailed methods, see Supplementary Material). The placental samples were snap frozen and stored at −80°C. DNA was extracted, and DNA methylation was measured using the Illumina EPIC 850k array (Illumina, San Diego, CA, USA). CpGs in which DNA methylation was altered were identified using a Wilcoxon signed-rank test. RNA was also extracted, and stranded RNA sequencing was performed; differentially expressed genes following 25(OH)D treatment were identified. In human placental villous fragments, 25(OH)D treatment altered DNA methylation at six CpG sites in the *RXRA* gene: decreased at four CpG sites (-0.80% to −2.67%, $p = 0.04$ and $p = 0.02$, respectively) and increased in two (1.10% to 1.41%, $p = 0.04$ and $p = 0.01$, respectively), as shown in Supplementary Table 6. Through RNA sequencing, RXRA gene expression was shown to increase following 25(OH)D treatment (log fold change 0.50, $p = 0.04$).

Discussion

In this study we have demonstrated, to our knowledge for the first time in a randomized controlled trial setting, that supplementation with cholecalciferol in pregnancy is associated with reduced methylation at specific regions near to the *RXRA* promoter in fetal DNA derived from the umbilical cord of the offspring. Percentage methylation levels measured by pyrosequencing were lower in the cholecalciferol supplemented group than the placebo group (statistically significantly at the cluster of CpG sites represented by CpG 5), raising the possibility of site-specificity for a molecular interaction between 25(OH)D in pregnancy and DNA methylation.[21]

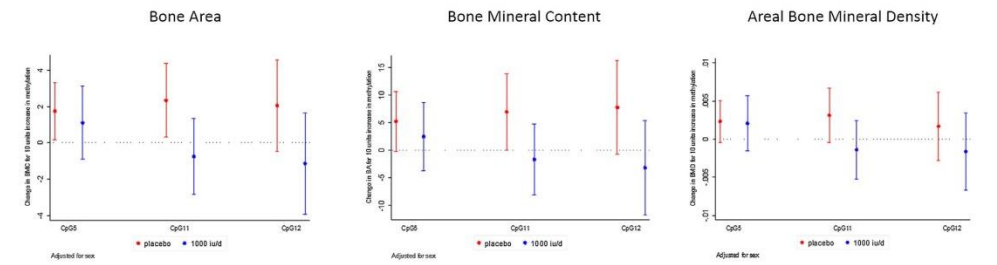

Fig. 3. Associations between *RXRA* methylation at CpG 5, CpG 11, and CpG 12 and whole-body minus head bone area (cm^2), bone mineral content (g), BMD (g/cm^2), adjusted for sex, by treatment group (placebo [red bars] or 1000 IU cholecalciferol daily [blue bars]). Outcomes expressed per 10% increase in methylation.

These results are consistent with our previous observational findings in the SWS, in which a negative association was found between an estimate of maternal-free 25(OH)-vitamin D and *RXRA* methylation at CpG 4/5,[5] measured using the Sequenom MassARRAY EpiTYPER (Sequenom Laboratories, San Diego, CA, USA). Additionally, the associations between *RXRA* methylation and neonatal bone indices in the placebo group replicated those observed previously in the SWS; conversely, in the present study, the direction of the association appeared to be reversed (albeit not reaching statistical significance) in the group whose mothers were supplemented with cholecalciferol. It is interesting that the methylation difference between treatment and placebo groups in the present study was greater in summer than winter births. The increase in 25(OH)D from baseline to 34 weeks was markedly greater for summer than winter deliveries, although the absolute difference between groups at 34 weeks was marginally less in summer than in winter, suggesting that greater increases in 25(OH)D across pregnancy might facilitate methylation differences consequent to vitamin D supplementation. However, given that RXRA interacts with several different nuclear hormone receptors, such as thyroid hormone receptor and PPAR-gamma, activation of either of which tends to have detrimental effects on bone, it is possible that we are seeing the net result of a complex series of interrelationships at this molecular level, with exogenous vitamin D perhaps modifying the balance in RXRA interaction between receptor types, resulting in heterogeneous associations between *RXRA* methylation and bone indices. Such considerations may be relevant both to the skeletal and to the seasonal differences we observed, although ultimately these questions must remain the focus of future research. Interestingly, we observed no consistent associations between maternal 25(OH)D in late pregnancy and *RXRA* methylation, but these measures were in different tissues, 6 weeks apart, and we were able to directly test whether treatment of perinatal tissue (placenta) with vitamin D would alter *RXRA* methylation. Thus, consistent with the findings from the MAVIDOS trial, in a small study of human placental villous fragments *RXRA* methylation appeared to be lowered at several CpG sites by the addition of 25(OH)D, and indeed *RXRA* expression upregulated overall, suggesting a specific role for the vitamin D–*RXRA* interaction.

Although the exact nature of the mechanistic underpinnings of our findings remains to be elucidated, there are several routes by which maternal 25(OH)D status might influence perinatal *RXRA* methylation. As previously stated, RXRA forms a heterodimer with several nuclear hormones known to influence bone metabolism, including $1,25(OH)_2$-vitamin D, perhaps implying that maternal 25(OH)D status plays a permissive role in the transcriptional regulation of the *RXRA* gene. Studies have shown that vitamin D may interact with the epigenome on multiple levels,[17,22–25] and our evaluation of public data from ENCODE suggests that methylation at the studied CpG sites is likely to have functional relevance, with evidence for DNase I hypersensitive regions, enhancer activity, and transcription factor binding. Furthermore, this suggested function within the DMR, which itself resides within the shore region of the 5′ CpG island. This location has been associated with influence on gene expression.[26] Epigenome-wide association studies (EWASs) have also provided some insight into the actions of vitamin D on DNA methylation. A small EWAS of DNA methylation in severely vitamin-D-deficient African-American adolescents demonstrated associations between vitamin D status and methylation in several genes, including genes involved in vitamin D metabolism such as the 24 and 25-hydroxylase genes. In the context of low serum vitamin D levels, the promoter of *CYP2R1* may become methylated; this is reversible on exposure to vitamin D.[27] Other studies have assessed the DNA methylation in CYP enzymes, which are part of the vitamin D metabolism pathway, and found a relationship between methylation of the genes *CYP2R1* (25-hydroxylase) and *CYP24A1* (24-hydroxylase) and variations in circulating 25(OH)D levels.[28] However, a study using the ALSPAC (Avon Longitudinal Study of Parents and Children) cohort and the Norwegian Mother and Child Cohort (MoBa) in which maternal 25(OH)D was measured in midpregnancy, demonstrated no convincing associations between maternal 25(OH)D status and DNA methylation in the umbilical cord blood (as opposed to umbilical cord tissue in our study) of 1416 newborn babies using Illumina 450k DNA methylation array analysis, thereby covering 473,731 CpG DNA methylation sites.[29] The authors suggested that to further identify associations, larger consortium studies, expanded genomic coverage, and the investigation of alternative cell types or 25(OH)D status at different gestational time points might be needed.

The data presented are from a placebo-controlled, double-blind, randomized trial, using the gold standards of pyrosequencing to determine CpG site-specific DNA methylation and DXA to assess bone mass. However, the limitations of our study must be considered. First, we have analyzed methylation in cells from whole umbilical cord; therefore, it is possible that the differential methylation we observed arose from different component cells in individual samples (eg, fibroblasts and epithelial cells). The difference in DNA methylation between treatment and control groups may thus partly reflect different proportions of cells and their cell-specific DNA methylation. However, any unaccounted cell heterogeneity may represent proportional differences that are related to the observed phenotypic outcomes,[30,31] and so potentially on the causal pathway. Second, owing to stipulations made during the ethics approval process, participants with baseline 25(OH)D concentrations less than 25 nmol/L or greater than 100 nmol/L could not be included. In addition, the study population did not include many women who were of nonwhite ethnicity, which again would affect the generalizability of our findings to multiethnic populations. Third, DXA assessment in neonates presents some difficulties, including the low absolute BMC of newborn babies and their tendency to move. However, the validity of DXA in small animals, of comparable size to neonates, has been documented[32] and appropriate DXA software was used. Fourth, some participants were taking vitamin D supplements in addition to the study drug, though supplement use was recorded at interview and did not differ between the treatment groups. Fifth, though we have previously excluded the presence of any SNPs at the CpG sites of interest at the *RXRA* locus by sequencing, we did not have information permitting exclusion of a genetic *cis* or *trans*-effect of local or distant SNPs, respectively. These could influence either associations between vitamin D supplementation and *RXRA* methylation, or influence both *RXRA* methylation and the child's bone phenotype. Sixth, we did not have measurements of 25(OH)D in umbilical cord blood; thus we were not able to directly assess a potential mediating role for 25(OH)D for *RXRA* methylation in the same organ at the same time. Finally, it should be noted that the analysis is

post hoc and that methylation outcomes were not prespecified in the original analysis plan, and so will require replication in further intervention studies.

In conclusion, we have shown in a randomized controlled trial that maternal supplementation with cholecalciferol from 14-weeks' gestation to delivery leads to lower levels of DNA methylation at the *RXRA* promoter in umbilical cord. This informs our understanding of early life mechanisms underpinning maternal vitamin D status, epigenetic change, and bone development, and may suggest a novel biomarker for a child's future bone health.

Disclosures

CC reports personal fees from ABBH, Amgen, Eli Lilly, GSK, Medtronic, Merck, Novartis, Pfizer, Roche, Servier and Takeda, outside the submitted work. NCH reports personal fees, consultancy, lecture fees and honoraria from Alliance for Better Bone Health, AMGEN, MSD, Eli Lilly, Servier, Shire, Radius Health, UCB, Consilient Healthcare and Internis Pharma, outside the submitted work. NJB reports remuneration from Internis Pharmaceuticals Ltd, outside the submitted work. ATP reports grants from Arthritis Research Council, during the conduct of the study. KMG reports reimbursement for speaking at Nestle Nutrition Institute conferences, grants from Abbott Nutrition & Nestec, outside the submitted work; in addition, KMG has a patent Phenotype Prediction pending, a patent Predictive Use of CpG Methylation pending, and a patent Maternal Nutrition Composition pending, not directly related to this work. HMI reports grants from Medical Research Council, Arthritis Research UK, European Union's Seventh Framework Programme, during the conduct of the study; and while not directly receiving funding from other bodies, members of her team have received funding from the following companies from other work: Danone, Nestec, Abbott Nutrition. MKJ reports personal fees from Stirling Anglia, Consilient Health and Internis, outside the submitted work. All other authors have no disclosures.

Acknowledgments

This work was supported by grants from Arthritis Research UK, the Medical Research Council (MRC #4050502589), the Bupa Foundation, the National Institute for Health Research (NIHR) Southampton Biomedical Research Centre, the University of Southampton and University Hospital Southampton NHS Foundation Trust, and the NIHR Oxford Biomedical Research Centre, University of Oxford. EC was supported by the Wellcome Trust (#201268/Z/16/Z). AP was funded by the MRC (programme code #U105960371). The work leading to these results was supported by the European Union's Seventh Framework Programme (#FP7/2007–2013), projects EarlyNutrition and ODIN under grant agreements #289346 and #613977, and by the BBSRC (HDHL-Biomarkers, #BB/P028179/1), as part of the ALPHABET project, supported by an award made through the ERA-Net on Biomarkers for Nutrition and Health (ERA HDHL), Horizon 2020 #696295. We are extremely grateful to Merck GmbH for the kind provision of the Vigantoletten supplement.

Authors' roles: All authors contributed to the preparation and approval of the final manuscript. EMC, NK, EC and NCH prepared the first draft. NK, EC, RM, EG, PC, JC, BA and IS undertook the laboratory analyses. CBG oversaw the bioinformatic analysis. EC, SD, SRC, HMI undertook the statistical analysis. NJB, SK, ATP, RF, SVG, AP, MKJ, NCH and RJM oversaw the MAVIDOS trial at the Oxford, Sheffield and Southampton sites. KAL supervised the laboratory analyses and mechanistic work. NCH and CC supervised the study and the preparation of the manuscript. CC is guarantor.

References

1. Gluckman PD, Hanson MA, Cooper C, Thornburg KL. Effect of in utero and early-life conditions on adult health and disease. N Engl J Med. 2008;359(1):61–73.
2. Harvey N, Dennison E, Cooper C. Osteoporosis: a lifecourse approach. J Bone Miner Res. 2014;29(9):1917–25.
3. Lillycrop KA, Slater-Jefferies JL, Hanson MA, Godfrey KM, Jackson AA, Burdge GC. Induction of altered epigenetic regulation of the hepatic glucocorticoid receptor in the offspring of rats fed a protein-restricted diet during pregnancy suggests that reduced DNA methyltransferase-1 expression is involved in impaired DNA methylation and changes in histone modifications. Br J Nutr. 2007;97(6):1064–73.
4. Burdge GC, Lillycrop KA, Phillips ES, Slater-Jefferies JL, Jackson AA, Hanson MA. Folic acid supplementation during the juvenile-pubertal period in rats modifies the phenotype and epigenotype induced by prenatal nutrition. J Nutr. 2009;139(6):1054–60.
5. Harvey NC, Sheppard A, Godfrey KM, et al. Childhood bone mineral content is associated with methylation status of the RXRA promoter at birth. J Bone Miner Res. 2014;29(3):600–7.
6. Curtis EM, Murray R, Titcombe P, et al. Perinatal DNA methylation at CDKN2A is associated with offspring bone mass: findings from the Southampton Women's Survey. J Bone Miner Res. 2017;32(10):2030–40.
7. Javaid MK, Crozier SR, Harvey NC, et al. Maternal vitamin D status during pregnancy and childhood bone mass at age 9 years: a longitudinal study. Lancet. 2006;367(9504):36–43.
8. Moon RJ, Harvey NC, Davies JH, Cooper C. Vitamin D and bone development. Osteoporos Int. 2015;26(4):1449–51.
9. Harvey NC, Holroyd C, Ntani G, et al. Vitamin D supplementation in pregnancy: a systematic review. Health Technol Assess. 2014;18(45):1–190.
10. Cooper C, Harvey NC, Bishop NJ, et al. Maternal gestational vitamin D supplementation and offspring bone health (MAVIDOS): a multicentre, double-blind, randomized placebo-controlled trial. Lancet Diabetes Endocrinol. 2016;4(5):393–402.
11. Harvey NC, Javaid K, Bishop N, et al. MAVIDOS Maternal Vitamin D Osteoporosis Study: study protocol for a randomized controlled trial. The MAVIDOS Study Group. Trials. 2012;13:13.
12. Jones KS, Assar S, Harnpanich D, et al. 25(OH)D2 half-life is shorter than 25(OH)D3 half-life and is influenced by DBP concentration and genotype. J Clin Endocrinol Metab. 2014;99(9):3373–81.
13. Sempos CT, Vesper HW, Phinney KW, Thienpont LM, Coates PM. Vitamin D status as an international issue: national surveys and the problem of standardization. Scand J Clin Lab Invest Suppl. 2012;243:32–40.
14. BLUEPRINT_Consortium. Quantitative comparison of DNA methylation assays for biomarker development and clinical applications. Nat Biotechnol. 2016;34(7):726–37.
15. Schulz KF, Grimes DA. Multiplicity in randomized trials I: endpoints and treatments. Lancet. 2005;365(9470):1591–5.
16. Newson R, B. Frequentist q-values for multiple-test procedures. Stata J. 2010;10(4):568–84.
17. The ENCODE Project Consortium. An integrated encyclopedia of DNA elements in the human genome. Nature. 2012;489(7414):57–74.
18. He Y, Carrillo JA, Luo J, et al. Genome-wide mapping of DNase I hypersensitive sites and association analysis with gene expression in MSB1 cells. Front Genet. 2014;5:308.
19. Schubeler D. Function and information content of DNA methylation. Nature. 2015;517(7534):321–6.
20. Burke RE, McGuire WL. Nuclear thyroid hormone receptors in a human breast cancer cell line. Cancer Res. 1978;38(11 Pt 1):3769–73.
21. Jones PA. Functions of DNA methylation: islands, start sites, gene bodies and beyond. Nat Rev Genet. 2012;13(7):484–92.

22. Carlberg C. Molecular endocrinology of vitamin D on the epigenome level. Mol Cell Endocrinol. 2017;453:14–21.
23. Takeyama K, Kato S. The vitamin D3 1alpha-hydroxylase gene and its regulation by active vitamin D3. Biosci Biotechnol Biochem. 2011;75(2):208–13.
24. Karlic H, Varga F. Impact of vitamin D metabolism on clinical epigenetics. Clin Epigenetics. 2011;2(1):55–61.
25. Fetahu IS, Höbaus J, Kállay E. Vitamin D and the epigenome. Front Physiol. 2014;5:164.
26. Irizarry RA, Ladd-Acosta C, Wen B, et al. The human colon cancer methylome shows similar hypo- and hypermethylation at conserved tissue-specific CpG island shores. Nat Genet. 2009;41 (2):178–86.
27. Zhu H, Wang X, Shi H, et al. A genome-wide methylation study of severe vitamin D deficiency in African American adolescents. J Pediatr. 2013;162(5):1004–9.e1.
28. Zhou Y, Zhao LJ, Xu X, et al. DNA methylation levels of CYP2R1 and CYP24A1 predict vitamin D response variation. J Steroid Biochem Mol Biol. 2014;144 Pt A:207–14.
29. Suderman M, Stene LC, Bohlin J, et al. 25-Hydroxyvitamin D in pregnancy and genome wide cord blood DNA methylation in two pregnancy cohorts (MoBa and ALSPAC). J Ster Biochem Mol Biol. 2016;159:102–9.
30. Bauer M, Fink B, Thurmann L, Eszlinger M, Herberth G, Lehmann I. Tobacco smoking differently influences cell types of the innate and adaptive immune system-indications from CpG site methylation. Clin Epigenetics. 2015;7:83.
31. Lappalainen T, Greally JM. Associating cellular epigenetic models with human phenotypes. Nat Rev Genet. 2017;18(7):441–51.
32. Brunton JA, Bayley HS, Atkinson SA. Validation and application of dual-energy x-ray absorptiometry to measure bone mass and body composition in small infants. Am J Clin Nutr. 1993;58(6):839–45.

Supplementary Material

Online Supplementary Table 1: Percentage DNA methylation at *RXRA* in umbilical cord tissue of offspring. DMR: Chromosome 9: 137215735- 137216064, Human genome hg19/GRCh37 build (Human genome hg19/GRCh37 build). Pyrosequencing was not performed at CpG 6 and 7.

CpG position	Distance from transcriptional start site (bases)	Human genome 19 coordinates	N	Min (25^{th}, 50^{th}, 75^{th} percentile) Max	Mean (SD)
1	-2686	137215735	446	16.9 (27.5, 31.7, 38.6) 70.6	34.0 (9.7)
2	-2682	137215739	449	37.2 (50.0, 54.9, 59.5) 89.5	55.5 (8.0)
3	-2673	137215748	450	21.0 (30.3, 34.8, 41.4) 70.0	36.6 (9.1)
4	-2649	137215772	444	32.5 (44.7, 49.3, 55.2) 80.4	50.7 (8.7)
5	-2642	137215779	447	29.0 (41.5, 46.5, 52.5) 81.4	47.7 (9.0)
6	-2554	137215867			
7	-2465	137215956			
8	-2406	137216015	449	44.6 (58.9, 63.0, 67.2) 84.5	63.1 (6.2)
9	-2391	137216030	448	29.4 (46.4, 50.5, 55.6) 80.6	51.5 (8.0)
10	-2387	137216034	447	46.9 (60.7, 64.7, 69.6) 88.9	65.5 (7.1)
11	-2385	137216036	446	37.8 (53.6, 57.5, 63.4) 84.9	58.6 (7.8)
12	-2357	137216064	446	46.1 (62.5, 66.1, 70.7) 86.1	66.5 (6.2)

Appendix E

Online Supplementary Table 2: CpG Clustering. Pearson's / Spearman's correlation of methylation levels at CpGs 1-9 within the *RXRA* region. 3 distinct clusters are defined. (A) Correlations in the MAVIDOS trial (dark green r≥0.90, pale green r≥0.80, yellow r≥0.70, orange r≥0.60, red r≥0.50). (B) Median absolute deviation (MAD) scores within the 3 clusters in MAVIDOS trial.

	RXRA CpG 1†	*RXRA* CpG 2	*RXRA* CpG 3†	*RXRA* CpG 4	*RXRA* CpG 5	*RXRA* CpG 8	*RXRA* CpG 9	*RXRA* CpG 10	*RXRA* CpG 11
RXRA CpG 1†	1								
RXRA CpG 2	0.89	1							
RXRA CpG 3†	0.93	0.93	1						
RXRA CpG 4	0.91	0.9462	0.91	1					
RXRA CpG 5	0.90	0.9202	0.89	0.9464	1				
RXRA CpG 8	0.69	0.7687	0.70	0.7715	0.7566	1			
RXRA CpG 9	0.78	0.8094	0.77	0.8182	0.8176	0.788	1		
RXRA CpG 10	0.78	0.8257	0.77	0.846	0.8312	0.8532	0.899	1	
RXRA CpG 11	0.79	0.8207	0.78	0.8451	0.835	0.8283	0.886	0.9345	1
RXRA CpG 12	0.57	0.6091	0.54	0.6578	0.6413	0.8265	0.6286	0.738	0.7297

† Spearman correlation used for CpG1 and CpG3

Online Supplementary Table 3: *RXRA* Median Absolute deviation scores

Cluster	CpG site	MAD score
CpG 1-5	1	5.26
	2	4.92
	3	5.35
	4	5.03
	5	**5.41**
CpG 8-11	8	4.16
	9	4.58
	10	4.25
	11	**4.66**
CpG 12	**12**	**3.98**

Online Supplementary Table 4: *RXRA* DNA methylation in cholecalciferol 1000 IU/day supplemented[a] and placebo[b] groups at all CpG sites studied. p-values < 0.05 are in bold. q-values were obtained using the Simes method.

CpG	n	% methylation Cholecalciferol 1000 IU/day[a]	% methylation Placebo[b]	Mean difference % methylation (a-b)	95% CI	p difference	q value
RXRA CpG 1†	446	31.4 (27.1,37.8)	32.3 (27.9,40.6)	-0.17	-0.35, 0.02	0.1	0.183
RXRA CpG 2	449	54.6 (7.5)	56.5 (8.4)	**-1.86***	**-3.34, -0.37**	**0.01**	0.100
RXRA CpG 3†	450	33.9 (29.7,40.7)	35.8 (31.0,42.5)	**-0.19***	**-0.37, -0.008**	**0.04**	0.100
RXRA CpG 4	444	49.8 (8.0)	51.5 (9.3)	**-1.70***	**-3.32, -0.08**	**0.04**	0.100
RXRA CpG 5	447	46.7 (8.2)	48.7 (9.7)	**-1.98***	**-3.65, -0.32**	**0.02**	0.100
RXRA CpG 8	449	62.7 (5.9)	63.6 (6.5)	-0.92	-2.07, 0.22	0.11	0.183
RXRA CpG 9	448	51.1 (7.5)	52.0 (8.5)	-0.95	-2.44, 0.53	0.21	0.233
RXRA CpG 10	447	65.1 (6.8)	66.0 (7.5)	-0.88	-2.20, 0.45	0.19	0.233
RXRA CpG 11	446	58.3 (7.5)	58.9 (8.1)	-0.67	-2.12, 0.78	0.36	0.360
RXRA CpG 12	446	66.1 (5.8)	66.9 (6.6)	-0.84	-1.99, 0.31	0.15	0.214

Online Supplementary Table 5: Relationships between perinatal methylation in umbilical cord at CpG sites within the *RXRA* region of interest and bone outcomes at birth (measured by DXA, whole body minus head), stratified by placebo and 1000IU / day cholecalciferol supplemented groups. Associations are adjusted for sex. β coefficients and 95% CIs have been multiplied by 10 and therefore represent the change associated with a 10% increase in methylation. p-values < 0.05 are in bold.

	BA, (cm^2)				**BMC, (g)**				**aBMD, (g/cm^2)**			
	Placebo		**1000 IU/d**		**Placebo**		**1000 IU/d**		**Placebo**		**1000 IU/d**	
	β (95% CI)	p	β (95% CI)	p	β (95% CI)	p	β (95% CI)	p	β (95% CI)	p	β (95% CI)	p
RXRA CpG 5	5.22 (-0.18, 10.62)	0.06	2.42(-3.78,8.61)	0.44	**1.75 (0.17, 3.33)**	**0.03**	1.08(-0.93, 3.08)	0.29	0.00(-0.00, 0.01)	0.10	0.00(-0.00, 0.01)	0.27
RXRA CpG 11	**6.96 (0.09, 13.82)**	**0.05**	-1.74(-8.17, 4.69)	0.59	**2.34 (0.32, 4.37)**	**0.02**	-0.78(-2.87, 1.31)	0.46	0.00(-0.00, 0.01)	0.08	-0.00(-0.01, 0.00)	0.46
RXRA CpG 12	7.76 (-0.77, 16.28)	0.07	-3.29(-11.86, 5.27)	0.45	2.05(-0.47, 4.57)	0.11	-1.18(-3.96, 1.60)	0.41	0.00(-0.00, 0.01)	0.46	-0.00(-0.01, 0.00)	0.51

(BA: bone area; BMC: bone mineral content; aBMD: areal bone mineral density)

Online Supplementary Figure 1: Location of CpG dinucleotides in the *RXRA* region. Region of interest: (chr9: 137215735- 137216064). (Human genome hg19/GRCh37 build). Local gene layout is shown with relevant distances marked in base-pairs (bp) from the transcriptional start site (TSS) of *RXRA*. The CpG dinucleotides of interest are marked on an annotated primary sequence.

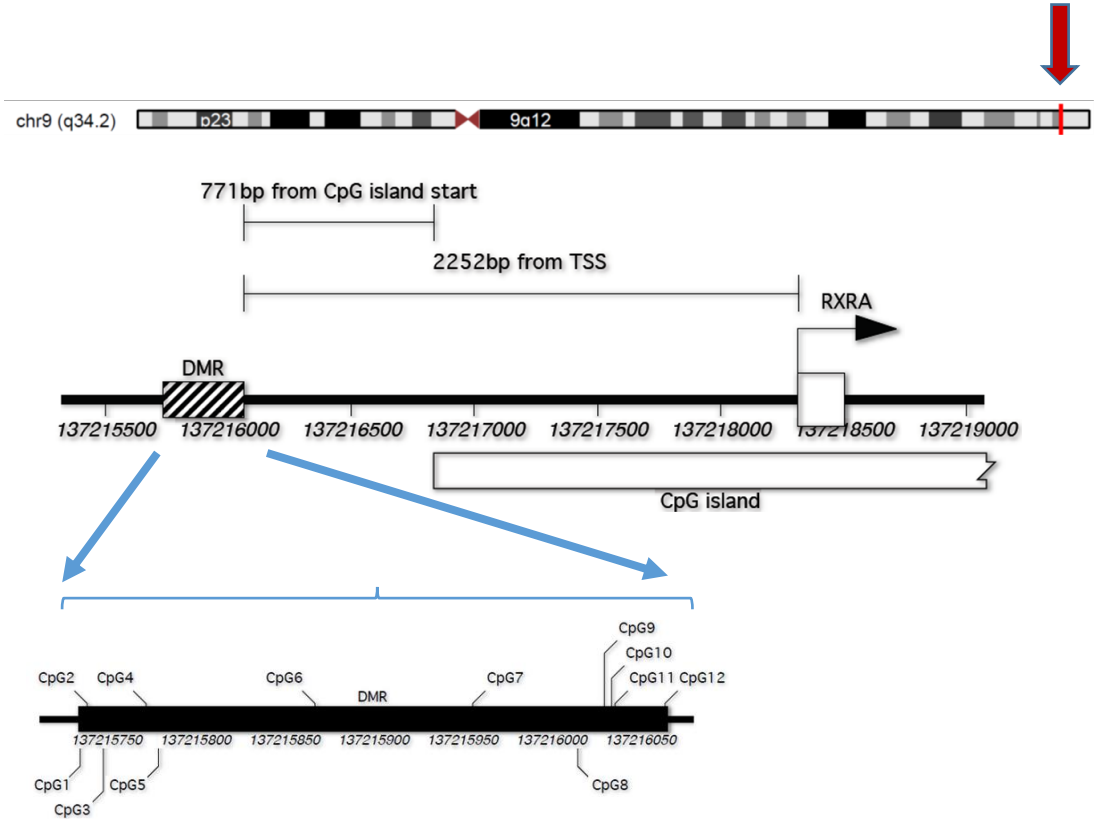

Online Supplementary Figure 2: UCSC- Human Genome Reference Sequence annotation for the *RXRA* region, Feb. 2009 (GRCh37/hg19) Assembly. The *RXRA* DMR is annotated in purple. DNase1 hypersensitivity (HS) clusters are displayed across 125 cell types, with examples of DNase1 HS peaks demonstrated in chorion and osteoblast cells. Enrichment of Transcription Factor binding sites (Transcription Factor CHIP-seq (161 factors) are outlined, with an example of peaks overlying the *RXRA* DMR in MCF-7 cells. Enhancer related mono-methylation of lysine 4 of the H3 histone protein (H3K4me1) are demonstrated. Genome segmentations from ENCODE across a variety of cells demonstrate the following predicted functional regions: in red, promoter regions; orange, enhancers; yellow, weak enhancers or open chromatin cis regulatory elements; blue, CTCF transcriptional repressor enriched element; grey, predicted repressed regions. A yellow weak enhancer region is shown in the region of the *RXRA* DMR.

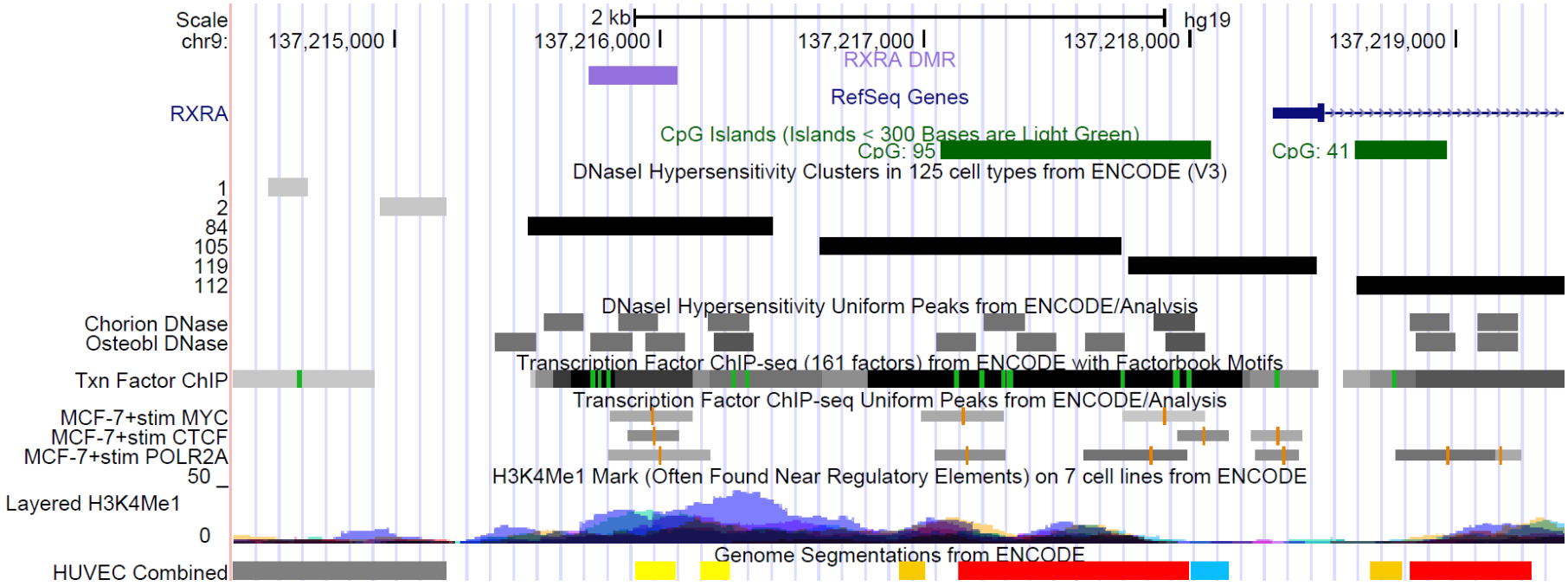

Online Supplementary Methods: Human Placental Data

Placental samples: The study was conducted according to the guidelines in the Declaration of Helsinki, and the Southampton and South West Hampshire Research Ethics Committee approved all procedures (REC 11/sc/0323). Written informed consent was obtained from all participating women.

Placentas (n = 6) were collected from healthy term pregnancies, not within the MAVIDOS trial, within 30 min of delivery. Placental villous tissue fragments were cultured at 37˚C for 8 h in Tyrode's buffer containing 0.7 mM albumin with or without 20 µM 25-hydroxyvitamin D [25(OH)D], and then snap frozen and stored at -80°C.

DNA Methylation: DNA was extracted from placental samples using the DNeasy Blood & Tissue Kit (Qiagen, UK) according to manufacturer's instructions. DNA methylation was measured using the Illumina EPIC 850K array and altered CpGs with Vitamin D treatment were identified using a Wilcoxon signed-rank test ($p < 0.05$).

RNA Sequencing: RNA was extracted from placental samples using the miRNeasy mini kit (Qiagen, UK) according to manufacturer's instructions. Stranded RNA sequencing was carried out by Expression Analysis (Durham, North Carolina, USA) using HiSeq 2x50bp paired-end sequencing on an Illumina platform. Analysis was performed by Expression Analysis to identify the differentially expressed genes following 25(OH)D treatment ($p < 0.05$), using their in-house developed RNA-Seq bioinformatics pipeline (version 9) which uses a variety of internally developed and open source programs (https://expressionanalysis.github.io/ea-utils/).

Online Supplementary Table 6

Comparison between *RXRA* methylation at CpG sites in proximity to the *RXRA* gene in human placental villous tissue fragments cultured with or without 20 μM cholecalciferol (n=6). Region: Chromosome 9: 137218286- 1137301309, Human genome hg19/GRCh37 build.

CpG	Distance from transcriptional start site (bases)	Human genome 19 coordinates	% difference in methylation (cholecalciferol treatment - no cholecalciferol treatment)	P-value
cg15266275	44772	137263193	-1.89	0.01
cg13689699	6890	137225311	1.41	0.01
cg14051721	82888	137301309	-2.67	0.02
cg02059519	32514	137250935	-0.80	0.04
cg09800519	-135	137218286	1.10	0.04
cg10984912	79935	137298356	-1.26	0.02

List of References

ABRAHAMS, V. M., KIM, Y. M., STRASZEWSKI, S. L., ROMERO, R. & MOR, G. 2004. Macrophages and apoptotic cell clearance during pregnancy. *Am J Reprod Immunol,* 51**,** 275-82.

ACHKAR, M., DODDS, L., GIGUERE, Y., FOREST, J. C., ARMSON, B. A., WOOLCOTT, C., AGELLON, S., SPENCER, A. & WEILER, H. A. 2015. Vitamin D status in early pregnancy and risk of preeclampsia. *Am J Obstet Gynecol,* 212**,** 511.e1-7.

AL-AMIN, A., HINGSTON, T., MAYALL, P., ARAUJO JUNIOR, E., FABRICIO DA SILVA, C. & FRIEDMAN, D. 2015. The utility of ultrasound in late pregnancy compared with clinical evaluation in detecting small and large for gestational age fetuses in low-risk pregnancies. *J Matern Fetal Neonatal Med,* 28**,** 1495-9.

ALBU, A. R., ANCA, A. F., HORHOIANU, V. V. & HORHOIANU, I. A. 2014. Predictive factors for intrauterine growth restriction. *J Med Life,* 7**,** 165-71.

AN, S., YEO, K., JEON, Y. & SONG, J. 2007. Crystal Structure of the Human Histone Methyltransferase ASH1L Catalytic Domain and Its Implications for the Regulatory Mechanism. *The Journal of Biological Chemistry,* 286**,** 8369-8374.

ANDERSON, P., TURNER, A. & MORRIS, H. 2012. Vitamin D actions to regulate calcium and skeletal homeostasis. *Clinical Biochemistry,* 45**,** 880-886.

APLIN, J. D. 2000. The cell biological basis of human implantation. *Baillieres Best Pract Res Clin Obstet Gynaecol,* 14**,** 757-64.

ARMAS, L. A., HOLLIS, B. W. & HEANEY, R. P. 2004. Vitamin D2 is much less effective than vitamin D3 in humans. *J Clin Endocrinol Metab,* 89**,** 5387-91.

BAIRD, J., BARKER, M., HARVEY, N. C., LAWRENCE, W., VOGEL, C., JARMAN, M., BEGUM, R., TINATI, T., MAHON, P., STROMMER, S., ROSE, T., INSKIP, H. & COOPER, C. 2016. Southampton PRegnancy Intervention for the Next Generation (SPRING): protocol for a randomised controlled trial. *Trials,* 17**,** 493.

BAKER, A. M., HAERI, S., CAMARGO, C. A., JR., ESPINOLA, J. A. & STUEBE, A. M. 2010. A nested case-control study of midgestation vitamin D deficiency and risk of severe preeclampsia. *J Clin Endocrinol Metab,* 95**,** 5105-9.

BANISTER, C. E., KOESTLER, D. C., MACCANI, M. A., PADBURY, J. F., HOUSEMAN, E. A. & MARSIT, C. J. 2011. Infant growth restriction is associated with distinct patterns of DNA methylation in human placentas. *Epigenetics,* 6**,** 920-7.

BARKER, D. 1989. The intrauterine and early postnatal origins of cardiovascular disease and chronic bronchitis. *In:* OSMOND, C. L., C. (ed.). Journal of Epidemiology and Community Health.

BARKER, D. J. 1990. The fetal and infant origins of adult disease. *Bmj,* 301**,** 1111.

BARKER, D. J. 1995. Fetal origins of coronary heart disease. *Bmj,* 311**,** 171-4.

BARKER, D. J., OSMOND, C., THORNBURG, K. L., KAJANTIE, E. & ERIKSSON, J. G. 2013. The shape of the placental surface at birth and colorectal cancer in later life. *Am J Hum Biol,* 25**,** 566-8.

BARKER, D. J., THORNBURG, K. L., OSMOND, C., KAJANTIE, E. & ERIKSSON, J. G. 2010. The surface area of the placenta and hypertension in the offspring in later life. *Int J Dev Biol,* 54**,** 525-30.

BENIRSCHKE, K., KAUFMANN, P. & BAERGEN, R. 2006. *Pathology of the Human Placenta*, Springer.

BERCIANO, J., GALLARDO, E., GARCI, A., RAMO, C., INFANTE, J. & COMBARROS, O. 2010. Clinical progression in Charcot–Marie-Tooth disease type 1A duplication: clinico-electrophysiological and MRI longitudinal study of a family. *Journal of Neurology,* 257**,** 1633-1641.

BERGH, P. A. & NAVOT, D. 1992. The impact of embryonic development and endometrial maturity on the timing of implantation. *Fertil Steril,* 58**,** 537-42.

BESTA, C., PRESSMANB, E., QUEENANB, R., COOPER, E. & O'BRIEN, K. 2019. Longitudinal changes in serum vitamin D binding protein and free 25-hydroxyvitamin D in a multiracial cohort of pregnant adolescents. *Journal of Steroid Biochemistry and Molecular Biology,* 186**,** 79-88.

BODNAR, L., SIMHAN, H., CATOV, J., ROBERTS, J., PLATT, R., DIESEL, J. & KLEBANOFF, M. 2014. Maternal vitamin d status and the risk of mild and severe preeclampsia. *Epidemiology,* 25**,** 207-14.

BOUW, G. M., STOLTE, L. A. M., BAAK, J. P. A. & OORT, J. 1976. Quantitative morphology of the placenta 1. Standardization of sampling. *European Journal of Obstetrics & Gynecology,* 6**,** 325-331.

BURKE, K. A., JAUNIAUX, E., BURTON, G. J. & CINDROVA-DAVIES, T. 2013. Expression and immunolocalisation of the endocytic receptors megalin and cubilin in the human yolk sac and placenta across gestation. *Placenta,* 34**,** 1105-9.

BURTON, G. & FOWDEN, A. 2015. The placenta: a multifaceted, transient organ. *Philosophical transactions of the Royal Society,* 370.

BURTON, G., REDMAN, C., ROBERTS, J. & MOFFETT, A. 2019. Pre-eclampsia: pathophysiology and clinical implications. *The BMJ,* 366.

CAPIATI, D., BENASSATI, S. & BOLAND, R. 2002. 1,25$(OH)_2$-Vitamin D_3 Induces Translocation of the Vitamin D Receptor (VDR) to the Plasma Membrane in Skeletal Muscle Cells. *Journal of Cellular Biochemistry,* 86**,** 128-135.

CARMELIET, G., DERMAUW, V. & BOUILLON, R. 2015. Vitamin D signaling in calcium and bone homeostasis: A delicate balance. *Best Practice & Research Clinical Endocrinology & Metabolism,* 29**,** 621-631.

CASTELLANO-CASTILLO, D., MORCILLO, S., CRUJEIRAS, A., SÁNCHEZ-ALCOHOLADO, L., CLEMENTE-POSTIGO, M., TORRES, E., TINAHONES, F. & MACIAS-GONZALEZ, M. 2019. Association between serum 25-hydroxyvitamin D and global DNA methylation in visceral adipose tissue from colorectal cancer patients. *BMC Cancer,* 19.

CETIN, I., DE SANTIS, M. S., TARICCO, E., RADAELLI, T., TENG, C., RONZONI, S., SPADA, E., MILANI, S. & PARDI, G. 2005. Maternal and fetal amino acid concentrations in normal pregnancies and in pregnancies with gestational diabetes mellitus. *Am J Obstet Gynecol,* 192**,** 610-7.

CHAVAN-GAUTAM, P., SUNDRANI, D., PISAL, H., NIMBARGI, V., MEHENDALE, S. & JOSHI, S. 2011. Gestation-dependent changes in human placental global DNA methylation levels. *Mol Reprod Dev,* 78**,** 150.

CHEN, Y. Y., POWELL, T. L. & JANSSON, T. 2016. 1,25-Dihydroxy vitamin D3 stimulates system A amino acid transport in primary human trophoblast cells. *Mol Cell Endocrinol,* 442**,** 90-97.

CHRISTAKOS, S., DHAWAN, P., VERSTUYF, A., VERLINDEN, L. & CARMELIET, G. 2016. Vitamin D: Metabolism, Molecular Mechanism of Action, and Pleiotropic Effects. *Physiol Rev,* 96**,** 365-408.

CHRISTAKOS, S., HEWISON, M., GARDNER, D. G., WAGNER, C. L., SERGEEV, I. N., RUTTEN, E., PITTAS, A. G., BOLAND, R., FERRUCCI, L. & BIKLE, D. D. 2013. Vitamin D: beyond bone. *Ann N Y Acad Sci,* 1287**,** 45-58.

CHRISTOFIDES, A., KARANTANOS, T., BARDHAN, K. & BOUSSIOTIS, V. 2016. Epigenetic regulation of cancer biology and anti-tumor immunity by EZH2. *Oncotarget,* 7**,** 85624-85640.

CLEAL, J., LOFTHOUSE, E., SENGERS, B. & LEWIS, R. 2018. A systems perspective on placental amino acid transport. *The Journal of Physiology,* 596**,** 5511-5522.

CLEAL, J. K., BROWNBILL, P., GODFREY, K. M., JACKSON, J. M., JACKSON, A. A., SIBLEY, C. P., HANSON, M. A. & LEWIS, R. M. 2007. Modification of fetal plasma amino acid composition by placental amino acid exchangers in vitro. *J Physiol,* 582**,** 871-82.

CLEAL, J. K., DAY, P. E., HANSON, M. A. & LEWIS, R. M. 2009. Measurement of housekeeping genes in human placenta. *Placenta,* 30**,** 1002-1003.

CLEAL, J. K., DAY, P. E., SIMNER, C. L., BARTON, S. J., MAHON, P. A., INSKIP, H. M., GODFREY, K., HANSON, M. A., COOPER, C., LEWIS, R. M., HARVEY, N. C. & GROUP, S. S. 2015. Placental

amino acid transport may be regulated by maternal vitamin D and vitamin D-binding protein: results from the Southampton Women's Survey. *British Journal of Nutrition*.

CLEAL, J. K., GLAZIER, J. D., NTANI, G., CROZIER, S. R., DAY, P. E., HARVEY, N. C., ROBINSON, S. M., COOPER, C., GODFREY, K. M., HANSON, M. A. & LEWIS, R. M. 2011. Facilitated transporters mediate net efflux of amino acids to the fetus across the basal membrane of the placental syncytiotrophoblast. *J Physiol,* 589**,** 987-97.

CLEAL, J. K. & LEWIS, R. M. 2016. Chapter 22 - The Placenta and Developmental Origins of Health and Disease A2 - Rosenfeld, Cheryl S. *The Epigenome and Developmental Origins of Health and Disease.* Boston: Academic Press.

CLEMENS, R., NEWBROUGH, S., CHUNG, E., GHEITH, S., SINGER, A., KORETZKY, G. & PETERSON, E. 2004. PRAM-1 Is Required for Optimal Integrin-Dependent Neutrophil Function. *Molecular and Cellular Biology,* 24.

COAD, J. & DUNSTALL, M. 2011. *Anatomy and Physiology for Midwives*, Elsevier.

CONSTANCIA, M., ANGIOLINI, E., SANDOVICI, I., SMITH, P., SMITH, R., KELSEY, G., DEAN, W., FERGUSON-SMITH, A., SIBLEY, C. P., REIK, W. & FOWDEN, A. 2005. Adaptation of nutrient supply to fetal demand in the mouse involves interaction between the Igf2 gene and placental transporter systems. *Proc Natl Acad Sci U S A,* 102**,** 19219-24.

COOPER, C., FALL, C., EGGER, P., HOBBS, R., EASTELL, R. & BARKER, D. 1997. Growth in infancy and bone mass in later life. *Ann Rheum Dis,* 56**,** 17-21.

COOPER, C., HARVEY, N. C., BISHOP, N. J., KENNEDY, S., PAPAGEORGHIOU, A. T., SCHOENMAKERS, I., FRASER, R., GANDHI, S. V., CARR, A., D'ANGELO, S., CROZIER, S. R., MOON, R. J., ARDEN, N. K., DENNISON, E. M., GODFREY, K. M., INSKIP, H. M., PRENTICE, A., MUGHAL, M. Z., EASTELL, R., REID, D. M. & JAVAID, M. K. 2016. Maternal gestational vitamin D supplementation and offspring bone health (MAVIDOS): a multicentre, double-blind, randomised placebo-controlled trial. *Lancet Diabetes Endocrinol,* 4**,** 393-402.

CORCORAN, J. J., NICHOLSON, C., SWEENEY, M., CHARNOCK, J. C., ROBSON, S. C., WESTWOOD, M. & TAGGART, M. J. 2014. Human uterine and placental arteries exhibit tissue-specific acute responses to 17beta-estradiol and estrogen-receptor-specific agonists. *Mol Hum Reprod,* 20**,** 433-41.

COSTA, M. A. 2016. The endocrine function of human placenta: an overview. *Reprod Biomed Online,* 32**,** 14-43.

COTTRELL, E. C., SECKL, J. R., HOLMES, M. C. & WYRWOLL, C. S. 2014. Foetal and placental 11beta-HSD2: a hub for developmental programming. *Acta Physiol (Oxf),* 210**,** 288-95.

CROZIER, S. R., HARVEY, N. C., INSKIP, H. M., GODFREY, K. M., COOPER, C. & ROBINSON, S. M. 2012. Maternal vitamin D status in pregnancy is associated with adiposity in the offspring: findings from the Southampton Women's Survey. *Am J Clin Nutr,* 96**,** 57-63.

CURTIS, E., KRSTIC, N., COOK, E., D'ANGELO, S., CROZIER, S., MOON, R., MURRAY, R., GARRATT, E., COSTELLO, P., CLEAL, J., ASHLEY, B., BISHOP, N., KENNEDY, S., PAPAGEORGHIOU, A., SCHOENMAKERS, I., FRASER, R., GANDHI, S., PRENTICE, A., JAVAID, K., INSKIP, H., GODFREY, K., BELL, C., LILLYCROP, K., COOPER, C., HARVEY, N. & GROUP, M. T. 2019. Gestational Vitamin D Supplementation Leads to Reduced Perinatal RXRA DNA Methylation: Results From the MAVIDOS Trial. *The Journal of Bone and Mineral Research,* 34**,** 231-240.

CUTTER, A. R. & HAYES, J. J. 2015. A brief review of nucleosome structure. *FEBS Lett,* 589**,** 2914-22.

DAMGAARD, R., WALKER, J., MARCO-CASANOVA, P., MORGAN, N., TITHERADGE, H., ELLIOTT, P., MCHALE, D., MAHER, E., MCKENZIE, A. & KOMANDER, D. 2016. The Deubiquitinase OTULIN Is an Essential Negative Regulator of Inflammation and Autoimmunity. *Cell,* 166**,** 1215-1230.

DARAKI, V., ROUMELIOTAKI, T., CHALKIADAKI, G., KATRINAKI, M., KARACHALIOU, M., LEVENTAKOU, V., VAFEIADI, M., SARRI, K., VASSILAKI, M., PAPAVASILIOU, S., KOGEVINAS, M. & CHATZI, L. 2018. Low maternal vitamin D status in pregnancy increases the risk of childhood obesity. *Paediatric Obesity,* 13**,** 467-475.

DAS, U. G. & SYSYN, G. D. 2004. Abnormal fetal growth: intrauterine growth retardation, small for gestational age, large for gestational age. *Pediatr Clin North Am,* 51**,** 639-54, viii.

DAUTZENBERGA, F., KILPATRICK, G., HAUGERC, R. & MOREAU, J. 2001. Molecular biology of the CRH receptors— in the mood. *Peptides,* 22**,** 753-760.

DAY, P. E., CLEAL, J. K., LOFTHOUSE, E. M., GOSS, V., KOSTER, G., POSTLE, A., JACKSON, J. M., HANSON, M. A., JACKSON, A. A. & LEWIS, R. M. 2013. Partitioning of glutamine synthesised by the isolated perfused human placenta between the maternal and fetal circulations. *Placenta,* 34**,** 1223-31.

DAY, P. E., NTANI, G., CROZIER, S. R., MAHON, P. A., INSKIP, H. M., COOPER, C., HARVEY, N. C., GODFREY, K. M., HANSON, M. A., LEWIS, R. M. & CLEAL, J. K. 2015. Maternal Factors Are Associated with the Expression of Placental Genes Involved in Amino Acid Metabolism and Transport. *PLoS One,* 10**,** e0143653.

DEATON, A. & BIRD, A. 2011. CpG islands and the regulation of transcription. *Genes and Development,* 25**,** 1010-1022.

DEISING, D., CORDES, T., FISCHER, D., DIEDRICH, K. & FRIEDRICH, M. 2006. Vitamin D – Metabolism in the Human Breast Cancer Cell Line MCF-7. *Anticancer Research,* 26.

DENNISON, E. M., SYDDALL, H. E., SAYER, A. A., GILBODY, H. J. & COOPER, C. 2005. Birth weight and weight at 1 year are independent determinants of bone mass in the seventh decade: the Hertfordshire cohort study. *Pediatr Res,* 57**,** 582-6.

DESHPANDE, S. & BALASINOR, N. 2018. Placental Defects: An Epigenetic Perspective. *Reproductive Sciences,* 25**,** 1143-1160.

DI, W. L., LACHELIN, G. C., MCGARRIGLE, H. H., THOMAS, N. S. & BECKER, D. L. 2001. Oestriol and oestradiol increase cell to cell communication and connexin43 protein expression in human myometrium. *Mol Hum Reprod,* 7**,** 671-9.

DOHERTY, G. J. & MCMAHON, H. T. 2009. Mechanisms of endocytosis. *Annu Rev Biochem,* 78**,** 857-902.

DOIG, C., SINGH, P., DHIMAN, V., THORNE, J., BATTAGLIA, S., SOBOLEWSKI, M., MAGUIRE, O., O'NEILL, L., TURNER, B., MCCABE, C., SMIRAGLIA, D. & CAMPBELL, M. 2013. Recruitment of NCOR1 to VDR target genes is enhanced in prostate cancer cells and associates with altered DNA methylation patterns. *Carcinogenesis,* 34**,** 248-256.

DOLPHIN, A. 2016. Voltage-gated calcium channels and their auxiliary subunits: physiology and pathophysiology and pharmacology. *The Journal of Physiology,* 594**,** 5369-5390.

DOMINSKI, Z., YANG, X., KAYGUN, H., DADLEZ, M. & MARZLUFF, W. 2003. A 3' Exonuclease that Specifically Interacts with the 3' End of Histone mRNA. *Molecular Cell,* 12**,** 295-305.

DOVNIK, A. & MUJEZINOVI, F. 2018. The Association of Vitamin D Levels with Common Pregnancy Complications. *Nutrients,* 10.

DURSUN, E. & GEZEN-AK, D. 2017. Vitamin D receptor is present on the neuronal plasma membrane and is co-localized with amyloid precursor protein, ADAM10 or Nicastrin. *PLoS ONE,* 12.

EDE, G., KESKIN, U., YENEN, M. & SAMUR, G. 2019. Lower vitamin D levels during the second trimester are associated with developing gestational diabetes mellitus: an observational cross-sectional study. *Gynecological Endocrinology*.

EDVARDSON, S., WANG, H., DOR, T. & ATAWNEH, O. Y., B. GARTNER, G CINNAMON, Y. CHEN, S. ELPELEG, S. 2016. Microcephaly-dystonia due to mutated PLEKHG2 with impaired actin polymerization. *Neurogenetics,* 17**,** 25-30.

EGGEMOEN, A., JENUM, A., MDALA, I., KNUTSEN, K., LAGERLØV, P. & SLETNER, L. 2017. Vitamin D levels during pregnancy and associations with birth weight and body composition of the newborn: a longitudinal multiethnic population-based study. *British Journal of Nutrition,* 117**,** 985-993.

EL HAJJ, N., PLIUSHCH, G., SCHNEIDER, E., DITTRICH, M., MULLER, T., KORENKOV, M., ARETZ, M., ZECHNER, U., LEHNEN, H. & HAAF, T. 2013. Metabolic programming of MEST DNA methylation by intrauterine exposure to gestational diabetes mellitus. *Diabetes,* 62**,** 1320-8.

ERIKSSON, J. G. 2016. Developmental Origins of Health and Disease - from a small body size at birth to epigenetics. *Ann Med,* 48**,** 456-467.

EYLES, D., TRZASKOWSKI, M., VINKHUYZEN, A., MATTHEISEN, M., MEIER, S., GOOCH, H., ANGGONO, V., CUI, X., TAN, M., BURNE, T., JANG, S., KVASKOF, D., HOUGAARD, D., NØRGAARD-PEDERSEN, B., COHEN, A., AGERBO, E., PEDERSEN, C., BØRGLUM, A., MORS, O., SAH, P., WRAY, N., MORTENSEN, P. & MCGRATH, J. 2018. The association between neonatal vitamin D status and risk of schizophrenia. *Nature,* 8.

FAAS, M. & DE VOS, P. 2018. Innate immune cells in the placental bed in healthy pregnancy and preeclampsia. *Placenta,* 69**,** 125-133.

FENSTER, S. & GARNER, C. 2002. Gene structure and genetic localization of the P*CLO* gene encoding the presynaptic active zone protein Piccolo. *The International Journal of Developmental Neuroscience,* 20**,** 161-171.

FERREIRA, J. C., CHOUFANI, S., GRAFODATSKAYA, D., BUTCHER, D. T., ZHAO, C., CHITAYAT, D., SHUMAN, C., KINGDOM, J., KEATING, S. & WEKSBERG, R. 2011. WNT2 promoter methylation in human placenta is associated with low birthweight percentile in the neonate. *Epigenetics,* 6**,** 440-9.

FEST, S., ALDO, P. B., ABRAHAMS, V. M., VISINTIN, I., ALVERO, A., CHEN, R., CHAVEZ, S. L., ROMERO, R. & MOR, G. 2007. Trophoblast-macrophage interactions: a regulatory network for the protection of pregnancy. *Am J Reprod Immunol,* 57**,** 55-66.

FETAHU, I. S., HOBAUS, J. & KALLAY, E. 2014. Vitamin D and the epigenome. *Front Physiol,* 5**,** 164.

FILIBERTO, A. C., MACCANI, M. A., KOESTLER, D., WILHELM-BENARTZI, C., AVISSAR-WHITING, M., BANISTER, C. E., GAGNE, L. A. & MARSIT, C. J. 2011. Birthweight is associated with DNA promoter methylation of the glucocorticoid receptor in human placenta. *Epigenetics,* 6**,** 566-72.

FOWDEN, A. L., VALENZUELA, O. A., VAUGHAN, O. R., JELLYMAN, J. K. & FORHEAD, A. J. 2016. Glucocorticoid programming of intrauterine development. *Domest Anim Endocrinol,* 56 Suppl**,** S121-32.

FROIMCHUK, E., JANG, Y. & GE, K. 2017. Histone H3 lysine 4 methyltransferase KMT2D. *Gene,* 627**,** 337-342.

FU, B., WANG, H., WANG, J., BAROUHAS, I., LIU, W., SHUBOY, A., BUSHINSKY, D. A., ZHOU, D. & FAVUS, M. J. 2013. Epigenetic regulation of BMP2 by 1,25-dihydroxyvitamin D3 through DNA methylation and histone modification. *PLoS One,* 8**,** e61423.

GACCIOLI, F. & LAGER, S. 2016. Placental Nutrient Transport and Intrauterine Growth Restriction. *Front Physiol,* 7**,** 40.

GALE, C. R., MARTYN, C. N., KELLINGRAY, S., EASTELL, R. & COOPER, C. 2001. Intrauterine programming of adult body composition. *J Clin Endocrinol Metab,* 86**,** 267-72.

GALLO, L. A., BARRETT, H. L. & DEKKER NITERT, M. 2016. Review: Placental transport and metabolism of energy substrates in maternal obesity and diabetes. *Placenta*.

GAO, L., LV, C., XU, C., LI, Y., CUI, X., GU, H. & NI, X. 2012. Differential Regulation of Glucose Transporters Mediated by CRH Receptor Type 1 and Type 2 in Human Placental Trophoblasts. *Endocrinology,* 153**,** 1464-1471.

GARCÍA-ACERO, M. & ACOSTA, J. 2017. Whole-Exome Sequencing Identifies a de novo AHDC1 Mutation in a Colombian Patient with Xia-Gibbs Syndrome. *Molecular Syndromology,* 8**,** 308-12.

GLUCKMAN, P. D. & HANSON, M. A. 2004. Living with the past: evolution, development, and patterns of disease. *Science,* 305**,** 1733-6.

GODFREY, K. M. 2002. The role of the placenta in fetal programming-a review. *Placenta,* 23 Suppl A**,** S20-7.

GRAMMATOPOULOS, D. 2007. The role of CRH receptors and their agonists in myometrial contractility and quiescence during pregnancy and labour. *Frontiers in Bioscience,* 12**,** 561-571.

GRUNDMANN, M. & VON VERSEN-HÖYNCK, F. 2011. Vitamin D - roles in women's reproductive health? *Reproductive Biology and Endocrinology,* 9**,** 146.

GUNJAN, A., PAIK, J. & VERREAULT, A. 2005. Regulation of histone synthesis and nucleosome assembly. *Biochimie,* 87**,** 625-635.

HACKER, A., FUNG, E. & KING, J. 2012. Role of calcium during pregnancy: maternal and fetal needs. *Nutrition reviews,* 70**,** 397-409.

HAGGARTY, P. 2010. Fatty acid supply to the human fetus. *Annu Rev Nutr,* 30**,** 237-55.

HAHN, D., BLASCHITZ, A., KORGUN, E. T., LANG, I., DESOYE, G., SKOFITSCH, G. & DOHR, G. 2001. From maternal glucose to fetal glycogen: expression of key regulators in the human placenta. *Mol Hum Reprod,* 7**,** 1173-8.

HALASZ, M. & SZEKERES-BARTHO, J. 2013. The role of progesterone in implantation and trophoblast invasion. *J Reprod Immunol,* 97**,** 43-50.

HALHALI, A., FIGUERAS, A. G., DIAZ, L., AVILA, E., BARRERA, D., HERNANDEZ, G. & LARREA, F. 2010. Effects of calcitriol on calbindins gene expression and lipid peroxidation in human placenta. *J Steroid Biochem Mol Biol,* 121**,** 448-51.

HANDSCHUH, K., GUIBOURDENCHE, J., TSATSARIS, V., GUESNON, M., LAURENDEAU, I., EVAIN-BRION, D. & FOURNIER, T. 2007. Human chorionic gonadotropin expression in human trophoblasts from early placenta: comparative study between villous and extravillous trophoblastic cells. *Placenta,* 28**,** 175-84.

HANSON, M. & GLUCKMAN, P. 2011. Developmental origins of noncommunicable disease: population and public health implications. *Am J Clin Nutr,* 94**,** 1754s-1758s.

HANSON, M. A. & GLUCKMAN, P. D. 2014. Early developmental conditioning of later health and disease: physiology or pathophysiology? *Physiol Rev,* 94**,** 1027-76.

HANSON, M. A. & GLUCKMAN, P. D. 2015. Developmental origins of health and disease--global public health implications. *Best Pract Res Clin Obstet Gynaecol,* 29**,** 24-31.

HARRIS, L. K., CROCKER, I. P., BAKER, P. N., APLIN, J. D. & WESTWOOD, M. 2011. IGF2 actions on trophoblast in human placenta are regulated by the insulin-like growth factor 2 receptor, which can function as both a signaling and clearance receptor. *Biol Reprod,* 84**,** 440-6.

HARVEY, N. C., HOLROYD, C., NTANI, G., JAVAID, K., COOPER, P., MOON, R., COLE, Z., TINATI, T., GODFREY, K., DENNISON, E., BISHOP, N., BAIRD, J. & COOPER, C. 2014a. Vitamin D supplementation in pregnancy: a systematic review. *NIHR Journals*.

HARVEY, N. C., JAVAID, K., BISHOP, N., KENNEDY, S., PAPAGEORGHIOU, A. T., FRASER, R., GANDHI, S. V., SCHOENMAKERS, I., PRENTICE, A. & COOPER, C. 2012. MAVIDOS Maternal Vitamin D Osteoporosis Study: study protocol for a randomized controlled trial. The MAVIDOS Study Group. *Trials,* 13**,** 13.

HARVEY, N. C., SHEPPARD, A., GODFREY, K. M., MCLEAN, C., GARRATT, E., NTANI, G., DAVIES, L., MURRAY, R., INSKIP, H. M., GLUCKMAN, P. D., HANSON, M. A., LILLYCROP, K. A. & COOPER, C. 2014b. Childhood bone mineral content is associated with methylation status of the RXRA promoter at birth. *J Bone Miner Res,* 29**,** 600-7.

HASHMI, I., NANDY, K. & SESHAN, K. 2019. Non-Medical Strategies to Improve Pregnancy Outcomes of Women with Gestational Diabetes Mellitus : A literature review. *Sultan Quaboos University Medical Journal,* 19.

HASSAN-SMITH, Z., JENKINSON, C., SMITH1, D., HERNANDEZ, I., MORGAN, S., CRABTREE, N., GITTOES, N., KEEVIL, B., STEWART, P. & HEWISON, M. 2017. 25-hydroxyvitamin D3 and 1,25-dihydroxyvitamin D3 exert distinct effects on human skeletal muscle function and gene expression. *PLoS ONE,* 12.

HAUGUEL, S., CHALLIER, J. C., CEDARD, L. & OLIVE, G. 1983. Metabolism of the human placenta perfused in vitro: glucose transfer and utilization, O2 consumption, lactate and ammonia production. *Pediatr Res,* 17**,** 729-32.

HAUGUEL-DE MOUZON, S. & SHAFRIR, E. 2001. Carbohydrate and fat metabolism and related hormonal regulation in normal and diabetic placenta. *Placenta,* 22**,** 619-27.

HAUSSLER, M. R., WHITFIELD, G. K., KANEKO, I., HAUSSLER, C. A., HSIEH, D., HSIEH, J. C. & JURUTKA, P. W. 2013. Molecular Mechanisms of Vitamin D Action. *Calcified Tissue International,* 92**,** 77-98.

HAY, D. L. & LOPATA, A. 1988. Chorionic gonadotropin secretion by human embryos in vitro. *J Clin Endocrinol Metab,* 67**,** 1322-4.

HEIKKINEN, J., MOTTONEN, M., KOMI, J., ALANEN, A. & LASSILA, O. 2003. Phenotypic characterization of human decidual macrophages. *Clin Exp Immunol,* 131**,** 498-505.

HEMACHANDRA, A. H., KLEBANOFF, M. A., DUGGAN, A. K., HARDY, J. B. & FURTH, S. L. 2006. The association between intrauterine growth restriction in the full-term infant and high blood pressure at age 7 years: results from the Collaborative Perinatal Project. *Int J Epidemiol,* 35**,** 871-7.

HERNANDEZ, C. J., BEAUPRE, G. S. & CARTER, D. R. 2003. A theoretical analysis of the relative influences of peak BMD, age-related bone loss and menopause on the development of osteoporosis. *Osteoporos Int,* 14**,** 843-7.

HII, C. & FERRANTE, A. 2016. The Non-Genomic Actions of Vitamin D. *Nutrients,* 8.

HOEK, H. 1998. The Dutch Famine and schizophrenia spectrum disorders. *In:* BROWN, A. S., E. (ed.). Social Psychiatry and Psychiatric Epidemiology.

HOLROYD, C. R., HARVEY, N. C., CROZIER, S. R., WINDER, N. R., MAHON, P. A., NTANI, G., GODFREY, K. M., INSKIP, H. M. & COOPER, C. 2012. Placental size at 19 weeks predicts offspring bone mass at birth: findings from the Southampton Women's Survey. *Placenta,* 33**,** 623-9.

HU, H., BRITTAIN, G., CHANG, J., PUEBLA-OSORIO, N., JIN, J., ZAL, A., XIAO, Y., CHENG, X., CHANG, M., FU, Y., ZAL, T., ZHU, C. & SUN, S. 2013. Otud7b controls noncanonical NF-κB activation via deubiquitination of TRAF3. *Nature,* 494**,** 371-374.

HUBERA, F., GREENBLATTB, S., DAVENPORTA, A., MARTINEZB, C., XUB, Y., VUC, L., NIMERB, S. & HOELZ, A. 2017. Histone-binding of DPF2 mediates its repressive role in myeloid differentiation. *PNAS,* 114**,** 6016-6021.

HUPPERTZ, B. 2008. The anatomy of the normal placenta. *Journal of Clinical Pathology,* 61**,** 1296-1302.

HUSSLEIN, H., HAIDER, S., MEINHARDT, G., PRAST, J., SONDEREGGER, S. & KNÖFLER, M. 2009. Expression, Regulation and Functional Characterization of Matrix Metalloproteinase-3 of Human Trophoblast. *Placenta,* 30**,** 284-291.

HUXLEY, R. R., SHIELL, A. W. & LAW, C. M. 2000. The role of size at birth and postnatal catch-up growth in determining systolic blood pressure: a systematic review of the literature. *J Hypertens,* 18**,** 815-31.

ILLSLEY, N. P. 2000. Glucose transporters in the human placenta. *Placenta,* 21**,** 14-22.

INSKIP, H. M., GODFREY, K. M., ROBINSON, S. M., LAW, C. M., BARKER, D. J. & COOPER, C. 2006. Cohort profile: The Southampton Women's Survey. *Int J Epidemiol,* 35**,** 42-8.

JAFFE, R. B., LEE, P. A. & MIDGLEY, A. R., JR. 1969. Serum gonadotropins before, at the inception of, and following human pregnancy. *J Clin Endocrinol Metab,* 29**,** 1281-3.

JAKOUBEK, V., BIBOVA, J. & HAMPL, V. 2006. Voltage-gated Calcium Channels Mediate Hypoxic Vasoconstriction in the Human Placenta. *Placenta,* 27**,** 1030-1033.

JAMES, J. L., STONE, P. R. & CHAMLEY, L. W. 2006. The regulation of trophoblast differentiation by oxygen in the first trimester of pregnancy. *Hum Reprod Update,* 12**,** 137-44.

JANSSON, T., WENNERGREN, M. & ILLSLEY, N. P. 1993. Glucose transporter protein expression in human placenta throughout gestation and in intrauterine growth retardation. *J Clin Endocrinol Metab,* 77**,** 1554-62.

JAVAID, M., CROZIER, S., HARVEY, N. C., GALE, C. R., DENNISON, E., BOUCHER, B. J., ARDEN, N. K., GODFREY, K. & COOPER, C. 2006. Maternal vitamin D status during pregnancy and childhood bone mass at age 9 years: a longitutinal study. *The Lancet,* 367**,** 36-43.

JIN, M. & GOLDENRING, J. 2006. The Rab11-FIP1/RCP gene codes for multiple protein transcripts related to the plasma membrane recycling system. *Biochimica et Biophysica Acta,* 1759**,** 281-295.

JONES, G., PROSSER, D. E. & KAUFMANN, M. 2014. Cytochrome P450-mediated metabolism of vitamin D. *J Lipid Res,* 55**,** 13-31.

JONES, G., STRUGNELL, S. A. & DELUCA, H. F. 1998. Current understanding of the molecular actions of vitamin D. *Physiological Reviews,* 78**,** 1193-1231.

JUNGE, K. M., BAUER, T., GEISSLER, S., HIRCHE, F., THURMANN, L., BAUER, M., TRUMP, S., BIEG, M., WEICHENHAN, D., GU, L., MALLM, J. P., ISHAQUE, N., MUCKE, O., RODER, S.,

HERBERTH, G., DIEZ, U., BORTE, M., RIPPE, K., PLASS, C., HERMANN, C., STANGL, G. I., EILS, R. & LEHMANN, I. 2016. Increased vitamin D levels at birth and in early infancy increase offspring allergy risk-evidence for involvement of epigenetic mechanisms. *J Allergy Clin Immunol,* 137**,** 610-3.

KARAMALI, M., BEIHAGHI, E., MOHAMMADI, A. & ASEMI, Z. 2015. Effects of High-Dose Vitamin D Supplementation on Metabolic Status and Pregnancy Outcomes in Pregnant Women at Risk for Pre-Eclampsia. *Hormone and Metabolic Research,* 47.

KARRAS, S. N., WAGNER, C. L. & CASTRACANE, V. D. 2017. Understanding vitamin D metabolism in pregnancy: From physiology to pathophysiology and clinical outcomes. *Metabolism*.

KAUSHAL, M. & MAGON, N. 2013. Vitamin D in pregnancy: A metabolic outlook. *Indian Journal of Endocrinology and Metabolism,* 17**,** 76-82.

KEPPLER, B. & ARCHER, T. 2008. Chromatin-modifying enzymes as therapeutic targets – Part 1. *Expert opinion on therapeutic targets,* 12**,** 1301-1312.

KIM, D., RYU, D., KOH, M., LEE, M., LIM, D., KIM, M., KIM, Y., CHO, W., LEE, C., PARK, S., KOO, S. & CHOI, H. 2011. Orphan Nuclear Receptor Estrogen-Related Receptor Gamma (ERRG) Is Key Regulator of Hepatic Gluconeogenesis. *The Journal of Biologcal Chemistry,* 287**,** 21628-21639.

KIM, M. S., FUJIKI, R., MURAYAMA, A., KITAGAWA, H., YAMAOKA, K., YAMAMOTO, Y., MIHARA, M., TAKEYAMA, K. & KATO, S. 2007. 1Alpha,25(OH)2D3-induced transrepression by vitamin D receptor through E-box-type elements in the human parathyroid hormone gene promoter. *Mol Endocrinol,* 21**,** 334-42.

LAMBERT, S., JOLMA, A., CAMPITELLI, L., DAS, P., YIN, Y., ALBU, M., CHEN, X., TAIPALE, J., HUGHES, T. & WEIRAUCH, M. 2018. The Human Transcription Factors. *Cell,* 172**,** 650-665.

LEWIS, R. M., CLEAL, J. K., NTANI, G., CROZIER, S. R., MAHON, P. A., ROBINSON, S. M., HARVEY, N. C., COOPER, C., INSKIP, H. M., GODFREY, K. M., HANSON, M. A. & JOHN, R. M. 2012. Relationship between placental expression of the imprinted PHLDA2 gene, intrauterine skeletal growth and childhood bone mass. *Bone,* 50**,** 337-42.

LEWIS, R. M., GREENWOOD, S. L., CLEAL, J. K., CROZIER, S. R., VERRALL, L., INSKIP, H. M., CAMERON, I. T., COOPER, C., SIBLEY, C. P., HANSON, M. A. & GODFREY, K. M. 2010. Maternal muscle mass may influence system A activity in human placenta. *Placenta,* 31**,** 418-22.

LI, X., LI, C., DONG, X. & GOU, W. 2014. MicroRNA-155 inhibits migration of trophoblast cells and contributes to the pathogenesis of severe preeclampsia by regulating endothelial nitric oxide synthase. *Mol Med Rep,* 10**,** 550-4.

LIU, N. Q. & HEWISON, M. 2011. Vitamin D, the placenta and pregnancy. *Archives of Biochemistry and Biophysics*.

LO, H., TSAI, C., CHEN, C., WANG, L., LEE, Y., CHEN, C., LIANG, C., CHEONG, M. & CHEN, H. 2017. Association of dysfunctional synapse defective 1 (SYDE1) with restricted fetal growth – SYDE1 regulates placental cell migration and invasion. *Journal of Pathology,* 241**,** 324-336.

LONGTINE, M., CVITIC, S., COLVIN, B., CHEN, B., DESOYE, G. & NELSON, N. 2017. Calcitriol regulates immune gene CD14 and CD180 to modulate LPS response in human trophoblasts. *Reproduction,* 154**,** 735-744.

LOU, Y., MOLNAR, F., PERAKYLA, M., QIAO, S., KALUEFF, A., ST-ARNAUD, R., CARLBERG, C. & TUOHIMAA, P. 2010. 25-Hydroxyvitamin D 3 is an agonistic vitamin D receptor ligand. *The Journal of Steroid Biochemistry and Molecular Biology,* 118**,** 162-170.

LOZANO, N. A., LOZANO, A., MARINI, V., SARANZ, R. J., BLUMBERG, R. S., BAKER, K., AGRESTA, M. F. & PONZIO, M. F. 2018. Expression of FcRn receptor in placental tissue and its relationship with IgG levels in term and preterm newborns. *Am J Reprod Immunol,* 80**,** e12972.

LUNDQVIST, J., WIKVALL, K. & NORLIN, M. 2012. Vitamin D-mediated regulation of CYP21A2 transcription — A novel mechanism for vitamin D action. *Biochimica et Biophysica Acta,* 1820**,** 1553-1559.

MACCANI, M. A., AVISSAR-WHITING, M., BANISTER, C. E., MCGONNIGAL, B., PADBURY, J. F. & MARSIT, C. J. 2010. Maternal cigarette smoking during pregnancy is associated with downregulation of miR-16, miR-21, and miR-146a in the placenta. *Epigenetics,* 5**,** 583-9.

MACCANI, M. A. & MARSIT, C. J. 2009. Epigenetics in the placenta. *Am J Reprod Immunol,* 62**,** 78-89.

MAHON, P., HARVEY, N., CROZIER, S., INSKIP, H., ROBINSON, S., ARDEN, N., SWAMINATHAN, R., COOPER, C. & GODFREY, K. 2010. Low maternal vitamin D status and fetal bone development: cohort study. *J Bone Miner Res,* 25**,** 14-9.

MARIN, R., RIQUELME, G., GODOY, V., DIAZ, P., ABAD, C., CAIRES, R., PROVERBIO, T., PINERO, S. & PROVERBIO, F. 2008. Functional and structural demonstration of the presence of Ca-ATPase (PMCA) in both microvillous and basal plasma membranes from syncytiotrophoblast of human term placenta. *Placenta,* 29**,** 671-9.

MAZAHERY, H. & VON HURST, P. R. 2015. Factors Affecting 25-Hydroxyvitamin D Concentration in Response to Vitamin D Supplementation. *Nutrients,* 7**,** 5111-42.

MCCREIGHT, J., SCHNEIDER, S., WILBURN, D. & SWANSON, W. 2017. Evolution of microRNA in primates. *PlosOne,* 12.

MEYER, M., BENKUSKY, N. & PIKE, J. 2014. 1,25-Dihydroxyvitamin D 3 Induced Histone Profiles Guide Discovery of VDR Action Sites. *The Journal of steroid biochemistry and molecular biology,* 144**,** 19-21.

MOHAMMADBEIGI, A., FARHADIFAR, F., SOUFI ZADEH, N., MOHAMMADSALEHI, N., REZAIEE, M. & AGHAEI, M. 2013. Fetal macrosomia: risk factors, maternal, and perinatal outcome. *Ann Med Health Sci Res,* 3**,** 546-50.

MOHR, A. M. & MOTT, J. L. 2015. Overview of microRNA biology. *Semin Liver Dis,* 35**,** 3-11.

MOLNAR, F. 2014. Structural considerations of vitamin D signaling. *Frontiers in Physiology,* 5**,** 22.

MOLNAR, F., SIGUEIRO, R., SATO, Y., ARAUJO, C., SCHUSTER, I., ANTHONY, P., PELUSO, J., MULLER, C., MOURINO, A., MORAS, D. & ROCHEL, N. 2011. 1α,25(OH) 2 -3-Epi-Vitamin D 3 , a Natural Physiological Metabolite of Vitamin D 3 : Its Synthesis, Biological Activity and Crystal Structure with Its Receptor. *PLOS One,* 6.

MOORE, L. D., LE, T. & FAN, G. 2013. DNA methylation and its basic function. *Neuropsychopharmacology,* 38**,** 23-38.

MOREAU, R., DAOUD, G., BERNATCHEZ, R., SIMONEAU, L., MASSE, A. & LAFOND, J. 2002. Calcium uptake and calcium transporter expression by trophoblast cells from human term placenta. *Biochimica et Biophysica Acta,* 1564**,** 325-332.

MORRISON, E., BOWERMAN, S., SYLVERS, K., WERESZCZYNSKI, J. & MUSSELMAN, C. 2018. The conformation of the histone H3 tail inhibits association of the BPTF PHD finger with the nucleosome. *eLIFE,* 7.

MURRAY, A. J. 2012. Oxygen delivery and fetal-placental growth: beyond a question of supply and demand? *Placenta,* 33 Suppl 2**,** e16-22.

MYREN, M., MOSE, T., MATHIESEN, L. & KNUDSEN, L. E. 2007. The human placenta - An alternative for studying foetal exposuree. *Toxicology in Vitro,* 21**,** 1332-1340.

NAPSO, T., YONG, H., LOPEZ-TELLO, J. & SFERRUZZI-PERRI, A. 2018. The Role of Placental Hormones in Mediating Maternal Adaptations to Support Pregnancy and Lactation. *Frontiers in Physiology,* 9.

NELISSEN, E. C., VAN MONTFOORT, A. P., DUMOULIN, J. C. & EVERS, J. L. 2011. Epigenetics and the placenta. *Hum Reprod Update,* 17**,** 397-417.

NOMURA, Y., LAMBERTINI, L., RIALDI, A., LEE, M., MYSTAL, E. Y., GRABIE, M., MANASTER, I., HUYNH, N., FINIK, J., DAVEY, M., DAVEY, K., LY, J., STONE, J., LOUDON, H., EGLINTON, G., HURD, Y., NEWCORN, J. H. & CHEN, J. 2014. Global methylation in the placenta and umbilical cord blood from pregnancies with maternal gestational diabetes, preeclampsia, and obesity. *Reprod Sci,* 21**,** 131-7.

NOVAKOVIC, B. & SAFFERY, R. 2012. The ever growing complexity of placental epigenetics - Role in adverse pregnancy outcomes and fetal programming. *Placenta***,** 959-970.

NOVAKOVIC, B., SIBSON, M., NG, H. K., MANUELPILLAI, U., RAKYAN, V., DOWN, T., BECK, S., FOURNIER, T., EVAIN-BRION, D., DIMITRIADIS, E., CRAIG, J. M., MORLEY, R. & SAFFERY, R.

2009. Placenta-specific methylation of the vitamin D 24-hydroxylase gene: implications for feedback autoregulation of active vitamin D levels at the fetomaternal interface. *J Biol Chem,* 284**,** 14838-48.

NOVAKOVIC, B., YUEN, R. K., GORDON, L., PENAHERRERA, M. S., SHARKEY, A., MOFFETT, A., CRAIG, J. M., ROBINSON, W. P. & SAFFERY, R. 2011. Evidence for widespread changes in promoter methylation profile in human placenta in response to increasing gestational age and environmental/stochastic factors. *BMC Genomics,* 12**,** 529.

NYKJAER, A., FYFE, J., KOZYRAKI, R., LEHESTE, J., JACOBSEN, C., NIELSEN, M., VERROUST, P., AMINOFF, M., CHAPELLE, A., MOESTRUP, S., RAY, R., GLIEMANN, J., WILLNOW, T. & CHRISTENSEN, E. 2001. Cubilin dysfunction causes abnormal metabolism of the steroid hormone 25(OH) vitamin D3. *PNAS,* 98**,** 13895-13900.

ORLOV, I., ROCHEL, N., MORAS, D. & KLAHOLZ, B. P. 2012. Structure of the full human RXR/VDR nuclear receptor heterodimer complex with its DR3 target DNA. *Embo Journal,* 31**,** 291-300.

PAINTER, R. C., ROSEBOOM, T. J. & BLEKER, O. P. 2005. Prenatal exposure to the Dutch famine and disease in later life: an overview. *Reprod Toxicol,* 20**,** 345-52.

PARIMI, P. & CALHAN, S. 2007. Glutamine supplementation in the newborn infant. *Seminars in fetal and neonatal medicine,* 12**,** 19-25.

PERAZZOLO, S., HIRSCHMUGL, B., WADSACK, C., DESOYE, G., LEWIS, R. M. & SENGERS, B. G. 2015. Computational modelling of fatty acid transport in the human placenta. *Conf Proc IEEE Eng Med Biol Soc,* 2015**,** 8054-7.

PEREIRA, F., BARBACHANO, A., SILVA, J., BONILLA, F., CAMPBELL, M. J., MUNOZ, A. & LARRIBA, M. J. 2011. KDM6B/JMJD3 histone demethylase is induced by vitamin D and modulates its effects in colon cancer cells. *Hum Mol Genet,* 20**,** 4655-65.

PEREIRA, F., BARBACHANO, A., SINGH, P. K., CAMPBELL, M. J., MUNOZ, A. & LARRIBA, M. J. 2012. Vitamin D has wide regulatory effects on histone demethylase genes. *Cell Cycle,* 11**,** 1081-9.

PERRIN, D., BALLESTAR, E., FRAGA, M. F., FRAPPART, L., ESTELLER, M., GUERIN, J. F. & DANTE, R. 2007. Specific hypermethylation of LINE-1 elements during abnormal overgrowth and differentiation of human placenta. *Oncogene,* 26**,** 2518-24.

PFEFFER, P. E., LU, H., MANN, E. H., CHEN, Y. H., HO, T. R., COUSINS, D. J., CORRIGAN, C., KELLY, F. J., MUDWAY, I. S. & HAWRYLOWICZ, C. M. 2018. Effects of vitamin D on inflammatory and oxidative stress responses of human bronchial epithelial cells exposed to particulate matter. *PLoS One,* 13**,** e0200040.

PILON, C., REBELLATO, A., URBANET, R., GUZZARDO, V., CAPPELLESSO, R., SASANO, H., FASSINA, A. & FALLO, F. 2015. Methylation Status of Vitamin D Receptor Gene Promoter in Benign and Malignant Adrenal Tumors. *Int J Endocrinol,* 2015**,** 375349.

PITALE, P., HOWSE, W. & GORBATYUK, M. 2016. Neuronatin Protein in Health and Disease. *The Journal of Cellular Physiology,* 232**,** 477-481.

PLASS, C. & SMIRAGLIA, D. 2006. Genome-wide Analysis of DNA Methylation Changes in Human Malignancies. *DNA Methylation: Development, Genetic Disease and Cancer. Current Topics in Microbiology and Immunology,* 310.

POTGENS, A. J., SCHMITZ, U., BOSE, P., VERSMOLD, A., KAUFMANN, P. & FRANK, H. G. 2002. Mechanisms of syncytial fusion: a review. *Placenta,* 23 Suppl A**,** S107-13.

PRIETL, B., TREIBER, G., PIEBER, T. & AMREIN, K. 2013. Vitamin D and Immune Function. *Nutrients,* 5**,** 2502-2521.

QIAO, Q., LI, Y., CHEN, Z., WAN, M., REINBERG, D. & XU, R. 2010. The structure of NSD1 reveals an autoregulatory mechanism underlying histone H3K36 methylation. *The Journal of Biological Chemistry,* 286**,** 8361-8368.

RACICOT, K., KWON, J. Y., ALDO, P., SILASI, M. & MOR, G. 2014. Understanding the complexity of the immune system during pregnancy. *Am J Reprod Immunol,* 72**,** 107-16.

RAGHUPATHY, R., AL MUTAWA, E., MAKHSEED, M., AZIZIEH, F. & SZEKERES-BARTHO, J. 2005. Modulation of cytokine production by dydrogesterone in lymphocytes from women with recurrent miscarriage. *Bjog,* 112**,** 1096-101.

RAHNAMA, F., SHAFIEI, F., GLUCKMAN, P. D., MITCHELL, M. D. & LOBIE, P. E. 2006. Epigenetic regulation of human trophoblastic cell migration and invasion. *Endocrinology,* 147**,** 5275-83.

REEVES, E. & JAMES, E. 2017. Tumour and placenta establishment: The importance of antigen processing and presentation. *Placenta,* 56**,** 34-39.

REICHETZEDER, C., DWI PUTRA, S. E., PFAB, T., SLOWINSKI, T., NEUBER, C., KLEUSER, B. & HOCHER, B. 2016. Increased global placental DNA methylation levels are associated with gestational diabetes. *Clin Epigenetics,* 8**,** 82.

REYNOLDS, R. M., JACOBSEN, G. H. & DRAKE, A. J. 2013. What is the evidence in humans that DNA methylation changes link events in utero and later life disease? *Clin Endocrinol (Oxf),* 78**,** 814-22.

RISNES, K. R., ROMUNDSTAD, P. R., NILSEN, T. I., ESKILD, A. & VATTEN, L. J. 2009. Placental weight relative to birth weight and long-term cardiovascular mortality: findings from a cohort of 31,307 men and women. *Am J Epidemiol,* 170**,** 622-31.

ROBINSON, M., MCCARTHY, D. & SMYTH, G. 2010. edgeR: a Bioconductor package for differential expression analysis of digital gene expression data. *Bioinformatics,* 26**,** 139-140.

ROCHEL, N., WURTZ, J. M., MITSCHLER, A., KLAHOLZ, B. & MORAS, D. 2000. The crystal structure of the nuclear receptor for vitamin D bound to its natural ligand. *Mol Cell,* 5**,** 173-9.

RON, M., LEVITZ, M., CHUBA, J. & DANCIS, J. 1984. Transfer of 25-hydroxyvitamin D3 and 1,25-dihydroxyvitamin D3 across the perfused human placenta. *Am J Obstet Gynecol,* 148**,** 370-4.

ROOS, S., JANSSON, N., PALMBERG, I., SALJO, K., POWELL, T. L. & JANSSON, T. 2007. Mammalian target of rapamycin in the human placenta regulates leucine transport and is down-regulated in restricted fetal growth. *J Physiol,* 582**,** 449-59.

ROOS, S., KANAI, Y., PRASAD, P. D., POWELL, T. L. & JANSSON, T. 2009a. Regulation of placental amino acid transporter activity by mammalian target of rapamycin. *Am J Physiol Cell Physiol,* 296**,** C142-50.

ROOS, S., POWELL, T. L. & JANSSON, T. 2009b. Placental mTOR links maternal nutrient availability to fetal growth. *Biochem Soc Trans,* 37**,** 295-8.

RUCHAT, S. M., HOUDE, A. A., VOISIN, G., ST-PIERRE, J., PERRON, P., BAILLARGEON, J. P., GAUDET, D., HIVERT, M. F., BRISSON, D. & BOUCHARD, L. 2013. Gestational diabetes mellitus epigenetically affects genes predominantly involved in metabolic diseases. *Epigenetics,* 8**,** 935-43.

RUDDOCK, N. K., SHI, S. Q., JAIN, S., MOORE, G., HANKINS, G. D., ROMERO, R. & GARFIELD, R. E. 2008. Progesterone, but not 17-alpha-hydroxyprogesterone caproate, inhibits human myometrial contractions. *Am J Obstet Gynecol,* 199**,** 391.e1-7.

SAITO, Y., HAMAMOTO, A. & KOBAYASHI, Y. 2013. Regulated control of melanin-concentrating hormone receptor 1 through posttranslational modifications. *Frontiers in endocrinology,* 4.

SAMARUT, E. & ROCHETTE-EGLY, C. 2012. Nuclear retinoic acid receptors: Conductors of the retinoic acid symphony during development. *Molecular and Cellular Endocrinology,* 348**,** 348-360.

SAMUEL, S. & SITRIN, M. 2008. Vitamin D's role in cell proliferation and differentiation. *Nutrition Reviews,* 66**,** 116-124.

SANDVIG, K., PUST, S., SKOTLAND, T. & VAN DEURS, B. 2011. Clathrin-independent endocytosis: mechanisms and function. *Curr Opin Cell Biol,* 23**,** 413-20.

SCHIMMACK, G., SCHORPP, K., KUTZNER, K., GEHRING, T., BRENKE, J., HADIAN, K. & KRAPPMANN, D. 2017. YOD1/TRAF6 association balances p62-dependent IL-1 signaling to NF-κB. *eLIFE,* 6.

SCHMITGES, F., RADOVANI, E., NAJAFABADI, H., BARAZANDEH, M., CAMPITELLI, L., YIN, Y., JOLMA, A., ZHONG, G., GUO, H., KANAGALINGAM, T., DAI, W., TAIPALE, J., EMILI, A., GREENBLATT, J. & HUGHES, T. 2016. Multiparameter functional diversity of human C2H2 zinc finger proteins. *Genome Research,* 26**,** 1742-1752.

SCHNEIDER, H. 2015. IFPA senior award lecture: Energy metabolism of human placental tissue studied by ex vivo perfusion of an isolated cotyledon. *Placenta,* 36 Suppl 1**,** S29-34.

SCHONTEICH, E., WILSON, G., BURDEN, J., HOPKINS, C., ANDERSON, K., GOLDENRING, J. & PREKERIS, R. 2008. The Rip11/Rab11-FIP5 and kinesin II complex regulates endocytic protein recycling. *The Journal of Cell Science,* 121**,** 3824-3833.

SCHUERMANN, D., WEBER, A. R. & SCHAR, P. 2016. Active DNA demethylation by DNA repair: Facts and uncertainties. *DNA Repair (Amst),* 44**,** 92-102.

SCHULZ, E. V., CRUZE, L., WEI, W., GEHRIS, J. & WAGNER, C. L. 2017a. Maternal vitamin D sufficiency and reduced placental gene expression in angiogenic biomarkers related to comorbidities of pregnancy. *J Steroid Biochem Mol Biol*.

SCHULZ, E. V., CRUZE, L., WEI, W., GEHRIS, J. & WAGNER, C. L. 2017b. Maternal vitamin D sufficiency and reduced placental gene expression in angiogenic biomarkers related to comorbidities of pregnancy. *J Steroid Biochem Mol Biol,* 173**,** 273-279.

SEELY, E. W., WOOD, R. J., BROWN, E. M. & GRAVES, S. W. 1992. Lower serum ionized calcium and abnormal calciotropic hormone levels in preeclampsia. *J Clin Endocrinol Metab,* 74**,** 1436-40.

SEROV, A. S., SALAFIA, C., GREBENKOV, D. S. & FILOCHE, M. 2016. The role of morphology in mathematical models of placental gas exchange. *J Appl Physiol (1985),* 120**,** 17-28.

SFERRUZZI-PERRI, A. 2018. Regulating needs: Exploring the role of insulin-like growth factor-2 signalling in materno-fetal resource allocation. *Placenta,* 33**,** 16-22.

SHE, Z. & YANG, W. 2015. SOX family transcription factors involved in diverse cellular events during development. *European Journal of Cell biology,* 94**,** 547-563.

SHEA, R. & BERG, J. 2017. Self-administration of vitamin D supplements in the general public may be associated with high 25-hydroxyvitamin D concentrations. *Annals of Clinical Biochemistry,* 54.

SHENGA, L., TURNER, A., BARRATT, K., KREMERE, R., MORRIS, H., CALLEN, D., ANDERSON, P. & TARULLI, G. 2019. Mammary-specific ablation of C*yp24a1 i*nhibits development, reduces proliferation and increases sensitivity to vitamin D. *The Journal of Steroid Biochemistry and Molecular Biology*.

SHIN, J. S., CHOI, M. Y., LONGTINE, M. S. & NELSON, D. M. 2010. Vitamin D effects on pregnancy and the placenta. *Placenta,* 31**,** 1027-1034.

SIGGS, O. & BEUTLER, B. 2012. The BTB-ZF transcription factors. *Cell Cycle,* 11**,** 3358-3369.

SIMNER, C., NOVAKOVIC, B., LILLYCROP, K., BELL, C., HARVEY, N., COOPER, C., SAFFERY, R., LEWIS, R. & CLEAL, J. 2017. DNA methylation of amino acid transporter genes in the human placenta. *Placenta,* 60**,** 64-73.

SIMNER, C. L. 2015. *Vitamin D transport and the effects on placental function and fetal growth.* Doctor of Philosophy, University of Southampton.

SINCLAIR, K., ALLEGRUCCI, C., SINGH, R., GARDNER, D., SEBASTIAN, S., BISPHAM, J., THURSTON, A., HUNTLEY, J., REES, W., MALONEY, C., LEA, R., CRAIGON, J., MCEVOY, T. & YOUNG, L. 2007. DNA methylation, insulin resistance, and blood pressure in offspring determined by maternal periconceptional B vitamin and methionine status. *PNAS,* 104.

SINGH, P. K., LONG, M. D., BATTAGLIA, S., HU, Q., LIU, S., SUCHESTON-CAMPBELL, L. E. & CAMPBELL, M. J. 2015. VDR regulation of microRNA differs across prostate cell models suggesting extremely flexible control of transcription. *Epigenetics,* 10**,** 40-9.

ST-PIERRE, J., HIVERT, M. F., PERRON, P., POIRIER, P., GUAY, S. P., BRISSON, D. & BOUCHARD, L. 2012. IGF2 DNA methylation is a modulator of newborn's fetal growth and development. *Epigenetics,* 7**,** 1125-32.

STABLES. D & RANKIN. J 2010. *Physiology in Childbearing with anatomy and related biosciences*, Elsevier.

STEINFELD, H., CHO, M., RETTERER, K., PERSON, R., SCHAEFER, B., DANYLCHUK, N., MALIK, S., BURNS WECHSLER, S., WHEELER, P., VAN, GASSEN, K., TERHAL, P., VERHOEVEN, V., VAN SLEGTENHORST, M., MONAGHAN, K., HENDERSON, L. & CHUNG, W. 2016. Mutations in *HIVEP2* are associated with developmental delay, intellectual disability and dysmorphic features. *Neurogenetics,* 17**,** 159-164.

SUTER, M., ABRAMOVICI, A., SHOWALTER, L., HU, M., SHOPE, C. D., VARNER, M. & AAGAARD-TILLERY, K. 2010. In utero tobacco exposure epigenetically modifies placental CYP1A1 expression. *Metabolism,* 59**,** 1481-90.

SVENSSON-ARVELUND, J., MEHTA, R. B., LINDAU, R., MIRRASEKHIAN, E., RODRIGUEZ-MARTINEZ, H., BERG, G., LASH, G. E., JENMALM, M. C. & ERNERUDH, J. 2015. The human fetal placenta promotes tolerance against the semiallogeneic fetus by inducing regulatory T cells and homeostatic M2 macrophages. *J Immunol,* 194**,** 1534-44.

TAMBLYN, J., HEWISON, M., WAGNER, C., BULMER, J. & KILBY, M. 2015. Immunological role of vitamin D at the maternal–fetal interface. *The Journal of endocrinology,* 224**,** 107-121.

TAYLOR, P. M. & RITCHIE, J. W. 2007. Tissue uptake of thyroid hormone by amino acid transporters. *Best Pract Res Clin Endocrinol Metab,* 21**,** 237-51.

THOMSON, M. 2013. The physiological roles of placental corticotropin releasing hormone in pregnancy and childbirth. *The Journal of Physiological Biochemistry,* 69**,** 559-573.

TIAN, X. & HOLICK, M. 1999. A liposomal model that mimics the cutaneous production of vitamin D3. Studies of the mechanism of the membrane-enhanced thermal isomerization of previtamin D3 to vitamin D3. *The Journal of Biological Chemistry,* 274**,** 4174-4179.

TRA, J., KONDO, T., LU, Q., KUICK, R., HANASH, S. & RICHARDSON, B. 2002. Infrequent occurrence of age-dependent changes in CpG island methylation as detected by restriction landmark genome scanning. *Mechanisms of Ageing and Development,* 123**,** 1487-1503.

TUCKEY, R., CHENG, C. & SLOMINSKI, A. 2018. The serum vitamin D metabolome: What we know and what is still to discover. *The Journal of steroid biochemistry and molecular biology*.

TUCKEY, R. C. 2005. Progesterone synthesis by the human placenta. *Placenta,* 26**,** 273-81.

UMU, S., LANGSETH, H., BUCHER-JOHANNESSEN, C., FROMM, B., KELLERC, A., MEESED, E., LAURITZEN, M., LEITHAUG, M., LYLEE, R. & ROUNGE, T. 2018. A comprehensive profile of circulating RNAs in human serum. *RNA Biology,* 15**,** 242-250.

VAZIRI, F., DABBAGHMANESH, M. H., SAMSAMI, A., NASIRI, S. & SHIRAZI, P. T. 2016. Vitamin D supplementation during pregnancy on infant anthropometric measurements and bone mass of mother-infant pairs: A randomized placebo clinical trial. *Early Hum Dev,* 103**,** 61-68.

VISIEDO, F., BUGATTO, F., SANCHEZ, V., COZAR-CASTELLANO, I., BARTHA, J. L. & PERDOMO, G. 2013. High glucose levels reduce fatty acid oxidation and increase triglyceride accumulation in human placenta. *Am J Physiol Endocrinol Metab,* 305**,** E205-12.

VITALE, S., LAGANÀ, A., RAPISARDA, A., SCARALE, M., CORRADO, F., CIGNINI, P., BUTTICÈ, S. & ROSSETTI, D. 2016. Role of urocortin in pregnancy: An update and future perspectives. *World Journal of clinical cases,* 4**,** 165-171.

WACKER, M. & HOLICK, M. 2013. Sunlight and vitamin D: A global perspective for health. *Dermato-endocrinology,* 5**,** 51-108.

WAN, L. Y., ZHANG, Y. Q., CHEN, M. D., LIU, C. B. & WU, J. F. 2015. Relationship of structure and function of DNA-binding domain in vitamin D receptor. *Molecules,* 20**,** 12389-99.

WANG, B., ITHIER, M., PAROBCHAK, N., YADAVA, S., SCHULKIN, J. & ROSEN, T. 2018a. Vitamin D stimulates multiple microRNAs to inhibit CRH and other pro-labor genes in human placenta. *Endocrine Connections,* 7**,** 1380-1388.

WANG, H., XIAO, Y., ZHANG, L. & GAO, Q. 2018b. Maternal early pregnancy vitamin D status in relation to low birth weight and small-for-gestational-age offspring. *The Journal of Steroid Biochemistry and Molecular biology,* 175**,** 146-150.

WANG, Y., SATOH, A., WARREN, G. & MEYER, H. 2004. VCIP135 acts as a deubiquitinating enzyme during p97–p47-mediated reassembly of mitotic Golgi fragments. *The Journal of Cell biology,* 164**,** 973-978.

WILCOX, C. R., HOLDER, B. & JONES, C. E. 2017. Factors Affecting the FcRn-Mediated Transplacental Transfer of Antibodies and Implications for Vaccination in Pregnancy. *Front Immunol,* 8**,** 1294.

WILHELM-BENARTZI, C. S., HOUSEMAN, E. A., MACCANI, M. A., POAGE, G. M., KOESTLER, D. C., LANGEVIN, S. M., GAGNE, L. A., BANISTER, C. E., PADBURY, J. F. & MARSIT, C. J. 2012. In

utero exposures, infant growth, and DNA methylation of repetitive elements and developmentally related genes in human placenta. *Environ Health Perspect,* 120**,** 296-302.

WINDER, N. R., KRISHNAVENI, G. V., HILL, J. C., KARAT, C. L., FALL, C. H., VEENA, S. R. & BARKER, D. J. 2011a. Placental programming of blood pressure in Indian children. *Acta Paediatr,* 100**,** 653-60.

WINDER, N. R., KRISHNAVENI, G. V., VEENA, S. R., HILL, J. C., KARAT, C. L., THORNBURG, K. L., FALL, C. H. & BARKER, D. J. 2011b. Mother's lifetime nutrition and the size, shape and efficiency of the placenta. *Placenta,* 32**,** 806-10.

XIE, L., MOUILLET, J. F., CHU, T., PARKS, W. T., SADOVSKY, E., KNOFLER, M. & SADOVSKY, Y. 2014. C19MC microRNAs regulate the migration of human trophoblasts. *Endocrinology,* 155**,** 4975-85.

XUE, J., SCHOENROCK, S. A., VALDAR, W., TARANTINO, L. M. & IDERAABDULLAH, F. Y. 2016. Maternal vitamin D depletion alters DNA methylation at imprinted loci in multiple generations. *Clin Epigenetics,* 8**,** 107.

YABE , S., ALEXENKO , A., AMITA , M., YANG , Y., SCHUST , D., SADOVSKY , Y., EZASHI , T. & ROBERTS, R. 2016. Comparison of syncytiotrophoblast generated from human embryonic stem cells and from term placentas. *PNAS,* 113.

YANG, X., PURDY, M., MARZLUFF, W. & DOMINSKI, Z. 2006. Characterization of 3'hExo, a 3' Exonuclease Specifically Interacting with the 3' End of Histone mRNA. *The Journal of Biological Chemistry,* 281**,** 30447-30454.

YUAN, L., LV, Y., LI, H., GAO, H., SONG, S., ZHANG, Y., XING, G., KONG, X., WANG, L., LI, Y., ZHOU, T., GAO, D., XIAO, Z., YIN, Y., WEI, W., HE, F. & ZHANG, L. 2015. Deubiquitylase OTUD3 regulates PTEN stability and suppresses tumorigenesis. *Nature Cell Biology,* 17.

ZERWEKH, J. 2008. Blood biomarkers of vitamin D status. *American Journal of Clinical Nutrition,* 87.

ZHANG, C., LI, Q., REN, N., LI, C., WANG, X., XIE, M., GAO, Z., PAN, Z., ZHAO, C., REN, C. & YANG, W. 2015a. Placental miR-106a approximately 363 cluster is dysregulated in preeclamptic placenta. *Placenta,* 36**,** 250-2.

ZHANG, T., COOPER, S. & BROCKDORFF, N. 2015b. The interplay of histone modifications – writers that read. *EMBO reports,* 16**,** 1467-1481.

ZHANG, Y., GONG, Y., XUE, H., XIONG, J. & CHENG, G. 2018. Vitamin D and gestational diabetes mellitus: a systematic review based on data free of Hawthorne effect. *BJOG,* 125**,** 1338-1339.

ZHAO, C., ZHANG, T., SHI, Z., DING, H. & LING, X. 2014. MicroRNA-518d regulates PPARalpha protein expression in the placentas of females with gestational diabetes mellitus. *Mol Med Rep,* 9**,** 2085-90.

ZHAO, G. & SIMPSON, R. 2010. Membrane Localization, Caveolin-3 Association and Rapid Actions of Vitamin D Receptor in Cardiac Myocytes *Steroids,* 75**,** 555-559.

ZHOU, Y., FISHER, S. J., JANATPOUR, M., GENBACEV, O., DEJANA, E., WHEELOCK, M. & DAMSKY, C. H. 1997. Human cytotrophoblasts adopt a vascular phenotype as they differentiate. A strategy for successful endovascular invasion? *J Clin Invest,* 99**,** 2139-51.

ZHOU, Y., ZHAO, L. J., XU, X., YE, A., TRAVERS-GUSTAFSON, D., ZHOU, B., WANG, H. W., ZHANG, W., LEE HAMM, L., DENG, H. W., RECKER, R. R. & LAPPE, J. M. 2014. DNA methylation levels of CYP2R1 and CYP24A1 predict vitamin D response variation. *J Steroid Biochem Mol Biol,* 144 Pt A**,** 207-14.

ZHU, J. & DELUCA, H. F. 2012. Vitamin D 25-hydroxylase - Four decades of searching, are we there yet? *Arch Biochem Biophys,* 523**,** 30-6.

ZHU, X. M., HAN, T., SARGENT, I. L., YIN, G. W. & YAO, Y. Q. 2009. Differential expression profile of microRNAs in human placentas from preeclamptic pregnancies vs normal pregnancies. *Am J Obstet Gynecol,* 200**,** 661.e1-7.